Author:
Allahyani, Mamdouh

Title:
Investigating the Roles SAFB Proteins Play in Controlling Haemopoiesis and in Acute Lymphoblastic Leukaemia

Investigating the roles SAFB proteins play in controlling haemopoiesis and in acute lymphoblastic leukaemia

Mamdouh Allahyani

A dissertation submitted to the University of Bristol in accordance with the requirements for the award of the degree of Doctor of Philosophy in the Faculty of Health Sciences, Bristol Medical School.

October 2019

40,303 words (main text only)

AUTHOR'S DECLARATION

I declare that the work in this dissertation was carried out in accordance with the requirements of the University's *Regulations and Code of Practice for Research Degree Programmes* and that it has not been submitted for any other academic award. Except where indicated by specific reference in the text, the work is the candidate's own work. Work done in collaboration with, or with the assistance of, others, is indicated as such. Any views expressed in the dissertation are those of the author.

SIGNED: ..... DATE: .....15/03/2020.....

ACKNOWLEDGMENTS

First and foremost, I would like to express my deepest appreciation to my supervisors, Professor James Uney and Dr Allison Blair for giving me this opportunity to pursue a PhD under their supervision. Their encouragement and support have helped me build my confidence as a researcher. I have benefited greatly from the strengths of this supervisory team and I am grateful for the both of you. It has been an amazing 4 years studying SAFB proteins and I have definitely enjoyed every bit of the journey. Without their advice motivation and guidance, this PhD would have been very challenging for me to complete.

I would also like to thank Dr Helen Scott and Dr Paraskevi Diamanti for their relentless help throughout the times when I was learning techniques. Their support, advice and practical help in the lab are appreciated and I am grateful to have worked alongside each of you. Their kindness and patience at answering my questions, even during holidays, meant so much to me. I would also like to thank my labmates, Nicola Buckner and Renata Raele for their patience and kindness for helping me and willingness to share their knowledge and expertise. Furthermore, I would like to thank my sponsor (Taif university, Saudi Arabia) for giving me a chance to further my studies here in the University of Bristol. I also would like to thank Dr Kate Heesom for conducting the mass spectrometry and Dr Phil Lewis for his help and advice on the analysis of the proteomic data. In addition, my thanks go to Dr Stephan Cross for his expertise and advice on image analyses.

A big thank to my parents, brothers and sisters for believing in me and for supporting me in every decision that I have made. Special thanks to my wife Samah who has provided me with a lot of love, support and reassurance and was with me in every step during this journey. She always has been incredibly supportive, encouraging and loving throughout my entire life. Not forgetting my son Gaith, who was born during my second year, for adding joy and happiness in my life.

Last but not least, the people who I hold dear, my peeps, I thank them for their unwavering support, great food and the (even more) excellent company. I cannot even imagine completing this PhD without them by my side. Many thanks to everyone else, who was with me throughout the ups and downs of my studies.

ABSTRACT

To investigate scaffold attachment factor B1 and 2 (SAFB1/2) function in acute lymphoblastic leukaemia (ALL), a transcriptomic differential array screen was interrogated and SAFB1 mRNA expression was found to be significantly lower in T cell ALL (T-ALL) cells compared to normal bone marrow (NBM) cells. Furthermore, the SAFB1/SAFB2 ratio was reduced significantly in both B cell precursor (BCP-) and T-ALL cells. I also found that SAFB2 protein expression was significantly elevated in both ALL subtypes and SAFB1 overexpression induced apoptosis within 48 hours in ALL cells. In contrast, apoptosis was not induced in NBM cells and fibroblasts following SAFB1 overexpression. These data suggest decreased SAFB1 protein expression may promote oncogenesis and overexpressing SAFB1 may form the basis for gene therapy strategies.

The stress response (as characterised by the induction of heat shock factor 1 (HSF1), heat shock proteins (HSPs) and formation of nuclear stress bodies (nSBs) and action of anti-cancer HSP90 inhibitors (celastrol and 17-DMAG) has been characterised in ALL cells. Experiments to characterise the ALL stress response found that HSF1 was constitutively overexpressed and HSF1 nuclear border expression was present in primary BCP-ALL and T-ALL cells following heat shock and 17-DMAG treatment compared with NBM. SAFB1/2 co-localises with HSF1 following a HS in HeLa cells and primary fibroblasts. However, neither SAFB1 nor SAFB2 was found to co-localise with HSF1 following a HS in ALL cells. These findings suggest the stress response differs in ALL cells and may render them more permissive to treatment with HSP90 inhibitors.

RGG/RG and SUMOylation mutants of SAFB1/2 were made to investigate the importance of post translational modifications (PTMs) in regulating SAFB1/2 interactions. Experiments revealed that SAFB1 SUMOylation mutants had a significantly increased interaction with the known oncogene, serine/arginine-rich splicing factor 1 (SRSF1), following heat shock. Results also showed that interactions between SAFB2 delta-RGG/RG methylation mutants and SRSF1 was reduced compared with wild-type SAFB2 under basal and heat shock conditions. Proteomic analyses of SAFB1/2 interactions were undertaken using Tandem Mass Tag Mass Spectrometry (TMT-MS) and bioinformatic analyses suggested they regulate RNA processing, splicing, transcription and translation. Interestingly SAFB2 bound more proteins than SAFB1 in T-ALL cells but bound significantly fewer proteins in HeLa cell. Together, these data highlight the pivotal role of SAFB1/2 play in regulating critical cellular processes and altered indicate SAFB1/2 expression ratios could be important in promoting tumorigenicity.

TABLE OF CONTENTS

LIST OF TABLES

LIST OF FIGURES

ABBREVIATIONS

17-DMAG	17 dimethylaminoethylamino-17-demethoxygeldanamycin
53BP1	P53 Binding Protein 1
AGM	Aorta-gonad- mesonephros
Aha1	Activator of Hsp90 ATPase protein 1
ALC1	Amplified in liver cancer 1
ALL	Acute lymphoblastic leukaemia
AML	Acute myeloid leukaemia
ADPC	Adenomatous polyposis coli-like
APLF	Aprataxin-PNK-like factor
ATP	Adenosine triphosphate
B/NK	B/ natural killer cell progenitors
BAZ1A	Bromodomain adjacent to zinc finger domain protein 1A
BBC3	Bcl-2-binding component 3
BCA	Bicinchoninic acid assay
BCP-ALL	B cell precursor ALL
bHLH	Basic helix-loop-helix
BiTE	Bispecific T-cell engager
BP	Biological processes
BRCA1	Breast cancer type 1 susceptibility protein 1
BRD4	Bromodomain-containing protein 4
BRG1	Brahma-related gene-1
BSA	Bovine serum albumin
CAR	Chimeric antigen receptor
CB	Cord blood
CBP	CREB-binding protein
CDC37	Cell division cycle 37
CHD1	Chromodomain-helicase-DNA-binding protein 1
Chip	Chromatin immunoprecipitation
CKS2	Cyclin-dependent kinase interacting protein
CLL	Chronic lymphocytic leukaemia
CML	Chronic myeloid leukaemia
CMP	Common myeloid progenitors
CNS	Central nervous system
co T-ALL	Cortical T-ALL
Co-IP	Co-Immunoprecipitation
CT	Cycle threshold
DAVID	Database for Annotation, Visualization and Integrated Discovery
DDR	DNA damage response
DMEM	Dulbecco's Modified Eagle Medium
DMP	Dimethyl pimelimidate dihydrochloride
DMSO	Dimethyl sulfoxide
DNMTs	DNA methyltransferases
DTT	Dithiothreitol

E/R	Glutamic acid/arginine
ECM	Extracellular matrix
EED	Polycomb protein
EGFR	Epidermal growth factor receptor
ERG	ETS related gene
ETP	Early T cell progenitors
EZH2	Enhancer of zeste homolog 2
FBS	Fetal bovine serum
FDR	False discovery rate
FLI1	Friend leukemia integration1 transcription factor
FLT3	Fms-like tyrosine kinase-3
FSC	Forward scatter
GATA1	Globin transcription factor-1
G-CSF	Granulocyte-colony stimulating factor
GM-CSF	Granulocyte macrophage colony stimulating factor
GMP	Granulocyte-monocyte progenitor
GO	Gene ontology
GVHD	Graft-versus-host disease
HAP	HnRNP A1 associated protein
HAT	Histone acetyltransferase
HCC	Hepatocellular carcinoma
HD	High dose
HDAC3	Histone deacetylase 3
HET	Hsp27 ERE TATA-binding protein
hnRNP	Heterogeneous nuclear ribonucleoproteins
HOX	Homeobox
HS	High similarity
HS	Heat shock
HSC	Haemopoietic stem cells
HSCT	Haemopoietic stem cell transplantation
HSFs	Heat-shock factors
HSP27	Heat shock protein 27
HSPs	Heat shock proteins
iCLIP	Individual nucleotide resolution cross-linking and immunoprecipitation
Ig	Immunoglobulin
IMDM	Iscove's Modified Dulbecco's Medium
IncRNA	Long non-coding RNA
ING5	Inhibitor of growth protein 5
IPTG	Isopropyl-1-thio-β-D-galactopyranoside
KEGG	Kyoto Encyclopaedia of Genes and Genomes
LN2	Liquid nitrogen
LB	Luria broth
LD	Lower dose
LEF	Lymphoid enhancer factor
LICs	Leukaemia initiating cells
LMO2	LIM domain only 2

LOH	Loss of heterozygosity
LY6K	Glycophosphatidyl-inositol-anchored membrane protein
MALAT1	Metastasis associated lung adenocarcinoma transcript 1
MCSF	Macrophage colony stimulating factor
MEF	Mouse embryonic fibroblasts
MEP	Megakaryocyte erythroid progenitors
MLP	Multi lymphoid progenitors
MRD	Measurable residual disease
MS	Mass spectrometry
MTA	Methylthioadenosine
MTAP	5-methylthioadenosine phosphorylase
MTT	MTT 3-(4,5-Dimethylthiazol-2-yl)-2,5-diphenyltetrazolium bromide
NCOR	Nuclear receptor co-repressor 1
NEAAs	Non-essential amino acids
NEAT1	Nuclear Enriched Abundant Transcript 1
NEDD9	Neural precursor cell expressed developmentally down-regulated protein 9
NF-κB	Receptor activator of nuclear factor kappa B
NGS	Next generation sequencing
NK	Natural killer cells
NLS	Nuclear localization signal
NOD/SCID	Non-obese diabetic–severe combined immune deficient
NRAS	Neuroblastoma ras viral oncogene homolog
nSBs	Nuclear stress bodies
NSG	NOD/LtSz-scid IL-2RYc null
NZY+	NZ amine (casein hydrolysate) and yeast
one-way ANOVA	One-way analysis of variance
OPG	Osteoprotegerin
ORF	Open reading frames
OS	Overall survival
PARylation	Poly(ADP ribosyl)ation
PAX5	Paired box 5
PBS	Phosphate buffer saline
PBST	PBS 0.02% tween
PFA	Paraformaldehyde
Ph-ALL	Philadelphia positive ALL
PI	Propidium Iodide
PPIs	protein-protein interactions network
PRCs	Polycomb repressive complexes
PRMT	protein arginine methyltransferases
PKR	Protein kinase R
PSA	Prostate-specific antigen
PTL	Parthenolide
Pu.1	Including purine box binding protein 1
R/G	Arginine/glycine
RBM23	Probable RNA-binding protein 23

RBP	RNA binding proteins
RIPA	Radioimmunoprecipitation assay
RPs	Ribosomal proteins
RRM	RNA-recognition motif
RTKs	Receptor tyrosine kinases
RT-qPCR	Real time quantitative polymerase chain reaction
Runx1/AML1	Runt-related transcription factor1/acute myeloid leukemia1
S/MARs	Scaffold/matrix attachment regions
SAFA	Scaffold attachment factor A
SAFB	Scaffold attachment factor B
SAP box	SAF-A/B, Acinus and PIAS domain
SATIII	Satellite-III
SCL/tal1	Stem cell leukemia/T cell acute lymphocytic leukemia-1
SD	Standard deviation
SDS	Sodium dodecyl sulfate
SFRS12	Splicing factor, arginine/serine-rich 12
SLM1	Cytoskeletal signalling protein
SLTM	SAF (scaffold attachment factor)-like transcription modulator
snRNA	Small nuclear RNA
SNRPD3	Small nuclear ribonucleoprotein Sm D3
SOC	Catabolite repression
SR	Serine–arginine-rich
SRSF1	Serine and arginine rich splicing factor 1
SSC	Side scatter
SUMO	Small ubiquitin-like modifier
SUZ12	Polycomb protein SUZ12
TAE	Tris / acetic acid / EDTA
T-ALL	T cell ALL
TCF	T-cell factor
TCR	T-cell receptor
TFIIH	Transcription factor IIH complex
TMT	Tandem Mass Tag
TNF	Tumour necrosis factor
Tra2	Transformer-2 sex-determining protein
TUG1	Taurine upregulated gene 1
two-way ANOVA	Two-way analysis of variance
UTR	Untranslated regions
VEGF	Vascular endothelial growth factor
XIST	X-inactive specific transcript
XOR	Xanthine oxidoreductase

CHAPTER 1 : General Introduction

1.1 SAFB proteins

1.1.1 Scaffold attachment factor B (SAFB) family

The RNA binding protein Scaffold attachment factor B1 (SAFB1) was identified by three different research groups; it was found by Renz and Fackelmayer (1996) as a protein that interacts with scaffold/matrix attachment regions (S/MARs) (1). These regions attach chromatin to the nuclear matrix and the chromatin loop domains formed at these attachment regions are also thought to be sites controlling transcription and replication (2). A second research group identified a protein that interacted with the heat shock protein 27 (hsp27) ERE TATA-box (hsp27 ERE TATA-box-interacting protein (HET)) and found it repressed the transcriptional activity of hsp27 (3). A third group identified a hnRNP A1 associated protein (HAP) by two-hybrid screening and subsequent sequencing determined that SAFB1, HET and HAP were identical (4). Subsequent to these findings, a paralogue of SAFB1 was found and termed SAFB2 (5) and our group more recently found a homologue, SAF (scaffold attachment factor)-like transcription modulator (SLTM) (6). SAFB1 and SAFB2 are located on human chromosome 19p13.3 in a bidirectional manner, separated by a 490 bp promoter (5) (Figure 1.1). SLTM is located on chromosome 15q22.1.

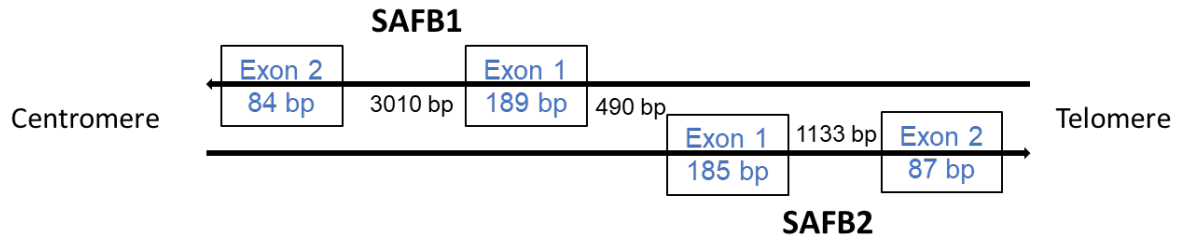

Figure 1.1 The chromosomal location of SAFB1 and SAFB2. *SAFB1* and *SAFB2* are located on chromosome 19p13 in a head to head arrangement, separated by a 490bp promoter.

1.1.2 SAFB proteins have a modular structure

SAFB1 and 2 proteins are highly similar at the amino acid level, sharing 74% homology. However, SLTM shares only 34% and 36% similarity with SAFB1 and SAFB2, respectively (Figure 1.2) (7). SAFB proteins are structurally similar and the

various functional domains share a very high homology (ranging from 65-100%) (Figure 1.2). These functional domains include a SAF-A/B, Acinus and PIAS domain (SAP box) located at the N-terminus, an RNA-recognition motif (RRM) and nuclear localization signal (NLS) located in the central region and glutamic acid/arginine (E/R) and arginine/glycine-rich (R/G) regions at the C-terminus. The C-terminus region is crucial for protein-protein interactions. They also share a region with no known function with high conservation termed the high similarity (HS) domain (8).

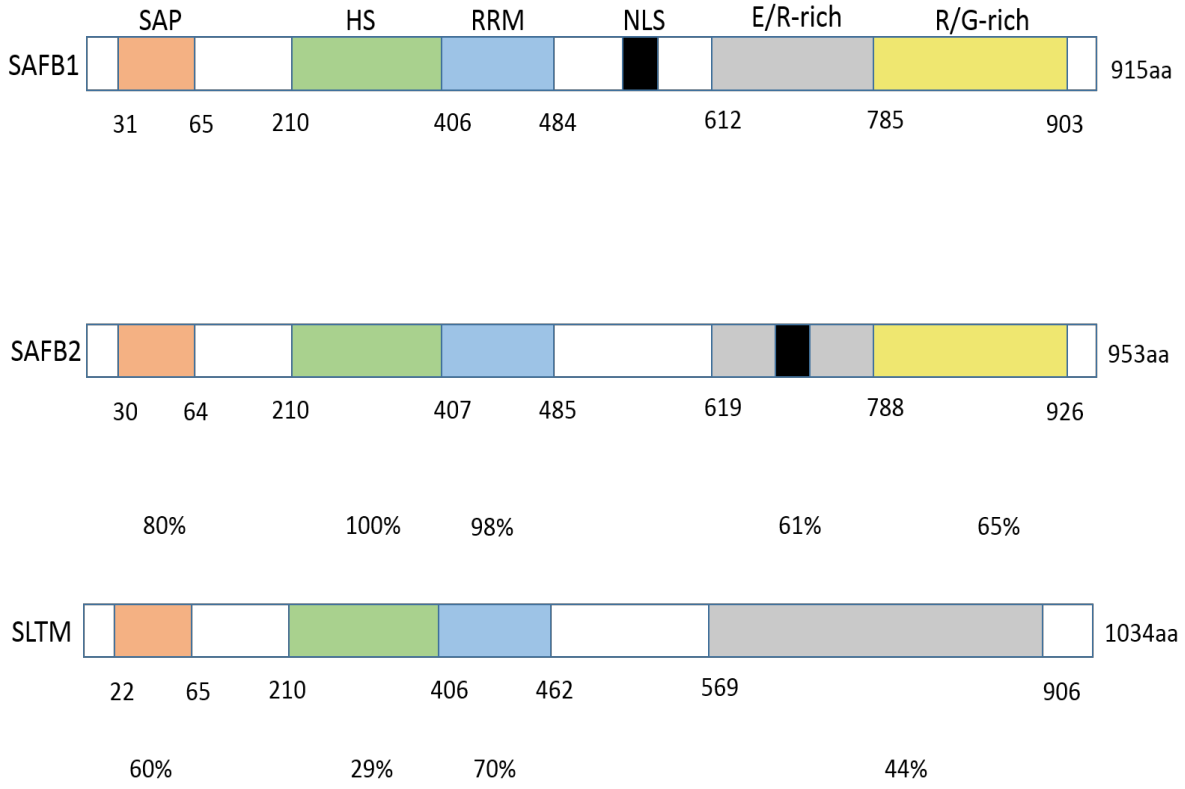

Figure 1.2 SAFB1, SAFB2 and SLTM protein domains and homologies. The diagram shows a region with no known function with high similarity (HS) the SAP-Box, RNA-recognition motif (RRM), nuclear localization signal (NLS), Glu/Arg rich (E/R) and Arg/Gly rich (R/G) domains. The amino acid homology of SAFB2 and SLTM compared to SAFB1 for each domain is given as a percentage.

1.1.3 SAFB proteins' expression profile and cellular localisation

SAFB1 is primarily expressed in the nucleus, while its paralogue SAFB2 is expressed in both the nucleus and cytoplasm (5). This suggests that SAFB2 has additional functions distinct from those of SAFB1 in the nucleus. This is supported by the

observation that SAFB2 is highly expressed in Sertoli cells compared to SAFB1 (9), suggesting SAFB1 and SAFB2 expression can be tissue specific and that they have distinct functions. SLTM is expressed in the nucleus and excluded from nucleolus, similar to SAFB1. SLTM partially co-localises with SAFB1 suggesting that proteins may share some functions (6).

Proteomic analysis demonstrated that SAFB proteins are widely expressed across different tissues, including the bone marrow tissues where leukaemia cells reside. For example, SAFB1 and SLTM were expressed at high levels in bone marrow cells, whereas SAFB2 was expressed at moderate levels (Figure 1.3) (10). Furthermore, all SAFB proteins were expressed at high levels in a wide range of tissues, including the thyroid gland, heart, lung, kidney and placenta. The expression of SAFB proteins has also been investigated in neuronal tissues. It was found that SAFB1 was expressed at high levels throughout the hippocampus (11). In contrast, SAFB2 and SLTM were expressed at moderate levels (Figure 1.3) (10). These data again suggest that SAFB proteins might play different roles in various tissues.

Endogenous genes targeted by SAFB were investigated in breast cancer cells using chromatin immunoprecipitation (Chip)-on-chip and gene expression analysis to extend our understanding about SAFB1/2 functions and to investigate which genes are controlled by SAFB1/2. Over 541 SAFB1/2 binding sites were identified and the majority of those binding SAFB1 coded for genes involved in regulating the immune system (interleukins, chemokines), followed by genes with roles in signalling and apoptosis, including Bcl-2-binding component 3 (BBC3), neural precursor cell expressed developmentally down-regulated protein 9 (NEDD9) and Osteoprotegerin (OPG) (12).

SAFB1 was reported to be important in growth regulation, development and reproduction (13). SAFB1-knockout mice exhibited a number of abnormalities, including dwarfism, infertility, defects in testes and in the development of the haemopoietic system, suggesting SAFB1 plays a critical role in haemopoiesis (13). In contrast, mice lacking SAFB2 were viable and showed no major defects in growth or infertility (14). These data suggest that SAFB1 and SAFB2 have unique physiological functions.

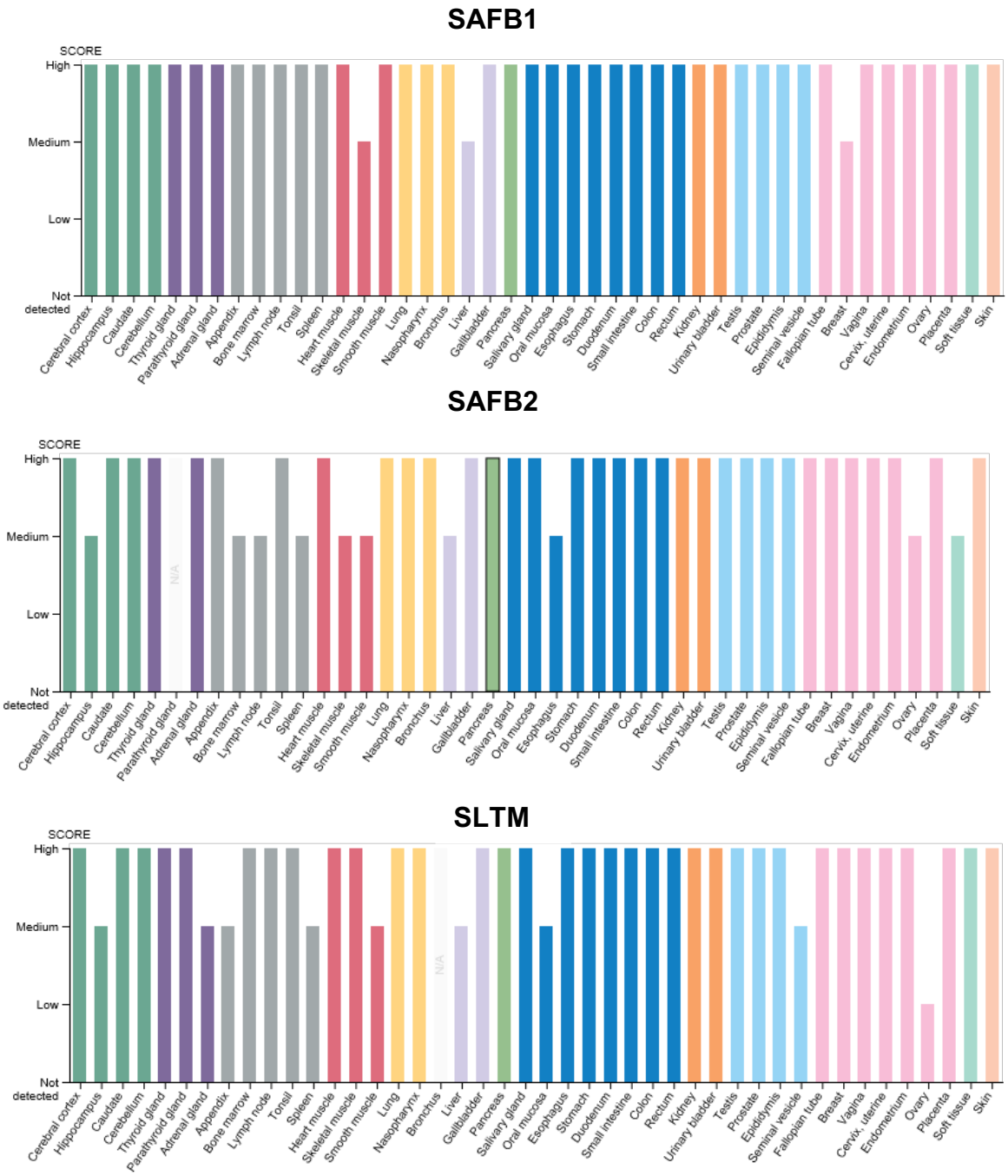

Figure 1.3 Protein expression of SAFB1, SAFB2 and SLTM proteins in 44 normal human tissues. Tissues were immunohistochemically stained and categorised into negative, low, medium and high based on staining intensities. Coloured bars represent tissues with similar features (10).

1.2 Functions of SAFB proteins

SAFB proteins have been implicated in a wide range of cellular processes, including transcriptional regulation, chromatin organisation, cellular stress response, DNA damage response, apoptosis, RNA splicing and metabolism (11). However, despite

evidence suggesting SAFB1 and SAFB2 may have some distinct functions, the majority of studies to date have only investigated SAFB1 with very few investigating SAFB2.

1.2.1 SAFB proteins in transcription

SAFB1 was identified as a protein that bound and repressed hsp27 promoter activity (3) and hence SAFB1 was believed to be a negative regulator of transcription. Another study reported that SAFB1 repressed *xanthine oxidoreductase* (XOR) expression (15). A wider study demonstrated that knockdown of SAFB1 and SAFB2 resulted in the induction of 457 genes and repression of 259 genes (12). The mechanisms by which SAFB proteins might repress transcription involved interaction with chromatin-modifying complexes, such as Polycomb repressive complexes (PRCs) and long non-coding RNA (lncRNAs). For example, a study found that SAFB1 represses the androgen receptor and SAFB1 knockdown resulted in higher transcription of prostate-specific antigen (PSA) in cultured prostate cells (16). Also, SAFB1 was shown to form a complex with Polycomb PRC2 components; Enhancer of zeste homolog 2 (EZH2), and Polycomb proteins SUZ12 and EED (16), suggesting that SAFB1 mediates transcriptional repression by this pathway. However, SAFB1 transcription is not always repressive; for example, SAFB1 knockdown was shown to inhibit the expression of skeletal muscle genes, indicating a positive regulatory role of SAFB1 (17). SAFB1 overexpression was shown to promote expression of muscle structural proteins. In contrast, SAFB1 knockdown was associated with inhibition of skeletal muscle gene expression. The interaction between SAFB1 and the polycomb PRC2 complex was suggested by the persistence of the Ezh2 component of PRC2 and the repressive histone marker H3K27me3 following SAFB1 knockdown (17). These data suggest that SAFB1 is necessary for chromatin transition from repression to the active state during myogenesis.

1.2.2 SAFB proteins in cellular stress response

SAFB1 was reported to be involved in regulating the response to a stress such as heat shock (HS). SAFB1 co-localised with HSF1 in nuclear stress bodies (nSBs) and was suggested to play a role in transcriptional control and alternative splicing in cells

following stress (4),(18). nSB formation requires ongoing transcription and was shown to be sensitive to RNase indicating that RNA is a main component (4),(19). Further studies found that a region close to the C-terminal [580–788aa] region of SAFB1 is needed upon HS to be recruited to the nSBs (20). Deletion of both the E/R and R/G at the C-terminal caused SAFB1 to translocate to the cytoplasm suggesting multiple C-terminal interactions govern SAFB1 function.

1.2.3 SAFB proteins in the DNA damage response

RNA binding proteins (RBPs) are known to play an important role in DNA repair (21). SAFB1 was shown to be rapidly recruited to DNA double-strand breaks and this was required for histone γH2AX to be efficiently phosphorylated (22) which governs DNA damage response (DDR) signalling. SAFB1 recruitment was dependent on poly(ADP ribosyl)ation (PARylation) pathway, which was rapidly activated in response to DNA breakage. PARylation also facilitates the recruitment of several chromatin modifiers, including aprataxin-PNK-like factor (APLF) and amplified in liver cancer 1 (ALC1) and repair factors, including breast cancer type 1 susceptibility protein (BRCA1) and P53 Binding Protein 1 (53BP1) to damaged sites (22). It was shown that a deletion mutant of SAFB1, lacking the R/G domain (aa 785–917) at the C-terminal, was sufficient for SAFB1 recruitment to damaged chromatin and was needed for PARP recruitment (22). These data suggest that SAFB1 is an essential component of the general response to DDR by rendering the chromatin permissive to DNA damage signalling.

1.2.4 SAFB proteins in apoptosis

High levels of SAFB1 were reported to arrest T24 (human bladder carcinoma) cells in the G_2-M phase suggesting a role in the control of cell division (23). The overexpression of SAFB1 also leads to multinuclearity and considerable changes in the cell cycle (23). Our group has also found that SLTM overexpression induces apoptosis (6). After activating apoptosis, SAFB1 expression (24) was seen in the nucleolus within 30 minutes. By 2 hours, most cells display peri-nucleolar staining of SAFB1. After 3-4 hours, the peri-nucleolar feature was absent (24) and this was found to be dependent on RNA binding. It was concluded that SAFB1 is required to direct the segregation of RNA during apoptosis. In addition to the role of SLTM in inducing

apoptosis, these data suggest that SAFB1 is likely to be involved in the programmed cell death pathway.

1.3 Post-translational modification of SAFB proteins

SAFB proteins have been found to undergo phosphorylation, ubiquitylation, SUMOylation, arginine methylation, PARylation and acetylation. However, this section focuses on phosphorylation, small ubiquitin-like modifier (SUMO)ylation and arginine methylation. SAFB1 was reported to be phosphorylated (2) and another study reported that all SAFB proteins became phosphorylated in response to DNA damage (25) and is required for the amplification of DDR signalling (22).

SUMOylation is dynamic process that conjugates the SUMO moiety on target proteins. It is involved in a diverse range of functions, such as DNA replication, genome stability, nuclear transport, and gene transcription (26). All SAFB proteins were proposed to be substrates for SUMOylation. SUMOylation was demonstrated on Lys 231 and Lys 294 of both SAFB1 and SAFB2 (27) and SUMOylation of SAFB1 has been shown to be mediated by SUMO-1 and SUMO 2/3 (28). SAFB1 SUMOylation status was linked to the stress response, with SAFB proteins becoming de-SUMOylated upon heat stress (27). Subsequently, it was found that SUMOylation was required for transcriptional repression to be mediated by SAFB1 (29). More recently, it was found that transcription of ribosomal proteins (RPs) was enhanced by SUMOylated SAFB1 (28).

Protein methylation can occur on arginine or lysine residues and is essential in the regulation of histone and non-histone proteins in many signal transduction pathways (30). The UniProt database showed that SAFB proteins were methylated on the RGG/RG arginine motif sites (aa 868–875 in SAFB1), located on the R/G rich domain within the C-terminal domain. However, how the methylation of SAFB proteins regulates cellular functions is not known. Arginine methylation regulates many processes, including gene expression, DNA damage repair and protein translocation (30). Also, evidence suggests that RGG/RG motifs are the substrates for protein arginine-N-methyltransferases (PRMT), i.e. PRMT1, PRMT3, PRMT5, PRMT6 and PRMT8 (31) which were shown to modify many protein functions and are implicated in health and disease (30).

1.4 SAFB proteins in cancer

There have been a number of studies suggesting that altered SAFB protein expression is linked to oncogenesis. Disruption of SAFB1 expression is associated with immortalisation in mouse embryonic fibroblasts (MEFs) (32). SAFB1 down regulation was associated with an increase in growth rate (23). SAFB1 mutations were identified in breast tumours but not in the normal adjacent tissue. The implications of SAFB1 mutations were not studied and further experiments are needed. A high loss of heterozygosity (LOH) of 78% was detected at the SAFB chromosomal locus in invasive breast cancer. A high rate of LOH is a feature of genes with roles in cancer suppression (33). Further analysis of 19p13 locus showed that adenomatous polyposis coli-like (APCL), a tumour suppressor candidate, is involved (33). SAFB2 was shown to be a substrate for breast cancer type 1 (BRCA1) and the latter was proven to enhance SAFB2 protein expression (33).

Lower levels of SAFB expression are associated with worse overall survival in breast cancer patients (34). SAFB1 expression was also lower in prostate cancer (16) and more recently, a group found low levels of SAFB1 promoted the activation of NF-κB signalling in colorectal cancer patients. Also, SAFB1 down regulation was correlated with poor survival and aggressive phenotype in colorectal cancer patients (35). Together these findings suggest that SAFB1 overexpression is associated with inhibition of cancer cells and SAFB1 was hypothesised to be a tumour suppressor gene. However, further experiments need to be performed to prove this hypothesis.

1.5 SAFB protein interactions with RNA and proteins

Spectrometric analyses found that SAFB1, SAFB2 and SLTM bind mRNA (36), (37), suggesting that SAFB proteins could be involved in mRNA processing. Therefore, individual nucleotide resolution cross-linking and immunoprecipitation (iCLIP) technology was used with deep sequencing to identify SAFB1 binding sites in the SH-SY5Y neuroblastoma cell line. SAFB1 binding with RNA was enriched in exons and associated with the purine rich pentamers GAAGA and AAGAA, occurring with the highest frequency in proximity to intron-exon and exon-intron boundaries, suggesting a role in mRNA splicing (38). In addition, SAFB1 binding was also enriched in ncRNAs, 3’ and 5’ untranslated regions (UTR) (38), suggesting roles in regulating gene

expression. Another group used the iCLIP technique to investigate the interaction of SAFB1 with RNA in MCF-7 breast cancer cells (39). Similar results were produced with enrichment in introns, open reading frames (ORFs), in 3' and 5' UTRs with higher enrichment in ncRNA. Using iCLIP technology, several ncRNA transcripts were bound to SAFB1, including metastasis associated lung adenocarcinoma transcript 1 (MALAT1), nuclear enriched abundant transcript 1 (NEAT1), taurine upregulated gene 1 (TUG1) and X-inactive specific transcript (XIST) which are involved in the regulation of gene regulation (38). Moreover, it was shown that SAFB1 is bound with many microRNA transcripts, including the miR-17-92 cluster (38). Knockdown of SAFB1 was associated with decrease in mature miR-19A expression and increase in the primary miR-17-92 transcript expression, indicating that SAFB1 is required for processing miR-19A (38). SAFB1 and the microRNA 17-92 were shown to regulate RNA processing (38).

In addition to RNA interactions, SAFB1 was shown to interact with several regulatory proteins (11), discussed below. It is important to consider the methodology used to identify protein-protein interactions. Two-hybrid assays have been used for protein-protein identification but are subject to false positive results. In contrast, co-immunoprecipitation technology provides a better picture for protein-protein interactions. However, the choice of the extraction conditions may influence the results. For example, high salt concentrations will help in identifying stable interactions but could miss important weaker interactions. Also, co-immunoprecipitation does not distinguish between direct and indirect interactions. SAFB1 was reported to interact with several heterogeneous nuclear ribonucleoproteins (hnRNP) proteins, including hnRNPC (4), hnRNPD (40), hnRNPG (9) and hnRNPPI (4). hnRNP proteins regulate many processes, including transcription, processing and transport of mRNA. The SR (serine–arginine-rich) proteins, such as serine and arginine rich splicing factor 1 (SRSF1), SRSF3, SRSF7 and SRSF9 interact with SAFB1. They play important roles in splicing and are concentrated in nSBs together with SAFB1. It was shown that SAFB1 interact with several RNA splicing proteins, including transformer-2 sex-determining protein (Tra2), SRSF9, SRp30c, SFRS12, cytoskeletal signalling protein (SLM1) and SLM2) (9). Splicing of Tra2 was found to be inhibited by SAFB1 (41) and SAFB2 (9). SAFB1 was identified to be a component of spliceosomes (42), macromolecular complexes of snRNA (small nuclear RNA molecules and small

nuclear ribonucleoproteins assisting in the removal of introns (43). However, SAFB1 was not found in an analysis of spliceosomes, suggesting a transient association between SAFB1 and spliceosomes (44). Furthermore, SAFB1 was shown to interact with proteins involved in transcription, such as RNA polymerase III (2) and p53 (45). SAFB1 was shown to bind with p53 and supress its activity (45). In addition, SAFB1 interacted with several proteins with roles in determining chromatin structure and function, including nuclear receptor co-repressor 1 (NCOR) (29), histone deacetylase 3 (HDAC3) (29), chromodomain-helicase-DNA-binding protein 1 (CHD1) (46), Brahma-related gene-1 (BRG1) (15) and matrin3 (47). CHD1 was shown to interact with HDAC3 and NCOR, a transcriptional corepressor, suggesting a role in chromatin remodelling.

1.6 Haemopoiesis

Haemopoiesis is the term used to describe the process of blood cell production; which emerges from haemopoietic stem cells (HSCs). HSCs are rare cells sitting at the top of haemopoietic hierarchy that have the ability to produce all blood cell types throughout a lifetime and they have the characteristics of self-renewal and differentiation (48).

Blood cell differentiation starts with HSCs, followed by multipotent progenitor cells, which are unique in their developmental capacity and then they become progressively lineage-restricted. One class of multipotent progenitor cells are multi lymphoid progenitors (MLP), which give rise to mature B, T and natural killer (NK) cells. Another subset of multipotent progenitor cells are common myeloid progenitors (CMP), which eventually give rise to mature erythrocytes, megakaryocytes, monocytes, granulocytes and dendritic cells (49). A schematic for blood lineages during haemopoiesis is shown in Figure 1.4.

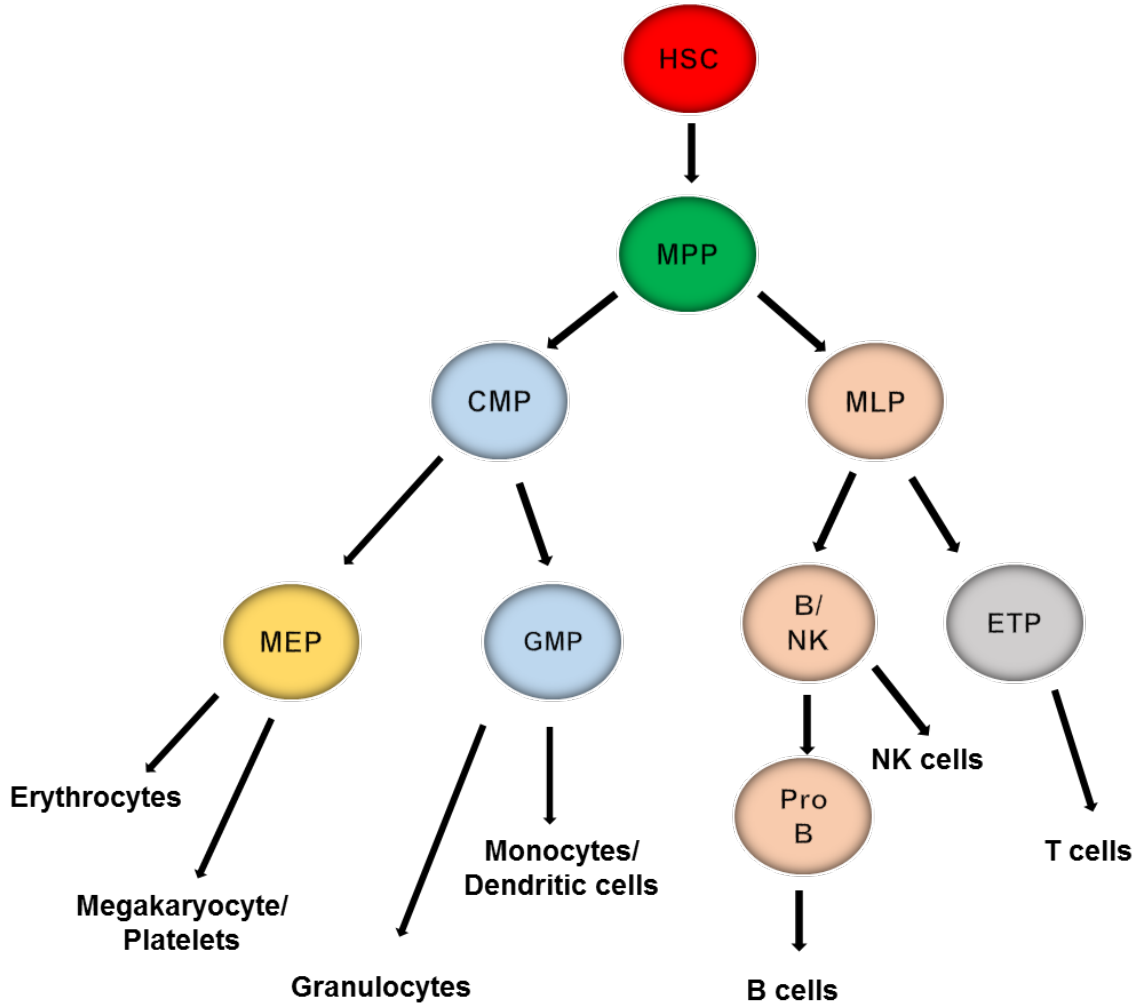

Figure 1.4 The differentiation of haemopoietic progenitor cells from HSCs. HSCs give rise to multipotent progenitors (MPP) which maintain the ability to differentiate into both myeloid and lymphoid lineages. Myeloid and lymphoid pathways diverge after from MPP into either common myeloid progenitors (CMP) or multi lymphoid progenitors (MLP). Progenitors then differentiate, with CMP giving rise to megakaryocyte erythroid progenitors (MEP) or granulocyte-monocyte progenitor (GMP) and MLP becoming early T cell progenitors (ETP) or B/ natural killer cell progenitors (B/NK). These progenitors then give rise to mature and specialised haemopoietic cells.

During embryonic and fetal development, haemopoiesis takes place in different anatomical sites, including the yolk sac, then the aorta-gonad- mesonephros (AGM) region, followed by the liver and eventually the bone marrow (50). The initial stage of haemopoiesis in the yolk sac called primitive which helps in the production of erythrocytes, facilitating oxygenation of rapidly growing embryo (50). Primitive haemopoiesis is transient and replaced by definitive haemopoiesis in the AGM region which gives rise to primitive HSCs. At the later stages of fetal development, the

functional HSCs migrate to the liver where they expand (51). The shift in locations during the fetal haemopoiesis is important as the embryo is developing. The bone marrow is the main site for haemopoiesis during adulthood as the bone marrow can provide the microenvironment needed to conserve the multipotency of HSCs (51). The bone marrow niche has the potential to maintain the HSC self-renewal and differentiation balance (52). Haemopoiesis also happens in the spleen and also in the thymus where T lymphocytes mature.

The HSC fate is associated with changes in gene expression. Regulation of HSC self-renewal and differentiation is controlled by various transcriptional factors, molecular signaling pathways and epigenetic modifiers. Several transcriptional factors were shown to regulate HSCs during embryogenesis, including purine box binding protein 1 (Pu.1), runt-related transcription factor1/acute myeloid leukemia1 (Runx1/AML1), globin transcription factor-1 (GATA1), GATA2, stem cell leukemia/T cell acute lymphocytic leukemia-1 (SCL/tal1), LIM domain only 2 (Lmo2), friend leukemia integration1 transcription factor (FLI1) and ETS related gene (ERG) (53). Pu.1, one of the most important factors that regulate haemopoiesis, is essential for B lymphocyte and monocyte differentiation (54). Pu.1 overexpression forced HSCs to differentiate into macrophages instead of B lymphocytes (53). Also, Pu.1 disruption resulted in a failure commitment of HSCs to differentiate into both myeloid and lymphoid lineages (53).

During adulthood the regulation of HSCs takes place in the bone marrow niche. The bone marrow niche contains cells and extracellular matrix (ECM). ECM provides the physical support and interacts with HSCs through adhesion molecules. Niche cells are responsible for HSC quiescence, proliferation and differentiation. Osteoblasts, one of the most important niche cells, secrete various cytokines such as granulocyte-colony stimulating factor (G-CSF), macrophage colony stimulating factor (MCSF), granulocyte macrophage colony stimulating factor (GM-CSF), interleukin (IL)-1, IL-6, IL-7, osteoprotegerin (OPG), receptor activator of nuclear factor kappa B (NF-κB), tumour necrosis factor (TNF)-α and vascular endothelial growth factor (VEGF), all of which are involved in the modulation of HSC function (53).

The balance between HSC self-renewal and differentiation is essential for the maintenance of hemopoieses and requires tight regulation. For example, the overexpression of the proto-oncogene c-Myc was shown to increase HSC differentiation. In contrast, c-Myc deficient HSCs lack the ability to generate lineage committed haemopoietic precursors (52), leading to the formation of immature granulocytes, erythrocytes and platelets. In addition to the role of the transcriptional factors in regulating HSCs, numerous signaling pathways are also implicated in regulating this process, including Notch and Wnt signaling pathways (55). Mis-regulation of the pathways involved in regulating HSC self-renewal and differentiation leads to cancer.

1.7 Acute lymphoblastic leukaemia

1.7.1 Background

Acute lymphoblastic leukaemia (ALL) is initiated in the bone marrow following the expansion of uncontrolled regulation in the early progenitor lineages during haemopoiesis. ALL is associated with several symptoms, including bruising and bleeding resulting from thrombocytopenia. ALL patients also exhibit other symptoms, such as pallor and fatigue resulting from anaemia (56). The involvement of extramedullary sites (thymus, liver, spleen, kidney and the testes in males) is common, occurring in 20% of patients. The central nervous system (CNS) involvement of those patients present in 5-8% of ALL cases and associated with poor prognosis (57).

ALL is the most common cancer in children, accounting for approximately 25% of all childhood malignancies occurring before age 15 years (58). Eighty percent of ALL cases occur in children (57), with the peak incidence at 3-5 years of age (56). An annual incidence of 3,000 in million children (59) diagnosed with ALL reported annually in the US. A total of 400 new cases of ALL are diagnosed annually in the UK in children younger than 15 years every year. The remission rate has increased dramatically from 10% to 90% (60). ALL is divided into B cell precursor ALL (BCP-ALL) and T cell ALL (T-ALL). BCP-ALL accounts for the majority (85%) of ALL cases (61). T-ALL patients have poorer prognosis compared to those with BCP-ALL (62). ALL is more common in males (62).

1.7.2 Genetic landscape in ALL

There are several chromosomal structural and genetic abnormalities associated with ALL patients (63). About 75% of ALL cases are associated with genetic alterations (61). Common genetic alterations in BCP-ALL and T-ALL are highlighted in Figure 1.5 (64). Significant improvements in cytogenetic and genomic technologies contributed to better understanding of the disease and provide prognostic and predictive markers for therapy (65),(66). Such advances will also provide novel markers which might help in ALL diagnosis and could be targeted with new therapies (64).

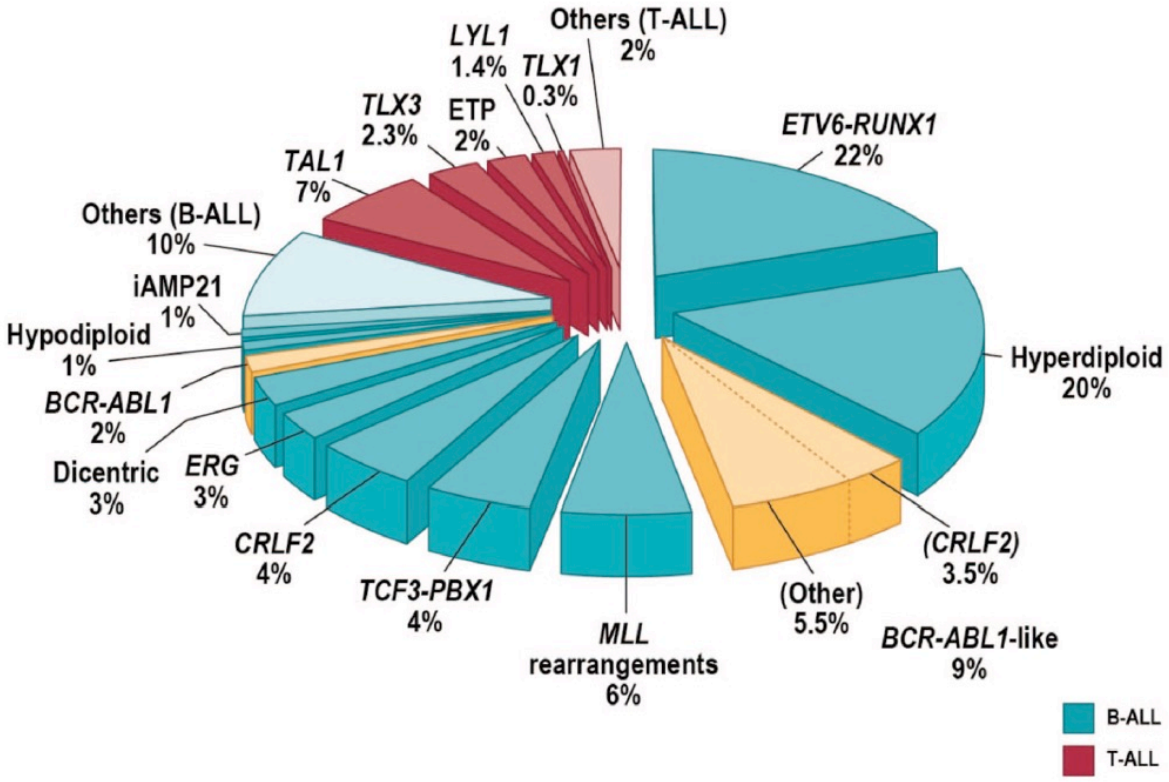

Figure 1.5 Genetic alterations in ALL. The figure highlights several genetic alterations in BCP-ALL (blue bars), including ETV6-RUNX1, resulting from t(12;21) (p13;q22); BCR-ABL1, resulting from t(9;22)(q34;q11) and TCF3-PBX1, resulting from t(1;19) (q23;p13). It also shows different alterations such as hyperdiploidy, hypodiploidy, MLL rearrangements, iAMP21, ERG and dicentric. In T-ALL, TAL1, TLX1, ETP, TLX3 and LYL1 were commonly found to be disregulated (red bars). The yellow bars represent different genetic alterations in ALL but mostly common in BCP-ALL, including BCR-ABL1-like and CRLF2 (64).

Genetic abnormalities in ALL can be structural aberrations, such as chromosomal translocations, and numerical aberrations such as hypodiploidy (<44 chromosomes)

and high hyperdiploidy (>50 chromosomes) (61). The translocation t(12;21) (p13;q22) resulting in the ETV6-RUNX1 fusion gene is the most common translocation (22%) in BCP-ALL patients and children with this mutation have good prognoses (63). The ETV6-RUNX1 fusion gene disrupts haemopoiesis as ETV6 and RUNX1 are important transcriptional factors mediating this process (61). The ETV6-RUNX1 translocation thought to cause alterations in B-cell progenitor self-renewal and differentiation but this is not sufficient to cause the disease as ETV6-RUNX1 did not induce leukaemia in transplanted mice, indicating that other factors are cooperating for BCP-ALL progression (61). Hyperdiploidy is another frequent abnormality (20%) in BCP-ALL patients and associated with good prognosis and 5-year overall survival (OS) rates >90% (63). However, some hyperdiploid patients relapse and this is due to the fact that many mutations were found to be frequently associated with hyperdiploidy, including fms-like tyrosine kinase-3 (FLT3), neuroblastoma ras viral oncogene homolog (NRAS) and paired box 5 (PAX5) (61). Hypodiploidy is less common (1%) compared with hyperdiploidy and associated with poor prognosis (64). Patients with hypodiploidy can be near haploid (24–31 chromosomes), low hypodiploid (32–39 chromosomes), hypodiploid (40–43 chromosomes) and near diploid (44 or 45 chromosomes) with lower chromosome numbers associated with poorer outcome (61).

The genetic landscape in T-ALL is different compared with the BCP-ALL genetic signature and generally associated with poor outcome. The most common regulator of T cells is NOTCH1, which regulates the commitment of haemopoietic progenitors to the T‑cell lineage during development, was found to be mutated in T-ALL (67). NOTCH1 mutations were found in 60% of T-ALL patients and associated with good prognosis (68). Genomic analyses found that the oncogenic transcriptional factors are associated with T-ALL subgroups. Such oncogenic transcription factors, include basic helix-loop-helix (bHLH) family members, such as TAL1 t(1;14)(p32;q11); LIM-only domain (LMO) genes, such as LYL1 t(7;19)(q34;p13) and *HOXA* homeobox (HOX) genes, such as TLX1 t(11;14)(p15;q11) and TLX3 t(11;14)(p15;q11) (68). The TAL1 is largest subgroup (7%) with other subgroups having lower frequency (69). TAL1 is an important regulator of HSC development (67). Another oncogenic transcription factor implicated in T-ALL is TLX3, which was found to be overexpressed in 20%-25%

in paediatric and 5% of adult T-ALLs (70),(71). TLX3 overexpression was associated with poor prognosis and high risk of relapse, while TLX1 overexpression was associated with good prognosis and low relapse risk (70),(71).

1.8 Treatment in ALL

Effective treatment strategies for ALL have been developed and the remission rate for paediatric ALL has reached 90% compared with 1960s when survival was just 10% (72). Despite the remarkable treatment success, prognosis remains poor for a subset of ALL patients (73). For example, patients with hypodiploidy and *MLL* rearrangements are associated with increased rates of treatment failure and relapse (73). However, evidence shows that around 50% of ALL patients with intermediate and low risk disease relapse (section 1.6.1) (74). These data demonstrate an unmet need to develop more effective therapies that reduce the risk of relapse. The chemotherapy doses can not be increased as it is associated with toxicity of normal cells. Therefore, developing more targeted therapies would be useful.

1.8.1 Treatment stages

The front line of chemotherapy for newly diagnosed patients with ALL consists of 5 phases, including induction, consolidation, interim maintenance, delayed intensification and maintenance (72). The induction therapy is the first phase of treatment and lasts for up 6 weeks to induce a complete remission (75). The second phase is consolidation which involves 2 blocks of chemotherapy at intervals with the aim to eliminate residual leukaemia cells and lasts for up to 9 months (75). The third phase is interim maintenance and aims to further destroy any residual leukaemia cells and lasts for 8 weeks (75). The fourth phase is delayed intensification which is important to improve a child's event-free survival and lasts for 8 weeks (72). The final phase is maintenance which aims to destroy any cancerous cells and prevent relapse and lasts for 84 days (72). Details of the current treatment in the UK and the drugs used are shown in Table 1.1, which is based on the UK-ALL 2011 trial protocol (76). In this trial, BCP-ALL patients are treated on either regimen A or B for 4 weeks, depending on age and WBC count. All T-ALL patients and high-risk cytogenetic cases

start on regimen B. During induction, patients are randomised and receive high dose (HD) dexamethasone for 14 days or a lower dose (LD) for 28 days (76) During interim maintenance and maintenance, patients are randomised again with vincristine and dexamethasone are given (76). Patient found to have near and low haploidy, iAMP21 or t(17:19) transfer onto regimen C at day 15, as do high risk cases with Down's syndrome.

Table 1.1 Chemotherapeutic drugs used to treat ALL patients in the UK.

Regimen A	
Induction	Vinc, Asp, Dex (HD 14d or 28d)
Consolidation	Merc
Interim maintenance	Merc, Meth (OR, IT), Vinc and Dex pulses
Delayed intensification	Vinc, Dox, Dex, Asp, Phos, Cyta, Merc
Maintenance	Merc, Meth (IT), Vinc and Dex pulses
Regimen B	
Induction	Vinc, Asp, Dex (HD 14d or 28d), Daun
Consolidation	Phos, Cyta, Merc
Interim maintenance	Merc, Meth (OR, IT), Vinc and Dex pulses
Delayed intensification	Vinc, Dox, Dex, Asp, Phos, Cyta, Merc
Maintenance	Merc, Meth (IT), Vinc and Dex pulses
Regimen C	
Augmented consolidation	Vinc, Phosph, Cyta, Merc, Asp
Augmented intensification	Vinc, Dox, Dex, Asp, Phos, Cyta, Merc
Maintenance	Merc, Meth (IT), Vinc and Dex pulses

Vinc = Vincristine; Asp = Pegasparginase; Cyta = Cytarabine; Daun = Daunorubicin; Dex = Dexamethasone; Merc = mercaptopurine; Meth = Methotrexate; Dox = doxorubicin; OR = Oral; IV = Intravenous; IT = Intrathecal; HD = High dose.

There is no consensus on the optimal drug doses/types but many factors are attributed to provide better treatment management (66). Chemotherapy intensity/type depends on the severity of the disease, age, leukocyte count and genetic abnormalities (77). For example, paediatric ALL patients over 10 years old, ALL with Philadelphia chromosome t(9;22), *MLL* rearrangements involving 11q23 and intrachromosomal

amplification of chromosome 21 (iAMP21) are high risk groups and require more intensive therapy (75). The Philadelphia chromosome t(9;22) is first found in CML and is characterised by the translocation of the q34 portion of chromosome 9 and the q11 locus of chromosome 22. The fusion gene produced (ABL1/BCR) links the tyrosine kinase ABL1 on chromosome 9 with the BCR gene on chromosome 22, resulting in a constitutively active kinase protein (75). Much attention must be paid to determine the best drugs to improve life quality of ALL patients.

It is widely believed that the initial response to therapy predicts outcome. Historically, initial assessment of treatment was evaluated morphologically. Currently, evaluating patients for measurable residual disease (MRD) is the standard method (57) and considered to be the best prognostic indicator of patient outcome. MRD analysis is used to determine the levels of residual leukaemia remaining after the induction therapy. Patients are stratified based on MRD status into low, intermediate and risk groups. At day 29, if ALL cell burden is below <0.005% the patient is classified as MRD low risk, while if there is evidence of MRD of ≥0.005%, patients are classified as MRD risk. At week 14, MRD risk patients are further classified into either MRD high risk (MRD ≥0.5%) or MRD intermediate risk (MRD <0.5%). MRD is determined using flow cytometry to detect abnormal WBS's known as leukaemia blasts based on surface markers and/or real time quantitative polymerase chain reaction (RT-qPCR) to detect immunoglobulin (Ig)/T-cell receptor (TCR) rearrangements (78). RT-qPCR can detect 1 ALL cell in 10^5 normal cells, while flow cytometry is less sensitive (1 ALL cell in 10^4) (79). Flow cytometry is a faster method for MRD analysis compared with RT-qPCR (80). The next generation sequencing (NGS)-based method is a newer addition to MRD analysis techniques with higher sensitivity capable of detecting 1 ALL cell in 10^6 normal cells (81),(82). However, its use is still limited due to cost.

1.9 Leukaemia initiating cells

The current chemotherapy used to treat ALL reduces the bulk of the leukaemia cells but these treatments may fail to eliminate leukaemia cells that can self-renew and differentiate, eventually leading to relapse (83). These cells are known as leukaemia initiating cells (LICs) and are found in various cancers, including T-ALL and BCP-ALL

as well as other solid cancers. LICs were initially proposed to be the population of cells expressing CD34 but lacking CD7 or CD4 in paediatric T-ALL (84). However, it was found that $CD34^+/CD4^-$ or $CD34^+/CD7^-$ cells from mature T-ALL cases did not possess LIC activity but have normal haemopoietic differentiation potential in non-obese diabetic–severe combined immune deficient (NOD/SCID) mice (85). Currently, NOD.Cg-*Prkdc*^{scid} *Il2rg*^{tm1Wjl}/SzJ NOD/LtSz-scid IL-2RY$_c$ null (NSG) mice are considered to be more permissive hosts than NOD/SCID mice for engrafting human BCP-ALL and T-ALL (86) and human haemopoietic cells (87), so they are used as a model to study the ability of human LICs to differentiate. Several T-ALL subpopulations, including $CD34^+/CD7^+$, $CD34^-/CD7^+$ and $CD34^-/CD7^-$ were able to engraft more successfully in NSG than NOD/SCID mice. However, $CD34^+/CD7^-$ engraftment in both mice was faster and required 2-100 fold fewer cells compared with other subpopulations such as $CD34^+/CD7^+$, $CD34^-/CD7^+$ and $CD34^-/CD7^-$ cells, suggesting that the $CD34^+/CD7^-$ cells were the most primitive subpopulation (86). In addition, the self-renewal ability of some T-ALL populations such as $CD34^+/CD7^+$, $CD34^-/CD7^+$ and $CD34^-/CD7^-$ subpopulations was more limited. In contrast, $CD34^+/CD7^-$ cells had stable levels of engraftment and were able to differentiate *in vivo* (86). CD99 was shown to be overexpressed and used as a diagnostic marker for MRD in T-ALL (88). Cells expressing $CD34^+/CD99^+$, $CD34^+/CD99^-$, $CD34^-/CD99^+$ and $CD34^-/CD99^-$ could propagate in NGS mice, suggesting that targeting CD99 alone is not an effective approach to eradicate the disease. However, $CD34^+/CD99^-$ cells were shown to have higher frequencies of LICs (89). These data suggest that using CD99 for MRD analyse may lead to false negative results, as not all LIC express it.

BCP-ALL LICs were described as the cells expressing $CD34^+/CD38^-$ in NOD/SCID mice in Philadelphia positive ALL (Ph-ALL) cases (90). Later, it was found that all different subpopulations of BCP-ALL cells, including $CD34^+/CD19^+$, $CD34^+/CD19^-$, $CD34^-/CD19^+$ and $CD34^-/CD19^-$ have LICs with different content (Discussed below). It was found that the majority of cells at sorting were $CD34^+/CD19^+$. It was also reported that most of the cells proliferating at week 6 were derived from the $CD34^+/CD19^-$ cells, suggesting that they are the most primitive subpopulation. In contrast, $CD34^-/CD19^+$ and $CD34^-/CD19^-$ cells had the lowest proliferative capabilities *in vitro* (91). LIC engraftment was compared in NOD/SCID and NSG mice. It was found that $CD34^+/CD19^+$, $CD34^+/CD19^-$ and $CD34^-$ cells have the ability to engraft in NSG mice.

The $CD34^+/CD19^-$ subpopulation showed the highest engraftment in both NOD/SCID and NSG with lower engraftment in NOD/SCID (86). $CD34^+/CD19^-$ cells have the ability to differentiate *in vivo* and induce the disease resembling that of the patient from which the sample was taken (86). Another study showed that $CD34^+/CD38^+/CD19^+$ and $CD34^+/CD38^-/CD19^+$ populations can initiate BCP-ALL in NOD/SCID mice (92). LICs have been shown to express CD133 and $CD133^+/CD19^-$ cells were capable of long-term culture *in vitro* and *in vivo* and can engraft serial NOD/SCID recipients (93).

Several papers have investigated the response of LICs to ALL treatment. It was reported that $CD133^+/CD19^-$ ALL cells were resistant to standard chemotherapeutic agents such as dexamethasone and vincristine (93). Parthenolide (PTL) is known to induce apoptosis and was analysed in our laboratory to evaluate its effect on ALL cells (94). It was found that PTL was effective against bulk ALL cells but was less effective towards $CD34^+/CD19^-$, $CD34^+/CD7^-$ and $CD34^-$ subpopulations, suggesting they are more drug resistant cells (94). HSP90 inhibitors (Celastrol and 17-DMAG) have been reported to be effective anti-cancer drugs used to treat ALL. Celastrol and 17-DMAG induce apoptosis in the bulk leukaemia in T-ALL and BCP-ALL cells. Using both drugs in combination were associated with significant reduction in viability in BCP-ALL and in LIC ($CD34^+/CD19^+$, $CD34^+/CD19^-$, $CD34^-/CD19^+$ and $CD34^-/CD19^-$) subpopulations (96).

1.10 Targeted therapy

Although chemotherapy has improved the patient response compared to 50 years ago, many complications remain, such as cardiac dysfunction, organ toxicity and the risk of secondary malignancies (73). In addition, relapse is another challenge which occurs in 20% of ALL patients and is associated with poor prognosis (69). Infection is the main cause for treatment related mortality, is reported to be between 2 and 4% (96). Thus, attention should be paid on identifying treatments with specific targets on ALL cells and thus causing less toxicities on normal cells. This led researchers to focus on specific targets that were dis-regulated and/or mutated in ALL rather than the non-specific targeting achieved by conventional chemotherapy (75). Many therapies were developed to selectively target cancer cells by targeting specific receptors/ proteins or

altered signalling pathways (73). Advances in understanding the genetic and biology of ALL has guided the research for drug development towards more specific molecular targets (97). Examples of targeted therapies are detailed below.

1.10.1 Tyrosine kinase inhibitors

ALL patients with Philadelphia chromosome (Ph+ ALL) are associated with poor prognosis and higher rates of relapse (73). Allogeneic haemopoietic stem cell transplantation (HSCT) following chemotherapy was the gold standard therapy for the maintenance of the complete remission to treat those patients. However, HSCT is associated with higher toxicities and graft-versus-host disease (GVHD) (98). Receptor tyrosine kinases (RTKs) are involved in a wide range of processes, including growth, differentiation and metabolism and dysregulation of RTKs is a common target, which is reported in human cancer. The fusion gene, BCR-ABL1 resulting from t(9;22)(q34;q11), in Ph+ leukaemia is a fusion of the tyrosine kinase ABL1 with the gene BCR (73). BCR-ABL1 is found in 3-5% in paediatric ALL (101). This translocation results in less control of cellular proliferation and it also has the potential to escape from apoptosis (73). Therefore, molecules that target RTKs have been considered as anti-cancer drugs used to treat Ph+ ALL patients (99). Imatinib was developed to target BCR-ABL1 and was the first-generation of tyrosine kinase inhibitors to treat Ph+ CML (100). Imatinib was reported to have excellent effect when combined with chemotherapy (100). In clinical trials, imatinib increased 3-year event-free survival rates to 80% compared with 30% with chemotherapy and this improvement was achieved with less toxicities (100). Although imatinib was promising, mutations in the kinase domain were developed and associated with resistance. Therefore, the second-generation tyrosine kinase inhibitors were developed (dasatinib) to overcome the kinase domain mutations, which was shown to have more potency than imatinib (73). Dasatinib was shown to eliminate BCR-ABL1 cells and induce apoptosis (102). However, the T315I mutation was shown to be resistant to dasatinib (73). Next, ponatinib was developed as the third-generation tyrosine kinase inhibitor and used for children with mutations in BCR-ABL1 (103) and T315I (104) in ALL Ph^+ patients.

1.10.2 Monoclonal antibody therapy

Another newer strategy in the treatment of ALL is the monoclonal antibody therapy and one approach of using this technology is targeting CD19. Targeting CD19 is an attractive approach as it is expressed at all stages in B lymphocytes. Blinatumomab is a promising monoclonal drug which has been used in the treatment of ALL. Blinatumomab is a bispecific T-cell engager (BiTE) antibody, which has the ability to bring the CD3+ T cells in contact with the CD19+ cells, resulting in the release of perforin and granzymes form cytotoxic T-cells and leading to target cell destruction (105),(73). Treatment with Blinatumomab resulted in the induction of remission and long-term survival rate for patients with relapsed BCP-ALL (106). However, not all BCP-ALL cells express $CD19^+$, so $CD19^-$ cells would not be targeted by this drug and have the potential to cause relapse.

Limited monoclonal options are avaliable for treatment of T-ALL comapred with BCP-ALL. The monclonal antibody alemtuzumab (anti-CD52) was studied in clinical trials, however, it ended due to toxicities (107). A New monoclonal antibody drug that needs further investiagtion is daratumumab (anti-CD38) as the majority of T-ALL cells express CD38 with low levels on normal lymphoid and meyloid cells (108). Daratumumab was shown to be effective against patient-derived xenografts (PDX) for T-ALL (109). However, not all T-ALL expresses $CD38^+$ cells. Evidence showed that $CD34^+/CD38^+/CD19^+$ and $CD34^+/CD38^-/CD19^+$ populations can initiate BCP-ALL in NOD/SCID mice (92).

1.10.3 Chimeric antigen receptor T cells

A novel method which uses engineered T lymphocytes to target leukaemia cells called chimeric antigen receptor (CAR) therapy is now an emerging and promising approach for ALL treatment. The CAR is introduced by viral transfection and composed of an extracellular target binding domain for a specific marker of the cancer cells (96). CAR-T technology has shown promise in various blood cancers (110),(111). One example of CAR-T technology is targeting the antigen CD19 for the treatment of BCP-ALL. CD19 CAR-T was successful in relapsed BCP-ALL in 70% of patients with MRD negative response (110). However, not all BCP-ALL cells express $CD19^+$ so $CD19^-$

cells will not be eliminated by CD19 CAR-T. It was also shown that BCP-ALL patients relapse after treatment with CD19 CAR-T with $CD19^-$ disease (105). $CD19^-$ cells were shown to have LIC activity which could account for the relapse.

There are fewer CAR-T therapies for T-ALL compared to BCP-ALL (107). It was shown that CAR-T cells can be used to target CD7 expressing cells (112). CD7 CAR-T cells were cytotoxic against T-cell lines and primary T-ALL cells (112). As normal T lymphocytes and NK cells express CD7 they are likely to be targeted by anti-CD7 CAR cells. However, not all T-ALL cells express CD7 antigen. $CD7^-$ cells were shown to have leukaemia initiating capacity. Recently, another group showed that CD1a-specific CAR was cytotoxic against refractory cortical T-ALL (co T-ALL) *in vitro* and *in vivo* with limited target to host cells (113). A general concern for CAR-T therapy is that engineered T cells induce high levels of cytokines (interleukin-6 and tumour necrosis factor), causing cytokine release syndrome, which can be fatal (96).

1.10.4 Heat shock protein 90 inhibitors

HSP90 is an ATP-dependent chaperone that comprises 1 to 2 % of the total protein in non-stressed conditions and exhibits twofold higher expression following stress (114). HSP90 is a homodimer and each monomer has an N-terminal domain, a flexible linker region, a middle domain and a C-terminal domain (114) (Figure 1.7). The N-terminal domain contains the adenosine triphosphate (ATP) binding site and is essential for co-chaperone and nucleotide binding. The middle domain is involved in binding both the client and co-chaperone proteins, while the C-terminal domain is essential to connect two monomers to form a dimer (114), which is important for protein client maturation.

HSP90 was proposed to be a promising target for cancer treatment for several reasons. Firstly, HSP90 has the ability to stabilise and activate a wide range of client proteins, including oncogenic tyrosine kinase (v-Src kinase), mutated oncogene (BCR/ABL, FLT3), tumour suppressor (p53 protein) and steroid receptors (115). These client proteins were shown to be important for the development, proliferation and survival of several cancers, such as breast cancer and leukaemias (116). Secondly, HSP90 is found at high levels in acute myeloid leukaemia (AML) and is correlated with poor prognosis (117). In addition, high levels of HSP90 were also shown in many solid

(including ovarian, breast, cervical, renal and oral cancers) and haematological cancers (such as myeloma and various leukaemias) suggesting a role in cancer growth and survival (114), due to disruption of the client proteins that associated with HSP90.

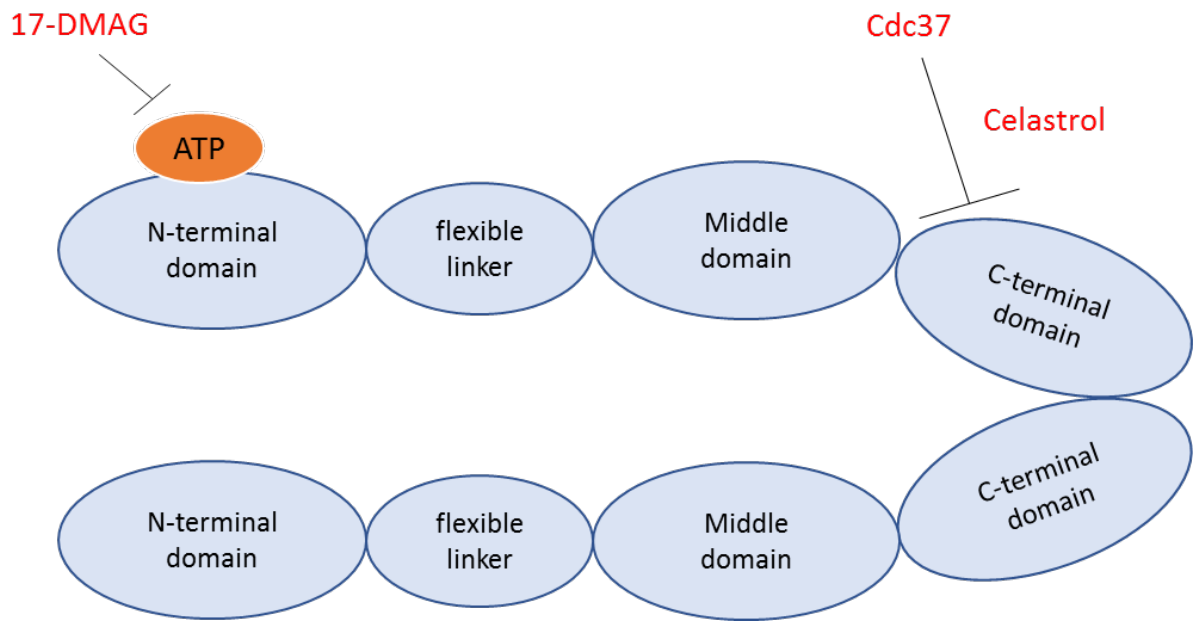

Figure 1.6 HSP90 dimer structure. Structural regions of HSP90 consist of N-terminal domain, a flexible linker region, a middle domain and a C-terminal domain. HSP90 inhibition sites by 17-DMAG and celastrol are shown.

As HSP90 is associated with and stabilises many client proteins (97), HSP90 inhibition leads to degradation of these proteins, therefore targeting HSP90 is a promising approach for anticancer therapy. There are many drugs that target specific pathways, including regulators of cell survival (BCL-2, ABT-263), oncogenic proteins such as BCR/ABL (Tyrosine kinase inhibitors) and cell-cycle regulating proteins such as the cyclins (Flavopiridol) (97). However, disruption of one target may not abrogate the cancer phenotype in most cancers. Thus, HSP90 with its many functions is proposed to be a good target for ALL treatment.

There are different mechanisms for HSP90 inhibition, including blocking the N-terminal domain ATP binding site, disturbing co-chaperone/HSP90 interaction and antagonism of client/HSP90 association (118). HSP90 inhibitors were first introduced in 1990s as a strategy for treating cancers and include geldanamycin and radiciol, both of which bind the ATP binding site leading to client protein degradation. However, their use in the clinic was limited due to poor solubility and significant toxicity (119). Two geldanamycin analogues, 17 allylamino-17 demethoxygeldanamycin (17-AAG; tanespimycin) and 17 dimethylaminoethylamino-17-demethoxygeldanamycin (17-DMAG; alvespimycin) were developed (119). 17-AAG was tested in more than 30 clinical trials but its effectiveness was limited with cytotoxicity and poor solubility. In contrast, 17-DMAG was shown to be less toxic and a water-soluble drug (120). 17-DMAG is in development in treatment for carcinomas and leukaemias (121),(122) and was proven to be cytotoxic to chronic myeloid leukaemia (CML) cells but not normal lymphocytes (123).

Inhibition of HSP90 has further expanded to various modulators of HSP90 machinery, such as the co-chaperones (124). HSP90 was reported to form complexes with co-chaperones, including cell division cycle 37 (Cdc37), HSP70 and activator of Hsp90 ATPase protein 1 (Aha1) (116). Cdc37 binds to the C-terminal ATP binding domain of HSP90 and is overexpressed in AML (125). These co-chaperones are involved in maintaining the client protein interactions and regulating HSP90 (125). Co-chaperones can also modulate the HSP90 ATPase rate and client protein recruitment (120). Therefore, inhibiting co-chaperones may be therapeutically beneficial, especially if combined with HSP90 inhibition.

The ability of celastrol to inhibit HSP90 was discovered more than 10 years ago when its mode of action is uncertain. Celastrol was initially shown to inhibit HSP90 by binding to the ATP binding site (126). Celastrol was also shown to reduce HSP90 ATPase activity in the human monocytic leukaemia cell line U937 (127). Conversely celastrol was reported to bind directly to the C-terminal region of HSP90, disrupting the interaction between HSP90 and the co-chaperone Cdc37 in 293T cells (124) and in pancreatic cancer cells (125) (Figure 1.6). The HSP90-cdc37 complex is important in regulating different kinases that are implicated in cancer progression, including epidermal growth factor receptor (EGFR) and BRAF kinases (119).

Since HSP90 inhibition leads to the release and subsequent misfolding of client proteins, HSP90 inhibitors were assessed for their ability to induce the cellular stress response. Celastrol was shown to induce HSF1 activation and hyperphosphorylation and subsequently HSP gene expression (128),(129). Furthermore celastrol was shown to upregulate HSP70 expression in Jurkat human leukaemia cell lines (130). Similarly, 17-DMAG treatment induces the activation of HSF1 and HSP70 induction *in vivo* (131).

1.10.4.1 The role of HSF1 in the stress response

Exposure of cells to high temperatures triggers a well-characterised protective response known as the heat shock response (HSR) or stress response (132). Heat shock proteins (HSPs) are produced following stress and are regulated by several heat-shock factors (HSF1– HSF4) with HSF1 being the master regulator of the stress response in humans (132). A variety of other stresses including osmotic shock, oxidative stress and heavy metals also trigger the stress response (4).

HSF1 is a monomer and bound to hsp90 in the cytoplasm under normal conditions Upon stress, it is released from hsp90 (usually due to competition with misfolded proteins), undergoes trimerisation (132) and is translocated to the nucleus where it binds to heat shock elements (HSEs) in HSP promoters (133) leading to HSP mRNA synthesis. HSF1 activation is regulated by many post-translational modifications, including phosphorylation, SUMOylation and acetylation (134). HSPs are highly expressed following stress and act as molecular chaperones to prevent protein misfolding and aggregation (132). There are several families of HSP proteins including HSP40, HSP60, HSP70 and HSP90 that have different cellular localisation and functions (97). Competition for Hsp90 binding in the cell is also known to result in the activation of HSF1 and the induction of a stress response. However, the stress response following HSP90 inhibitors (inducer of the stress response) has never been thoroughly explored in primary ALL cells.

Upon stress, in addition to HSP production, HSF1 also transcribes G-rich long non-coding satellite-III (SatIII) RNAs (135) mediating nSBs formation (136). nSBs were first identified in HeLa cells exposed to heat shock (137) and later HSF1 was found to be concentrated at these sites (138),(139). SatIII RNA is located on the pericentromeric heterochromatic q12 band of chromosomes 9, 12 and 15 (140). The binding of HSF1 to the SatIII locus mediates the recruitment of the histone acetyltransferase (HAT) CREB-binding protein (CBP) (139) and SatIII is transcribed by RNA polymerase II (141). SatIII RNAs act as scaffolds to recruit other proteins such as SAFB1, SRSF1 and 9G8 thus forming nSBs (4),(135),(139). nSBs are known to be transient storage sites for splicing factors and RNA binding proteins (142). Splicing factors and RNA binding protein sequestration is thought to be a significant strategy to restrain splicing machinery components from the damage induced from the stress (143). A schematic of nSBs formation following heat shock is illustrated in Figure 1.7.

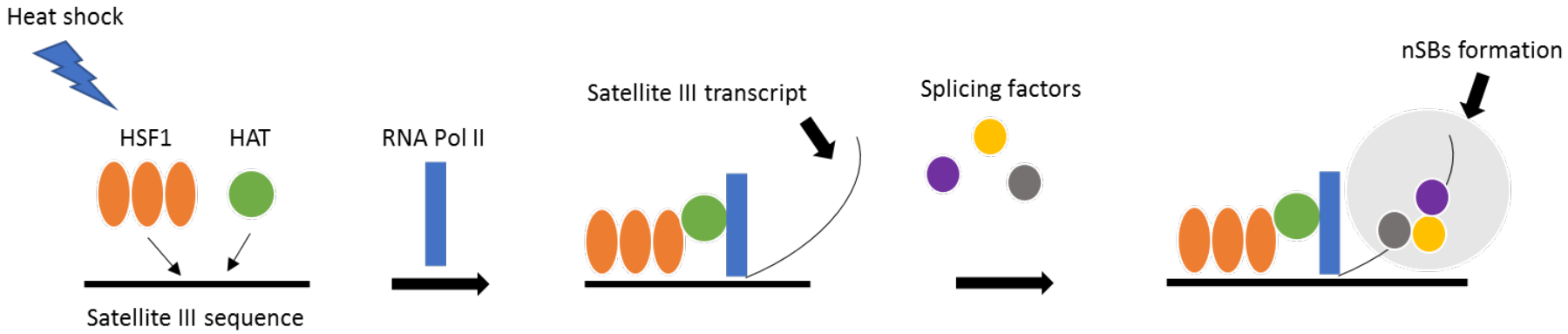

Figure 1.7 Heat shock induces nSB formation. HSF1 trimerises following heat shock and binds to satellite III sequences recruiting histone acetyltransferase (HAT) CREB-binding protein. RNA polymerase is also recruited to initiate transcription. Different splicing factors, including SAFB1 are recruited to satellite III transcripts leading to nSBs formation.

1.10.4.2 HSF1 in cancer

HSF1 activities extend far beyond the classical stress response and accumulating evidence has linked HSF1 with oncogenesis (144). HSF1 activation in cancer is caused by many factors, such as tumour microenvironment, aneuploidy and reactive oxygen species (134). HSF1 activation occurs to allow cancer cells to cope with the proteomic instability (147) and is associated with poor prognosis in prostate, lung, colon (145),(148) and melanoma cancers (149). HSF1 was found to be overexpressed in prostate cancer cell lines (150), human breast cancer cells (148), chronic lymphocytic leukaemia (CLL) (151) and found in the nucleus of CLL B cells but not in normal B cells (152). HSF1-knockout mice are less susceptible to tumorigenesis induced by oncogenic Ras or mutant p53 (153). HSF1-knockout mice showed impaired growth, invasion and metastasis of xenograft hepatocellular carcinoma (HCC) (154) and melanoma cells (155). HSF1 knockdown is associated with less proliferation and survival rates of cancer cells (156). These studies clearly emphasise the significant role of HSF1 in cancer progression and survival (156). CHIP seq analyses found that HSF1 binds more genes in highly malignant cells in comparison to less aggressive breast cancer cells, many of which (e.g. cyclin-dependent kinase interacting protein (CKS2), glycophosphatidyl-inositol-anchored membrane protein (LY6K) and probable RNA-binding protein 23 (RBM23)) were not classical heat shock genes (145), suggesting that HSF1 supports highly malignant cancers. HSF1 was shown to be regulated by polyploidy generation in prostate cancer cells, suggesting a role in genomic stability and tumour progression (146).

1.11 Project aims

Although SAFB1 has been implicated in carcinogenesis in several cancers, the biological functions and underlying mechanisms of SAFB1 and SAFB2 in the progression of paediatric ALL patients are largely unknown. Treatment with HSP90 inhibitors induces apoptosis in ALL cells (95) and several publications report that HSP90 inhibition induces a heat shock response (157,122,158). SAFB1 is reported to be sequestered into nSBs in HeLa cells following heat shock and co-localises with the transcription factor HSF1. However, SAFB1, SAFB2 and HSF1 localisation/expression was not explored in primary ALL cells following heat shock and treatment with HSP90i. SAFB1 and SAFB2 were shown to be methylated and SUMOylated and SAFB1 was reported to interact with several proteins. However, whether the methylation and SUMOylation status of SAFB1/2 influences their binding partners in primary ALL have never been investigated.

The overall aims of this thesis were therefore to:

(i) Characterise SAFB1 and SAFB2 expression in ALL

(ii) Compare the stress response in HeLa and ALL cells following heat shock and treatment with HSP90 inhibitors

(iii) Investigate SAFB1 and SAFB2 interactions in HeLa and ALL cells and explore the influence of its methylation and SUMOylation on the interaction with SRSF1

CHAPTER 2 :

Materials and Methods

2.1 Primary ALL and NBM samples

Bone marrow (BM) cells from children (median age, 11 years; range, 2 - 18) diagnosed with T-ALL (n=14) and BCP-ALL (n=18) at diagnosis or relapse were collected with approval of University Hospitals Bristol NHS Trust. Patient characteristics are shown in Table 2.1. Normal BM (NBM) cells from healthy donors were used as controls. Samples' selection was based on the availability of materials. Most patients were males and taken at diagnosis, however, some patients were taken at the time of relapse. MRD status of patients were classified as low, intermediate and risk groups. Patients karyotype were variable and associated with good or poor prognosis.

2.1.1 Mononuclear cell isolation

Mononuclear cells were isolated from ALL and normal bone marrow (NBM) by density centrifugation. Bone marrow samples were mixed with an equal volume with Iscove's Modified Dulbecco's Medium (IMDM, Invitrogen, Paisley, UK) and layered carefully on one volume of Histopaque®-1077 (Sigma-Aldrich, Poole, UK) and centrifuged at 1500g for 20 minutes. For example, 4ml of bone marrow sample is mixed with 4ml of IMDM and layered with 4ml of Histopaque®-1077. Blood components were separated with mononuclear cells and platelets being retained in a single layer above the ficoll layer. The mononuclear cells were collected, washed with 10ml of IMDM and centrifuged at 350g for 5 minutes to remove platelets. The supernatant was removed, the cell pellet was resuspended in 10ml of IMDM and centrifuged at 1000g for 5 minutes. The supernatant was removed and the cell pellet was resuspended in red cell lysis buffer (Miltenyi Biotec, Bisley, UK) for 10 minutes at room temperature. Cells were centrifuged at 500g for 5 minutes and the cell pellet was resuspended in 10ml of IMDM. The supernatant was removed and the isolated mononuclear cells were resuspended in 90% fetal bovine serum (FBS) and 10% dimethyl sulfoxide (DMSO). Samples were cryopreserved in liquid nitrogen (LN_2) until use. Upon use cells were thawed in a water bath at 37^{o}C then 10ml of FBS was added drop-wise to the cells. The cells were then washed with 10ml of FBS and IMDM at 1:1 ratio and viability checked by a MACSQuant 10 flow cytometer (Miltenyi Biotec) using Propidium Iodide (PI, Miltenyi Biotec). Cells were resuspended in RPMI 1650, penicillin (50U/ml), L-glutamine (2mM), streptomycin (50µg/ml) and 20% FBS (all Sigma-Aldrich) prior to treatment.

Table 2.1 Patient sample characteristics

ID	Classification	Karyotype	Age (y)	Sex	Disease status	MRD risk Status*
1	T-ALL	t(11;14)	2	M	Relapse	Low
2	T-ALL	46XY	14	M	Diagnosis	Risk
3	T-ALL	del 6q	3	F	Diagnosis	Risk
4	T-ALL	del 6q	2	M	Diagnosis	Risk
5	T-ALL	N/A	6	M	Diagnosis	Low
6	T-ALL	t(9;22)	10	M	Diagnosis	Risk
7	T-ALL	N/A	8	M	Diagnosis	Risk
8	T-ALL	+4, +9	15	M	Relapse	Risk
9	T-ALL	N/A	15	M	Diagnosis	Low
10	T-ALL	del 6q	14	M	Diagnosis	Risk
11	T-ALL	N/A	5	M	Diagnosis	N/A
12	T-ALL	N/A	12	M	Diagnosis	N/A
13	T-ALL	del 4q	15	M	Diagnosis	Low
14	T-ALL	46XY	8	M	Diagnosis	Low
15	Pre-pre B	High hyperdiploidy	8	M	Diagnosis	Risk
16	Pre B	-1 + Mar	2	F	Diagnosis	Low
17	Pre B	+4, +9	2	M	N/A	Low
18	Pre B	46XY	8	M	Diagnosis	Risk
19	Pre B	t(12;21)	2	M	Diagnosis	Low
20	BCP	N/A	10	F	Diagnosis	Low
21	Pre-pre B	del 6q	4	M	Diagnosis	Risk
22	Pre B	dic(9;20)	4	F	Diagnosis	Low
23	Pre B	t(12;21)	3	M	Diagnosis	Low
24	Pre B	iAMP21	11	M	Diagnosis	Intermediate
25	Pre B	46XY	16	M	Diagnosis	Risk
26	Pre B	-1 + Mar	10	F	Diagnosis	Low
27	Pre B	t(12;21)	17	M	Relapse	Low
28	Pre B	t(12;21)	5	M	Diagnosis	Low
29	Pre B	t(12;21)	18	M	Diagnosis	Low
30	BCP					
31	Pre B	46XY	3	F	Diagnosis	Low
32	Pre B	46XY	12	F	Diagnosis	Intermediate

* MRD (measurable residual disease) risk status at day 29 of treatment; N/A, not avaliable

2.2 Cell culture

2.2.1 Human cervical cancer cell line (HeLa cells)

HeLa cells were used in this thesis for practice and optimisation purposes. HeLa cells were maintained in Dulbecco's Modified Eagle Medium (DMEM) supplemented with penicillin (50U/ml), L-glutamine (2mM) and streptomycin (50µg/ml) and 10% FBS (all Sigma-Aldrich). Cells were grown in T75 flasks and maintained at 37^0C in 5% CO_2. Cells were passaged twice a week with complete media changes.

2.2.2 Mouse embryonic fibroblasts (MEFs)

MEFs were used as a highly proliferating cell model to assess the effect of SAFB1 overexpression. MEFs were maintained in DMEM supplemented with penicillin (50U/ml), L-glutamine (2mM) and streptomycin (50µg/ml), 10% FBS, 0.01% β - mercaptoethanol and 1% non-essential amino acids (NEAAs) (all Sigma-Aldrich). Cells were grown in T75 flasks and maintained at 37^{o}C in 5% CO_2. Cells were passaged once a week with a complete media change.

2.2.3 Primary T-ALL

Prior to Co-IP, primary T-ALL cells were plated at 5x10^{5} cells/ml in 30 well plates in serum free media, supplemented with IL-3 (50µg/ml), IL-7 (25µg/ml), stem cell factor (50µg/ml) (all Miltenyi Biotec) and bovine serum albumin (BSA), insulin, and transferrin (BIT) 9500 serum substitute (stemcell technologies, Cambridge, UK). Viability and cell count were checked regularly using the annexin V-PI flow cytometric assay. Cells were harvested after 10 days with half media change after 5 days in co-IP lysis buffer. Cell lysis and protein assays were performed as described previously (section 2.12) in co-IP lysis buffer (Table 2.10).

2.3 Plasmid preparation

2.3.1 Transformation

pEGFP.SAFB1, pEGFP.SAFB2 and pRRL.sin.cppt.CMV.EGFP.WPRE were transformed into 50µl of chemically competent E.coli cells such as Stbl3 or DH5α (Invitrogen, UK), incubated on ice for 30 minutes, heat shocked at 42^{0}C for 45 seconds and then placed immediately on ice for 2 minutes. A volume of 250µl of super optimal broth with catabolite repression (SOC, Invitrogen) media was added, incubated at 37^{o}C for one hour and plated overnight on luria broth (LB, Invitrogen) agars with appropriate antibiotic (50µg/ml kanamycin, Sigma-Aldrich) or (100µg/ml ampicillin, Sigma-Aldrich). Several colonies were picked and grown in 3ml LB with ampicillin and/or kanamycin antibiotics for at least 5 hours at 37^{o}C.

2.3.2 Plasmid purification

One to three millilitres of bacterial culture was purified on a miniprep scale to isolate plasmid DNA using QIAprep Spin Miniprep Kit (Qiagen, Manchester, UK) according to the manufacturer's instructions. Five hundred millilitres of bacterial culture were purified on a maxiprep scale using the density gradient centrifugation method. Five hundred millilitres of LB were incubated with 1ml of bacterial culture and incubated overnight in a shaking incubator at 37^{o}C. The bacterial culture was centrifuged at 1800g for 30 minutes at room temperature. The supernatant was removed and the cell pellet was resuspended in 18ml of solution 1. Two millilitres of lysozyme solution and 40ml of solution 2 was added, then the pot was inverted 6 times and left for 10 minutes at room temperature to lyse bacteria. Twenty millilitres of solution 3 were added, the pot was inverted 6 times and left for 10 minutes on ice to neutralise the lysate. All solutions used are detailed in Table 2.2. The lysate was centrifuged at 1800g for 20 minutes at 4^{o}C. The supernatant was filtered and 0.6 volume isopropanol was added, mixed once and left for 10 minutes at room temperature to precipitate plasmid DNA. The tubes were centrifuged at 4000g for 20 minutes at room temperature. The supernatant was removed and the pellets were left to dry. The pellets were dissolved in TE buffer (1M Tris pH8 and 500mM EDTA). An equal mass of caesium chloride (CsCl, Sigma-Aldrich) was dissolved in the DNA solution. Ethidium bromide was added and centrifuged at 4000g for 12 minutes at room temperature. The supernatant was transferred into a Beckman optiseal ultracentrifuge tube and topped up with TE/CsCl (1:1). The tube was placed in an NVTi65 rotor (Beckman Coulter) and centrifuged overnight at 475000g. The pink band (plasmid DNA) was collected carefully, mixed with butanol (Sigma-Aldrich) several times to remove ethidium bromide from the DNA. The DNA was transferred into a 50ml falcon tube, 10ml dH_2O and 45ml of ethanol was added. The tube was mixed, left in the fridge for 20 minutes to precipitate plasmid DNA and centrifuged at 4000g for 20 minutes at 4^{o}C. The supernatant was removed and the DNA pellet was washed with 70% ethanol. The tube was centrifuged at 4000g for 5 minutes at 4^{o}C. Ethanol was removed, the pellet was left to dry and resuspended in dH_2O. Plasmid DNA concentrations were measured using NanoDrop 2000/2000c Spectrophotometers (Thermo Fisher, Cambridge, UK).

Table 2.2 Maxi-prep solutions

Solution 1	**Final Concentration**
Glucose	5mM
Tris pH8	25mM
EDTA	10mM
Lysozyme solution	**Final Concentration**
Lysozyme	5mM
Tris pH8	10mM
Solution 2	**Final Concentration**
NaOH	200mM
SDS	1 %
Solution 3	**Final Concentration**
Potassium Acetate	3M
Glacial acetic acid	11.5 %

2.3.3 Restriction Endonuclease reactions

Appropriate restriction enzymes were chosen using Serial Cloner software to check the size of the plasmids. All restriction enzymes and buffers were purchased from (NEB, Hitchin, UK) or (Roche, Welwyn Garden, UK). All restriction enzyme reactions were carried out in a total volume of 20µl for 1-2 hours according to the manufacturer's instructions.

2.3.4 Agarose gel electrophoresis and sequencing

One percent agarose gels were prepared using agarose (Melford, Suffolk, UK) and 100ml of TAE (Tris / acetic acid / EDTA) buffer with 0.5µg of ethidium bromide (Sigma-Aldrich). Digested plasmid DNA samples were mixed with 0.17 volumes of 6 X loading buffer and run on the gel in TAE buffer at 100-110 V until sufficient separation of DNA fragments was achieved. One kilobase (1kb) DNA ladder (NEB) was used to estimate the DNA length. Gels were visualised and photographed using a UV transilluminator (Bioimaging systems). Plasmid DNA was sequenced by Source Bioscience (https://www.sourcebioscience.com/) using Sanger sequencing and appropriate primers.

2.3.5 Plasmid transfection

For plasmid transfection experiments, HeLa cells were plated in 24 well-plates, at $1x10^4$ cells/ml. Primary ALL and NBM cells were plated at $1x10^6$ cells/ml in 96 well plates prior to transduction. Cells were then transfected with appropriate plasmids using Lipofectamine 2000 (Invitrogen) and Optimem (Gibco) according to the manufacturer's instructions. A concentration of 500ng of plasmid DNA/ml was used throughout.

2.4 Adenoviral transduction

Primary ALL and NBM cells were plated at $1x10^6$ cells/ml in 96 well plates prior to transduction. Ad.CMV.EGFP.SAFB1 and Ad.CMV.EGFP.SAFB2 were used at a multiplicity of infection (MOI) of 50. As a control, Ad.CMV.EGFP was used. Cells were then left at 37^oC in 5% CO_2 and 5% O_2 for 24 and 48 hours prior to assessing viability.

2.5 Mutagenesis

SAFB1 mutagenesis was performed using QuikChange II XL Site-Directed Mutagenesis Kit (Agilent technologies, UK) according to the manufacturer's instructions. pEGFP.SAFB1 plasmid was used as a template to mutate the arginine methylation sites (aa557, aa754, aa811, aa868, aa874, aa884 and aa902). All primers were ordered from (Sigma-Aldrich, UK) according to protocol guidelines, as shown in Table 2.3. Arginine was replaced with Lysine sequence (shown in red) in the mutagenic primers.

Table 2.3 Mutagenic primers

Mutation	Sequence
Mutation 1: aa557 (RG)	**F: 5'** CACAAAGTCAGGAAGTAAGGGGACCGAACGGAC **R: 5'** GTCCGTTCGGTCCCCTTACTTCCTGACTTTGTG
Mutation 2: aa754 (RG)	**F: 5'** GACCACAGGGACAAGGGCCGCTACCCCG **R: 5'** CGGGGTAGCGGCCCTTGTCCCTGTGGTC
Mutation 3: aa811 (RG)	**F: 5'** GGATGAGCGAGGGCAAGGGGCTGCCTCCTCC R: 5' GGAGGAGGCAGCCCCTTGCCCTCGCTCATCC
Mutation 4: aa868 (RGG), Mutation 5: aa874 (RG)	**F: 5'** CCACATGATGAACAAGGGAGGAATGTCAGGGAAGGGCAGCTTTGC R 5' GCAAAGCTGCCCTTCCCTGACATTCCTCCCTTGTTCATCATGTGG
Mutation 6: aa884 (RG)	**F: 5'** GGCGGGGCCTCCAAGGGCCACCCCATCC R: 5' GGATGGGGTGGCCCTTGGAGGCCCCGCC
Mutation 7: aa902 (RG)	**F: 5'** GGAGGCCAGAGCAAGGGGAGCAGGCCC **R: 5' GGGCCTGCTCCCCTTGCTCTGGCCTCC**

The reaction mix for the first mutation (aa557) was prepared, containing 1x reaction buffer, 10ng plasmid template (pEGFP.SAFB1), 125ng forward and reverse primers, dNTPs mix, quick solution and Pfu HF polymerase (50µl total volume). The cycling parameters are shown in Table 2.4.

Table 2.4 Cycling parameters

Segment	Cycles	Temperature	Time
1	1	95°C	1
2	18	95°C 60°C 68°C	50 seconds 50 seconds 1 minute/kb of plasmid length
3	1	68°C	7 minutes

Following cycling, the reaction tubes were immediately placed on ice for 2 minutes. One microlitre of the *Dpn* I restriction enzyme was added. After mixing, the reactions were incubated at 37°C for 1 hour to digest non-mutated plasmid. Two microlitre of β-ME mix were mixed with 45µl of XL10-Gold ultracompetent cells. The mix was

incubated on ice for 10 minutes with gentle swirling every 2 minutes. Two microlitre of the Dpn I-treated plasmid was added to ultracompetent cells and incubated on ice for 30 minutes. The tubes were heat shocked at 42^{o}C for 30 seconds and then incubated on ice for 2 minutes. A volume of 0.5ml of preheated (42°C) NZ amine (casein hydrolysate) and yeast (NZY+) broth was added to each tube and incubated at 37^{o}C for an hour. A total of 250µl of the transformation reaction was plated on LB agar plates containing 80µg/ml X-gal and 20 mM Isopropyl-1-thio-β-D-galactopyranoside (IPTG) and kanamycin antibiotic. The plates were incubated at 37^{o}C for >16 hours. Plasmid purification, agarose gel electrophoresis and sequencing were performed as described previously (section 2.3). The mutated plasmid was used as a template to perform the next mutation. The final plasmid with all sites (aa557, aa754, aa811, aa868, aa874, aa884 and aa902) mutated was used for the subsequent experiments.

2.6 Heat shock (HS)

HeLa cells were seeded at 1x10^{3} cells/ml in 200µl DMEM in 96 well plates and maintained for 48h prior to heat shock. In some instances, HeLa cells were transfected with 500ng plasmid DNA/ml. Primary ALL and NBM cells were grown at 1x10^{6} cells/well in 200µl DMEM in 96 well plates. Cells were then transferred to a heat block at 42^{o}C within the incubator for 80 minutes with either no recovery period or a 1 hour recovery at 37^{o}C with 5% CO_2. In addition, some cells were not heat shocked as controls.

2.7 Heat shock protein 90 inhibitors

Celastrol and 17-DMAG (Stratech Scientific Ltd,Cambridge, UK) were dissolved in DMSO at a 1mM stock concentration. The required concentrations were achieved by diluting in DMEM supplemented with 10% FBS and L-glutamine (2mM) to obtain final concentrations of 10µM, 5µM, 1µM, 0.1µM, 0.01µM, 0.001µM, 0.0001µM and 0.00001µM. Cells treated with DMSO were used as controls and DMSO concentration was kept constant. To measure cell death following HSP90i treatment, HeLa cells were seeded at 4x10^{4} cells/ml in 500µl DMEM in 24 well plates, while primary ALL and NBM cells were seeded at 8x10^{4} cells/ml in 250µl DMEM in 96 well plates. Cells were

treated with different concentrations of both 17-DMAG and/or celastrol and left for 24 and 48 hours. Cells were then fixed and immunostained for SAFB1, SAFB2, HSF1, SRSF1 and HSP70 (Section 2.8). Also, Hela cell lysates were subjected to Western blotting analyses to measure HSP70 expression. At 48 hours post treatment, HeLa cells were also incubated with MTT 3-(4,5-Dimethylthiazol-2-yl)-2,5-diphenyltetrazolium bromide (MTT, Sigma-Aldrich) product (section 2.11). However, primary ALL and NBM cells were evaluated for viability using Annexin-V/PI flow cytometric assay (section 2.9).

2.8 Immunofluorescence

Wells were coated with an appropriate volume of 0.1% poly-l-lysine (Sigma-Aldrich-P8920) for 5 minutes and subsequently washed carefully with phosphate buffer saline (PBS). Wells were left to dry for 5 minutes and then primary ALL and NBM cells were seeded and incubated for 1 hour at 37^0C in the incubator prior to treatment. Media was removed and cells were washed once with PBS before fixation with 4% paraformaldehyde (PFA) for 10-15 minutes. Cells were blocked and permeabilised with 0.3% Triton X-100 with 0.05% donkey serum in PBS for 1 hour with gentle rocking. Cells were incubated overnight at 4^0C with primary antibodies (Table 2.5). After 3x10 minute washes with PBS with gentle rocking, cells were incubated with the appropriate secondary antibodies for 1 hour at room temperature (Table 2.6). After 3 x 10 minute washes with PBS, cells were stained with Hoechst (1µg/mL) for 15 minutes with gentle rocking and cells were washed twice with PBS. Images were taken using a confocal laser microscope (Perkin Elmer Opera LX system) at 63x magnification. Fluorescence intensities and the number of nuclear stress bodies were detected using ImageJ software. For HSF1 nuclear border expression, nuclear outlines were first determined using blue and red fluorescence channels using ImageJ. Each nucleus object was then split into two objects: an edge object, comprising a 5-pixel wide region at the edge of the nucleus, and the remaining central region. Red channel intensity was measured for each of these two objects and the ratio of edge intensity to centre intensity calculated.

Table 2.5 Primary antibodies

Antibody	Dilution	Company	Catalogue
SAFB1 (rabbit)	1 in 200	Bethyl	A300-811A
SAFB2 (rabbit)	1 in 200	Bethyl	A301-112A
HSF1 (rat)	1 in 200	ENZO Life sciences	ADI-SPA-950
SRSF1 (mouse)	1 in 200	Thermo Fisher Scientific	32-6400
HSP70 (mouse)	1 in 200	ENZO Life sciences	ADI-SPA-810-D

Table 2.6 Secondary antibodies

Antibody	Dilution	Company	Catalogue
donkey anti rabbit IgG Cyanine 3	1 in 200	Jackson Laboratories	711-165-152
donkey anti rat IgG Cyanine 3	1 in 200	Jackson Laboratories	712-165-150
donkey anti rabbit IgG Cyanine 2	1 in 200	Jackson Laboratories	711-225-152
donkey anti mouse IgG Alexa Fluor 488	1 in 200	Thermo Fisher Scientific	R37114

2.9 Annexin V/PI apoptosis assay

After plasmid transfection and adenoviral transduction, primary ALL and NBM cells were washed and stained with Annexin V-FITC at 1:20 (Miltenyi Biotec) for 10 minutes in the dark. Cells were resuspended in Annexin V buffer (100µl) and PI (1µl) was added. Viability and apoptosis were measured using a MACSQuant 10 flow cytometer (Miltenyi Biotec). As an example, lymphocytes were gated according to side scatter (SSC) and forward scatter (FSC) based on the size and granularity of cells, respectively (Figure 2.1A). The gating strategy was set up based on unstained cells (Figure 2.1B). Cells are considered to be viable when PI and Annexin-V are negative. Cells in late apoptosis are positive for PI and Annexin-V. Early apoptotic cells are PI negative and Annexin-V positive. Dead cells are positive for both PI only (Figure 2.1C). Data was analysed using FlowJo software version 7.10.

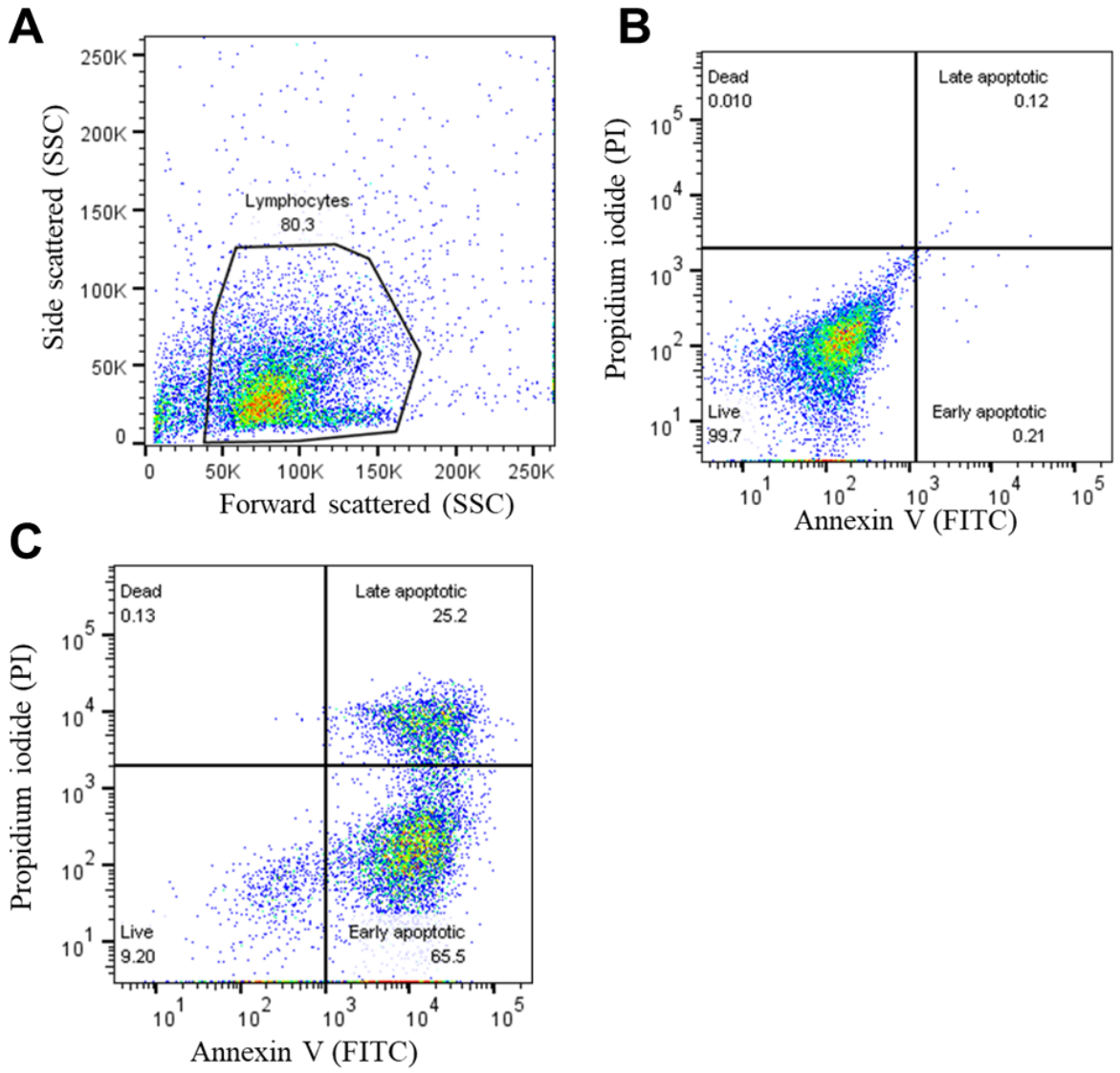

Figure 2.1 Gating strategy for flow cytometric analyses using Annexin-V/PI. (A) Lymphocytes were gated according to SSC and FSC based on the size and granularity of cells (B) Gating was set up based on un-stained cells. (C) Dead, apoptotic and live cells can be discriminated based on PI and annexin-V and cells are alive when PI and Annexin-V (FITC) are negative. Numbers on the dot plots indicate percentages of lymphocytes.

2.10 Drug effect calculations

The Annexin-V/PI flow cytometry method or MTT assay were used to measure the effect of drugs on viability. As an example, 17-DMAG was used at increasing concentrations to generate a dose response curve and find a dose that kill half of cells treated, known as the half maximal inhibitory concentration (IC_{50}). Following that, a second best fit curve was generated and the IC_{50} value was measured based on the best fit curve equation using GraphPad Prism software (version 6.04, Figure 2.2).

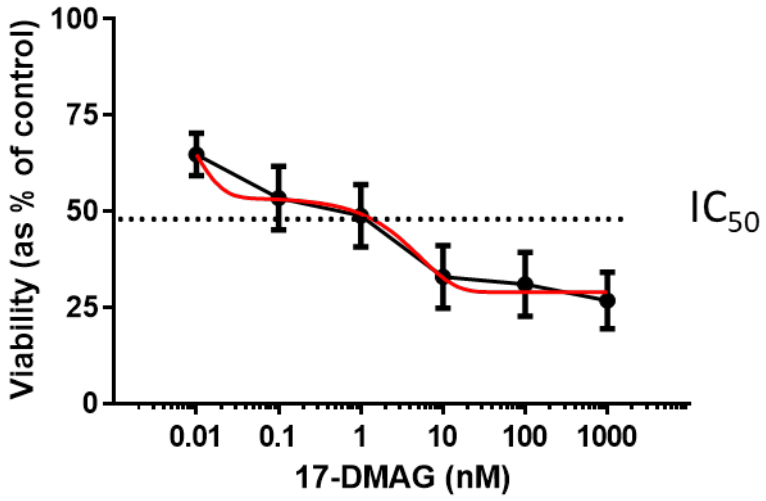

Figure 2.2 17-DMAG dose response curve.
Viability of BCP-ALL at 24 hours post 17-DMAG treatment (0.01-1000nM) was calculated using annexinV/PI assay. A second order best fit curve (red) shows the IC_{50} based on the viability.

2.11 MTT Assays

Viability of HeLa and MEF cells was assessed using the MTT assay, which estimates metabolic activity of cells by measuring the mitochondrial-dependent conversion of MTT to a coloured formazan product. MTT (0.5mg/ml) was added directly to each well and incubated in 5% CO_2 at 37°C for 3h. The medium was then aspirated and 200µl acidified isopropanol was added to solubilise the coloured formazan product that is deposited in viable cells. Absorbance was read at 550nm on a scanning multiwell

spectrophotometer (Bio-Rad, London, UK), after agitating the plates on a shaker for 5 minutes.

2.12 Quantitative Polymerase Chain Reaction (qPCR)

2.12.1 RNA extraction

RNA was isolated from primary BCP-ALL, T-ALL and NBM cells using ReliaPrep RNA cell miniprep system (Promega, Southampton, UK) according to the manufacturer's instructions. Briefly, cells were washed with cold PBS and lysed in BL buffer supplemented with 1-thioglycerol. A 20-gauge needle was used to further lyse the cells and shear genomic DNA. Isopropanol was added to precipitate the RNA before transferring the lysate to the ReliaPrep mini column. After centrifugation, DNase was added and incubated for 15 minutes at room temperature to digest DNA. After several washes, RNA was eluted in 30μl of dH_2O. RNA concentration and purity was assessed using Nano drop (Thermo Fisher) and stored at -80^0C.

2.12.2 cDNA synthesis

RNA was reverse transcribed using GoScript Reverse Transcription system (Promega) according to the manufacturer's instructions. Briefly, Random primers (0.5 μg) were mixed with 80ng/μl of RNA and incubated at 70^0C for 5 minutes (denaturation step), then placed on ice. The reverse transcription reaction mix was prepared, containing RT buffer (1x), $MgCl_2$ (2mM), PCR nucleotides mix (0.5mM), recombinant RNasin ribonuclease inhibitor (20 unit) and GoScript reverse transcriptase. The RNA/primer sample and reverse transcription reaction mix were combined and incubated at 25^0C for 5 minutes (annealing step). Next, the tubes were incubated at 42^0C for 60 minutes (cDNA synthesis step), followed by incubation at 70^0C for 15 minutes to inactivate reverse transcriptase. The cDNA was diluted in nuclease free water prior to qPCR.

2.12.3 Real-time qPCR for SAFB1 and SAFB2 expression

cDNA samples were mixed with SYBR green master mix (Applied Biosystems, Warrington, UK) and 300nM of forward and reverse primers (Table 2.7) from (Sigma-Aldrich) in 96 well plates. The SYBR green dye binds to double strand DNA and this results in fluorescence, indicating cDNA amplification is taking place. Each amplification is measured as a cycle threshold (CT). GAPDH and Beta actin were used as endogenous controls to normalise CT values. Samples were run by Step-One Plus Real-Time PCR Systems (Applied Biosystems).

Table 2.7 Primer sequences

Gene	Sequence
SAFB1	F'-GAGGGACCGAACGGACTGTAG R'-TGGCTGATTTGCGATCCTG
SAFB2	F'-GAGCGGACGGTCGTGATG R'-ACTTGCGATCCTGACTCTTGG
GAPDH	F'-TGCACCACCAACTGCTTAGC R'-GGCATGGACTGTGGTCATGAG
Beta actin	F'-CCCCTGAACCCCAAGGC R'- CAGAGGCGTACAGGGATAGCAC

2.12.4 Analysis

SAFB1 and SAFB2 relative expression was calculated using the ΔΔCT method. Briefly, CT values were normalised against the mean of the endogenous controls, GAPDH and Beta actin and then to the calibrator sample (NBM). Then the normalised values (ΔΔCT) were converted to the linear scale ($2^{-\Delta C\Delta CT}$) to give fold change comparison between samples.

2.13 Western blotting

2.13.1 Cell lysis and protein assays

Cells were washed twice with cold PBS and were then scraped in radioimmunoprecipitation assay (RIPA) buffer (50mM Tris-HCL pH8, 150mM NaCl, 1% Triton X 100, 1% sodium deoxy cholate and 0.1% SDS, all from Sigma-Aldrich)

with phosphatase inhibitor phosSTOP and protease inhibitor complete mini (Roche). Lysates were transferred to a pre-cooled Eppendorf tube and centrifuged at 20000g for 30 min at 4^0C to remove cell debris. The supernatant was frozen at - 80^0C until use. The protein concentration was measured using the bicinchoninic acid assay (BCA assay, Thermo Fisher, USA). The BCA working solution was made according to the suggested ratio by the supplier. A volume of 2μl of protein samples and known protein standards were loaded into 96 well plates. After that, 98μl of BCA working solution was added and incubated at 37^0C for 60 minutes. The colorimetric change was measured at 567nm absorbance using a plate reader (Glomax, Promega).

2.13.2 Sodium dodecyl sulfate poly acrylamide (SDS) gel electrophoresis

Eight percent acrylamide gels (0.1% SDS, 8% acrylamide gel, 150mM Tris pH8.8, 0.1% APS, TEMED) were cast in Mini Protean II apparatus (Bio-Rad). Once polymerised a stacking gel (0.025% SDS, 8% acrylamide gel, 250mM Tris pH6.8, 0.025% APS, TEMED) was added on and a comb used to form sample wells. A volume of 2 X sample loading buffer (100mM Tris base, 25% glycerol, 2% SDS, 0.01% bromophenol and 10% mecaptoethanol, Dithiothreitol, 0.5M) (all Sigma-Aldrich) was added to protein samples (usually 20μg). Samples were heated at 100^0C for 5 minutes to denature proteins prior to loading. Samples along with a broad range protein standard (NEB) were loaded to the gel and electrophoresed at 100V.

2.13.3 Transfer, staining and detection of proteins

The gel transfer was performed using Trans-Blot Turbo system (Bio-Rad) according to the manufacturer's instructions. Briefly, the gel was placed on top of the membrane and stacks in the cassette. Additional stacks were arranged on the top. The cassette was closed and transfer performed for 10 minutes using the high molecular weight protocol suggested by the manufacturer. The membrane was blocked in 5 % milk (dried skimmed milk, Marvel) and PBS 0.1 % tween for an hour with rocking. The film was incubated overnight at 4^0C with the primary antibodies and diluted in PBS 0.1 % tween and 1 % milk (Table 2.8). SAFB1 and SAFB2 antibodies were previously validated (Rivers *et al.*, 2015). After 3 x 10 minute washes with PBS 0.1 % tween, the membrane was incubated at room temperature for 1 hour with the appropriate

secondary antibodies and diluted in PBS 0.1 % tween and 1 % milk (Table 2.9). After 3 x 10 minute washes with PBS 0.1 % tween, the membrane was then incubated for 5 minutes with enhanced chemiluminescence (ECL) reagent (Pierce) and the membrane was exposed to an autoradiographic film (Amersham, GE Healthcare, Freiburg, Germany). The relative protein expression was calculated by densitometry using ImageJ and normalised to Alpha tubulin to control for loading.

Table 2.8 Primary antibodies

Antibody	Dilution	Company	Catalogue
SAFB1 (rabbit)	1 in 1000	Bethyl	A300-811A
SAFB2 (rabbit)	1 in 1000	Bethyl	A301-112A
SRSF1 (mouse)	1 in 1000	Thermo Fisher Scientific	32-6400
SRSF1 (rabbit)	1 in 1000	Abcam	Ab38017
HSP70 (mouse)	1 in 1000	ENZO Life sciences	ADI-SPA-810-D
Alpha tubulin (mouse)	1 in 2000	Sigma	T5168

Table 2.9 Secondary antibodies

Antibody	Dilution	Company	Catalogue
anti mouse IgG HRB-linked whole Ab	1 in 10000	GE healthcare	NA391
anti rabbit IgG HRB-linked whole Ab	1 in 10000	GE healthcare	NA394

2.14 Co-Immunoprecipitation (co-IP)

For co-IP of endogenous proteins HeLa cells were seeded in 10cm dishes at $1x10^5$ cells/ml and incubated for 48h. For co-IP of EGFP tagged proteins HeLa cells were seeded in 10cm dishes at $5x10^4$ cells/ml, the next day cells were transfected with SAFB1-EGFP or SAFB2-EGFP plasmid (15μg/dish). Cells were incubated for 48h before lysis.

2.14.1 Cross-linking of antibodies for co-IP

Three micrograms of antibody (rabbit SAFB1 (A300-811A, Bethyl), rabbit SAFB2 (A301-112A, Bethyl), rabbit IgG (2729, cell signalling, USA) mouse EGFP (Memorial Sloan-Kettering, USA) and mouse IgG (14-4714-82, Invitrogen) were incubated with 20μL Pierce Protein G magnetic beads (Thermo Fisher) and PBS 0.02% tween (PBST), taking the final volume to 1ml and rotated at 4˚C overnight. Following incubation, beads were applied to a magnet and supernatant was removed. Beads were washed with PBST 3 x 10 seconds with tubes inverted a few times. Beads were washed again 3 x for 10 seconds in coupling buffer (0.2M triethanolamine (Sigma-Aldrich) in PBS with 0.01% Tween-20) at pH9. Next, beads were crosslinked in 20mM Dimethyl pimelimidate dihydrochloride (DMP, Sigma-Aldrich) in coupling buffer for 1 hour at room temperature. The crosslinked antibodies were quenched in 50mM ethanolamine (Sigma-Aldrich) in PBST for 30min at room temperature. After quenching, beads were washed in elution buffer (0.2M glycine (Sigma-Aldrich) pH2.5 with PBST with vortexing to remove uncrosslinked antibody. The crosslinked beads were resuspended in PBST and stored at 4^0C until use.

2.14.2 SAFB1 and SAFB2 co-IP

Three micrograms of crosslinked IgG were washed 3 x in PBST. Beads were rotated with the protein lysates of interest for 6 hours in the cold room at 4^0C to remove background interacting events. After incubation, beads were applied to a magnet and the supernatant collected (pre-cleared lysate). A total of 500μg pre-cleared lysate was incubated with 3μg of cross-linked antibody overnight at 4^0C. The next day, beads were applied to a magnet and the supernatant was removed and kept (immunodepleted lysate). The beads were washed 6 x with 500μL co-IP lysis buffer with gentle mixing. Beads were always kept on ice between washes. After the final wash, 2/3 of the volume of beads was stored at -80^0C for proteomic analyses. The remainder was resuspended in 2 X SDS gel buffer and Dithiothreitol (DTT, 0.5M), boiled at 100^0C for 5 minutes and analysed via western blot (Section 2.12).

Table 2.10 Co-IP lysis buffer

	Final Concentration
Tris (pH 7.5)	20 mM
NaCl	150 mM
EDTA (disodium salt dehydrate, Sigma E5134)	1 mM
EGTA (Sigma E3889)	1 mM
IGEPAL CA-630	1 %
Sodium pyrophosphate (tetrabasic decahydrate, Sigma S6422)	2.5 mM
Sodium orthovanadate (Sigma S6508)	1 mM
B-glycerophosphate (disodium salt hydrate, Sigma G9422)	1 mM
Protease Inhibitors (added fresh)	1X

2.15 Mass spectrometry (MS)

2.15.1 Tandem Mass Tag (TMT) labelling

SAFB1, SAFB2 and IgG co-IP samples were prepared and analysed by MS by the Proteomics Facility, University of Bristol. Immunoprecipitated samples were digested on the beads with trypsin and labelled with TMT ten-plex reagents according to the manufacturer's instructions (Thermo Fisher Scientific), then pooled. Samples were then fractionated by high pH reversed-phase chromatography using an Ultimate 3000 liquid chromatography system (Thermo Fisher Scientific). Samples were analysed by Nano-LC Mass Spectrometry.

2.15.2 Data analyses

The raw data files were quantified using Proteome Discoverer software v1.4 (Thermo Fisher Scientific) and searched against the UniProt Human database. The abundance of proteins was filtered using 5% false discovery rate (FDR). Data were log2

transformed so they are normally distributed. The fold change for SAFB1 and SAFB2 against the corresponding IgG for each biological replicate was calculated and the fold change average was also calculated. Paired T test were performed. Proteins with <2 unique peptides were removed. Only proteins with statistical significance ($P<0.05$) compared to the corresponding IgG were considered for further analyses.

2.16 SAFB genes expression by Microarray analysis

Microarray analyses were previously performed on different primary human cell samples, using Agilent Whole Human Genome Oligo Microarrays (Miltenyi Biotec, Germany). RNA samples were taken from HSCs and peripheral blood cells from healthy individual, patients with BCP-ALL and T-ALL. For BCP-ALL, the bulk leukaemia population was obtained as well as lymphocytes that were sorted for the presence or absence of surface cell markers CD34 and CD19. Similarly for T-ALL, the bulk leukaemia population was obtained as well as lymphocytes that were sorted for the presence or absence of surface cell markers CD34 and CD7. For our purposes, SAFB genes expression were plotted as mean with standard deviation (SD) and as SAFB1/2 ratio.

2.17 Statistical analysis

The data were analysed using GraphPad Prism software version 6.04 (La Jolla, CA, USA). Differences in SAFB gene expression, viability following treatment with HSP90i (17-DMAG and celastrol), plasmid transfection, adenoviral transduction and changes in protein expression following heat shock and HSP90i in HeLa cells were analysed using one-way analysis of variance (one-way ANOVA), with Tukey post hoc analysis of means. Dose response curves following HSP90i and changes in protein expression following heat shock and HSP90i in primary ALL and NBM cells were analysed using two-way analysis of variance (two-way ANOVA) with Bonferroni post hoc analysis of means. GraphPad Prism 6.04 was used to determine the IC_{50} following HSP90i treatment. When a p value of < 0.05 was found, the data were deemed to be statistically significant.

CHAPTER 3 :

Characterising SAFB1 and SAFB2 expression and function in primary T-ALL and BCP-ALL

3.1 Introduction

There remains a need to identify novel molecular pathways, markers and genetic alterations in ALL to assist in the development of new more effective treatments (56). SAFB1 interacts with S/MARs, which serve as anchors to attach chromatin to the nuclear matrix (1), and the chromatin loop domains formed at these attachment regions are thought to be sites controlling transcription and replication (2). The SAFB1 interaction with S/MARs is mediated via its SAP domain, and thereby mediates association with the nuclear matrix and promotes or represses transcription. Evidence also suggests that SAFB1 may direct the reorganization and segregation of nuclear RNA and DNA prior to endonuclease-mediated DNA cleavage during apoptosis (24). SAFB1 has been shown to interact with a number of alternative RNA splicing regulators (159) and to have a high affinity for RNA polymerase II suggesting it may be a component of the spliceosome (2),(160),(161). A variety of cellular stresses leads to the formation of nSBs which are accumulation sites for RNA-binding proteins involved in pre-mRNA splicing. SAFB1 co-localises with nSBs, which was suggested to play a role in transcriptional control and alternative splicing in cells following stress (4). There have also been a number of papers suggesting that altered SAFB protein expression is linked to oncogenesis (7,11, 8,39). High levels of SAFB1 were reported to arrest cells in the G_2-M phase suggesting a role in the control of cell division (23). An observation supported by studies that show the disruption of SAFB1 expression led to cell immortalisation (32). SAFB1 mutations were identified in breast tumours but not in the normal adjacent tissue. The consequences of SAFB1 mutations were not well established and further experiments are needed. A high loss of heterozygosity (78%) was also detected at the SAFB chromosomal locus in invasive breast cancer (33). Decreased SAFB expression is associated with colorectal cancer (35), prostate cancer (16) and a worse overall survival of breast cancer patients (34). Together these findings suggest that low levels of SAFB1 may alter gene expression (particularly those associated with the control of the cell cycle and apoptosis) and chromatin state, thereby promoting tumorigenicity.

The aims of this chapter were to investigate:

(i) The hypothesis that SAFB1 expression is decreased in BCP-ALL and T-ALL

(ii) Whether increasing SAFB1 expression in ALL cells has a compensatory pro-apoptotic effect?

(iii) The effect of SAFB1 overexpression on dividing and non-dividing normal cells.

3.2 Results

3.2.1 Investigating the expression of SAFB1 and SAFB2 in primary T-ALL and BCP-ALL

Prior to investigating the effect of overexpressing SAFB1 in primary T-ALL and BCP-ALL cells, endogenous mRNA levels of SAFB1 and SAFB2 in leukaemia cells were measured. We initially interrogated microarray data (www.ebi.ac.uk/arrayexpress, accession number E-MTAB-4006) obtained from the BM from 5 BCP-ALL, 5 T-ALL patients and 5 healthy individuals to investigate SAFB1 expression levels in primary cancer cells (89). We found that SAFB1 expression levels were significantly lower in T-ALL patients (3.70±1.77, $P<0.05$) but not BCP-ALL patients (6.28±1.24) when compared to NBM controls (5.47±0.70, Figure 3.1A). SAFB1 and SAFB2 expression is controlled by a bidirectional promoter and knocking down SAFB1 expression results in the up-regulation of SAFB2 levels (39) (results not shown) and we would therefore predict an inverse relationship between SAFB1 and SAFB2 expression. Interestingly, when our array data was interrogated it was found SAFB2 mRNA levels were significantly increased in BCP-ALL (8.10±1.744, $P<0.05$) and T-ALL cells (7.63±2.15, $P<0.01$) when compared to NBM (4.88±2.26, Figure 3.1B) and the SAFB1/SAFB2 ratio was significantly reduced in both BCP-ALL (0.77±0.10, $P<0.05$) and T-ALL cells (0.50±0.27, $P<0.01$, Figure 3.1C). Together, these results suggest that SAFB2 levels may be elevated in T-ALL cells to compensate for a decrease in SAFB1 expression/function.

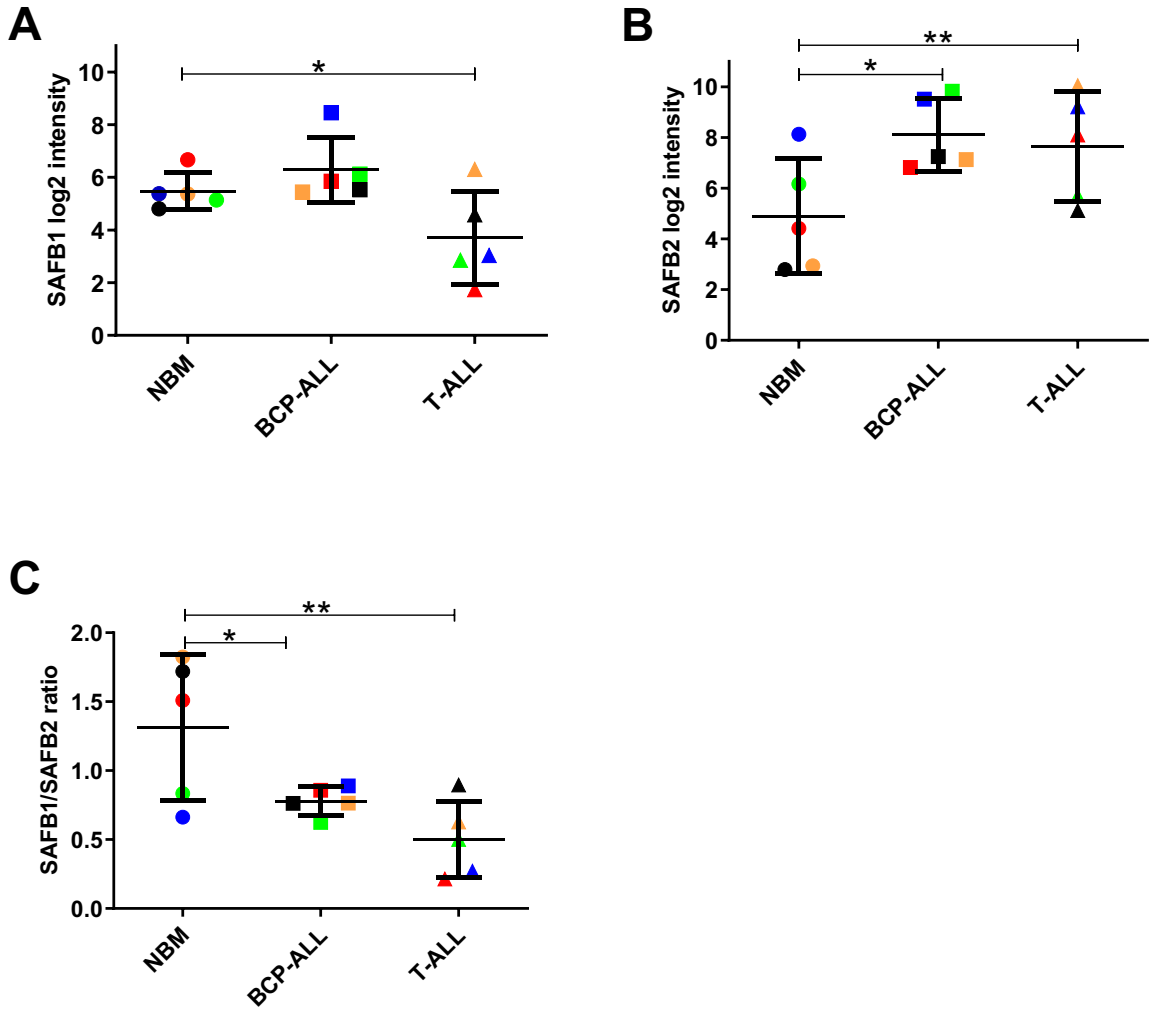

Figure 3.1 Comparison of SAFB mRNA expression in normal and leukaemia cells.
(A) SAFB1 and (B) SAFB2 gene expression in samples from BCP-ALL (n=5), T-ALL cases (n=5) and from NBM (n=5) analysed using Agilent Whole Genome Oligo microarrays. Data shows side by side comparisons of log2 signal intensities from individual samples. (C) SAFB1/SAFB2 expression ratios in cells derived from BCP-ALL and T-ALL patients and NBM. Circles, squares and triangles represent NBM, BCP-ALL and T-ALL samples, respectively and each colour represents a single sample. Results were analysed by one-way ANOVA. Values represent mean±SD. * = $P<0.05$ and ** = $P\leq0.01$.

Previous work from our group found that several subpopulations contain LICs in BCP-ALL and can maintain the disease, including ($CD34^+/CD19^+$, $CD34^+/CD19^-$, $CD34^-/CD19^+$, $CD34^-/CD19^-$) in BCP-ALL and $CD34^+/CD7^+$, $CD34^+/CD7^-$, $CD34^-/CD7^+$, $CD34^-/CD7^-$ in T-ALL. Therefore, we aimed to investigate whether the altered expression of SAFB1 and SAFB2 is also seen in these populations.

Results showed that SAFB1 and SAFB2 mRNA expression was not significantly different between $CD34^+/CD19^+$, $CD34^+/CD19^-$, $CD34^-/CD19^+$, $CD34^-/CD19^-$ BCP-ALL subpopulations compared with $CD34^+/CD38^-$ HSC (Figure 3.2A and B). The SAFB1/SAFB2 ratio was similar in $CD34^+/CD19^+$ (0.78±0.12), $CD34^+/CD19^-$ (0.90±0.51) and $CD34^-/CD19^-$ (0.71±0.11) BCP-ALL subpopulations compared with HSCs (0.62±0.37) and no significant difference was seen. However, $CD34^-/CD19^+$ cells had higher mean ratio than HSCs but was not statistically significant (1.48±0.85, Figure 3.2C).

Similarly, SAFB1 and SAFB2 mRNA expression was not altered in $CD34^+/CD7^+$, $CD34^+/CD7^-$, $CD34^-/CD7^+$, $CD34^-/CD7^-$ T-ALL subpopulations compared with HSCs (Figure 3.2D and E). There was no significant difference in SAFB1/SAFB2 ratios between $CD34^+/CD7^+$ (0.61±0.13), $CD34^+/CD7^-$ (1.03±0.70), $CD34^-/CD7^+$ (0.64±0.04), $CD34^-/CD7^-$ (0.47±0.09) T-ALL subpopulations compared with HSCs. In contrast, $CD34^+/CD7^-$ cells had higher mean ratio (0.78±0.12) than HSCs (0.62±0.37) but was not statistically significant (Figure 3.2F).

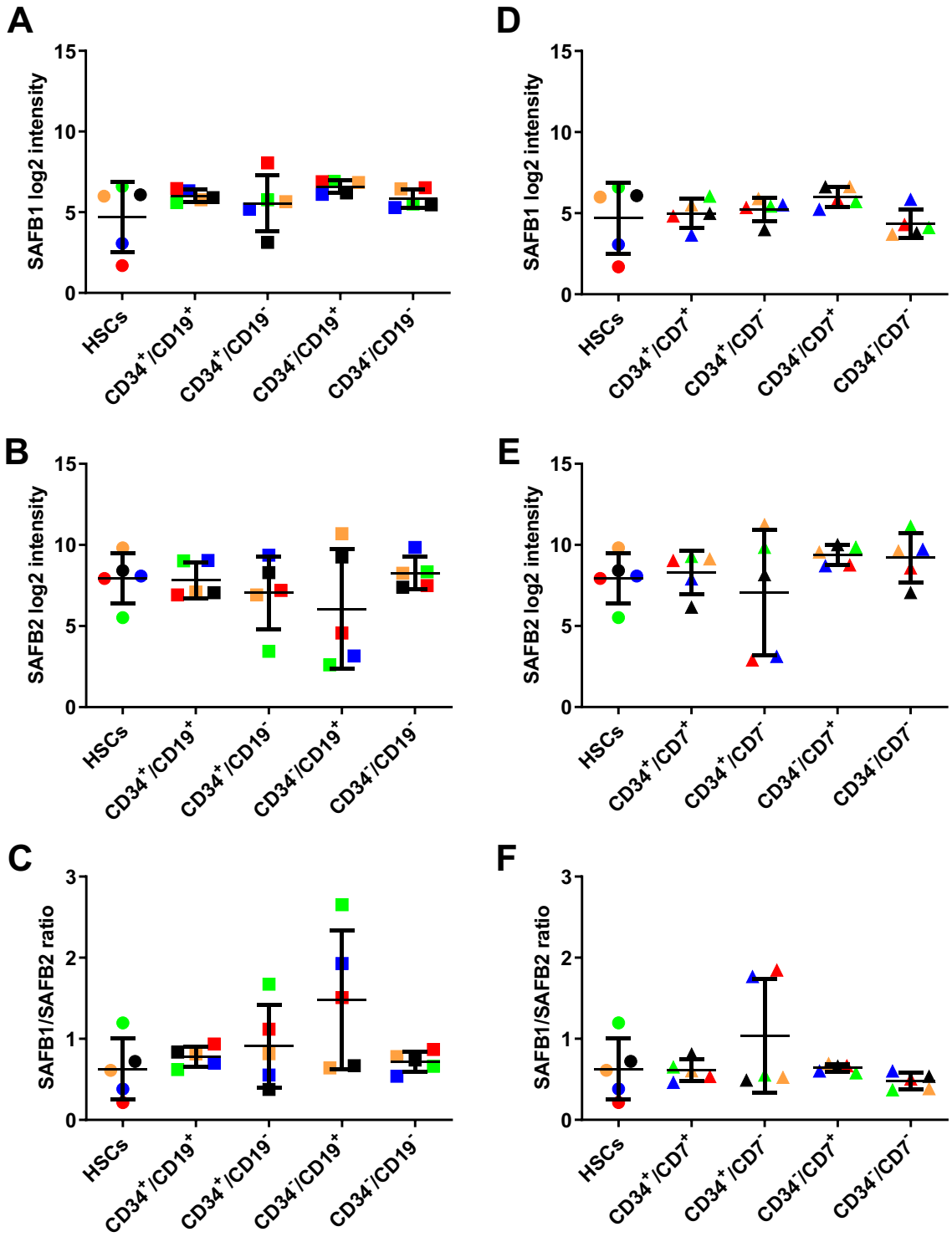

Figure 3.2 SAFB mRNA expression in HSCs and LICs.

SAFB1 and SAFB2 gene expression in LICs in (A-C) BCP-ALL (n=5) and (D-E) T-ALL cases (n=5) compared with HSCs. (A, B, D, E) Data shows side by side comparisons of log2 signal intensities from individual samples. (C, F) SAFB1/SAFB2 expression ratios in cells derived from BCP-ALL and T-ALL patients and HSCs. Circles, squares and triangles represent normal HSCs, BCP-ALL and T-ALL samples, respectively and each colour represents a single sample. Results were analysed by one-way ANOVA. Values represent mean±SD.

To validate SAFB1 and SAFB2 mRNA expression, RNA was extracted from BCP-ALL, T-ALL and NBM cells. cDNA was generated and SAFB1 and SAFB2 mRNA levels were measured via qPCR. Results showed that SAFB1 expression was significantly lower in T-ALL (0.67±0.14, $P<0.05$) but not BCP-ALL patients (1.22±0.10) compared with NBM (Figure 3.3A). Moreover, SAFB2 expression was significantly increased in T-ALL (1.73±0.11) and BCP-ALL (1.56±0.21, $P<0.01$) when compared with NBM (Figure 3.3B). These results confirm the altered SAFB1/SAFB2 expression rations observed from the microarray data.

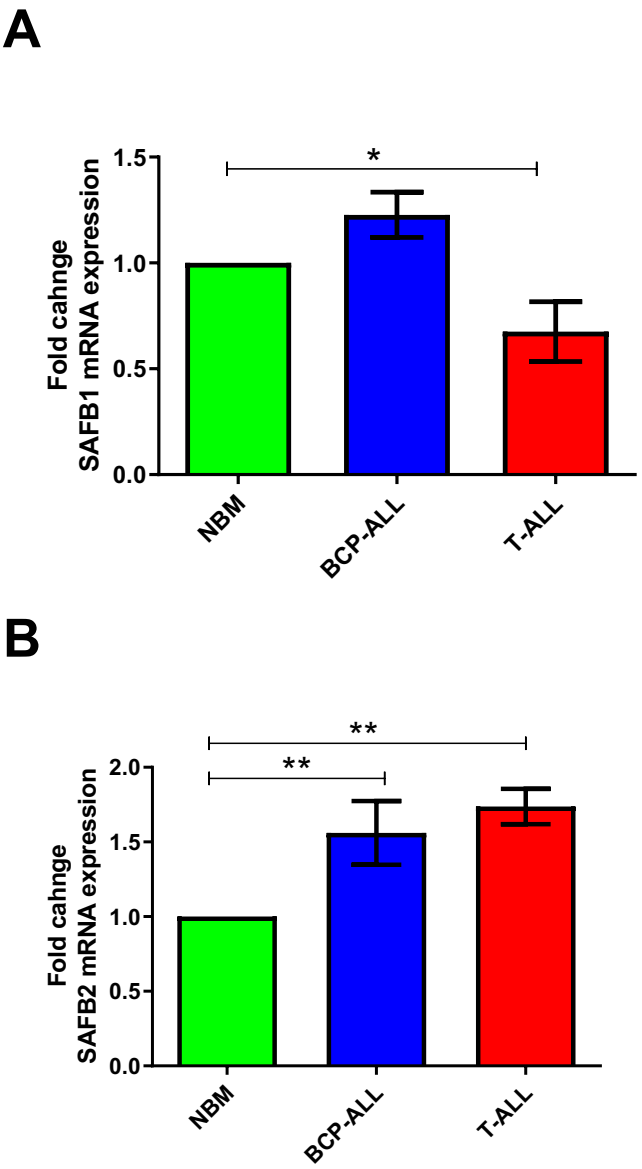

Figure 3.3 Validating SAFB1/2 mRNA expression in normal and leukaemia cells.
RNA was harvested from samples from BCP-ALL (n=3), T-ALL cases (n=3) and from 3 NBM donors. cDNA was generated to measure (A) SAFB1 and (B) SAFB2 relative mRNA expression using qPCR. GAPDH and beta-actin were used as endogenous genes. Data represent fold change from control cells (NBM). Results were analysed by one-way ANOVA. Values represent mean±SD. *=P<0.05, **=P≤0.01.

To see if the changes in SAFB1 mRNA levels and SAFB1/SAFB2 expression ratios reflected altered SAFB1/SAFB2 protein levels, BCP-ALL and T-ALL cells were immunocytochemically stained using previously validated specific anti-SAFB1 and anti-SAFB2 antibodies (Rivers *et al.*, 2015). The results showed SAFB1 and SAFB2 were expressed at comparable levels in NBM cells (6.12±1.18 and 4.98±1.10) respectively. SAFB2 levels were significantly increased in both BCP-ALL (15.43±1.90, $P<0.05$) and T-ALL cells (24.69±2.48, $P\leq0.001$) compared with SAFB1 (6.44±3.20, 3.93±1.29) in both ALL subtypes respectively (Figure 3.4).

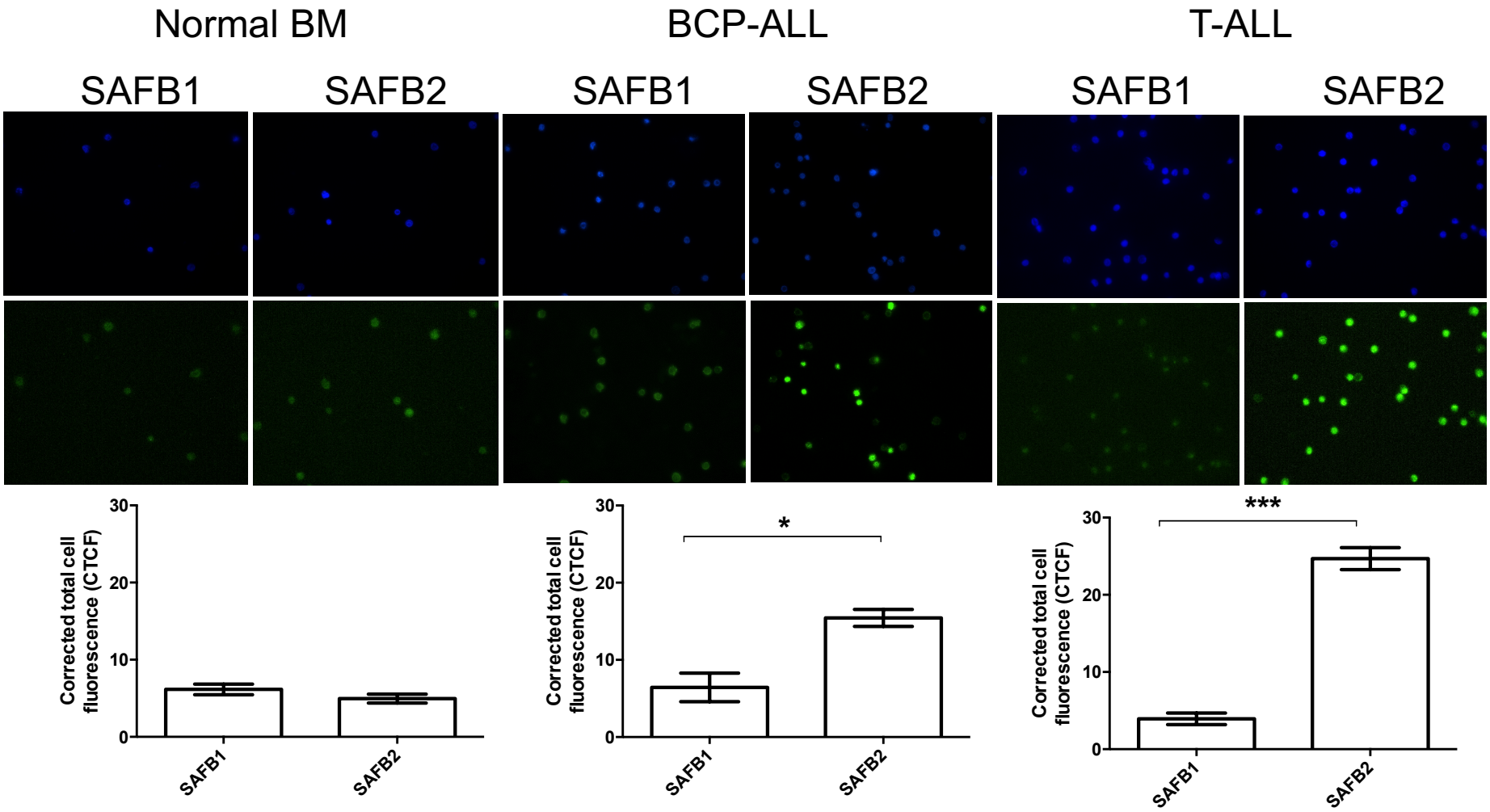

Figure 3.4 SAFB1 and SAFB2 expression in NBM and ALL cells.
Photomicrographs of DAPI nuclear staining (upper panels) and SAFB1 and SAFB2 immunocytochemical staining (lower panels) in NBM, BCP-ALL and T-ALL cells. Bar graphs show SAFB1 and SAFB2 expression and correspond to the conditions detailed in the panels above. Values are means±SD of 3 independent experiments. *=$P<0.05$, ***= $P\leq0.001$.

3.2.2 Studying whether rebalancing SAFB expression can induce apoptosis in cancer cells

T-ALL, BCP-ALL and NBM cells were transfected with pEGFP.SAFB1 plasmid or adenoviral vector expressing EGFP-SAFB1. Cells were left for 24 and 48 hours before being fixed with 4% PFA and images were taken to assess EGFP positive cells. Results showed that both plasmid transfection and adenoviral transduction resulted in high efficiency of EGFP-SAFB1 expression in primary ALL and NBM cells at 24 hours (Figure 3.5). There is no difference in the pictures in terms of cell number of ALL cells, indicating that cells are undergoing apoptosis. Similar observations were seen at 48 hours.

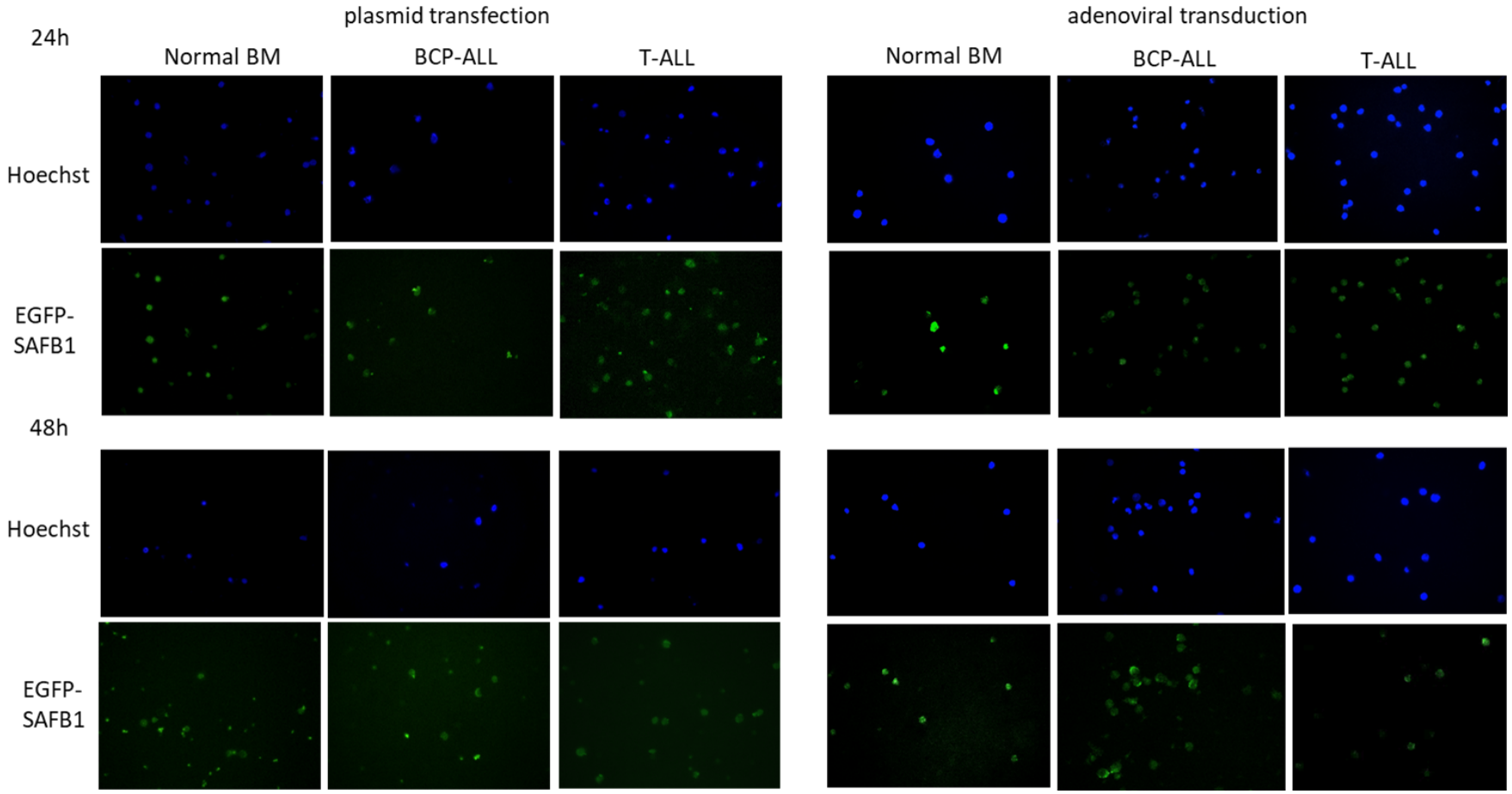

Figure 3.5 Assessing SAFB1 transfection/transduction efficiency in NBM and ALL cells. EGFP-SAFB1 was overexpressed in BCP-and T-ALL and NBM cells via plasmid transfection and adenoviral transduction and transfection efficiency was assessed after 24 (upper panels) and 48 (lower panels) hours by fluorescence microscopy. Hoechst was used for nuclear visualisation.

We next explored the effects of overexpressing SAFB1 on T-ALL and BCP-ALL cells and used annexin/PI assays to measure apoptosis. T-ALL, BCP-ALL and NBM cells were transfected with pEGFP.SAFB1 plasmid and adenoviral vector expressing SAFB1. Cells were left for 24 and 48 hours and viability was assessed. Results showed that overexpressing SAFB1 via adenoviral transduction induced apoptosis in BCP-ALL and T-ALL cells but not in NBM cells 24 and 48 hours after transfection (Figure 3.6A). Adenoviral transduction resulted in higher apoptosis than NBM with (52.02±5.65%) and (55.21±5.92%, $P \leq 0.001$) viability in BCP-ALL and T-ALL cells at 24 hours, respectively, while viability of ALL subtypes was 34.94±5.32% and 35.21±5.92% at 48 hours (Figure 3.6A) respectively. NBM cells were relatively resistant to adenoviral transduction with less apoptosis was induced following SAFB1 overexpression. Using plasmid transfection, both ALL subtypes viability was significantly reduced ($P \leq 0.01$, $P < 0.05$) at 24 and 48 hours, respectively (Figure 3.6B). Viability of both BCP-ALL and T-ALL cells were 71.40±5.58% and 73.09±3.59% at 24 hours, respectively. However, BCP-ALL and T-ALL viabilities were further reduced to 55.57±4.06% and 42.60±22.47% at 48 hours, respectively (Figure 3.6B). Viability of NBM cells was not significantly altered following plasmid transfection.

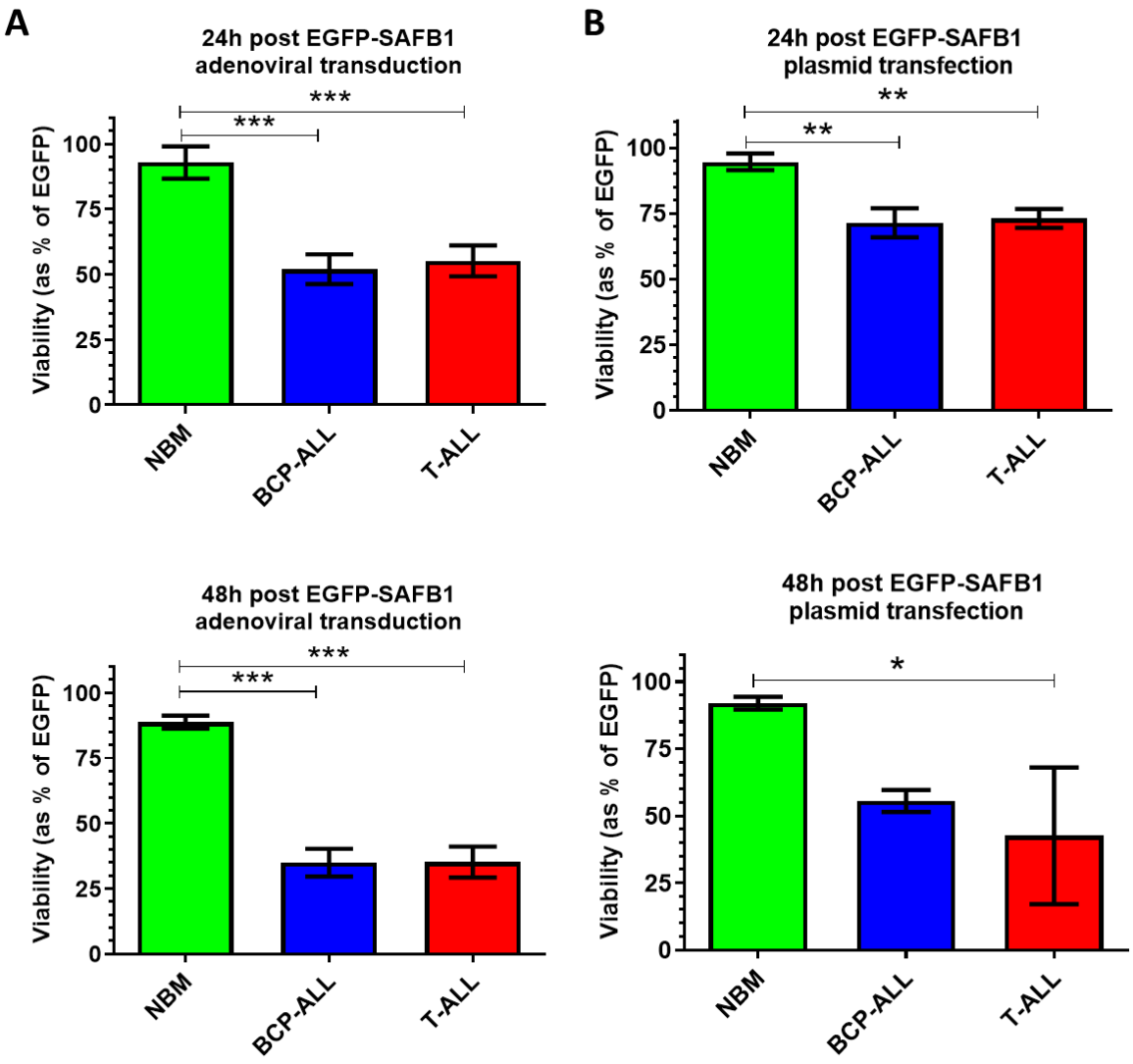

Figure 3.6 SAFB1 overexpression induces apoptosis in ALL cells.
SAFB1 was overexpressed in BCP-ALL, T-ALL and NBM cells via adenoviral transduction and plasmid transfection and viability was measured after 24 and 48 hours by flow cytometry using Annexin V and PI. Viability was determined as a percentage of the EGFP positive cells. Data represent mean±SD of 3 independent samples for each cell type. *=P<0.05, **=P≤0.01, *** =P≤0.001.

Next, the effect of SAFB2 overexpression on T-ALL and BCP-ALL cells was studied and the annexin/PI assays were used to measure apoptosis. T-ALL, BCP-ALL and NBM cells were transfected with pEGFP.SAFB2 plasmid and adenoviral vector expressing SAFB2. Cells were left for 24 and 48 hours and viability was assessed. Results showed that adenoviral transduction resulted in higher apoptosis in BCP-ALL (64.95±8.12%) and T-ALL cells (62.95±10.67%, $P \leq 0.01$) viability compared with NBM at 24 hours, while viability of ALL subtypes was 55.94±4.42% and 48.25±10.91% at 48 hours (Figure 3.7A) respectively. NBM cells were relatively resistant to adenoviral transduction with less apoptosis was induced following SAFB2 overexpression. Using plasmid transfection, both ALL subtypes viability was significantly reduced ($P<0.05$) at 24 and 48 hours, respectively (Figure 3.7B). Viability of both BCP-ALL and T-ALL cells were significantly reduced (79.29±9.41%, $P<0.05$) and (83.27±8.77%) compared with NBM at 24 hours, respectively. In addition, BCP-ALL and T-ALL viabilities were further reduced to 63.40±6.58% and 58.52±4.78% at 48 hours, respectively (Figure 3.7B). Viability of NBM cells was not significantly altered following plasmid transfection.

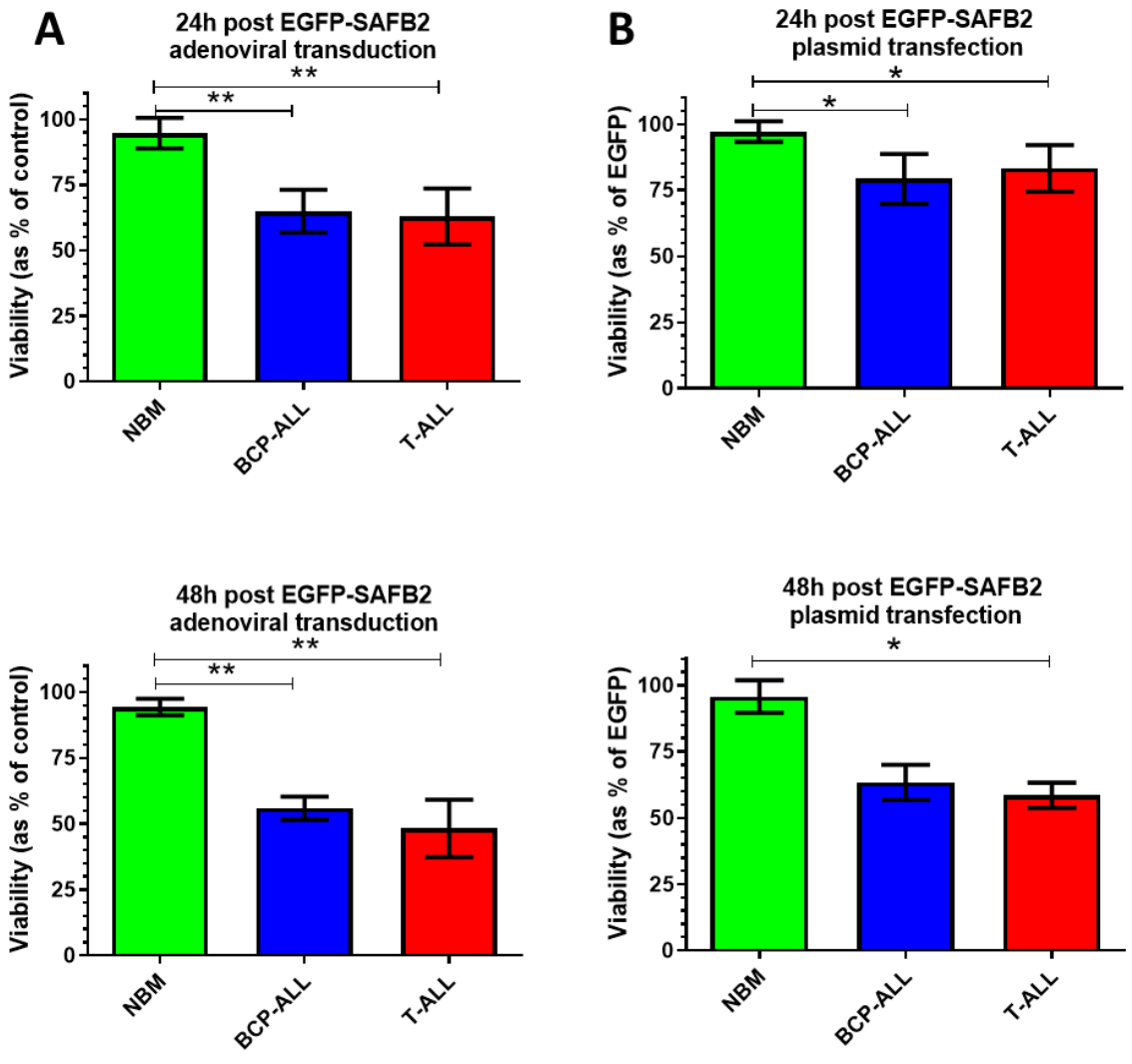

Figure 3.7 SAFB2 overexpression induces apoptosis in ALL cells.
SAFB2 was overexpressed in BCP-ALL, T-ALL and NBM cells via adenoviral transduction and plasmid transfection and viability was measured after 24 and 48 hours by flow cytometry using Annexin V and PI. Viability was determined as a percentage of the EGFP positive cells. Data represent mean±SD of 3 independent samples for each cell type. *=P<0.05, **=P≤0.01.

3.2.3 SAFB1 overexpression in non-cancerous dividing and non-dividing cells

Data showed that SAFB1 overexpression induced apoptosis in primary ALL cells (Figure 3.6). Therefore, it was interesting to investigate the effect of expressing SAFB1 in normal dividing MEFs and non-dividing primary neurons. MEFs were transfected with pEGFP.SAFB1 and left for 24 and 48 hours. The transfection efficiency was assessed and viability was measured by MTT activity. MTT was used as a measurement and correlate with viability. Results showed that transfection efficiency was high (Figure 3.8A) and transfection of mitotic MEF cells with SAFB1 did not mediate any significant alterations (P=0.40) in viability at 24 and 48 hours (Figure 3.8B).

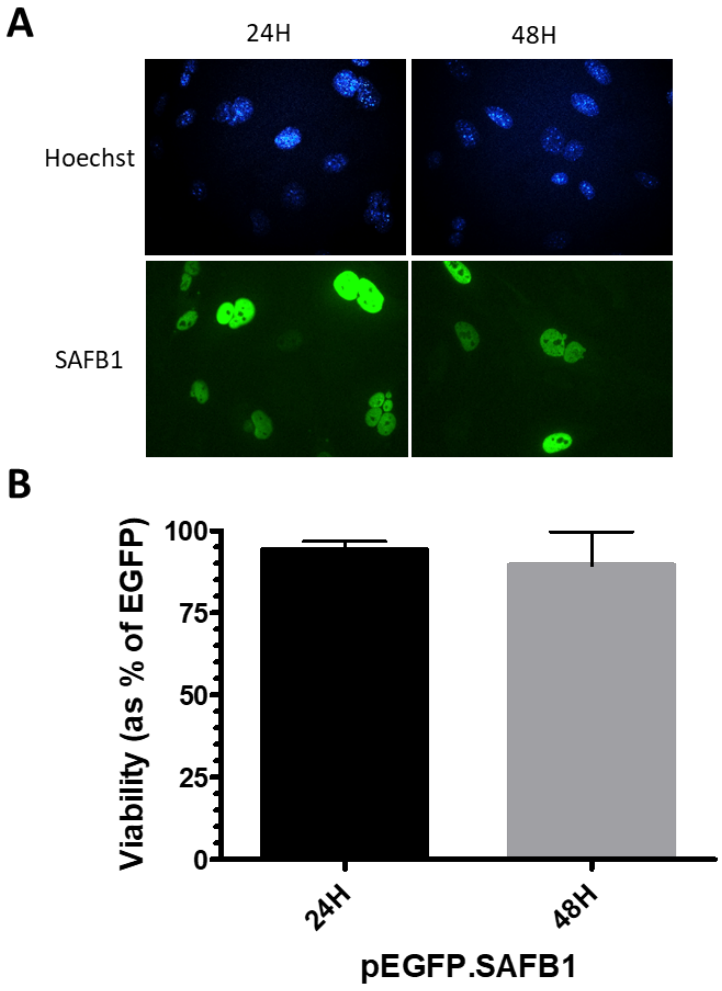

Figure 3.8 SAFB1 overexpression does not induce cell death in primary MEFs.
Primary MEFs were transfected with pEGFP.SAFB1 and left for 24 and 48 hours. (A) Transfection efficiency was assessed and (B) viability was measured by MTT activity at 24 and 48 hours. Viability was determined as a percentage of the EGFP positive cells. Values represent mean±SD.

Previous work in the lab showed that SAFB1 overexpression was closely associated with chromatin. Therefore, experiments performed by Youn-Bok Lee in the lab assessed the effect of expressing SAFB1 in non-dividing primary neurons. Primary cortical and hippocampal neurons were transduced with Ad.HA.SAFB1 at MOIs of 50, 100 and 200 (titres that killed SH-SY5Y cells after two days) and found there was no change in viability as assessed by MTT activity (Figure 3.9A) and immunocytochemical analysis of morphological and nuclear integrity (Figure 3.9B).

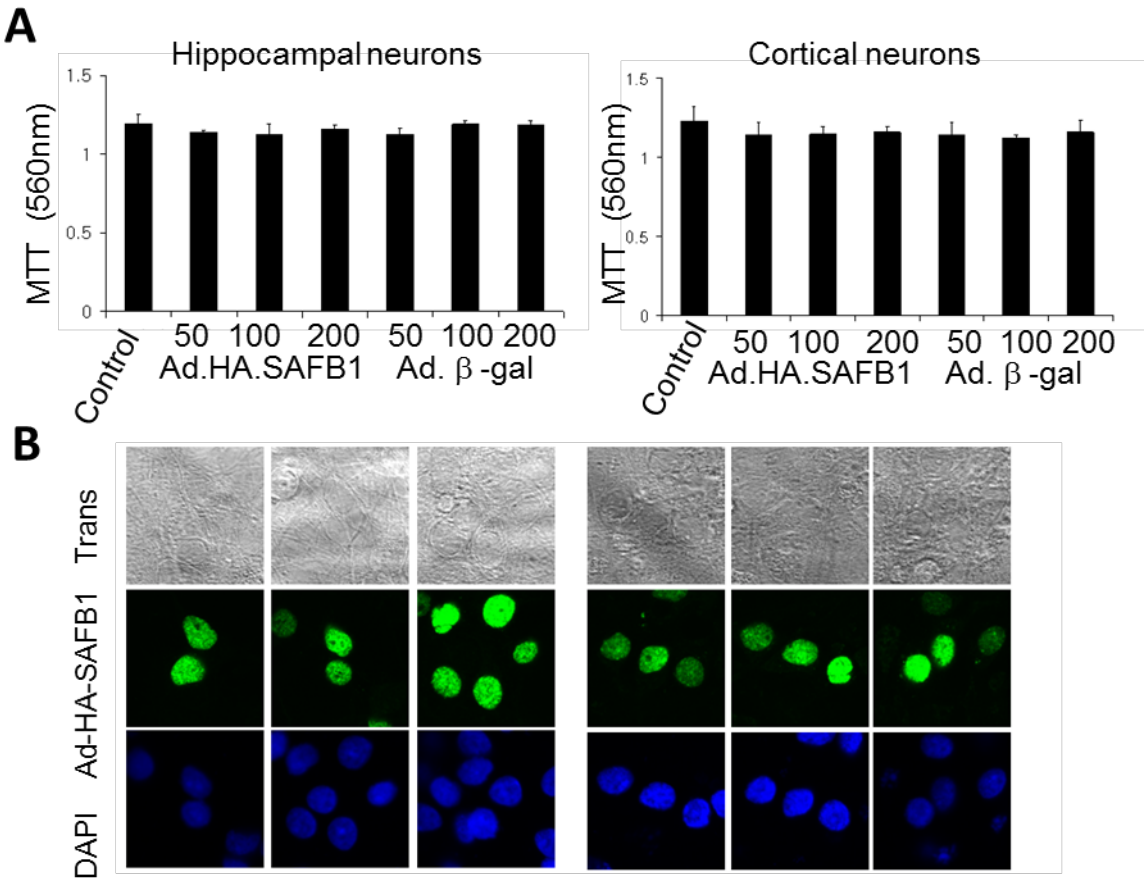

Figure 3.9 SAFB1 overexpression does not induce cell death in post-mitotic primary neurons. (A) Primary cortical and hippocampal neurons were transduced with Ad.HA.SAFB1 at various MOIs and MTT activity measured 6 days later. (B) Photomicrographs of primary hippocampal and cortical neurons transduced with Ad.HA.SAFB1 and detected using an anti-HA tag Ab. The confocal images also show DAPI stained neurons.

3.3 Discussion

SAFB1 and SAFB2 are known to interact with important regulators of tumorigenesis and the deletion of SAFB1 is associated with cellular immortalisation (32). In addition, decreased expression of SAFB1 has been found in prostate (16), breast (34) and colorectal cancers (35). However, it is not known if such alterations in SAFB1 are restricted to solid tumours. Consequently, we examined the expression profile of SAFB1 and its paralogue SAFB2 in primary BCP- and T-ALL cells. Initial analysis of microarray data showed that SAFB1 mRNA expression was significantly lower in T-ALL cells compared to BCP-ALL and NBM cells. We also report for the first time that SAFB2 protein expression was significantly elevated in both ALL subtypes. Interestingly, we also found that the SAFB1/SAFB2 ratio was reduced significantly in both BCP- and T-ALL cells compared with NBM. SAFB1 and SAFB2 are under the control of a bidirectional promoter and knocking down SAFB1 or SAFB2 results in a compensatory increase in SAFB2 and SAFB1, respectively (39). The mechanism has not been studied but presumably is a feedback mechanism for SAFB1/2 regulation. Thus, these results suggest that the altered transcriptional activity associated with ALL and other cancers promotes a decrease in the SAFB1/SAFB2 protein expression ratio. SAFB proteins regulate, chromatin structure, polymerase II activity (2), DNA repair (22), the cell cycle (23), apoptosis (24) and splicing (159). Considering these important roles in regulating gene expression and the cell cycle, these results suggest that aberrant SAFB1/2 protein expression may be associated with the development of tumorgenicity.

Next, it was interesting to evaluate the pattern of SAFB1 and SAFB2 expression within LICs in BCP-ALL. Data showed that there was no significant difference in SAFB1 and SAFB2 expression between BCP-ALL subpopulations. However, it was found that the ratio of SAFB1/SAFB2 in $CD34^-/CD19^+$ cells were higher compared with HSCs. The $CD34^-/CD19^+$ cells are known to have less proliferative capacity subpopulations to maintain the disease compared to other LIC subpopulations (91),(86),(94), indicating that this population may have a less aggressive function. Also, the expression of SAFB1 and SAFB2 within T-ALL subpopulations was investigated. Results showed that SAFB1/SAFB2 ratio seems to be higher in $CD34^+/CD7^-$ cells compared with HSCs. However, the higher SAFB1/2 ratio was only observed in 2/5 cases, indicating

that $CD34^+/CD7^-$ cells might not be associated with reduced functional capacity. Further experiments are needed to understand these observations. $CD34^+/CD7^-$ cells are known to be the most primitive subpopulation in T-ALL and have more LICs, compared to other LIC subpopulations which enable them to differentiate *in vivo* and maintain the disease (84), (86).

Previously it was found that overexpression of SAFB1 was highly effective at activating protein kinase R (PKR) and inhibiting protein translation. Further to these findings, ectopically expressed SAFB1 was closely associated with chromatin and mediated the formation of multinucleated cells indicating powerful effects on pathways governing the cell cycle. In this study it was found that SAFB1 overexpression was associated with initiating apoptosis in both primary T-ALL and BCP-ALL cells. However, SAFB1 did not mediate these actions in a range of normal cells including NBM, fibroblasts or primary neuronal cells. We have previously shown that SAFB1 plays a role in the apoptotic process, helping to reorganize and segregate nuclear RNA and DNA prior to endonuclease-mediated DNA cleavage (162). In addition, the SAF protein SLTM, (which shares 30% homology with SAFB1) when overexpressed has also been shown to induce apoptosis in cancer lines (6). These results suggest that compared to normal dividing cells, cancer cells are uniquely sensitive to SAFB1 protein overexpression. There are a number of possible explanations for the potential pro-apoptotic actions of ectopically expressed SAFB1: (i) SAFB1 binds active chromatin (euchromatin) unique to cancer cells prior to and during replication and hence disrupts cell division. This possibility is supported by the observation that SAFB1 has been shown to interact with a number of important modifiers of chromatin structure e.g. CHD1, NCOR, HDAC3, BRG1, Matrin 3 (reviewed in (39),(11)). SAFB1 was also shown to form a complex with the growth inhibitory kinase MST1 and the histone methyltransferase EZH2 at chromatin sites in association with PRC2 (16). (ii) SAFB1 alters the unique transcriptional activity of cancer cells by interacting with promoter regions (e.g. with TA rich regions and E-box regions via its SAF box) and/or by interacting with transcription factors (via its C-terminal domain) such as p53, c-Jun, oestrogen receptor and PPAR gamma. (iii) SAFB1 alters the splicing of cancer promoting genes. For instance, we have shown that SAFB1 regulates the splicing of Oncomir-1 (miR-17-92 cluster), MALAT1, ELK3 and MAP3K7 (38). SAFB proteins are subject to a number of PTMs and it is possible that cancer specific changes, for instance in SAFB protein

methylation, phosphorylation and/or SUMOylation may promote oncogenesis. For example, cellular stress is known prevent the SUMOylation of SAFB1 and inhibit its ability to mediate transcriptional repression (29).

The effect of SAFB2 overexpression on ALL cells was also examined. In the current study, it was shown that SAFB2 overexpression induced apoptosis in both primary T-ALL and BCP-ALL cells to less extent compared with SAFB1. However, SAFB2 overexpression did not induce apoptosis in NBM cells. The potential pro-apoptotic effect of SAFB2 is not well established compared with SAFB1 role and further experiments are warranted to define these observations. However, there are a number of possible reasons for the potential pro-apoptotic actions of SAFB2 overexpression: (i) SAFB2 could be competing with SAFB1, as SAFB2 was shown to co-localise with SAFB1 (9) (ii) SAFB1 and SAFB2 are under the control of a bidirectional promoter and it could be that a feedback mechanism for SAFB1/2 regulation can be involved.

We report for the first time that the expression ratio of SAFB1 and SAFB2 is reduced in both paediatric BCP-ALL and T-ALL cases. SAFB1 levels have previously been reported to be lowered in prostate, breast and colorectal cancers and also be associated with poor prognosis. The lower expression of SAFB1 in T-ALL correlates with these patients generally having a worse outcome than BCP-ALL cases. These results therefore suggest that altering the expression levels/function of these important regulators of gene expression and the cell cycle may promote oncogenesis. We also investigated the pro-apoptotic properties of SAFB1/2 and the results showed that SAFB1 inhibited translation (Youn-Bok Lee, personal communication) and induced apoptosis within 48 hours of expression. In contrast the overexpression of SAFB1 in NBM cells, fibroblasts and non-dividing primary hippocampal and cortical neurons did not result in a reduction in viability or mediate apoptosis. Considering the selectivity of cellular disruption mediated by SAFB1, its overexpression may form the basis for gene therapy strategies aimed at mediating cell death in cancer cells. Such strategies could be significantly less toxic to non-cancerous cells and thereby decrease treatment related mortality.

CHAPTER 4 : Investigating the effect of anti-cancer drugs (HSP90 inhibitors) on the stress response in HeLa cells, primary BCP-ALL and T-ALL cells

4.1 Introduction

Hsp90 has important roles in cell survival and it is an important regulator of the stress response (163). Hsp90 functions to promote protein folding, prevents misfolding (163) and HSP90 is often associated with HSP70 and co-chaperones such as Cdc37 (117). HSP90 is found to be highly expressed in many solid (prostate, lung) and haematological (leukaemia) cancers (116) and is associated with poor prognosis (163),(117). HSP90 inhibition leads to degradation of client proteins, such as oncogenic tyrosine kinase v-Src, mutated oncogene Bcr/Abl, tumour suppressor p53 protein and steroid receptors. Therefore, targeting HSP90 is a promising approach for anticancer therapy (163),(115). Several HSP90 inhibitors have been identified, including 17-DMAG and celastrol. Both drugs induce apoptosis in T-ALL and BCP-ALL cells. Both drugs in combination also reduce viability in BCP-ALL LIC ($CD34^+/CD19^+$, $CD34^+/CD19^-$, $CD34^-/CD19^+$ and $CD34^-/CD19^-$) subpopulations. However, neither of the HSP90 inhibitors had a cytotoxic effect on normal cord blood (CB) and HSCs (95). Furthermore, when T-ALL cells were treated with both drugs in combination and inoculated into NSG mice, engraftment of all LIC ($CD34^+/CD7^+$, $CD34^+/CD7^-$, $CD34^-/CD7^+$ and $CD34^-/CD7^-$subpopulations) was prevented 2/3 of cases (95). In the third case, a patient in relapse, engraftment was only prevented in $CD34^-/CD7^-$ cells. However, engraftment was reduced in unsorted, $CD34^+/CD7^+$ and $CD34^-/CD7^+$ cells.

Competition for Hsp90 binding in the cell is also known to result in the activation of HSF1 and the induction of a stress response. HSF1 is the master regulator of the stress response and in its active state HSF1 also transcribes lncSatIII RNAs and recruits other proteins such as SRSF1 and 9G8 into nSBs to regulate splicing (20). HSF1 activities extend far beyond the stress response and accumulating evidence has linked HSF1 with oncogenesis (144). HSF1 activation is associated with poor prognosis in prostate, lung, colon (148),(164),(145) and melanoma cancers (149). HSF1 was found to be overexpressed in prostate cancer cell lines (150), CLL (151) and found in the nucleus of leukaemia B cells but not in normal B cells (152). SAFB1 also co-localises with HSF1 in nSBs and it was suggested to play a role in transcriptional control and alternative splicing in cells following stress (4),(142).

Whether cancer cells respond to Hsp90i inhibitors by inducing a stress response is not known. In addition, the contribution of stress response induction to cancer cell viability has not been investigated.

Therefore, the aims of this chapter were to:
(i) Characterise the stress response by observing nSBs formation by assessing the expression/localisation of SAFB1, SAFB2 and HSF1 following heat shock and measuring HSP70 induction in HeLa cells.

(ii) Investigate whether HSP90 inhibitors also induce a stress response in HeLa cells

(iii) Assess the ability of ALL cancer cells to generate nSBs by monitoring the distribution of HSF1, SAFB1 and SAFB2 following heat shock.

(iv) Validate the effect of HSP90 inhibitors on the viability of ALL cancer cells and assess their efficacy when used in combination.

(v) Validate the effectiveness of pharmacological inducers (HSP90i) of a stress response by measuring HSP70 induction and expression/localisation of SAFB1, SAFB2 and HSF1 in ALL cancer cells.

4.2 Results

4.2.1 Establishing the base line stress response following heat shock and HSP90 inhibitors in HeLa cells

HSF1 is the master transcription factor in humans and is known to mediate the transcription of SATIII and also to be recruited into nSBs (20). SAFB1 is known to be recruited to nSBs and it is frequently used as a marker of nSB formation. SAFB2, a paralogue of SAFB1 with high similarity at the amino acid level and until recently it has been difficult to generate SAFB2 specific antibodies. However, antibodies specific to SAFB1 and SAFB2 are now available and therefore their localisation was compared following a stress response in cancer cells.

Prior to investigating the effect of HSP90 inhibitors on HSP70 induction and nSB formation cells were heat shocked and HSP70 expression and nSB formation were measured to allow comparison. To achieve this, HeLa cells were heat shocked at 42^0 C for 1 hour followed by 0 hours recovery (HS+NR) and left for a 1 hour recovery period (HS+R) and the expression of HSP70, HSF1, SAFB1 and SAFB2 measured immunocytochemically. Prior work in the laboratory (39) and live imaging analysis of stress body formation using Incucyte analyses (performed by Renate Raele) showed that a one hour heat shock consistently produced stress body formation. This work also showed that following a heat shock plus 1 hour recovery the majority of stress bodies had lost HSF1 staining and therefore represented an intermediate recovery period.

Under basal conditions, HSP70 was found to be expressed in the nucleus and cytoplasm but excluded from the nucleolus. Following HS (HS+NR), HSP70 was overexpressed and found to be more concentrated in the nucleolus (Figure 4.1A). The translocation of HSP70 into the nucleolus was more pronounced following the recovery period (HS+R). To quantify HSP70 expression the intensity of HSP70 immunofluorescence was calculated using ImageJ. HSP70 was overexpressed significantly following HS+NR (81.75±3.59, $P \leq 0.01$) and HS+R (66.75±4.78, $P < 0.05$) compared with basal conditions (Figure 4.1B).

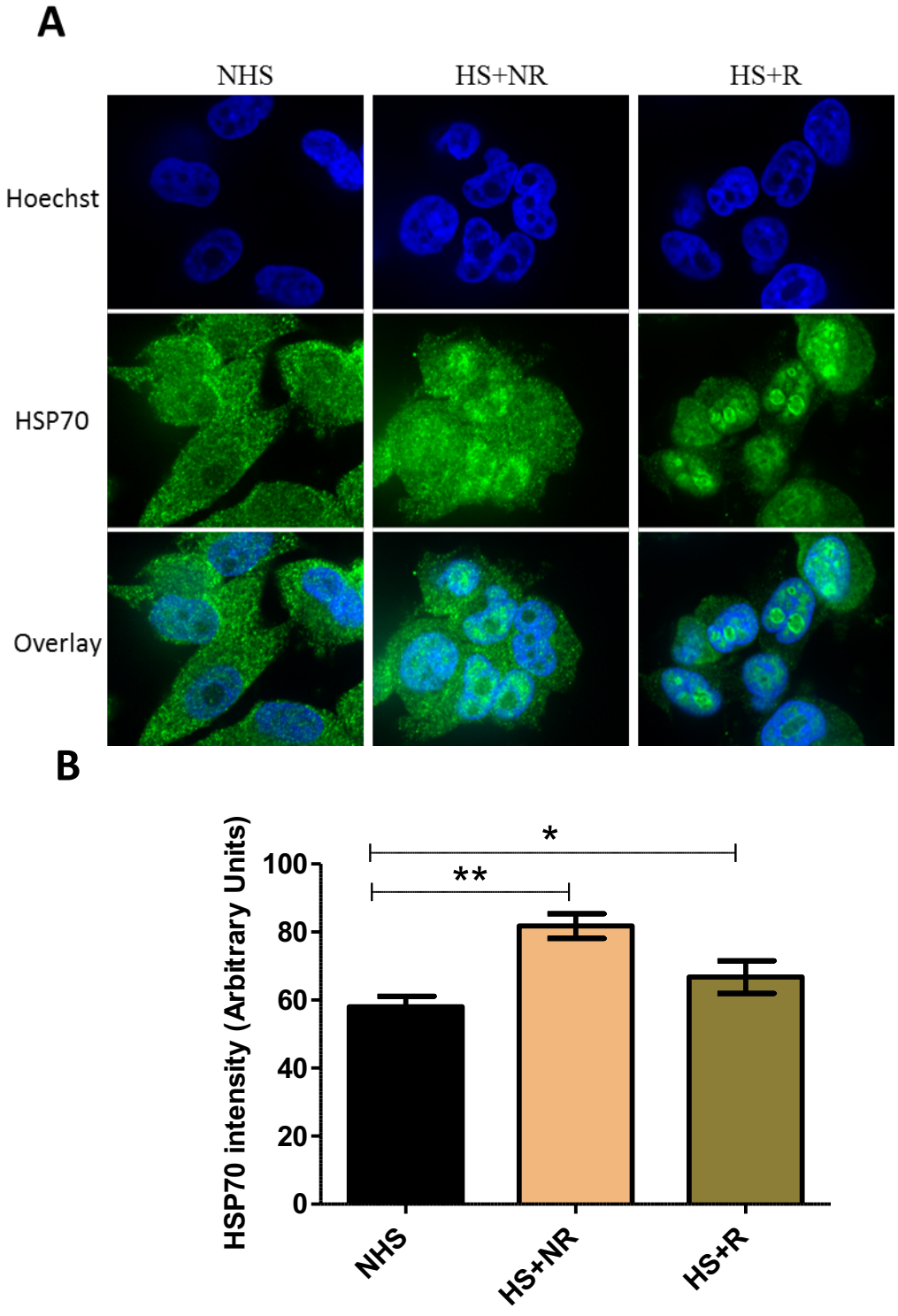

Figure 4.1 HSP70 induction after HS. (A) HeLa cells were heat shocked at 42^0C and immunostained with an anti-HSP70 primary antibody and visualised with Alexa 488 secondary antibody (green). Cells were also stained with Hoechst for nuclear visualisation (blue). Images were captured using a 63x lens confocal laser microscope. (B) Bar graph represents HSP70 intensities using ImageJ. Data was analysed by one-way ANOVA. Values represent mean±SD of 4 independent replicates. * = $P<0.05$ ** = $P\leq0.01$.

HeLa cells were immunostained with anti-SAFB1 and anti-HSF1 primary antibodies and visualised with Cy3 and Cy2 secondary antibodies respectively. Cells were stained with Hoechst for nuclear visualisation. Under basal conditions, SAFB1 and HSF1 were diffusely expressed in the nucleus with HSF1 also being expressed in the cytoplasm. Immediately after HS (HS+NR), SAFB1 distribution was unchanged, while HSF1 (the main marker for nSBs) started to form large nuclear puncta characteristic of nSBs. SAFB1 was not recruited into HSF1 puncta following heat shock (HS+NR). After the recovery period (HS+R), SAFB1 also started to form nuclear puncta with some colocalising with HSF1 in nSBs (Figure 4.2A). Analyses showed the number of cells with colocalised SAFB1 and HSF1 puncta (used as a measure of SAFB1 positive nSBs) was significantly greater in the HS+R (45.50±6.19, $P \leq 0.001$) compared with HS+NR and controls (NHS, Figure 4.2B).

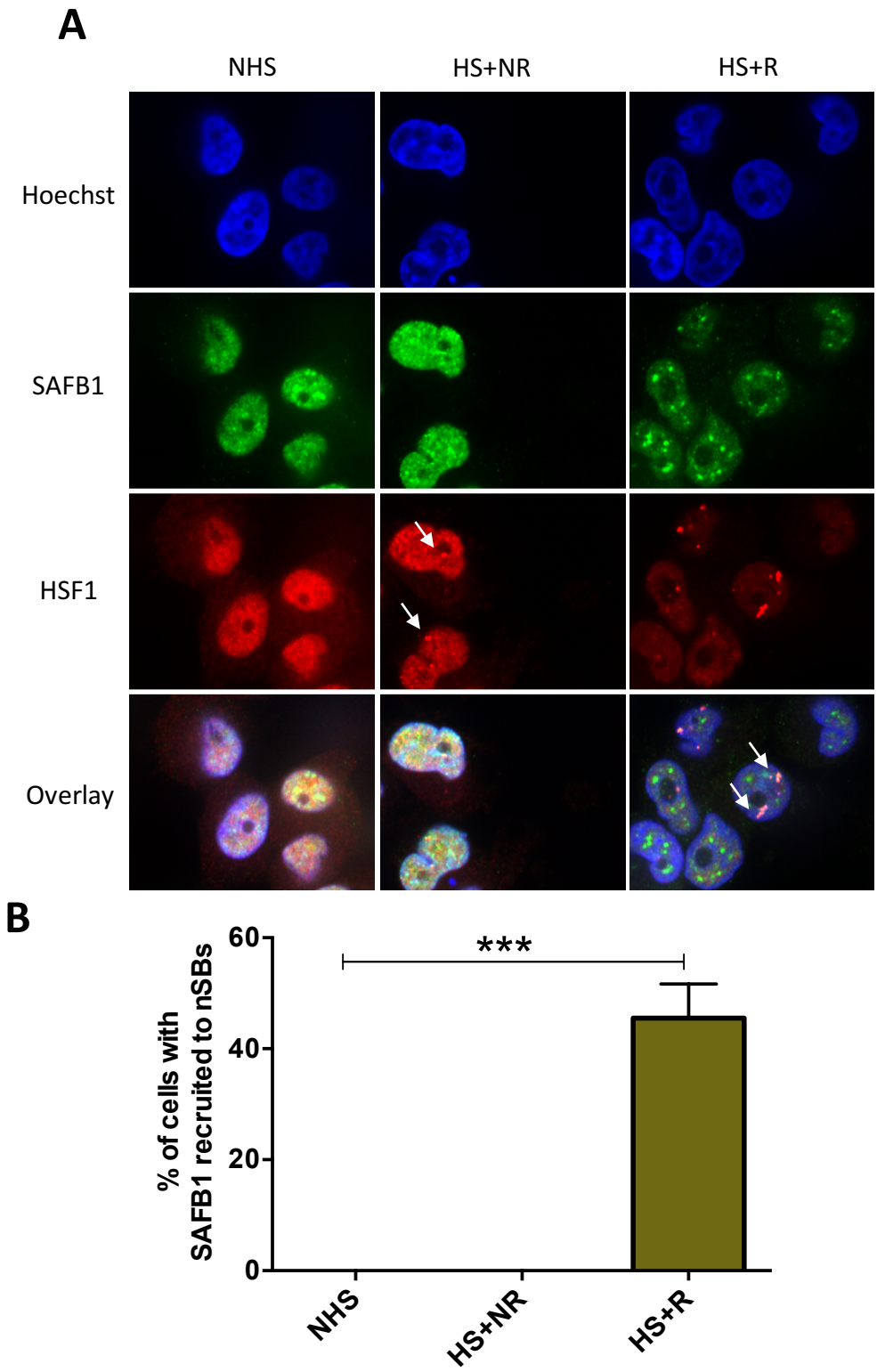

Figure 4.2 SAFB1 recruitment into nSBs after HS. (A) HeLa cells were heat shocked at 42^0 C and immunostained with anti-SAFB1 and anti-HSF1 primary antibodies and visualised with Cy2 (green) and Cy3 (red) secondary antibodies respectively. Hoechst was used to stain the nucleus (blue). Images were captured using a 63x lens confocal laser microscope. (B) The percentage of cells with nSBs were counted in 200 cells indicated by arrows. Data was analysed by one-way ANOVA. Values represent mean±SD of 4 independent replicates. *** = $P \leq 0.001$.

HeLa cells were also immunostained with anti-SAFB2 and anti-HSF1 primary antibodies and visualised with Cy3 and Cy2 secondary antibodies respectively. Cells were stained with Hoechst for nuclear visualisation. Under basal conditions, SAFB2 and HSF1 were diffusely expressed in the nucleus with HSF1 also being expressed in the cytoplasm. Immediately after HS (HS+NR), SAFB2 was found in puncta, some of which overlapped with HSF1 (Figure 4.3A). After the recovery period (HS+R), a greater number of SAFB2 puncta were found colocalised with HSF1 (Figure 4.3A). SAFB2 puncta appeared larger than those seen with SAFB1 and were more frequently colocalised with HSF1 than SAFB1 following HS+R (76.76±4.09, $P \leq 0.001$) compared with HS+NR (44.63±10.82) and controls (NHS, Figure 4.3B).

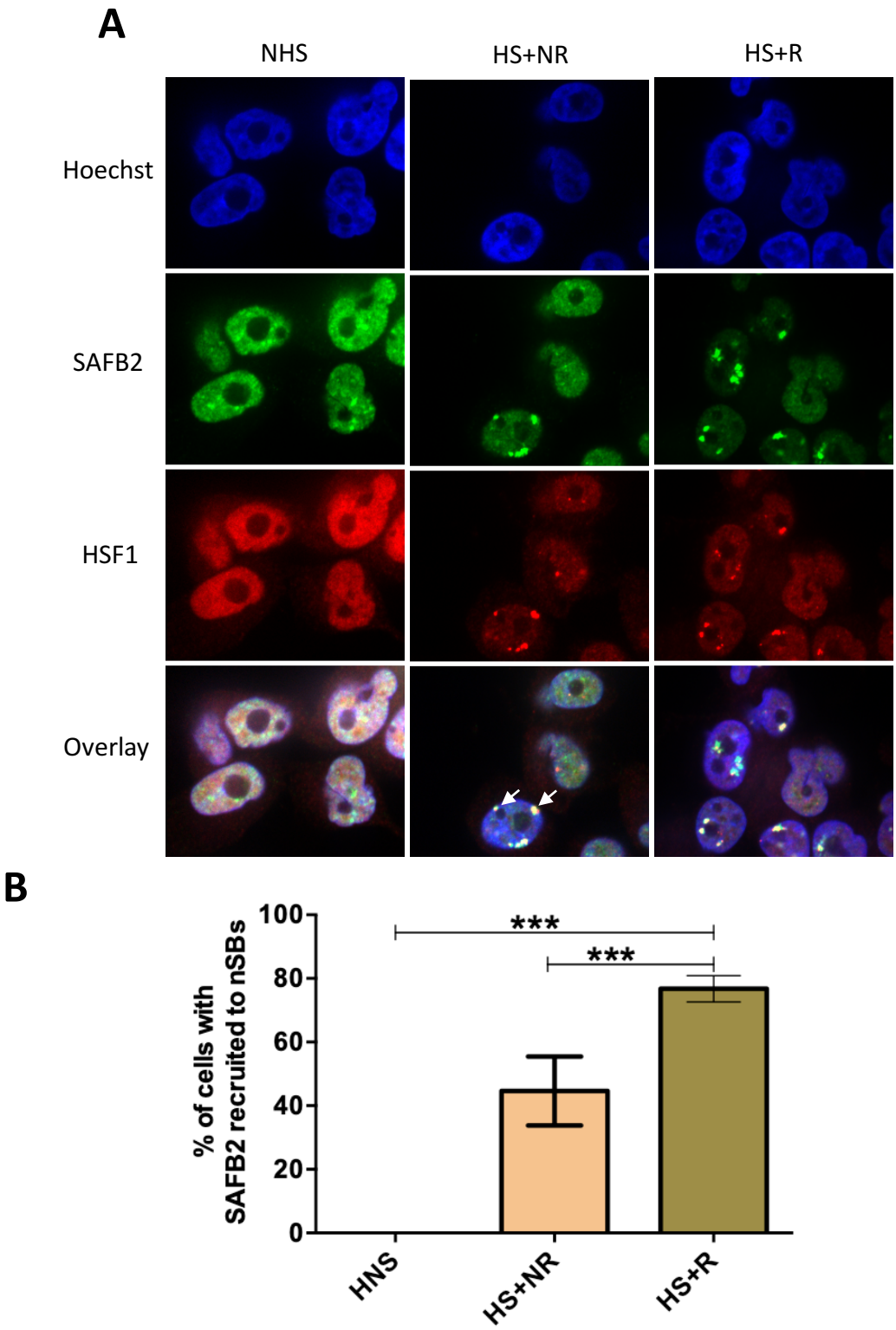

Figure 4.3 SAFB2 recruitment into nSBs after HS. (A) HeLa cells were heat shocked at 42^0 C and immunostained with anti-SAFB2 and anti-HSF1 primary antibodies and visualised with Cy2 (green) and Cy3 (red) secondary antibodies respectively. Hoechst was used to stain the nucleus (blue). Images were captured using a 63x lens confocal laser microscope. (B) The percentage of cells with nSBs were counted in 200 cells indicated by arrows. Data was analysed by one-way ANOVA. Values represent mean±SD of 4 independent replicates. *** = $P \leq 0.001$.

HeLa cells were treated with increasing concentrations of 17-DMAG or celastrol ranging from 0.01nM to 10μM for 24 and 48 hours then viability was monitored using the MTT assay. Two time points were used to obtain the best time point with effective cytotoxicity as previous work in our laboratory found that 17-DMAG was effective on primary ALL at 24h and celastrol was more effective at 48h (95). Viability experiments were conducted to obtain the IC_{50} (section 2.10) to investigate the contribution of stress response induction to cancer cell viability at doses that kill 50%. Also, the aim was to see whether cancer cells are more sensitive to HSP90 inhibitors than normal cells via the stress response pathway. The results showed that viability was not altered in response to celastrol at doses below 1μM, with a decrease in viability from 90.40±13.80% to 37.00±8.18 85% at 24 hours and 92.28±13.85% to 22.45±5.29% at 48 hours between 1 and 2μM. Therefore, further concentrations of celastrol were used to generate a dose response curve. Doses below 2μM showed a gradual reduction in viability, with a significant difference at 2μM (22.45±5.29%, $p<0.05$) compared to un-treated cells (Figure 4.4A). In contrast, cells started to respond to 17-DMAG, with a significant difference observed at 0.1 (70.91±4.22%), 1 (53.5±2.90%) and 10μM (16.31±4.19%, $p\leq0.01$) compared to un-treated cells (Figure 4.4B).

Moreover, it was essential to investigate viability following the application of the various doses of both drugs by determining the half-maximal inhibitory concentration (IC_{50}) values. Results revealed a higher IC_{50} for 17-DMAG compared to celastrol at 24 hours with 4.04μM versus 1.72μM, while the IC_{50} was similar at 48h with 1.78μM and 1.68μM for 17-DMAG and celastrol, respectively. Subsequently, the IC_{50} doses of both drugs were used in combination to treat HeLa cells and viability was evaluated using the MTT assay. The combined treatment with both 17-DMAG/Celastrol (DM-Ce) resulted in higher toxicity (35.75±7.38% viable) at 24 hours and (28.17±2.03% viable, $p\leq0.001$) at 48 hours compared to treatment with celastrol alone (52.17±7.60% viable) and (43.16±19.00% viable), respectively. However, there was no significant difference between DM-Ce and 17-DMAG at either timepoint ($p\leq0.26$, Figure 4.4C and D). 17-DMAG resulted in higher toxicity compared with celastrol (43.80±7.38% to 52.17±7.60% viable, $p<0.05$) and (36.83±2.32% to 65.16±19.00% viable, $p\leq0.001$) at 24 and 48 hours, respectively.

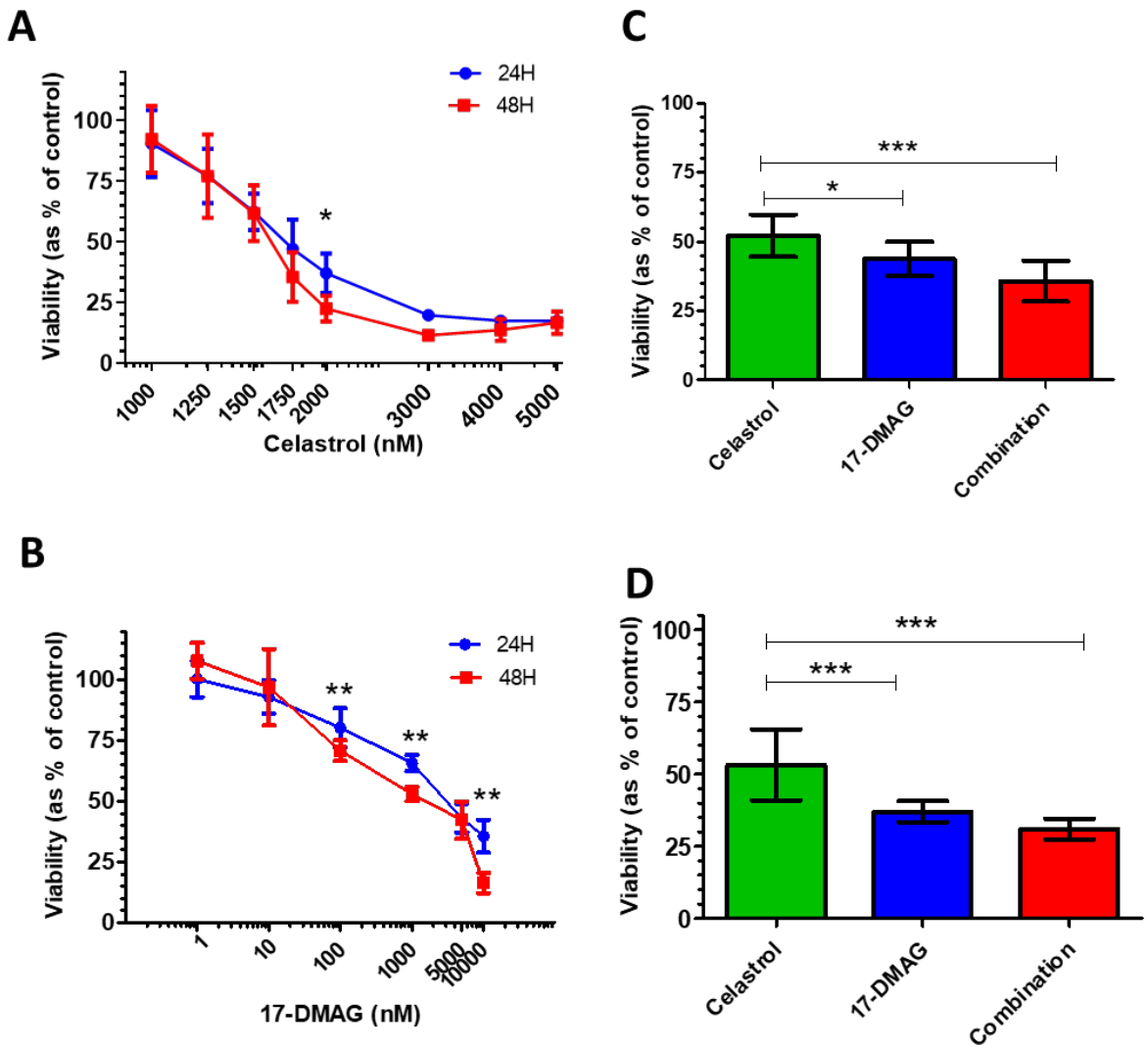

Figure 4.4 Response of HeLa cells to HSP90i. HeLa cells were treated with increasing concentrations of (A) celastrol (1-5 μM) and (B) 17-DMAG (1-10 μM) alone to calculate the IC_{50} doses. Cells were treated with the IC_{50} doses alone and in combination for (C) 24h and (D) 48h. Viability was assessed using MTT assay. Viability was determined as a percentage of the untreated control cells. Data was analysed by one-way ANOVA (C and D) and two-way ANOVA (A and B). Values represent mean±SD of 4 independent replicates. * = $P<0.05$; ** = $P\leq0.01$; *** = $P\leq0.001$.

Heat shock induced the stress response as characterised by HSP70 induction and nSB formation (Figure 4.1, 4.2, 4.3). However, the stress response assessed by HSP70 induction was not characterised following other stresses such as HSP90 inhibitors (17-DMAG and celastrol), using IC_{50} doses. It is not known whether HeLa cells contribute to cell death by dysregulation of the stress response. HSP70 expression is reported to be a reliable measurement of the efficiency of HSP90 inhibition (164). For example, 17AAG (a hydrophobic inhibitor of the HSP90 activity) was reported to cause a 4-6 fold increase in HSP70 expression in several cell lines, including MCF-7, PC-3, Myc-CaP, A549 and HT 1080 (158). To investigate this, HeLa cells were treated using IC_{50} doses with 17-DMAG (1.78μM) and celastrol (1.68μM) as single agents and in combination for 48 hours and the stress response characterised by HSP70, HSF1, SAFB1 and SAFB2 immunocytochemistry. HeLa cells were immunostained with an anti-HSP70 as described in section 4.2.1. Under basal conditions, HSP70 was expressed mainly in the cytoplasm with low expression in the nucleus and a similar pattern was observed following celastrol treatment (Figure 4.5A), suggesting it had no effect on HSP70 induction. However, increased HSP70 expression was seen in the nucleus and cytoplasm following 17-DMAG alone and DM-Ce and the cell morphology was also altered (Figure 4.5A) with the cells appearing larger. To quantify HSP70 expression, the intensity of HSP70 immunofluorescence was calculated using ImageJ. Treatment with celastrol resulted in a slight increase in HSP70 (208.80±49.03) but was not significantly different to control cells or 17-DMAG. In contrast, treatment with 17-DMAG alone and DM-Ce resulted in higher expression of HSP70 (360.90±60.30 and 424.60±180.00, $P<0.05$), respectively compared to controls (95.23±19 Figure 4.5B). Moreover, analysis of HSP70 by western blotting also showed an increase in HSP70 expression following 17-DMAG and DM-Ce (Figure 4.5C).

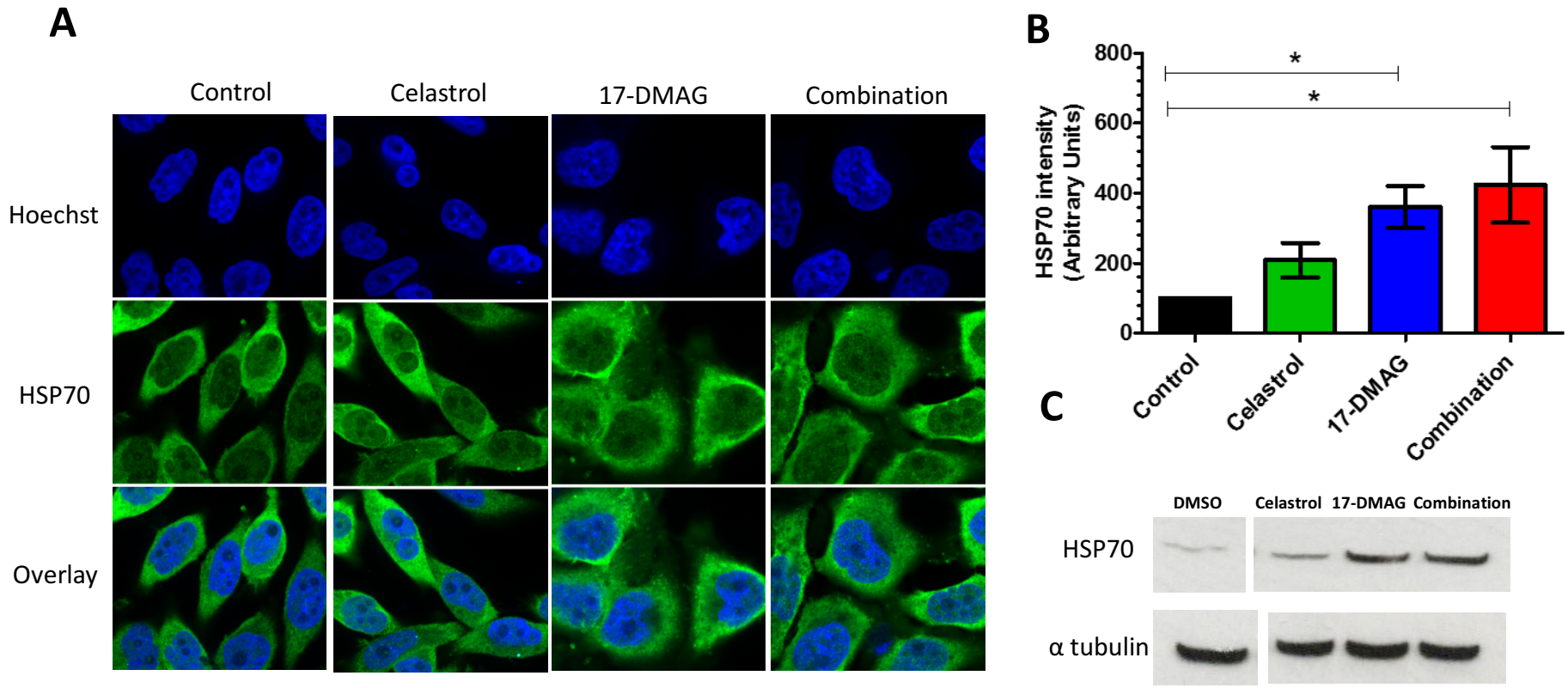

Figure 4.5 HSP70 induction following treatment with HSP90 inhibitors. (A) HeLa cells were treated with celastrol, 17-DMAG and DM-Ce using the IC_{50} doses for 48h. Cells were then immunostained with an anti-HSP70 primary antibody and visualised with Alexa 488 secondary antibody (green). Cells were also stained with Hoechst for nuclear visualisation (blue). Images were captured using a 63x lens confocal laser microscope. (B) Bar graph represents HSP70 intensities calculated in 200 cells using ImageJ. Data was analysed by one-way ANOVA. Values represent mean±SD of 3 independent experiments. * = $P<0.05$. (C) A representative WB showing HSP70 induction following HSP90 inhibitors from 3 independent experiments.

Next, the aim was to investigate whether 17-DMAG and celastrol trigger nSB formation in a similar way to heat shock and whether SAFB1 is recruited into nSBs. HeLa cells were immunostained with anti-SAFB1 and anti-HSF1 primary antibodies as described in section 4.2.1. Under basal conditions, SAFB1 and HSF1 are expressed in the nucleus with HSF1 also expressed weakly in the cytoplasm (Figure 4.6A). Following celastrol treatment, SAFB1 formed several small puncta within the nucleus whilst HSF1 remained diffuse in the nucleus and cytoplasm, suggesting celastrol did not induce the nSB stress response. Following treatment with 17-DMAG alone and DM-Ce, HSF1 was observed in a few punctate structures similar to nSBs. However, although SAFB1 puncta were observed following treatment with 17-DMAG alone and DM-Ce, these did not colocalise with HSF1 puncta (Figure 4.6A). HS+NR treatment induced HSF1 puncta co-localised with SAFB1, as seen previously (Figure 4.2) and also caused SAFB1 to have a more punctate distribution in the nucleus. Subsequently, the percentage of cells with HSF1 puncta was counted following HSP90 inhibitors and HS+NR. Results showed that HS+NR treated cells had a higher number of HSF1 puncta (59.52±10.32%, $P \leq 0.001$) compared with 17-DMAG alone (18.16±4.07%) and DM-Ce (17.36±3.67%, Figure 4.6B). Cells with HSF1 puncta following treatment with 17-DMAG alone were similar compared with DM-Ce. There were no HSF1 puncta following treatment with celastrol.

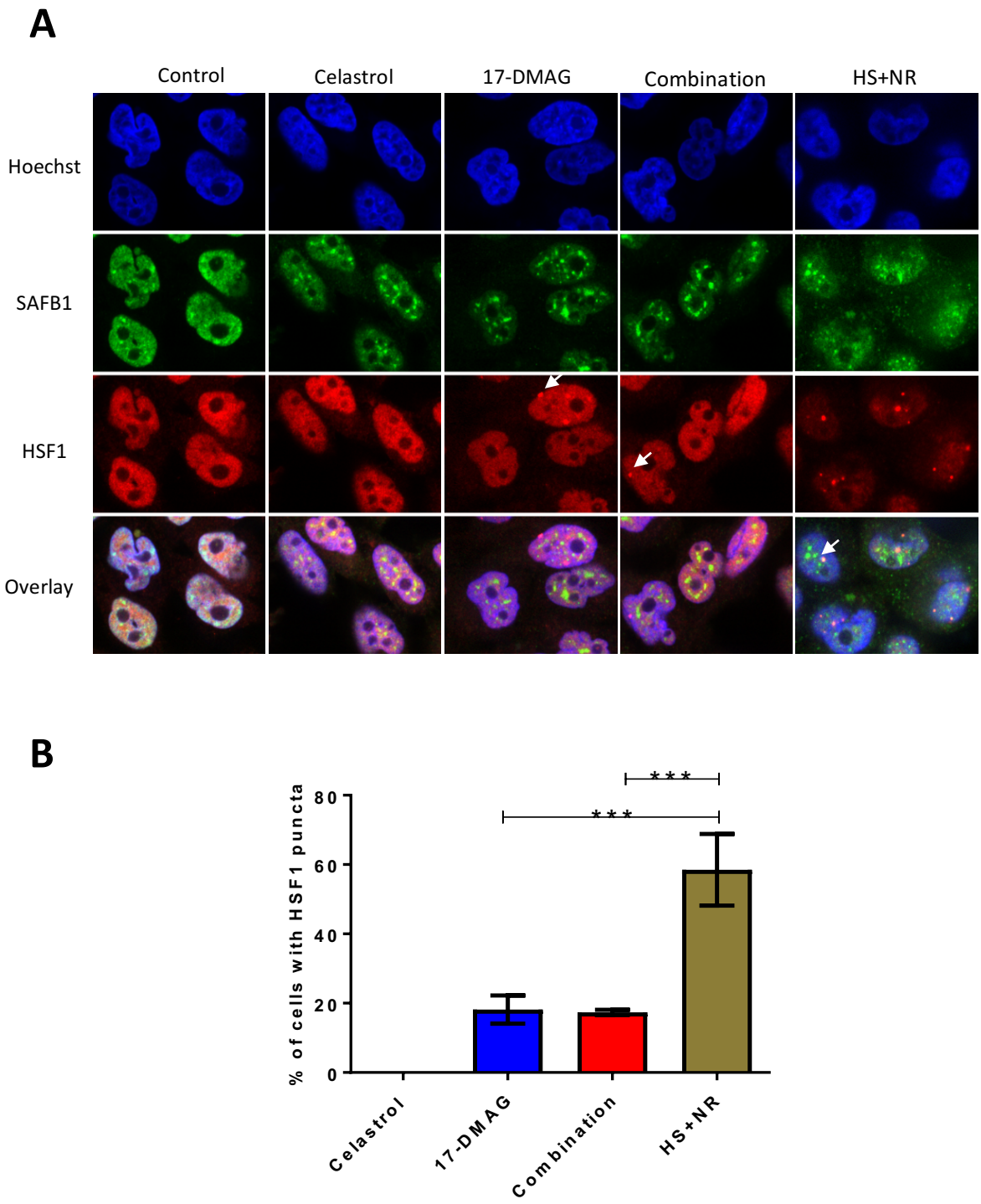

Figure 4.6 SAFB1 and HSF1 localisation following treatment with HSP90 inhibitors. (A) HeLa cells were treated with celastrol, 17-DMAG and DM-Ce using the IC_{50} doses for 48h. Cells were immunostained with anti-SAFB1 and anti-HSF1 primary antibodies and visualised with Cy2 (green) and Cy3 (red) secondary antibodies respectively. Hoechst was used to stain the nucleus (blue). Images were captured using a 63x lens confocal laser microscope. (B) The percentage of cells with HSF1 puncta were counted in 200 cells indicated by arrows using ImageJ. Data was analysed by one-way ANOVA. Values represent mean±SD of 4 independent replicates. *** = P≤0.001.

Also, we investigated whether 17-DMAG and celastrol alters SAFB2 expression and lead to its recruitment into nSBs as seen following heat shock. Cells were immunostained with anti-SAFB2 and anti-HSF1 as described in section 4.2.1. Under basal conditions, SAFB2 and HSF1 are expressed in the nucleus with HSF1 being also expressed weakly in the cytoplasm. Results also showed that following celastrol treatment, SAFB2 expression was not altered and HSF1 staining remained diffuse in the nucleus and cytoplasm, suggesting celastrol is not inducing a stress response. In contrast, HSF1 was found in nuclear puncta following treatment with 17-DMAG alone and with DM-Ce. However, unlike after heat shock, SAFB2 was not recruited into HSF1 puncta following 17-DMAG treatment (Figure 4.7A). HS+NR treatment induced HSF1 puncta, as seen previously, and also caused SAFB2 to be recruited into nSBs overlapping with HSF1. Subsequently, the percentage of cells with HSF1 puncta was counted following treatment with inhibitors and HS+NR. In agreement with the data in Figure 4.6B results showed that HS+NR had higher percentage (64.25±6.48%) of HSF1 puncta compared with 17-DMAG alone (14.37±1.37%) and DM-Ce (12.39±1.10%, $P \leq 0.001$, Figure 4.7B). In contrast, treatment with celastrol did not result in HSF1 puncta.

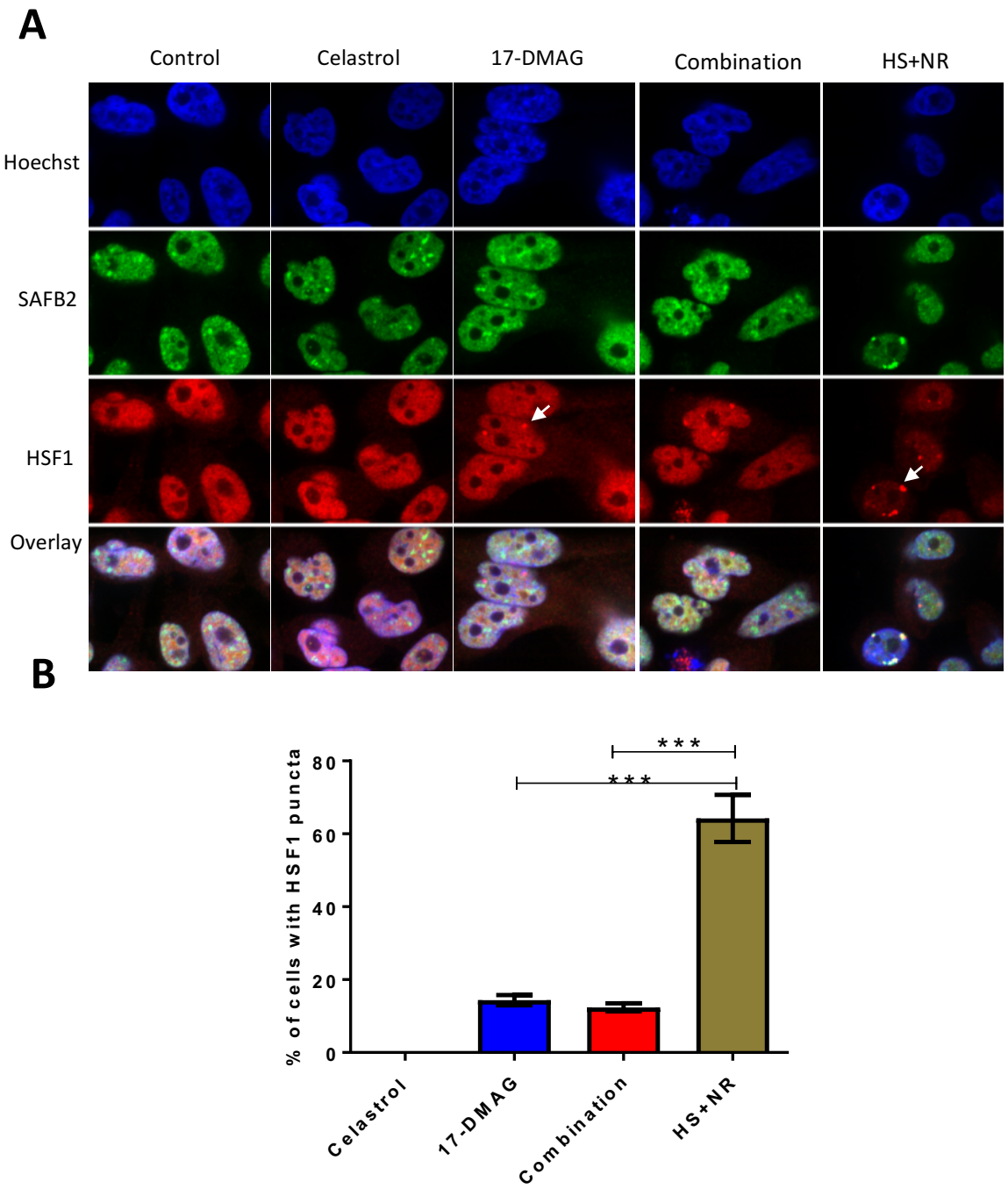

Figure 4.7 SAFB2 and HSF1 localisation following treatment with HSP90 inhibitors. (A) HeLa cells were treated with celastrol, 17-DMAG and DM-Ce using the IC_{50} doses for 48h. Cells were immunostained with anti-SAFB2 and anti-HSF1 primary antibodies and visualised with Cy2 (green) and Cy3 (red) secondary antibodies respectively. Hoechst was used to stain the nucleus (blue). Images were captured using a 63x lens confocal laser microscope. (B) The percentage of cells with HSF1 puncta were counted in 200 cells indicated by arrows using ImageJ. Data was analysed by one-way ANOVA. Values represent mean±SD of 4 independent replicates. *** = P≤0.001.

4.2.2 Investigating the stress response following heat shock in primary ALL cells

The ability of primary ALL cells to generate nSBs following heat shock and induce HSP70 has never been explored. Further, the altered SAFB1 and SAFB2 expression ratio found in BCP-ALL and T-ALL cancers, suggest the nuclear stress response may be altered in ALL cells. To characterise the stress response in ALL, compared to normal haemopoietic cells, BCP-ALL (n=3), T-ALL (n=3), and NBM (n=3) cells were heat shocked at 42^0 C for 1 hour and followed by 0 hours recovery (HS+NR) or 1 hour recovery (HS+R). Cells were immunostained with an anti-HSP70 primary antibody as described in section 4.2.1. to examine the stress response.

Under basal conditions, HSP70 was expressed mainly in the cytoplasm. After HS+NR and HS+R, HSP70 was expressed in the nucleus and cytoplasm of NBM (Figure 4.8A), BCP-ALL (Figure 4.8B) and T-ALL cells (Figure 4.8C), indicating that cells are under stress. To quantify the nuclear HSP70 expression, the fluorescence intensity was measured. HSP70 expression was significantly increased following heat shock (HS+NR) in BCP-ALL (from 5.66±1.54 to 9.50±1.32) and T-ALL (from 5.89±1.09 to 9.33±1.52, $P<0.05$) compared with controls (NHS, Figure 4.8D). However, no significant difference in HSP70 expression was observed following heat shock (HS+NR) and the recovery period (HS+R) in BCP-ALL and T-ALL compared with NBM. HSP70 expression was found to be lower following the recovery period (HS+R) compared with HS+NR in NBM (7.36±1.50), BCP-ALL (7.27±1.47) and T-ALL (97.99±1.24) but no significant difference was observed.

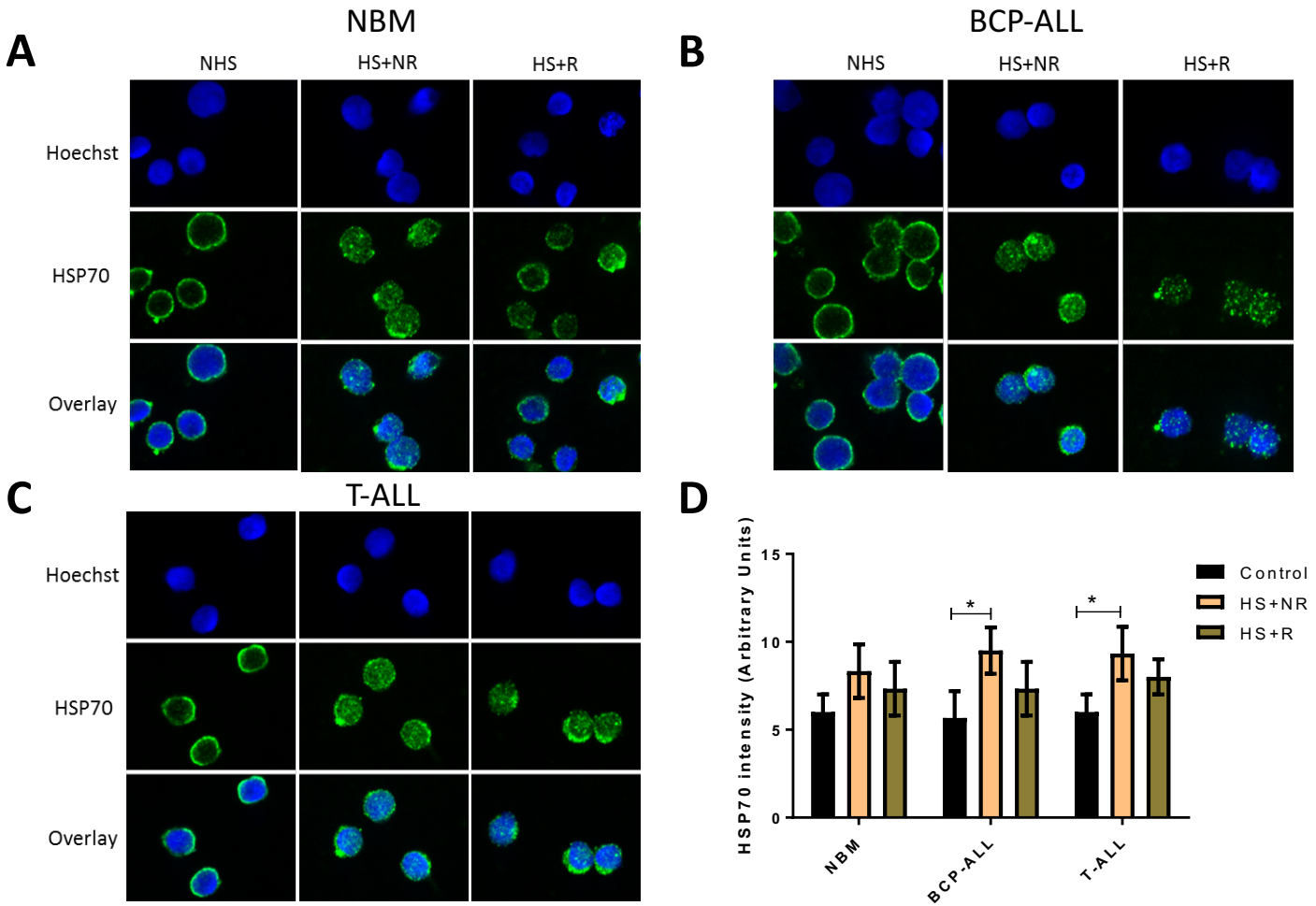

Figure 4.8 HSP70 induction after HS in ALL. (A) NBM, (B) BCP-ALL and (C) T-ALL cells were heat shocked at 42^0 C and immunostained with an anti-HSP70 primary antibody and visualised with Alexa 488 secondary antibody (green). Cells were also stained with Hoechst for nuclear visualisation (blue). Images were captured using a 63x lens confocal laser microscope. (D) Bar graph represents HSP70 intensities calculated in 200 cells (2 replicates) using ImageJ in 3 independent experiments. Data was analysed by two-way ANOVA. Values represent mean±SD of 3 independent patient samples. * = P<0.05.

SAFB1 and HSF1 were found to be recruited into nSBs following heat shock (HS+R) in HeLa cells (Figure 4.2). To monitor the distribution of HSF1 and SAFB1 expression in primary ALL, cells were immunostained with anti-SAFB1 and anti-HSF1 primary antibodies as described in section 4.2.1. Under basal conditions, SAFB1 was expressed in the nucleus, whereas HSF1 was found in the nucleus and cytoplasm in all cell types. After HS+NR and HS+R, HSF1 expression was altered, with a weaker diffuse nuclear and pronounced nuclear border expression observed in NBM (Figure 4.9A), BCP-ALL (Figure 4.9B) and T-ALL (Figure 4.9C). SAFB1 expression remained the same and was not recruited into HSF1 sites. To quantify SAFB1 and HSF1 expression, the fluorescence intensity was measured. There was no significant difference in SAFB1 expression in BCP-ALL (13.95±1.94 and 15.33±2.08) and T-ALL cells (15.46±2.25 and 12.36±3.51) compared with NBM (12.89±2.64 and 12.66±1.54) following heat shock (HS+NR) and the recovery period (NH+R, Figure 4.9D) respectively. There was a significant increase in HSF1 expression under basal conditions in BCP-ALL (18.33±2.09) and T-ALL (19.66±2.15, $P<0.05$) cells compared with NBM (13.29±1.58, Figure 4.9E). Also, there was a slight increase in HSF1 expression in BCP-ALL (13.38±3.05) and T-ALL cells (15.42±1.96) following heat shock (HS+NR) compared with NBM (9.98±1.88) but no significant difference was observed. Next, the percentage of cells with the HSF1 nuclear border staining was counted. Results showed that HSF1 nuclear border staining increased significantly following HS+NR in BCP-ALL (68.40±16.28) and T-ALL (58.08±13.00, $P\leq0.01$) compared with NBM (12.00±2.23, Figure 4.9F). There was also a significant increase in HSF1 nuclear border staining following HS+R in BCP-ALL (61.26±12.17) and T-ALL (43.38±8.15, $P\leq0.01$) compared with NBM (17.35±2.70).

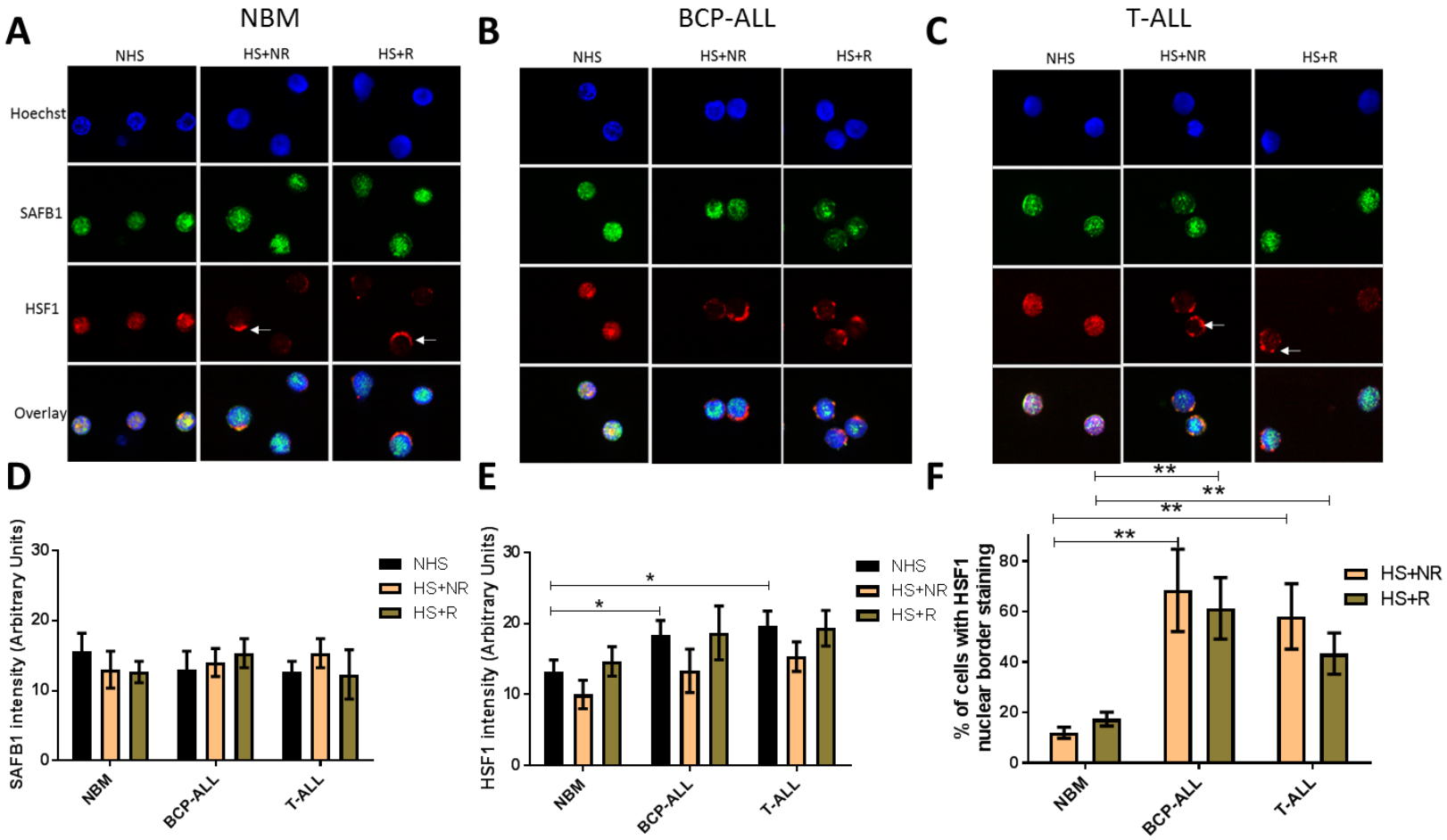

Figure 4.9 SAFB1 and HSF1 expression in ALL after HS. (A) NBM, (B) BCP-ALL and (C) T-ALL cells were heat shocked at 42^0 C and immunostained with anti-SAFB1 and anti-HSF1 primary antibodies and visualised with Cy2 (green) and Cy3 (red) secondary antibodies respectively. Hoechst was used to stain the nucleus (blue). Images were captured using a 63x lens confocal laser microscope. (D-F) Bar graph represents SAFB1, HSF1 intensities and the percentage of cells with HSF1 nuclear border staining respectively quantified in 200 cells (2 replicates) indicated by white arrows using ImageJ. Data was analysed by two-way ANOVA. Values represent mean±SD of 3 independent patient samples. * = $P<0.05$, ** = $P\leq0.01$.

Anti-SAFB2 and anti-HSF1 primary antibodies were used to immunostain ALL cells as described in section 4.2.1. Under basal conditions, SAFB2 was expressed in the nucleus, whereas HSF1 was found in the nucleus in all cell types (Figure 4.10A-C). Following heat shock, SAFB2 expression remained unchanged. To quantify SAFB2 expression the fluorescence intensity was measured. Like SAFB1, there was no significant difference in SAFB2 expression in BCP-ALL (16.33±3.21, 15.39±2.11, 12.66±1.52) and T-ALL cells (15.67±2.51, 12.88±2.64, 12.29±3.54) compared with NBM (12.61±1.45, 13.87±1.92, 15.34±2.10) under basal conditions and following heat shock (HS+NR) and the recovery period (NH+R, Figure 4.10D) respectively. As in Figure 4.9F the percentage of cells with the HSF1 nuclear border staining was counted as previously described. Consistent with data in Figure 4.9D, results showed that HSF1 nuclear border staining increased following HS+NR in BCP-ALL (74.20±6.83) and T-ALL (61.40±11.12, $P \leq 0.01$) compared with NBM (15.40±3.84, Figure 4.10F). There was a significant increase in HSF1 nuclear border staining following HS+R in BCP-ALL (61.40±11.12) and T-ALL (47.36±6.21, $P \leq 0.01$) compared with NBM (17.40±2.70). There was no significant difference following heat shock (HS+NR) compared with the recovery period (NH+R) in BCP-ALL (74.20±6.83, 61.40±11.12), T-ALL (61.40±11.12, 47.36±6.21) compared with NBM (15.40±3.84, 17.40±2.70, Figure 4.10F).

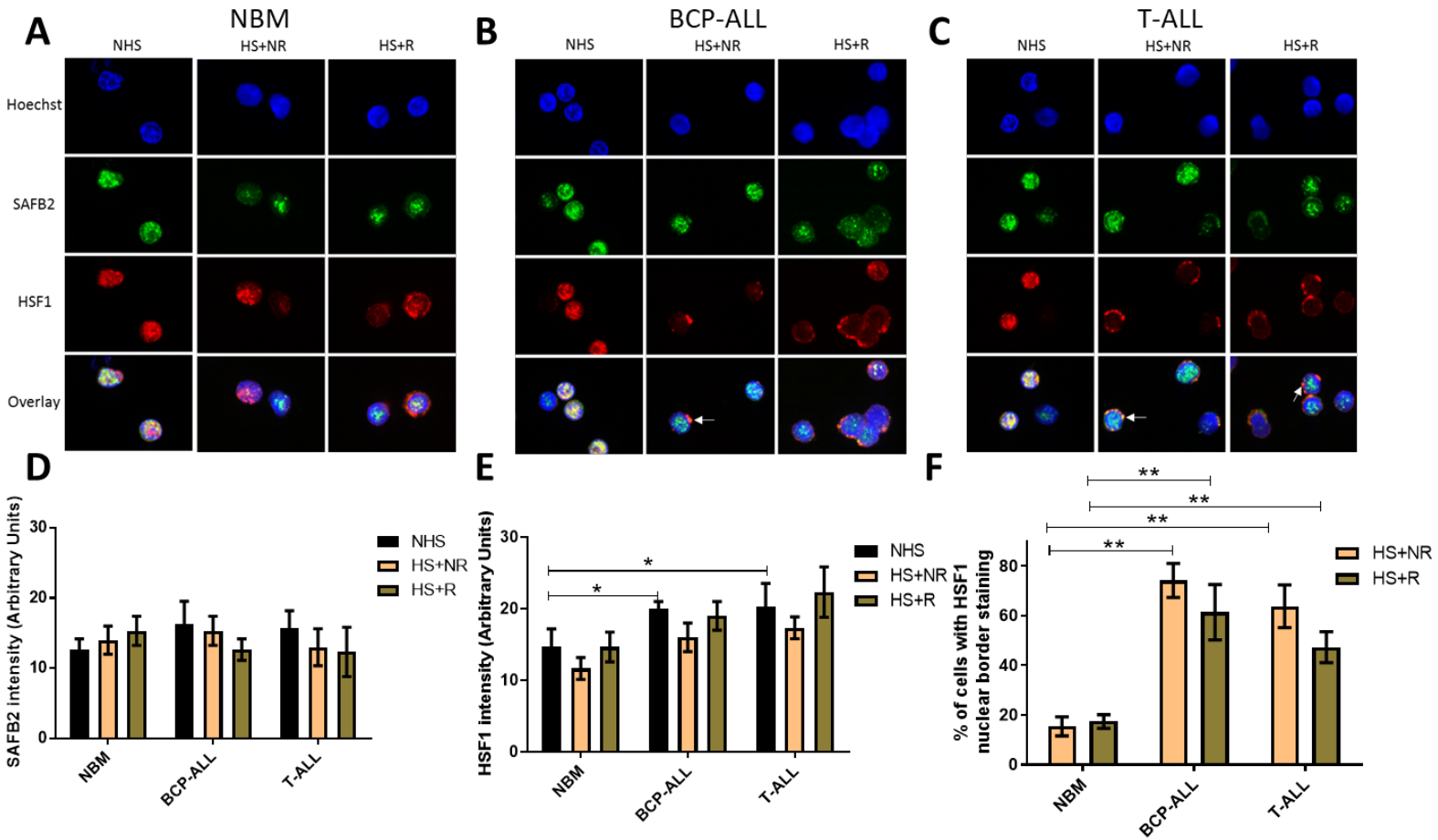

Figure 4.10 SAFB2 and HSF1 expression in ALL after HS. (A) NBM, (B) BCP-ALL and (C) T-ALL cells were heat shocked at 42^0 C and immunostained with anti-SAFB2 and anti-HSF1 primary antibodies and visualised with Cy2 (green) and Cy3 (red) secondary antibodies respectively. Hoechst was used to stain the nucleus (blue). Images were captured using a 63x lens confocal laser microscope. (D-F) Bar graph represents SAFB2, HSF1 intensities and the percentage of cells with HSF1 nuclear border staining respectively quantified in 200 cells (2 replicates) indicated by white arrows using ImageJ. Data was analysed by two-way ANOVA. Values represent mean±SD of 4 independent patient samples. * = $P<0.05$, ** = $P\leq0.01$.

4.2.3 Effect of HSP90 inhibitors on the viability of primary ALL cells

As inhibitors of HSP90 are used to preferentially kill cancers cells *in vitro* we investigated the effect of HSP90 inhibitors on the viability of ALL cells. BCP-ALL, T-ALL and NBM cells (all, n=4) were treated with increasing concentrations of 17-DMAG and celastrol as single agents for 24 and 48 hours and viability was monitored using Annexin-V and PI (Figure 4.11). Initial results showed that cells from 4 T-ALL cases treated with a concentration range from 0.01 to 1000nM celastrol were unaffected at concentrations up to 100nM with a drop in viability from 73.66±13.10% to 29.98±12.63% at 24h and from 67.61±11.19% to 23.22±9.98% at 48h between 100 and 1000nM doses, suggesting that the drug's effectiveness was within this range. Therefore, additional concentrations of celastrol within this range were used to treat cells from 4 additional T-ALL cases to give a dose response curve and determine the IC_{50}. Similarly, T-ALL cells responded to 17-DMAG at concentrations just under 1000nM, so further concentrations up to 2000nM were used to generate a dose response curve and calculate the IC_{50}. The IC_{50} for celastrol in T-ALL was 467.03nM at 24h and 431.37nM at 48h. In contrast, the IC_{50} for 17-DMAG in T-ALL was 861.20nM at 24h and 574.64nM at 48h. BCP-ALL cells responded to lower doses of celastrol (IC_{50} of 50.55nM at 24h and 47.69nM at 48h) and 17-DMAG (IC_{50} of 6.63nM at 24h and 0.83nM at 48h) than T-ALL. In contrast, NBM cells were relatively resistant with viabilities of 63.36±4.52% and 56.82±7.39% at the highest doses of celastrol (1μM) and 62.58±7.73% and 54.07±13.49% of 17-DMAG (2μM) at 24 and 48h, respectively.

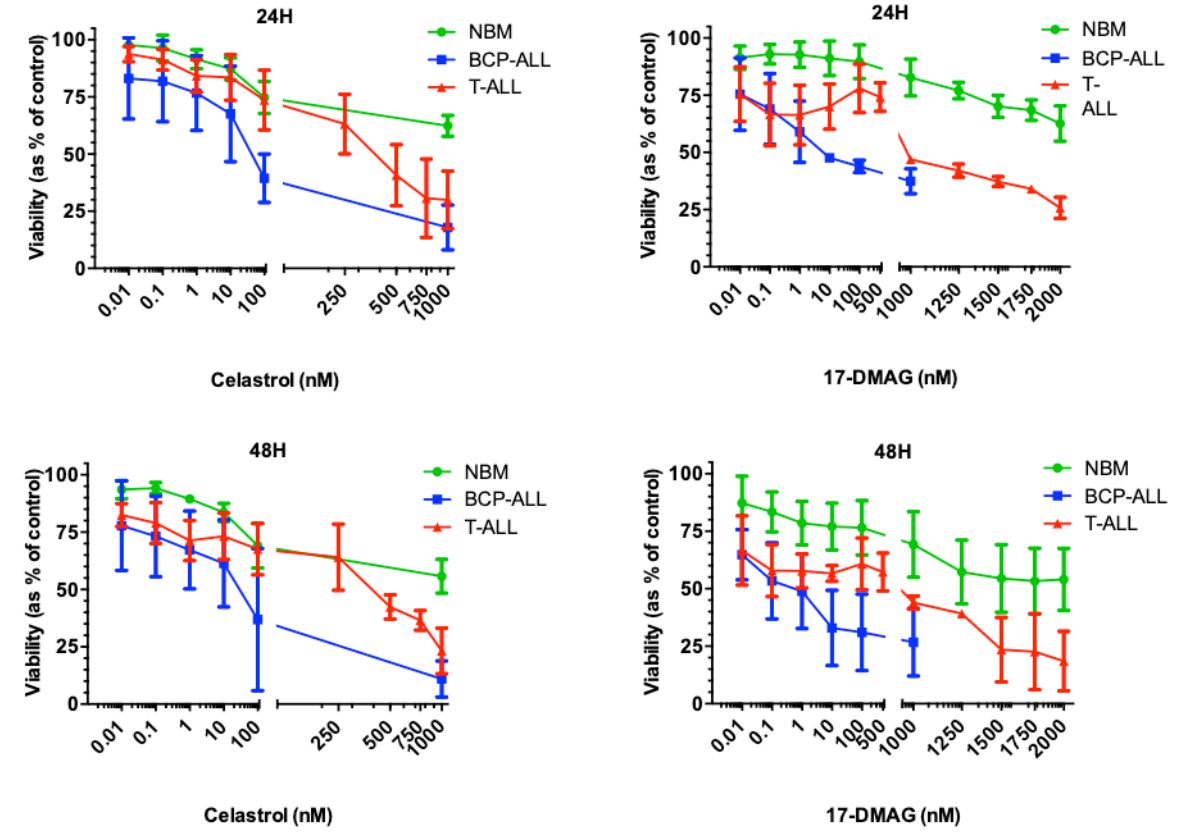

Figure 4.11 Response of primary ALL cells to HSP90i. BCP-ALL, T-ALL and NBM cells were treated with increasing concentrations of celastrol (0.01-1000nM) and 17-DMAG (0.01-2000nM) for 24 and 48 hours. Viability was assessed using annexin-V/PI assay. Viability was determined as a percentage of the untreated control cells. Data was analysed by two-way ANOVA. Values represent mean±SD of 4 independent patient samples.

17-DMAG and celastrol induced apoptosis in BCP-ALL cells when used as single agents. Subsequently, the effects of using both drugs in combination were examined and the Chou Talalay test was used to determine whether effects were additive, synergistic or antagonistic. The Chou Talalay method is calculated on the basis of median-effect equation and the mass-action law theory (153). The IC_{50} doses were used in this method with 2 and 4-fold higher (IC_{50}*2, IC_{50}*4) and lower (IC_{50}/2, IC_{50}/4) doses. The doses selected were based on IC_{50} values of 17-DMAG (6.63nM at 24h and 0.83nM at 48h) and celastrol (50.55nM at 24h and 47.69nM). The dose range for 17-DMAG was 1.6-26.5nM for 24h and 0.20-3.3nM for 48h, whilst the dose range for celastrol was 12.63-202.nM for 24h and 11.92-190.76nM for 48h. Combining 17-DMAG with celastrol showed no effect on cytotoxicity for 24 and 48 hours at any dose compared to either drug alone (Figure 4.12). Results also showed that the combined drugs at the IC_{50} dose reduced viability slightly to 46.75±8.22% compared with individual drugs at 24h where celastrol and 17-DMAG reduced viability to 51.26±11.16% and 55.08±12.45%, respectively (Figure 4.12A). Data in Figure 4.12B showed that combining both drugs resulted in slight reduction in viability to 52.28±7.42% compared with 56.48±4.73% and 60.08±9.82% with celastrol and 17-DMAG alone, respectively at 48h. However, this was not significantly different compared with individual drugs.

The effects of each drug as a single agent or in combination were used to derive the combination index (CI). The CI gives a quantitative measurement and reveals whether the drug has an additive effect (CI = 1), synergistic effect (CI < 1), or antagonistic effect (CI > 1). Results showed that combining both drugs resulted in drug antagonism for 24 and 48 hours indicated by high CI values in all doses tested. Using both drugs at the lowest combination dose (IC_{50}/4) resulted in CI value of 1.1 at 24h. The CI was slightly higher (1.3) following treatment with IC_{50} and IC_{50}*4. Furthermore, there was an increase in the CI following the treatment with IC_{50}*2 with CI value of 2. However, the highest CI was seen with IC_{50}/2 dose at 24h, reaching 2.2 (Figure 4.12). Results showed that IC_{50}/4, IC_{50}/2, IC_{50} and IC_{50}*4 resulted in a CI values of 1.4, 1.6, 1.6 and 1.9 respectively at 48h. The highest CI was observed at IC_{50}*2, reaching 2.2 (Figure 4.12).

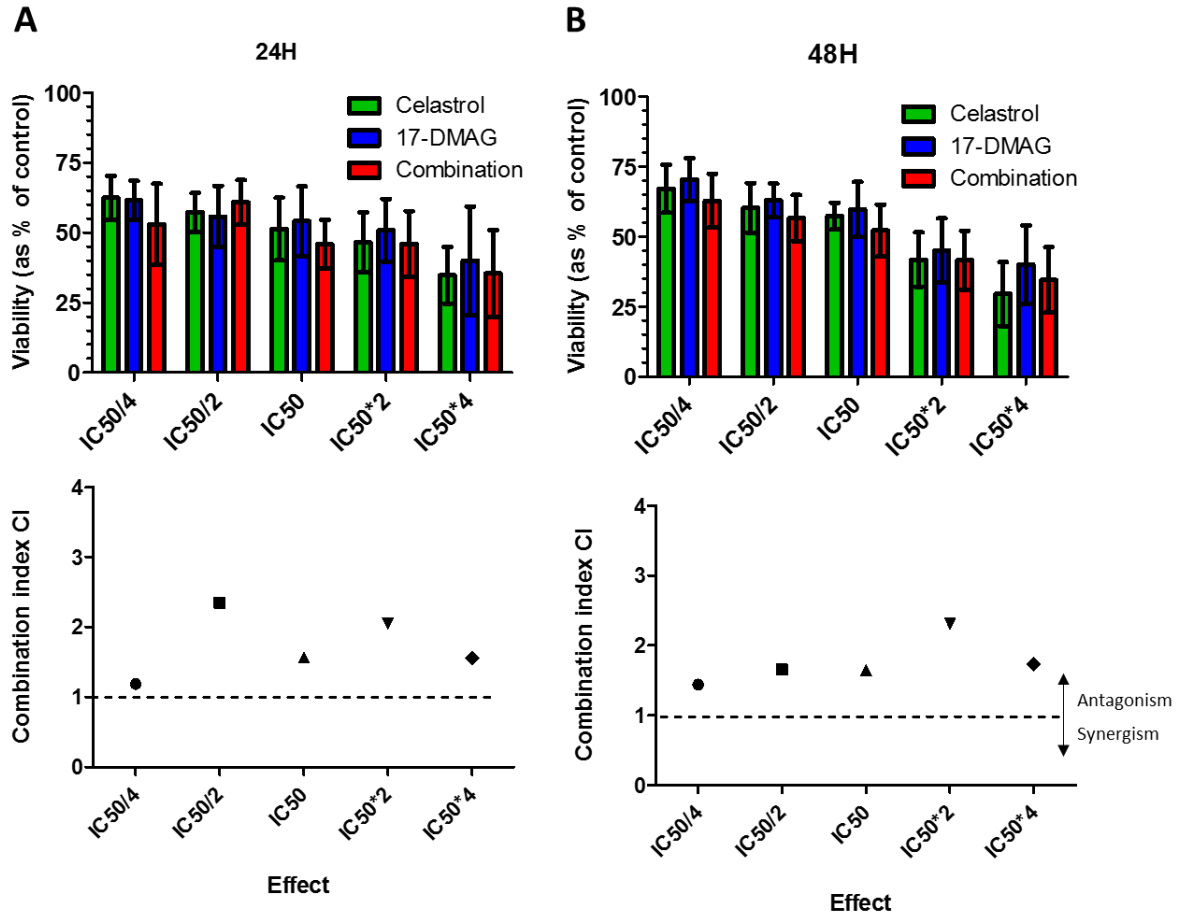

Figure 4.12 Drug synergy of celastrol and 17-DMAG in BCP-ALL. (A) BCP-ALL cells were treated with celastrol (12.63-202.nM, green), 17-DMAG (1.6-26.5nM, blue) and in combination (red) for 24 hours. (B) Cells were also treated with 17-DMAG (0.20-3.3nM, green), celastrol (11.92-190.76nM, blue) and in combination (red) for 48 hours. Viability was assessed using annexin-V/PI assay. Values represent mean±SD of 3 independent patient samples. Data was analysed by two-way ANOVA. The combination index represents the drug antagonism between 17-DMAG and celastrol at 24 and 48 hours.

Similar to BCP-ALL, 17-DMAG and celastrol induced apoptosis in T-ALL cells when used as single agents. Next, it was investigated whether using both drugs in combination enhanced cytotoxicity. As in Figure 4.12, 17-DMAG and celastrol were combined to assess cytotoxicity using the Chou Talalay test. The doses selected were based on IC_{50} values of 17-DMAG (6.63nM at 24h and 0.83nM at 48h) and celastrol (50.55nM at 24h and 47.69nM). The dose range for 17-DMAG was 1.6-26.5nM for 24h and 0.20-3.3nM for 48h, while the dose range for celastrol was 12.63-202.nM for 24h and 11.92-190.76nM for 48h. Results showed that combining 17-DMAG with celastrol showed no effect on viability for 24 and 48 hours in doses tested compared to either drug alone. Data in Figure 4.13A showed that combining the drugs at IC_{50} reduced viability to 49.23±7.68% compared with either drug alone at 24h, where viability was 58.32±6.78% and 61.93±4.95% with celastrol and 17-DMAG, respectively. Also, data in Figure 4.13B showed a slight reduction in viability to 45.83±18.03% with the combined drugs compared with 53.65±6.18% and 55.20±16.65% with celastrol and 17-DMAG alone, respectively at 48 hours. However, it was not significant.

Combined dosing of 17-DMAG with celastrol showed drug antagonism indicated by high CI values for 24 and 48 hours, reaching 3 at $IC_{50}/2$ dose at 24h (Figure 4.13). The CI value was 2 at IC_{50} and $IC_{50}/4$ doses, whilst the higher doses (IC_{50}*2, IC_{50}*4) resulted in higher CI values at 2.5 and 2.8 at 24h, respectively. At the 48h time point, the CI values were similar at IC_{50} and $IC_{50}/4$ doses, (1.5). However, the CI values were higher following treatment with IC_{50}*2 and IC_{50}*4 with 1.8 and 1.9 respectively. The highest CI was observed at $IC_{50}/2$, reaching 2.1 (Figure 4.13).

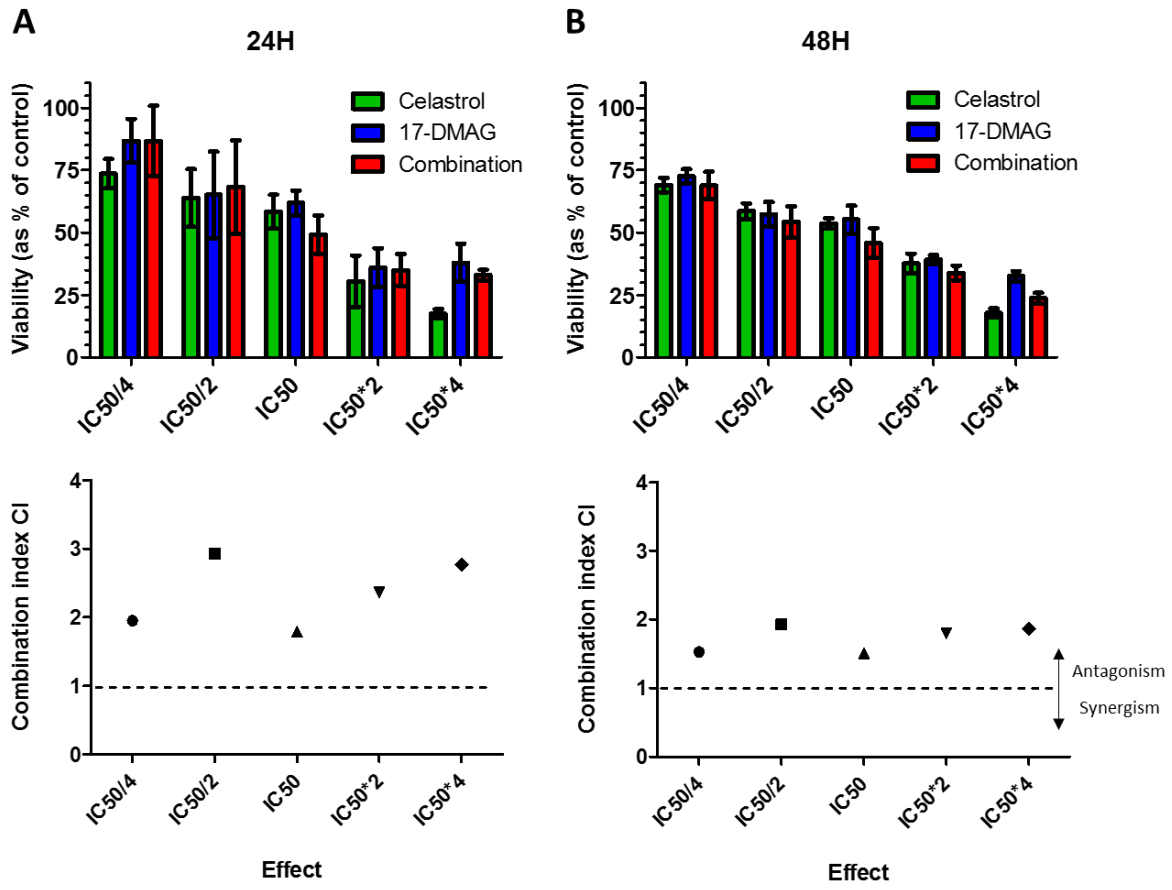

Figure 4.13 Drug synergy of celastrol and 17-DMAG in T-ALL. (A) T-ALL cells were treated with celastrol (116.8-1669.2nM, green), 17-DMAG (215.3-3444.8nM, blue) and in combination (red) for 24 hours. (B) Cells were also treated with 17-DMAG (143.6-2298.4nM, green), celastrol (107.8-1725.2nM, blue) and in combination (red) for 48 hours. Viability was assessed using annexin-V/PI assay. Values represent mean±SD of 3 independent patient samples. Data was analysed by two-way ANOVA. The combination index represents the drug antagonism between 17-DMAG and celastrol at 24 and 48 hours.

4.2.4 Validating the effectiveness of pharmacological inducers (HSP90i) of a stress response in primary ALL cells

17-DMAG caused HSP70 induction in HeLa cells. However, it has not been investigated if HSP70 is induced following HSP90i (17-DMAG and celastrol) in primary ALL cells. To this end, BCP-ALL, T-ALL and NBM cells (n=3) were treated with IC_{50} doses for 24h as described in Figure 4.12 and Figure 4.13. Cells were immunostained with an anti-HSP70 primary antibody as described in section 4.2.1. Under basal conditions, HSP70 was expressed mainly in the cytoplasm in all cell types. Following celastrol and 17-DMAG treatments, there was an increase in the nuclear expression of HSP70 in NBM (Figure 4.14A), BCP-ALL (Figure 4.14B) and T-ALL (Figure 4.14C) cells, indicating that cells are under stress. Quantification of the nuclear HSP70 fluorescence intensity revealed that HSP70 was significantly overexpressed following 17-DMAG in BCP-ALL (9.95±1.24, $P<0.05$) and T-ALL (11.22±1.48) compared with NBM (7.06±1.56, Figure 4.14D). Furthermore, HSP70 was overexpressed following 17-DMAG in BCP-ALL (from 5.87±1.08 to 9.95±1.24), T-ALL (from 6.33±0.60 to 11.22±1.48) and NBM (from 4.90±1.00 to 7.06±1.56, $P<0.05$) compared with controls (no treatment). There was no increase in the nuclear expression of HSP70 following celastrol in BCP-ALL and T-ALL compared with NBM. There was an increase in HSP70 expression following DM-Ce in BCP-ALL (9.33±1.52) and T-ALL (10.66±2.51) cells compared with NBM (6.37±1.71) but there was no significant difference.

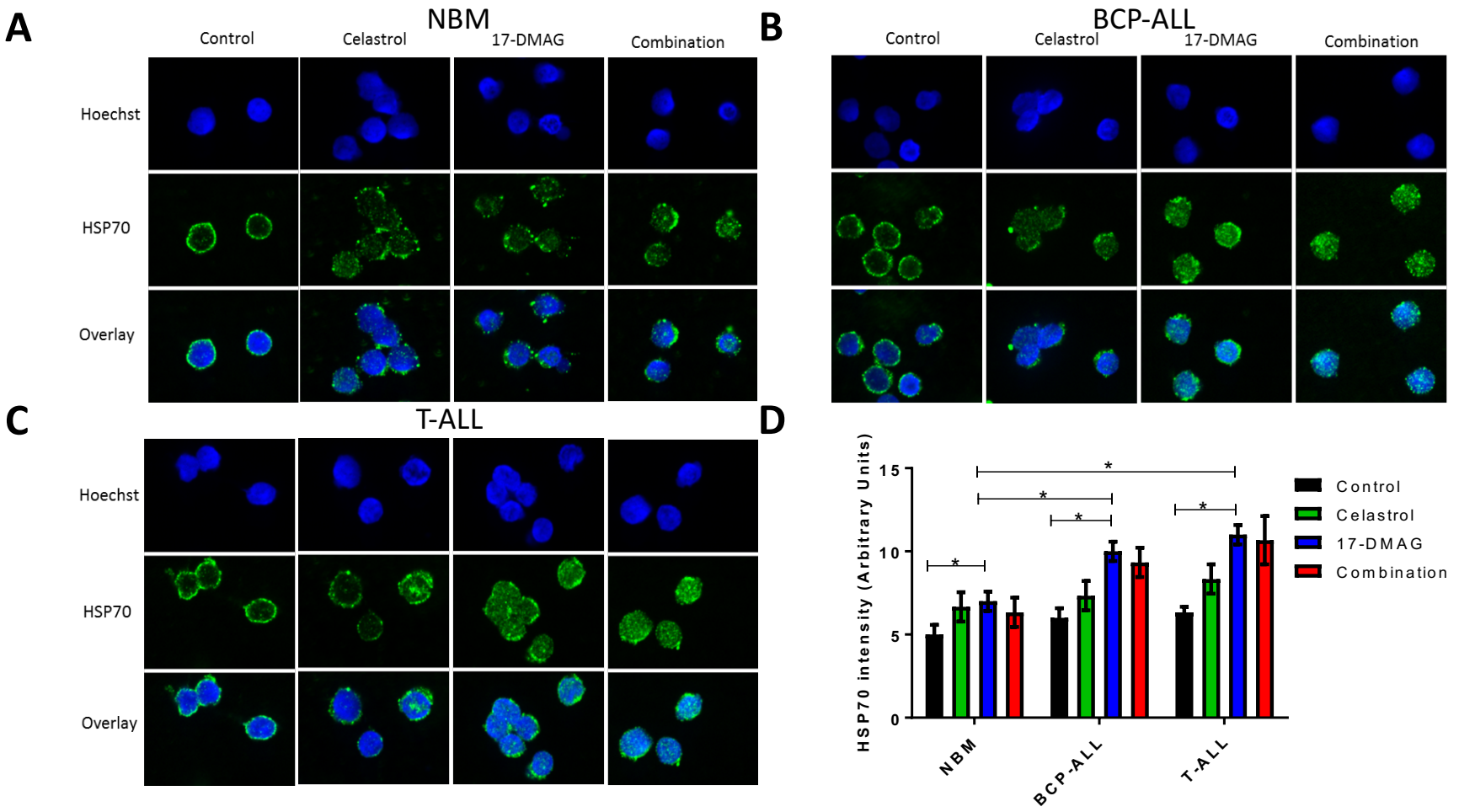

Figure 4.14 HSP70 induction in ALL after HSP90i treatment. (A) NBM, (B) BCP-ALL and (C) T-ALL cells were treated with celastrol, or 17-DMAG and DM-Ce using the IC_{50} doses for 24h. Cells were immunostained with an anti-HSP70 primary antibody and visualised with Alexa 488 secondary antibody (green). Cells were also stained with Hoechst for nuclear visualisation (blue). Images were captured using a 63x lens confocal laser microscope. (D) Bar graph represents HSP70 intensities calculated in 200 cells (2 replicates) using ImageJ. Data was analysed by two-way ANOVA. Values represent mean±SD of 4 independent patient samples. * = P<0.05.

To monitor the distribution of HSF1 and SAFB1 following 17-DMAG and celastrol in primary ALL cells were immunostained with anti-SAFB1 and anti-HSF1 primary antibodies as described in section 4.2.1. Under basal conditions, SAFB1 was expressed in the nucleus, whereas HSF1 was found in the nucleus and cytoplasm in all cell types. Data also showed that SAFB1 expression remained the same following celastrol and 17-DMAG treatment with no SAFB1 being recruited into HSF1 sites. After celastrol and 17-DMAG treatment, HSF1 expression was altered, with both diffuse nuclear and pronounced nuclear border expression being commonly observed in NBM (Figure 4.15A), BCP-ALL (Figure 4.15B) and T-ALL (Figure 4.15C) in a similar manner to what was seen following heat shock. To quantify SAFB1 and HSF1 expression the fluorescence intensity was measured. Under basal conditions, there was no significant difference in SAFB1 expression in BCP-ALL (12.12±2.64) and T-ALL (12.66±1.52) compared with NBM (15.88±1.88, Figure 4.15D). Data also showed that there was no significant difference in SAFB1 expression in BCP-ALL (12.95±1.90, 15.33±2.08, 13.66±2.11) and T-ALL (15.33±2.08, 12.33±3.51, 13.33±3.21) compared with NBM (12.97±2.64, 12.66±1.52, 13.33±2.51) following celastrol, 17-DMAG and DM-Ce treatment (Figure 4.15D), respectively. Under basal conditions, there was a significant difference in HSF1 expression in BCP-ALL (18.33±2.08) and T-ALL (19.66±2.10, $P<0.05$) cells compared with NBM (13.29±1.58, Figure 4.15E). However, HSF1 expression remained relatively unchanged following celastrol (10.91±1.90), 17-DMAG (12.66±1.62) or DM-Ce (13.33±2.46) in NBM compared with the control (13.29±1.58). However, HSF1 expression was reduced in BCP-ALL (13.87±1.78, 15.33±2.28, 13.73±2.39, 18.33±2.08) and T-ALL (13.53±2.22, 14.30±2.58, 13.47±3.21, 19.66±2.10) following celastrol, 17-DMAG or DM-Ce compared with the control cells but no significant difference was seen. The percentage of cells with the HSF1 nuclear border staining was counted. Results showed that HSF1 nuclear border staining increased following 17-DMAG in BCP-ALL (58.55±8.46) and T-ALL (59.25±8.42, $P<0.05$) compared with NBM (26.17±7.82, Figure 4.15F). Also, there was an increase in HSF1 nuclear border staining following DM-Ce in BCP-ALL (64.50±3.31) and T-ALL (64.50±2.64) but there was no significant difference compared with NBM (31.20±8.90). In contrast, celastrol caused a reduction in HSF1 nuclear border staining in BCP-ALL (11.37±2.42), T-ALL (16.25±4.42) and NBM (21.82±1.85) compared with 17-DMAG (Figure 4.15F).

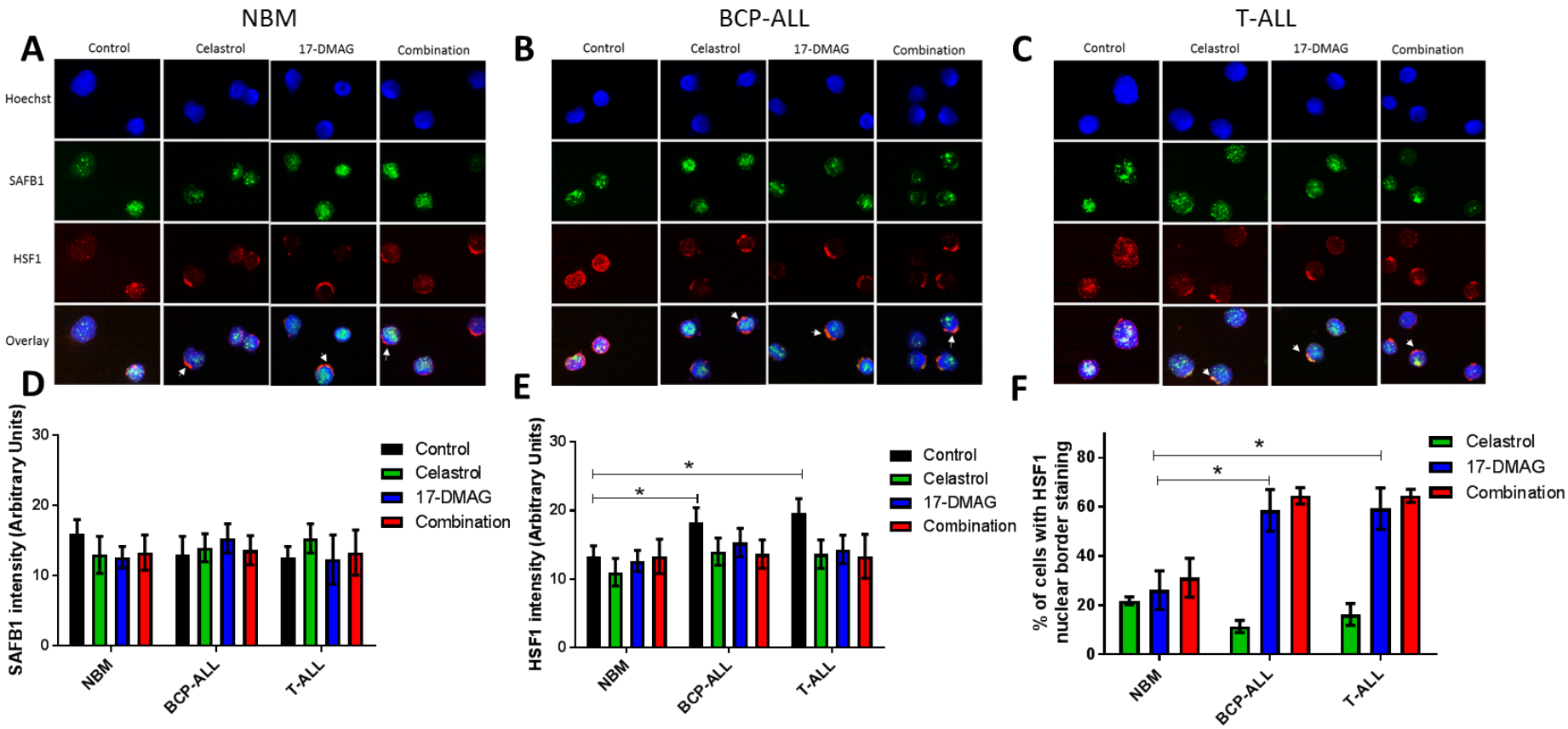

Figure 4.15 SAFB1 and HSF1 expression in ALL after HSP90i treatment. (A) NBM, (B) BCP-ALL and (C) T-ALL cells were treated with celastrol, or 17-DMAG and DM-Ce using the IC_{50} doses for 24h. Cells were immunostained with anti-SAFB1 and anti-HSF1 primary antibodies and visualised with Cy2 (green) and Cy3 (red) secondary antibodies respectively. Cells were also stained with Hoechst for nuclear visualisation (blue). Images were captured using a 63x lens confocal laser microscope. (D-F) Bar graph represents SAFB1, HSF1 intensities and the percentage of cells with HSF1 nuclear border staining respectively quantified in 200 cells (2 replicates) indicated by white arrows using ImageJ. Data was analysed by two-way ANOVA. Values represent mean±SD of 4 independent patient samples. * = $P<0.05$.

Primary ALL cells were also immunostained with anti-SAFB2 and anti-HSF1 primary antibodies as described in section 4.2.1. Under basal conditions, SAFB2 was expressed in the nucleus, whereas HSF1 was found in the nucleus and cytoplasm in all cell types. SAFB2 expression remained unchanged following celastrol and 17-DMAG with no SAFB2 being recruited into HSF1 sites. After celastrol and 17-DMAG, HSF1 expression was altered, with a diffuse nuclear and pronounced nuclear border expression being commonly observed in NBM (Figure 4.16A), BCP-ALL (Figure 4.16B) and T-ALL (Figure 4.16C). To quantify SAFB2 expression the fluorescence intensity was measured. Under basal conditions and following celastrol and 17-DMAG treatment as single drugs or in combination, there was no significant difference in SAFB2 expression in BCP-ALL (16.33±3.21, 13.98±1.91, 15.43±2.61, 13.73±2.58) and T-ALL (15.83±2.51, 15.13±2.31, 12.33±3.41, 13.03±3.23) compared with NBM (12.65±1.52, 12.63±2.64, 12.33±2.41, 12.24±2.11, Figure 4.16D). Consistent with data in Figure 4.15E, there was a slight decrease in HSF1 expression following celastrol and 17-DMAG treatment as individual or combined drugs (DM-Ce) compared with the control cells but no significant difference was observed. However, there was a significant difference in HSF1 expression under basal conditions in BCP-ALL (18.33±2.08) and T-ALL (19.66±2.10, $P<0.05$) cells compared with NBM (13.29±1.58, Figure 4.16E). HSF1 expression remained relatively the same following celastrol, 17-DMAG and DM-Ce treatments in NBM. The percentage of cells with the nuclear border staining was counted. Consistent with Figure 4.15 the results showed that HSF1 nuclear border staining increased following 17-DMAG in BCP-ALL (58.55±8.46) and T-ALL (59.25±8.42, $P<0.05$) compared with NBM (26.17±7.82, Figure 4.16F). Also, there was an increase in HSF1 nuclear border staining following DM-Ce in BCP-ALL (64.50±3.31) and T-ALL (64.50±2.64) but no significant difference was observed compared with NBM (31.20±8.90). In contrast, HSF1 nuclear border staining was comparable across all treatment conditions in NBM. However, HSF1 nuclear border staining was significantly increased in BCP-ALL (58.55±8.46, 64.50±3.31, 11.50±26.13) and T-ALL (59.25±8.42, 64.50±2.64, 17.15±3.32) following 17-DMAG and DM-Ce compared to samples treated with celastrol (Figure 4.16F).

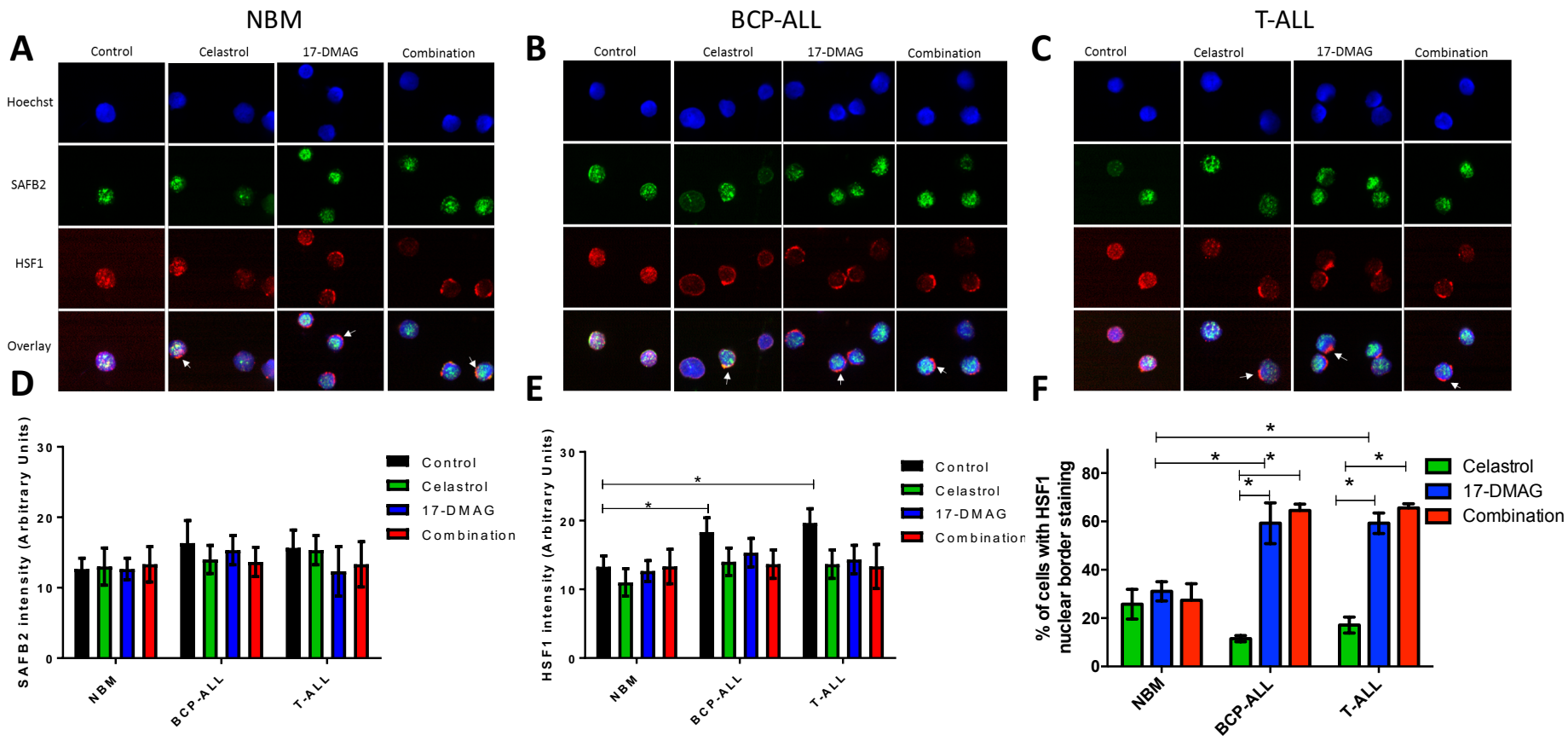

Figure 4.16 SAFB2 and HSF1 expression in ALL after HSP90i treatment. (A) NBM, (B) BCP-ALL and (C) T-ALL cells were treated with celastrol, or 17-DMAG and DM-Ce using the IC_{50} doses and left for 24h. Cells were immunostained with anti-SAFB2 and anti-HSF1 primary antibodies and visualised with Cy2 (green) and Cy3 (red) secondary antibodies respectively. Cells were also stained with Hoechst for nuclear visualisation (blue). Images were captured using a 63x lens confocal laser microscope. (D-F) Bar graph represents SAFB2, HSF1 intensities and the percentage of cells with HSF1 nuclear border staining respectively quantified in 200 cells (2 replicates) indicated by white arrows using ImageJ. Data was analysed by two-way ANOVA. Values represent mean±SD of 4 independent patient samples. * = P<0.05.

4.3 Discussion

The HSP90 inhibitor anti-cancer drugs (celastrol and 17-DMAG) are considered to be inducers of stress response (128),(129),(131) and also induce apoptosis in T-ALL and BCP-ALL cells (95). The transcriptional factor HSF1 controls different transcriptional programmes, such as oncogenic progression, cell cycle regulation and metabolism and HSF1 expression was found to be altered in a wide range of cancers (150),(151). Evidence also shows that SAFB1 localises to nSBs. However, it is not known if its paralogue, SAFB2, also transloctes to nSBs following a stress. The stress response has not been extensively studied following the treatment of cells with HSP90 inhibitors. In HeLa cells, which are known to induce a typical stress response, SAFB1, SAFB2 and HSF1 were recruited into nSBs following heat shock with different kinetics; SAFB2 and HSF1 being recruited first in HeLa cells. This may indicate SAFB2 is needed to stabilise Sat III lncRNAs and/or plays a role in recruiting further proteins to nSBs. Heat shock also caused HSP70 induction. 17-DMAG but not celastrol increased HSP70 expression and induced HSF1 puncta but SAFB1 and SAFB2 were not recruited into HSF1 puncta. HeLa cells treated with17-DMAG and celastrol in combination resulted in higher toxicity (35.75±7.38% viable) at 24 hours and (28.17±2.03% viable) at 48 hours compared to treatment with celastrol alone (52.17±7.60% viable) and (43.16±19.00% viable), respectively. However, there was no significant difference between DM-Ce and 17-DMAG at either timepoint. These data show that 17-DMAG acts as an effective inducer of Hsp70 transcription. As both of these drugs are effective at reducing viability (albeit at different concentrations) these data suggest they may do so via different mechanisms.

During HS, SAFB1 was previously shown to be recruited to distinct bodies, called nSBs during a recovery period at 37^0 C after HS (4), while the role of SAFB2, a paralogue of SAFB1, in cellular stress has not been studied. The present study suggests that SAFB1 is not immediately recruited into nSBs in HeLa cells. SAFB1 starts to move into nSBs after 1 hour of recovery following HS in HeLa cells. HSF1 is the main regulator of HS and so its expression was evaluated in parallel with SAFB1 and SAFB2. The changing expression and kinetics of SAFB2 following HS have not been previously studied. Interestingly, immediately after heat shock at 42^0 C for 1h in HeLa cells HSF1 was found to be recruited into nSBs and co-localised with SAFB2,

suggesting that SAFB2 moves into nSBs earlier than SAFB1. This may indicate SAFB2 is needed to stabilise lncRNAs and/or plays a role in recruiting further proteins to nSBs. Weighardt *et al.* (1999) studied the kinetics of SAFB1 and HSF1 following HS in HeLa cells (4). They found that HSF1 and SAFB1 formed nSBs following HS at 42^0 C for 30 minutes. At 45 and 60 minutes following HS, SAFB1 co-localisation with HSF1 was observed and they accumulated into nSBs. After a 3 hour recovery, SAFB1 was still concentrated in these granules, whereas HSF1 had diffused back to the nuclear compartment. However, in the current study it was found that SAFB2 goes into nSBs immediately after HS, whereas SAFB1 did not. This difference could be explained by the fact that SAFB1 was transfected into cells (i.e. endogenous SAFB1 was not being detected) and that the SAFB1 antibody used by Weighardt et al was cross reacting with SAFB2 and possibly they were detecting SAFB2 not SAFB1.

It was not known whether primary ALL cells have the ability to elicit a functional cellular stress response following heat shock and/or anti-cancer drug (HSP90i) treatment. In primary human ALL cells and NBM, SAFB1 and SAFB2 expression was not altered following heat shock. HSF1 expression was however significantly increased in BCP-ALL and T-ALL compared with NBM. In addition, HSF1 was found enriched at the nuclear border in primary NBM, BCP-ALL and T-ALL cells. HSF1 nuclear border aggregation was more abundant in BCP-ALL and T-ALL cells compared to NBM following HS. The HeLa cell response to stress is considered typical (see discussion below) in that it is similar to that elicited by many other cell types (i.e. the transcription of heat shock proteins and SatIII transcripts/nSBs formation occurs). These data show NBM cells differ in their stress response (did not form nSBs) compared to HeLa cells. Further, primary T-ALL and BCP-ALL cancer cells differ when compared to NBMs as HSF1 expression is significantly altered with higher percentage of HSF1 aggregation at the nuclear border (but no discrete nuclear puncta are seen) following heat shock and 17-DMAG treatment. Under normal conditions, HSF1 is normally diffusely enters the nucleus upon stress. In this study, HSF1 was aggregating at the nuclear border (detected by measuring the average intensities of HSF1 in the nucleus and cytoplasm-explained in the Method section) upon stress in ALL cells, which is unusual staining pattern and has never shown in other cells (HeLa cells). It is not known what does that mean but could be that HSF1 is not fully activated in these cells and further experiments are needed to define these observations. To differentiate localisation of

cytoplasmic and nuclear proteins, cytoplasmic markers techniques (e.g. immunofluorescence staining) could be employed to assess whether HSF1 is also detected in the cytoplasm. In addition, neither NBM or primary T-ALL and BCP-ALL cells were found to have SAFB2 containing nSBs following HS or 17-DMAG treatment. However, BCP-ALL and T-ALL cells were more sensitive to treatment with 17-DMAG and celastrol than NBM cells. These data show that NBM cells cannot induce a heat shock response. However, T-ALL and BCP-ALL cells show altered HSF1 expression and respond to HS and 17-DMAG by increasing hsp70 expression.

HSF1 nuclear border staining was not co-localised with either SAFB1 or SAFB2 after HS in primary human cells. Previous reports suggest that the expression of HSF1 is up-regulated in various tumours, including prostate, colon and lung cancers (145). The altered stress response could be linked to the altered levels of HSF1 reported above and the altered expression of SAFB1/SAFB2 ratio observed in BCP-ALL and T-ALL in chapter 3. Other reports found that the stress within cancer microenvironment is caused by many factors, including hypoxia and low pH. These factors might be altering HSF1 levels to accommodate the stress (134,147). In addition, it was reported that HSF1 levels were reduced in human T-cells following heat shock, consistent with the data presented in this chapter (166). Thus, this might influence its ability to generate the normal stress response. Also, it was suggested that lymphocyte activation is essential to elicit a proper cytoprotective response. Activated B and T lymphocytes were reported to be more protective following stress (167),(168). The lower percentage of cells with HSF1 nuclear border staining observed under basal conditions and following treatment with HSP90i in NBM cells compared with ALL cells might be linked to cellular differentiation. HSF1 was reported to control the cellular differentiation which might be altered during tumorigenesis. For example, monocytes have less potential to differentiate into macrophages *in vivo* and *in vitro* $HSF1^{-/-}$ mouse models (169).

Environmental perturbation (hypertonic stresses, heavy metals) and specific cellular conditions (HS) activate the stress response to maximise cellular survival (165). An immediate block of several cellular processes is triggered in response to stress, including DNA replication, transcription, mRNA export and translation (18). The initial identification of nSBs was based on the accumulation of HSF1 in stressed cells. The

formation of nSBs is not only induced by HS but also in response to chemical and hypertonic stresses (18). Furthermore, HSF1 nSBs have been detected in many cell lines, including HeLa, A431 and HOS as well as in primary human cells, including epithelial and fibroblasts (4). nSBs were found to be the sites of many pre-mRNA processing factors, including SF2/ ASF, 9G8 and SRp30c. The assembly of nSBs is a unique process that is found on distinct chromatin regions, consisting of Sat III DNA sequences that are only found at pericentromeric heterochromatin on specific chromosomes such as 9, 12 and 15 (18) with implications in regulating alternative splicing.

For cells to elicit a proper cellular stress response, in addition to nSB formation, HSPs are produced following stress to prevent protein mis-folding and aggregation. Treating HeLa cells with HSP90i such as 17-N-allylamino-17-demethoxygeldanamycin (17AAG) is known to induce a stress response as evaluated by higher HSP70 expression, which was found in the nucleus and cytosol following stress (170),(130),(171). Celastrol causes cell death in human leukaemia cell lines (Jurkat) and human glioblastoma cell lines (U251N) (130). Another class of HSP90 inhibitors used in this chapter, 17-DMAG but not celastrol, caused higher induction of HSP70 expression in HeLa and human BCP-ALL and T-ALL cells compared with NBM cells. Interestingly, although a previous report showed that celastrol caused up-regulation of inducible HSP70 in HeLa cells and SH-SY5Y (130), our data showed that celastrol did not trigger higher induction of HSP70. Although celastrol resulted in the formation of HSF1 nuclear border staining, the percentage of cells with this observation was far less compared with 17-DMAG. Similar observations were seen in BCP-ALL and T-ALL cells in which SAFB2 and SAFB1 were not co-localised with HSF1 following 17-DMAG and celastrol. These data suggest that 17-DMAG is inducing a different cellular response to celastrol and are likely explained by the fact 17-DMAG is a more effective inhibitor of HSP90 and celastrol has additional actions. 17-DMAG directly targets the ATP site of HSP90 (122), whereas celastrol indirectly inhibits HSP90 by causing disruption to HSP90 and the co-chaperone Cdc37 (130). These data suggest that the mechanisms regulating the cellular stress response (assessed by HSF1 and HSP70 expression) in BCP-ALL and T-ALL is altered compared with NBM cells.

In conclusion, the altered expression of SAFB1 and SAFB2 observed in primary BCP-ALL and T-ALL influenced the mechanisms regulating the stress response in malignant cells. In addition, HSF1 was found to be overexpressed in primary BCP-ALL and T-ALL cells following HS and HSP90i treatment, indicating that the stress response is altered. Furthermore, HSP90 inhibitors (17-DMAG and celastrol) killed primary BCP-ALL and T-ALL cells but not NBM cells at the same dose. This may occur due to the altered expression of HSF1 being toxic in BCP-ALL and T-ALL cells and/or pathways not related to HSP90 inhibition are activated. The altered stress response in ALL, as typified by the lack of SAFB2 containing nSBs, also suggest an altered stress response could be involved. For instance, nSB sequester transcription and RNA processing factors and are thought to thereby shut down transcription and translation during stress. If this does not occur, the chaperone/stress proteins induced during stress will bind constitutive proteins and interfere with their correct processing, thereby increasing cell dysregulation.

CHAPTER 5 : Characterising SAFB1 and SAFB2 protein: protein interactions using TMT Mass spectrometry

5.1 Introduction

SAFB proteins are involved in regulating many cellular functions, including gene expression (38), the cellular stress response (19), DNA repair, apoptosis (22), RNA processing and splicing (38). However, little is known about the differences/similarities between the function of SAFB1 and SAFB2 in regulating these pathways. Therefore, identifying the unique and shared SAFB1 and SAFB2 protein partners would help elucidate the roles of each of these proteins.

SAFB1 and 2 proteins are highly similar at the amino acid level, sharing 74% overall homology (7) with the various functional domains of SAFB proteins sharing higher homologies (ranging from 65-100%). The C-terminus region contains the domains crucial for protein-protein interactions and the various partner complexes formed are responsible for SAFB protein functionality (8). SAFB1 is primarily expressed in the nucleus, while SAFB2 is expressed in both the nucleus and cytoplasm (5). This suggests that SAFB2 has additional functions distinct from those of SAFB1. However, despite evidence suggesting SAFB1 and SAFB2 may have some distinct functions, the majority of studies to date have investigated SAFB1 functions with very few investigating SAFB2.

RNA binding proteins (such as SAFB1/2) need to interact with a number of partner proteins to mediate their actions. In addition, a number of PTMs, for example in response to stress and regulatory signals regulate these protein:protein interactions. SAFB1 has been reported to interact with hnRNPs, nuclear receptors (4),(40),(9) and SR proteins, such as SRSF1 (2). It was also reported that both SAFB1 and SRSF1 are recruited into nSBs following heat shock (2). Another study showed that deletions within the C-terminal protein interaction domain (638-788 aa region) of SAFB1 prevented binding to nSBs (20). In addition, deletion of both the E/R and R/G caused SAFB1 to translocate to the cytoplasm suggesting multiple C-terminal interactions govern SAFB1 function. SAFB proteins have been found to undergo several PTMs (SUMOylation, methylation), which are important in regulating protein-protein interactions (2),(25),(27),(28), (11). The E/R and R/G domains of SAFB1/2 contain RGG/RG motifs (30) that may be methylated differentially to mediate important cellular functions such as RNA binding and protein-protein interactions (11),(172),(173). Little

is known about the significance of the arginine methylation of SAFB proteins in regulating the cellular response to stress, however preliminary data in our laboratory showed that SH-SY5Y cells treated with AdOx (a pan methylation inhibitor) altered the nuclear distribution of SAFB1 and SRSF1, suggesting methylation of these proteins plays a role in their constitutive functions. The significance of SAFB protein SUMOylation status in mediating protein-protein interactions has not been studied. However, SAFB1 SUMOylation status was linked to the stress response, with SAFB proteins becoming de-SUMOylated upon heat stress (27). Also, it was found that SUMOylation was required for transcriptional repression to be mediated by SAFB1 (29). However, it is not known whether methylation and/or SUMOylation regulate the interaction between SRSF1 and SAFB1 or SAFB2 following heat shock.

Hence, although a number of studies have identified specific SAFB1 binding partners there have been no comprehensive proteomic analyses to identify the protein binding partners of SAFB1 and SAFB2. In addition, the influence of arginine (RGG/RG) methylation and SUMOylation on SAFB1/2 protein interactions has not been studied.

The aims of this chapter were therefore to:

i. Investigate whether SAFB1 and SAFB2 RGG/RG and SUMOylation motifs regulate the protein interactions of SAFB1 and SAFB2
ii. Identify SAFB1/2 protein interactions using Tandem Mass Tag Mass Spectrometry (TMT-MS) following pulldown assays in HeLa and T-ALL cells
iii. Use bioinformatic tools to map the biological processes and functional pathways that SAFB1 and SAFB2 regulate
iv. Highlight the novel pathways regulated by SAFB1 and SAFB2 identified by the proteomic analysis

5.2 Results

5.2.1 Exploring whether RGG/RG and SUMOylation motifs regulate interactions between SAFB1/SAFB2 and SRSF1

SAFB1 and SAFB2 are known to be post-translationally modified (PTM) and several sites for RGG/RG methylation and stress-dependent SUMOylation have been identified. SAFB1 was reported to interact with SRSF1, (also a component of nSBs) under stress and non-stress conditions (2). It was hypothesised that SAFB2 may also interact with SRSF1 and if this were the case interactions with SRSF1 could be used to investigate the role PTMs play in regulating SAFB1/2 function. Thus, SAFB1 methylation deficient (Δ-methylation) mutants were made at 7 sites (R557, R811, R868, R874, R844, R754, R902 aa) using a site directed mutagenesis kit to switch arginine (R) residues for lysine (K). SAFB2 Δ-methylation mutants (Renata Raele) and SAFB1/2 deficient (Δ-SUMOylation, K231 and K294 aa) mutants (Nicola Buckner) were also made in our lab at 8 sites (R773, R897, R903, R883, R932, R566, R835, R842 aa). A schematic diagram showing the mutagenesis steps is shown (Figure 5.1A) and full details of the mutagenesis method is described in chapter 2.

SAFB1 methylation sites are indicated in arrows within the SAFB1 sequence (Figure 5.1B) located at the C-terminal in the protein-protein interaction domain. To check for successful site directed mutagenesis, mutated SAFB1 plasmids were checked for the conversion of the arginine codon (CGT/CGC/CGA/CGG/AGA/AGG) to lysine (AAA/AAG) by Sanger sequencing. The whole SAFB1 construct was sequenced using flanking primers. Results showed that all 7 arginine methylation sites of SAFB1 was successfully converted to lysine, highlighted in red (Figure 5.1C).

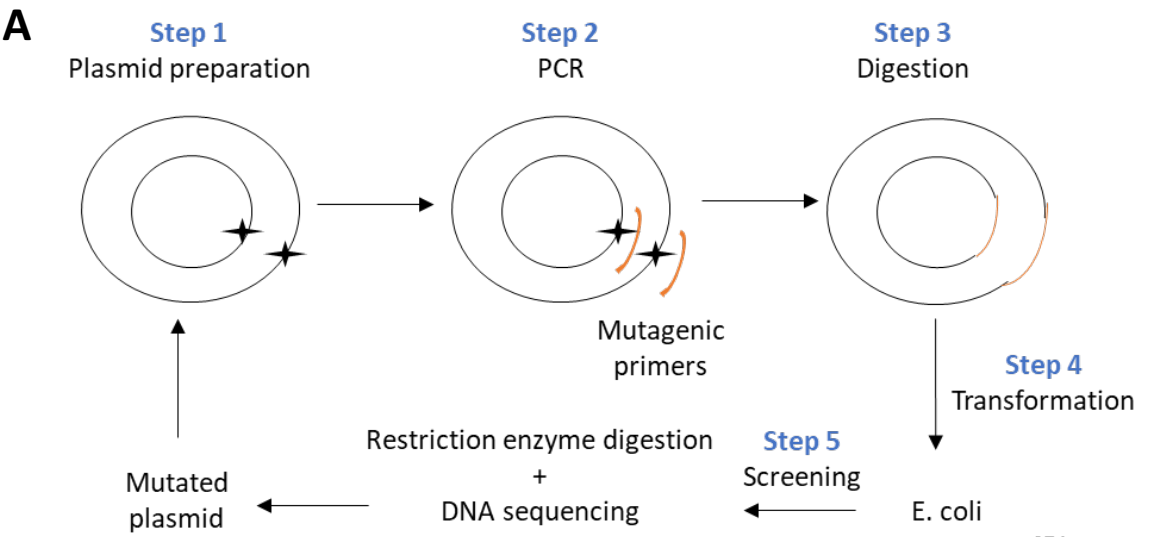

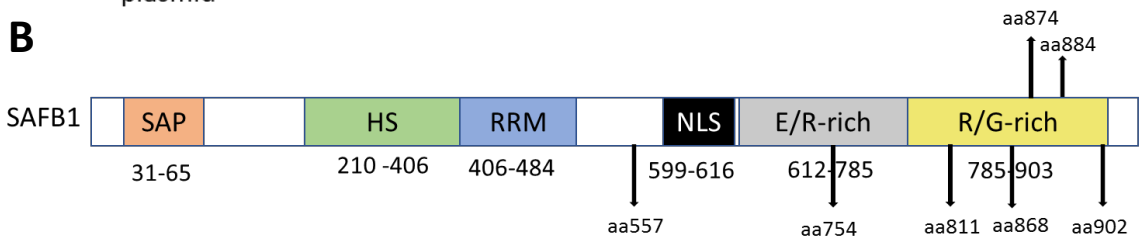

C

Full SAFB1 methylation mutants seq

ATGGCGGAGACTCTGTCAGGCCTAGGTGATTCTGGAGCGGCGGGCGCGGCGGCTCTGAGCTCCGCCTCGTCAGAGACCGG
GACGCGGCGCCTCAGCGACCTGCGAGTGATCGATCTGCGGGCGGAGCTGAGGAAACGGAATGTGGACTCGAGCGGCAACA
AGAGCGTTTTGATGGAGCGGCTGAAGAAGGCAATTGAAGATGAAGGTGGTAATCCTGACGAAATTGAAATTACCTCCGAG
GGAAACAAGAAAACATCAAAGAGGTCTAGCAAAGGGCGCAAACCAGAAGAAGAGGGTGTGGAAGATAACGGGCTGGAGGA
AAACTCTGGGGATGGACAGGAGGATGTTGAGACCAGTCTGGAGAACTTGCAGGACATCGACATCATGGATATCAGTGTGT
TGGATGAAGCAGAAATTGATAATGGAAGCGTTGCAGATTGTGTCGAAGACGATGATGCTGATAACCTCCAGGAGTCCCTG
TCGGATAGTAGAGAGCTAGTCGAGGGGGAAATGAAAGAGCTTCCGGAGCAGCTTCAGGAACATGCTATAGAGGACAAAGA
AACTATAAACAATTTAGATACTTCATCATCTGACTTCACTATATTACAGGAAATTGAAGAGCCATCCCTGGAGCCAGAAA
ATGAGAAAATACTCGACATTTTGGGGGAAACTTGTAAATCTGAGCCAGTAAAAGAAGAAAGTTCCGAGCTGGAGCAGCCA
TTTGCACAGGACACAAGTAGCGTGGGGCCAGACAGAAAGCTTGCGGAGGAAGAGGACCTATTTGACAGCGCCCATCCGGA
AGAGGGTGATTTAGATTTGGCCAGCGAGTCAACAGCACACGCTCAGTCGAGCAAGGCAGACAGCCTGTTAGCGGTAGTGA
AAAGGGAGCCCGCGGAGCAGCCAGGCGATGGCGAGAGGACGGACTGTGAGCCTGTAGGGCTAGAGCCGGCAGTTGAGCAG
AGTAGTGCGGCCTCCGAGCTCGCGGAGGCCTCTAGCGAGGAGCTCGCAGAAGCACCCACGGAAGCCCCAAGCCCAGAAGC
CAGAGATAGCAAAGAAGACGGGAGGAAGTTTGATTTTGACGCTTGTAATGAAGTCCCTCCGGCTCCTAAAGAGTCCTCAA
CCAGTGAGGGCGCTGATCAGAAAATGAGTTCTCCCGAAGATGACTCGGATACAAAAAGGCTTTCCAAAGAGGAAAAGGGT
CGCAGCAGTTGTGGTAGAAATTTCTGGGTTAGTGGACTCTCTTCTACAACCAGAGCTACAGATTTGAAGAATCTTTTCAG
CAAATATGGGAAGGTGGTGGGCGCCAAGGTTGTGACAAATGCCCGGAGTCCTGGAGCTCGCTGTTACGGTTTTGTCACGA
TGTCCACAGCAGAAGAGGCCACAAAATGCATTAACCACCTGCACAAGACGGAGCTCCACGGAAAGATGATCTCCGTGGAG
AAAGCCAAAAATGAACCTGTGGGAAAGAAAACCTCTGACAAAAGAGACAGTGACGGGAAAAAGGAGAAGTCGAGCAACAG
TGACAGATCTACAAACCTTAAGAGGGATGATAAATGTGACAGAAAAGATGATGCTAAGAAGGGTGACGACGGAAGTGGAG
AAAAGAGTAAGGACCAAGATGATCAGAAACCTGGCCCCTCAGAGCGATCTCGAGCCACAAAGTCAGGAAGTAAGGGACC
GAACGGACTGTAGTAATGGATAAATCCAAAGGGGTGCCTGTGATTAGTGTAAAAACGTCCGGGTCCAAAGAGAGAGCTTC
CAAAAGCCAGGATCGCAAATCAGCCAGCAGAGAGAAGCGGTCCGTCGTGTCCTTTGATAAGGTCAAGGAGCCTCGGAAGT
CAAGAGACTCAGAGTCCCATAGCAGGGTGCGTGAACGCAGTGAACGCGAACAACGCATGCAGGCGCAGTGGGAGCGCGAG
GAGCGTGAGCGGCTGGAGATTGCCCGAGAGAGGCTGGCCTTCCAGCGCCAGCGGCTGGAGCGGGAGCGCATGGAGCGGGA
ACGGCTGGAGCGCGAACGCATGCACGTGGAGCACGAGCGCAGGCGCGAGCAGGAGCGCATCCACCGTGAGCGCGAGGAGC
TGAGGCGCCAGCAGGAACTGCGCTATGAGCAGGAGCGGCGGCCCGCGGTGCGGCGGCCCTACGACCTGGACCGGCGAGAT
GATGCCTATTGGCCGGAAGCCAAGCGGGCCGCCCTGGATGAGCGCTACCATTCTGACTTTAACCGCCAGGACCGCTTCCA
CGACTTTGACCACAGGGACAAGGCCGCTACCCCGACCACTCGGTGGACAGGAGAGAAGGTTCAAGGTCAATGATGGGAG
AACGAGAAGGACAGCATTACCCAGAACGCCATGGAGGACCAGAGCGCCACGGCCGGGACTCCCGCGATGGCTGGGGGGGC
TATGGCTCTGACAAGAGGATGAGCGAGGGCAAGGGGCTGCCTCCTCCCCCCAGGGGCAGACGTGACTGGGGGGACCATGG
CCGAAGAGAGGATGACCGGTCATGGCAGGGCACGGCCGACGGGGGCATGATGGACAGGGATCACAAGAGGTGGCAAGGTG
GCGAGAGAAGCATGTCCGGTCACTCCGGGCCTGGCCACATGATGAACAAGGAGGAATGTCAGGGAAGGCAGCTTTGCC
CCAGGCGGGGCCTCCAAGGCCACCCCATCCCACACGGTGGCATGCAGGGCGGGTTTGGAGGCCAGAGCAAGGGAGCAG
GCCCAGCGATGCCCGCTTCACTCGCCGCTACTGA

Figure 5.1 Generation and validation of SAFB1 Δ-methylation mutants. (A) Schematic diagram showing the steps involved in mutagenesis. (B) SAFB1 domains with a total of 7 methylation arginine sites indicated in arrows. (C) SAFB1 Δ methylation mutants were created using a site directed mutagenesis kit and the conversion of the arginine to lysine was validated using Sanger sequencing (highlighted in red).

To investigate the effect of methylation and SUMOylation on the interaction between SRSF1 with SAFB1 under basal conditions and following heat shock, co-IPs were performed on HeLa cells transfected with EGFP-SAFB1 mutants. Cells were transfected with SAFB1 wild type (WT), SAFB1 Δ methylation and Δ SUMOylation mutants for 48 hours. Cells were then heat shocked at 42^0 C for 1 hour followed by 0 hours recovery (HS+NR) and 1 hour recovery (HS+R). Next, co-IPs were performed on HeLa lysate with anti-EGFP antibodies and IgG control. Immunoprecipitates were analysed by Western blotting and probed with SAFB1 and SRSF1 antibodies. Densitometry was performed on SRSF1 IP relative to SAFB1 IP and values represent mean± SD. Under basal conditions (non-heat shock), the SAFB1 Δ-methylation and SAFB1 Δ-SUMOylation proteins interaction with SRSF1 was reduced (0.66±0.13) and (0.60±0.11) compared with the WT-SAFB1 control (0.85±0.20), however this was not significant (Figure 5.2). Following heat shock (HS+NR), there was a significant reduction in the interaction between WT-SAFB1 (0.41±0.15, $P<0.05$) and SRSF1 following HS+NR compared with the WT-SAFB1:SRSF1 interaction (0.85±0.20) measured under basal conditions (Figure 5.2). There was however, no significant difference in the interaction of SAFB1 Δ-methylation (0.38±0.04) and SAFB1 Δ-SUMOylation (0.40±0.18) mutants with SRSF1 when compared to the WT-SAFB1 control. After the recovery period (HS+R), there was no significant difference between the interactions of WT-SAFB1 and SRSF1 when comparing HS+NR (0.41±0.15) to HS+R (0.49±0.23). However, the WT-SAFB1:SRSF1 interaction one hour after HS (HS+R) remained less than that observed with no heat shock (NHS). No significant change in the SAFB1 Δ-methylation:SRSF1 interaction was observed when compared to WT-SAFB1:SRSF1 values under any of the conditions. However, the interaction between the SAFB1 Δ-SUMOylation mutant and SRSF1 was significantly increased (0.85±0.08, $P<0.05$) when compared to SAFB1-WT:SRSF1 (0.49±0.23) under HS+R and SAFB1 Δ-SUMOylation interaction under HS+NR (0.40±0.18, Figure 5.2).

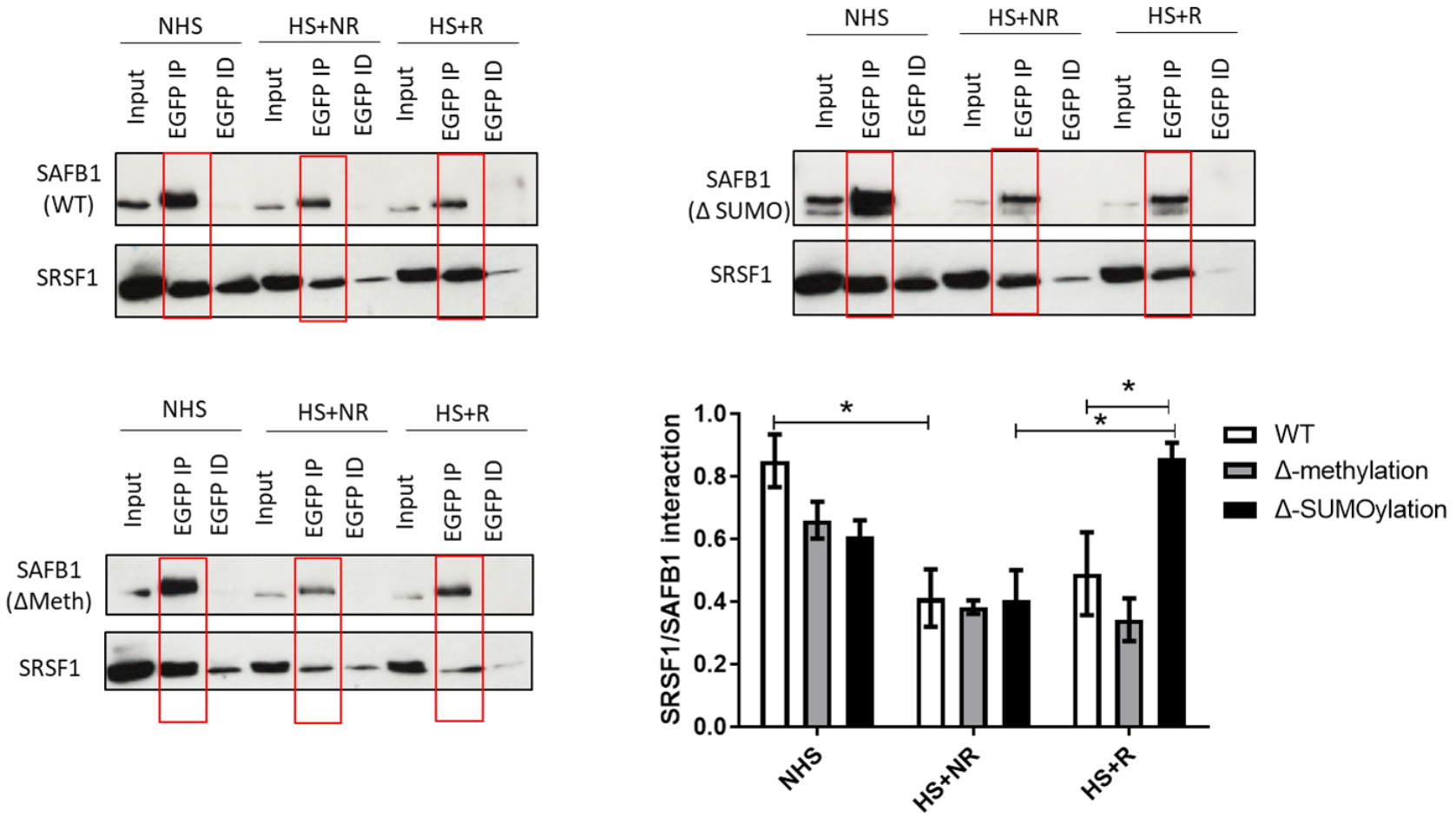

Figure 5.2 Investigating the interaction between SAFB1 and SRSF1. HeLa cells were transfected with EGFP-SAFB1 (WT), EGFP-SAFB1 Δ-methylation and EGFP-SAFB1 Δ-SUMOylation for 48 hours. Cells were subjected to either control (NHS), heat shock with no recovery (HS+NR) or heat shock and recovery (HS+R). Co-IPs were performed with EGFP or IgG antibodies. The immunoprecipitates were run on WB and probed with SAFB1 (Bethyl) and SRSF1 (Abcam) antibodies. Input and immunodepleted (ID) lysates were run as controls. Densitometry was performed on SRSF1 IP relative to SAFB1 IP. Co-IP results are from 3 independent experiments. Values represent mean± SD. * = P<0.05.

The influence of methylation and SUMOylation on the interaction between SRSF1 with SAFB2 was also explored under basal conditions and following heat shock using co-IPs on HeLa cells transfected with EGFP-SAFB2 mutants. Cells were transfected with SAFB2 WT, SAFB2 Δ methylation and Δ SUMOylation mutants for 48 hours. Cells were then heat shocked at 42^0 C for 1 hour followed by 0 hours recovery (HS+NR) and 1 hour recovery (HS+R). Next, co-IPs were performed on HeLa cell lysate with EGFP antibodies and IgG control. Co-IPs were analysed by Western blotting and probed with SAFB2 and SRSF1 antibodies. Densitometry was performed on SRSF1 IP relative to SAFB2 IP and values represent mean± SD. Under basal conditions, there was a significant reduction ($P \leq 0.01$) in the interaction between the SAFB2 Δ-methylation mutant (mean+SD=0.26±0.14) and SRSF1 when compared with WT-SAFB2 basal levels (0.81±0.15), indicating the methylation of SAFB2 increases binding to SRSF1. There was no significant reduction in the interaction between the SAFB2 Δ-SUMOylation (0.68±0.23) mutant and SRSF1 under basal conditions (Figure 5.3). There was however a significant reduction in the interaction between WT-SAFB2 and SRSF1 (0.33±0.07, $P<0.05$) following heat shock (HS+NR) compared with basal conditions (0.81±0.15, NHS, Figure 5.3). There was also a decrease in the WT-SAFB2:SRSF1 interaction following HS+NR (as with SAFB1) although there was no significant difference when methylation and SUMOylation mutants were compared to HS+NR control (WT-SAFB2). However, there was a significant reduction in the interaction between the SAFB2 Δ-methylation mutant and SRSF1 following HS+R (0.37±0.15, $P<0.05$) compared with the WT-SAFB2 (0.85±0.13). Likewise, the interaction between SAFB2 Δ-SUMOylation with SRSF1 was decreased (0.70±0.16) but was not significantly different compared to WT-SAFB2 (Figure 5.3).

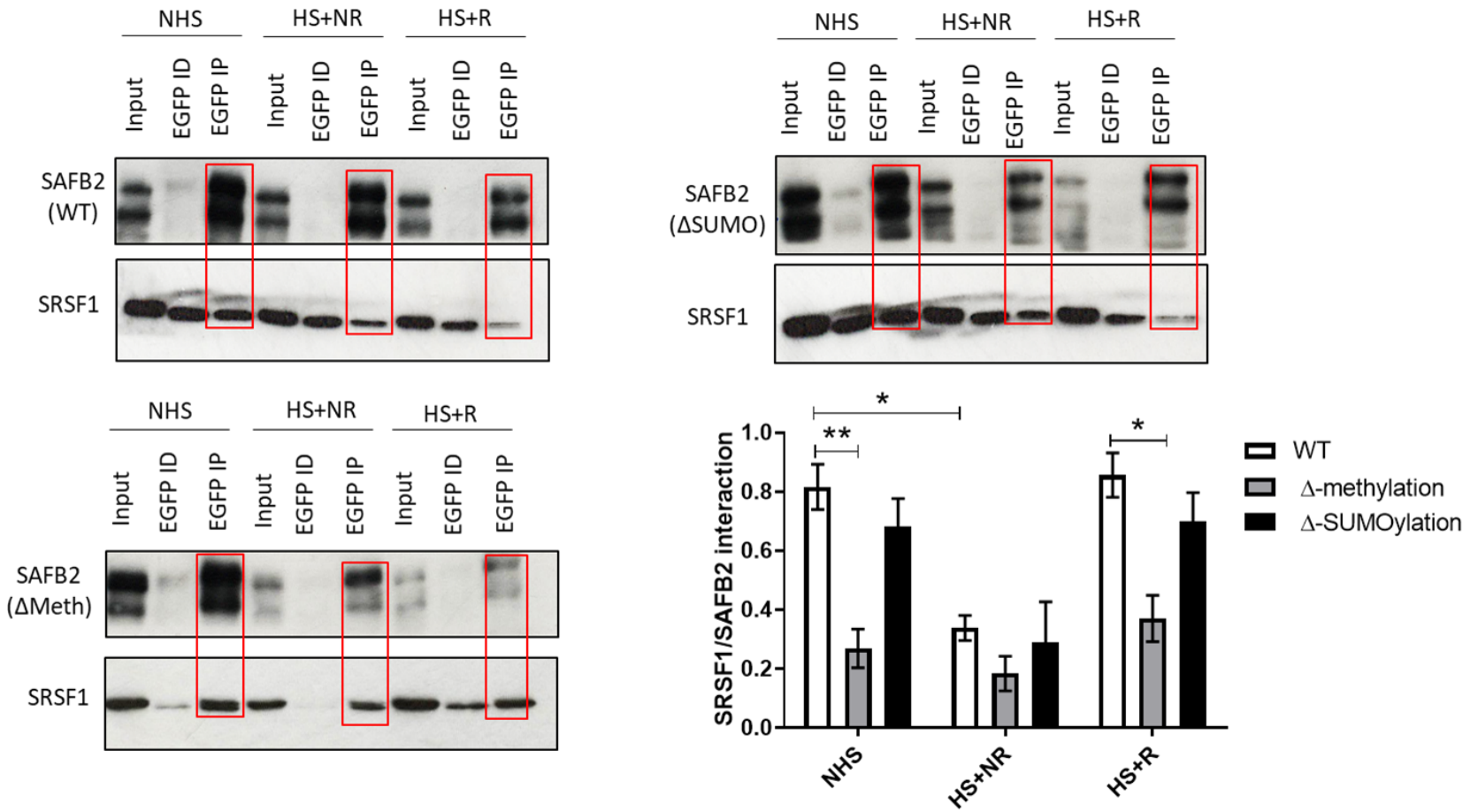

Figure 5.3 Investigating the interaction between SAFB2 and SRSF1. HeLa cells were transfected with EGFP-SAFB2 (WT), EGFP-SAFB2 Δ-methylation and EGFP-SAFB2 Δ-SUMOylation for 48 hours. Cells were subjected to either control (NHS), heat shock with no recovery (HS+NR) or heat shock and recovery (HS+R). Co-IPs were performed with EGFP or IgG antibodies. The immunoprecipitates were run on WB and probed with SAFB2 (Bethyl) and SRSF1 (Abcam) antibodies. Input and immunodepleted (ID) lysates were run as controls. Densitometry was performed on SRSF1 IP relative to SAFB2 IP. Co-IP results are from 3 independent experiments. Values represent mean± SD. * = $P<0.05$, ** = $P\leq0.01$.

5.2.2 TMT-MS analysis

In order to identify SAFB1/2 protein interactions, TMT-MS analysis was used. The mass spectrometry was conducted by Dr Kate Heesom at the Proteomic facility (University of Bristol). The first step in this process uses antibodies specific to SAFB1 and SAFB2 to carry out co-IP assays and the co-IP protocol is described. HeLa and T-ALL cell lysates were incubated with antibodies and SAFB1 and SAFB2 bound proteins immunoprecipitated (and compared to an isotype IgG control). SAFB1, SAFB2 and IgG antibodies were conjugated to protein G beads and incubated with the cell lysate overnight. Successful immunoprecipitation was confirmed by Western blotting for the presence of SAFB1 and SAFB2 and their known interacting proteins. The schematic workflow for SAFB1 and SAFB2 and TMT-MS analyses are shown (Figure 5.4A). Co-IP samples were desaturated by trypsin, TMT labelled, pooled, fractionated, cleaned and analysed by mass spectrometry. Data analyses and quantification were performed using Proteome discoverer software (Figure 5.4B).

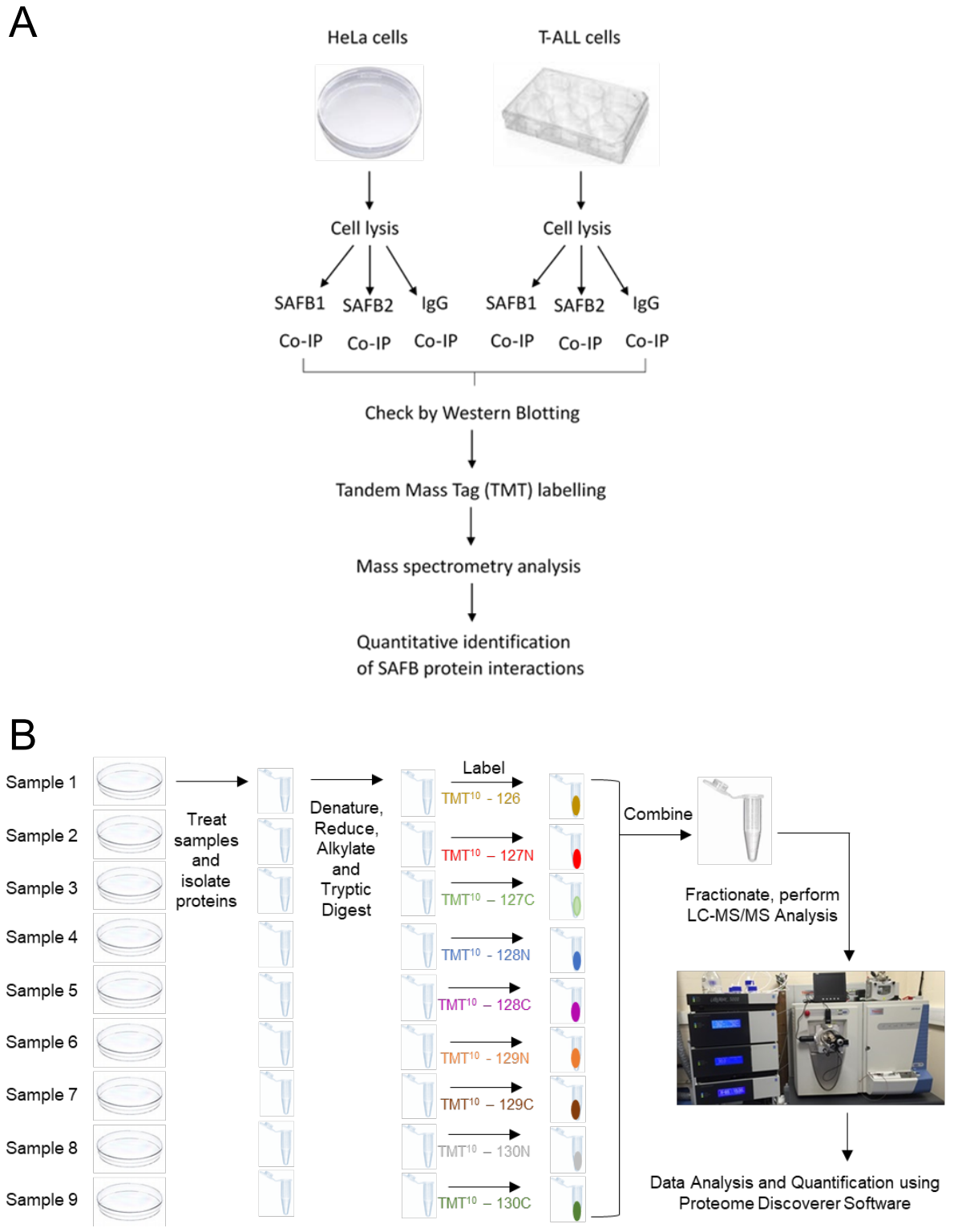

Figure 5.4 Schematic workflow for analysis of SAFB1 and SAFB2 partners in HeLa and T-ALL cells. (A) Five hundred micrograms of protein cell lysate were used for co-IP. Either SAFB1, SAFB2 or IgG co-IPs were performed generating 9 samples from 3 independent experiments for each cell type. The immune-complex in co-IPs were checked by Western blotting. (B) All samples were TMT labelled, pooled, fractionated, cleaned and analysed by mass spectrometry.

5.2.3 Optimisation of co-IP from HeLa cell lysates

Immunoprecipitation of SAFB1 and SAFB2 was carried out with and without the crosslinking of antibodies to the magnetic beads. A second aim was to validate a new custom made SAFB1 antibody. We produced our SAFB1 antibody (custom-made) by Invitrogen to save money and with the hope to obtain better specificity.

Initial co-IPs showed an IgG heavy (50kDa) and light (25kDa) chain band on the blots and the molecular weight of the latter was similar to the SRSF1 band (27kDa). Therefore, crosslinking the SAFB1 and SAFB2 antibodies to the beads was evaluated as a method to reduce non-specific IgG interactions and enable the better detection of SRSF1.

HeLa cell lysate was immunoprecipitated with SAFB1 (Bethyl and Invitrogen), SAFB2 (Bethyl) or IgG antibodies with and without crosslinking beads. IP was assessed by Western blotting and probing for SAFB1 and SAFB2 (Figure 5.5). Results revealed that SAFB1 IP was successful with both the Bethyl and Invitrogen antibodies. The SAFB1 band was depleted in the SAFB1 immunodepleted lane suggesting SAFB1 was mostly captured by the beads. Following crosslinking, the heavy chain IgG band was greatly diminished. The light chain IgG band was completely removed. Reducing IgG will help in removing non-specific interactions during TMT-MS analyses. Similarly, SAFB2 co-IP was successful and the SAFB2 band was detected, which was not found in the IgG lane. Also, most of the non-specific IgG band was removed following crosslinking (Figure 5.5).

These results revealed that crosslinking antibodies to beads was beneficial in removing most of non-specific IgG and also improved the efficiency of the IP itself. Therefore, antibodies crosslinked to beads were used in subsequent experiments.

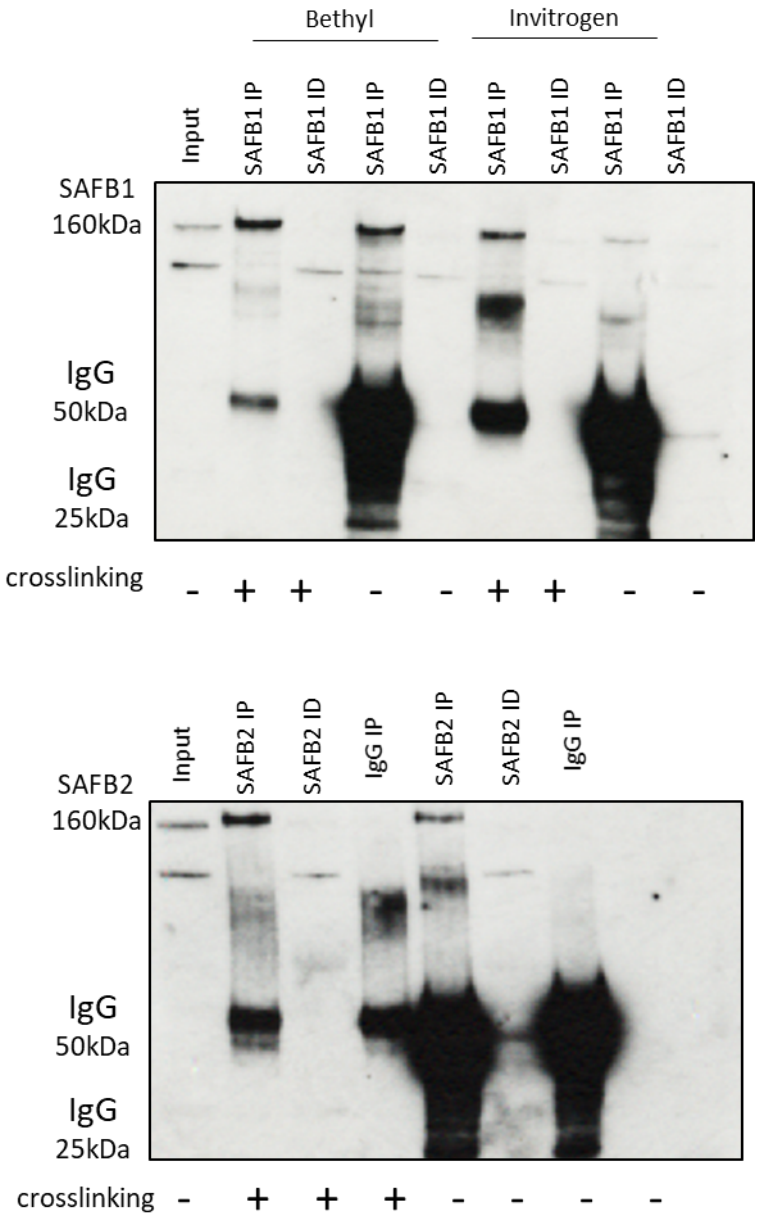

Figure 5.5 Comparing antibody crosslinking to beads. HeLa cell lysate (500µg) was incubated with SAFB1 (Bethyl and Invitrogen), SAFB2 (Bethyl) and IgG (Invitrogen) antibodies either crosslinked to protein G beads or without crosslinking. The immunoprecipitate was run on Western blots and probed with SAFB1 (Bethyl) and SAFB2 (Bethyl) antibodies. Input and immunodepleted lysates (ID) were run as controls.

5.2.4 Validation of co-IP from HeLa cell lysates

In order to confirm the immunoprecipitation was working, Hela cell lysates were coimmunoprecipitated with SAFB1 and SAFB2 and probed with SAFB1/2 antibodies and an SRSF1 antibody (as SRSF1 is a known binding partner of SAFB1). The results showed that SAFB1 was present in the IP and that immunodepletion reduced the SAFB1 band suggesting that it was mostly captured by the beads (Figure 5.6). Also, there was no SAFB1 band in the IgG IP sample, suggesting the SAFB1 IP was specific. SRSF1 was detected in the SAFB1 IP sample but not in the IgG IP sample, indicating the interaction of SRSF1 with SAFB1 was specific (Figure 5.6). SRSF1 was found in SAFB1 immunodepleted lane, indicating that not all the SRSF1 is bound to SAFB1.

Similarly, SAFB2 IP was successful and a SAFB2 band was detected, which was not found in the IgG lane. The SAFB2 band was depleted in the SAFB2 immunodepleted lane suggesting most of it was bound to the beads. Like SAFB1, SRSF1 was coimmunoprecipitated with SAFB2 with some fractions of SRSF1 found in the SAFB2 immunodepleted lane. However, no SRSF1 was seen in the IgG lane suggesting SRSF1 interaction with SAFB2 was specific (Figure 5.6).

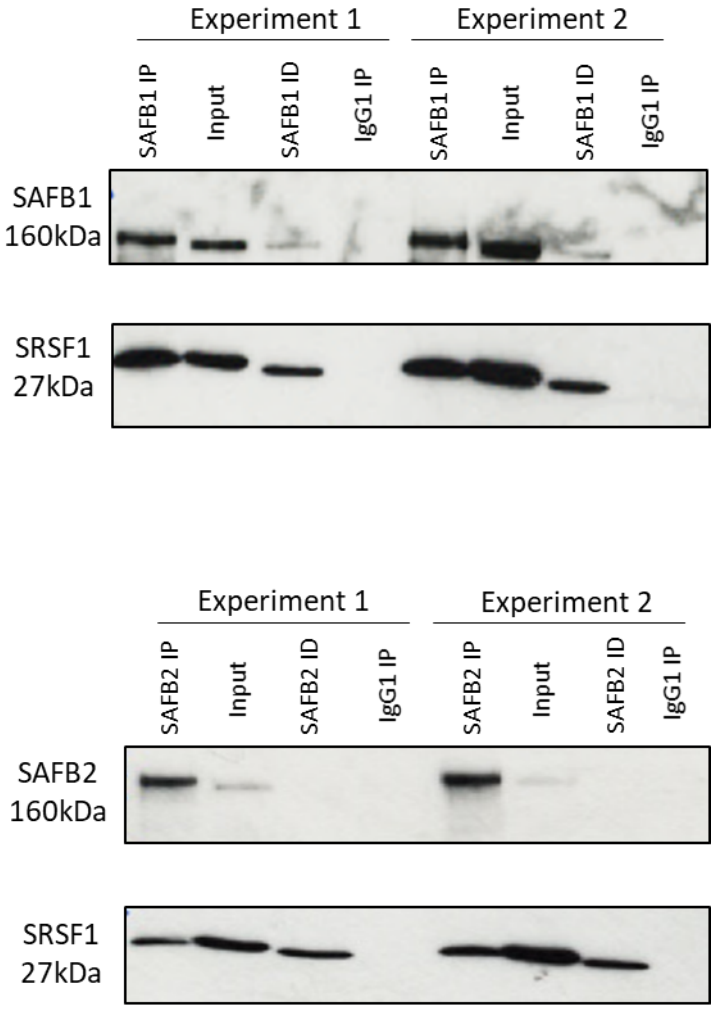

Figure 5.6 Investigating the interaction between SAFB1 or SAFB2 with SRSF1 in HeLa cells. Co-IP was performed with 500µg of pre-cleared lysate with SAFB1 (Invitrogen), SAFB2 (Bethyl) or IgG (Invitrogen) antibody crosslinked beads. The immunoprecipitate was run on Western blots and probed with SAFB1 (Bethyl), SAFB2 (Bethyl) and SRSF1 (Invitrogen) antibodies. Input and immunodepleted (ID) lysates were run as controls. Co-IP was performed on 3 independent experiments. Representative blots of only 2 independent experiments are shown.

5.2.5 Validation of co-IP in primary T-ALL cell lysates

The next aim was to assess co-IP of SAFB1 and SAFB2 interacting proteins from primary T-ALL cell lysates. To this end, SAFB1, SAFB2 and IgG co-IPs were performed using primary T-ALL lysates (n=3) following the protocol optimised using HeLa cell lysates. Co-IPs were assessed by western blotting and probed with SAFB1, SAFB2 and SRSF1 antibodies. Consistent with the HeLa cell data in Figure 5.6, IP was successful and a SAFB1 band was detected in the T-ALL IP samples (Figure 5.7). Also, immunodepletion reduced the SAFB1 band, suggesting most SAFB1 was captured by the beads. Furthermore, no IgG band was detected in SAFB1 IP lane suggesting the IP was specific. An interaction between SRSF1 and SAFB1 was detected with SRSF1 present in the IP sample with low levels compared with HeLa cell data. However, more SRSF1 was found in the SAFB1 immunodepleted lane. However, no SRSF1 was seen in the IgG lane suggesting that the SRSF1 interaction with SAFB1 was specific (Figure 5.7).

Similarly, the SAFB2 band was successfully detected in the SAFB2 IP sample but not the IgG IP sample. The immunodepletion diminished the SAFB2 band suggesting that it was mostly captured by the beads. Unlike in HeLa cells, the interaction between SRSF1 and SAFB2 was not detected, suggesting low level of interaction compared with HeLa cell data or the interaction is lost. However, the SRSF1 band was found in the SAFB2 immunodepleted lane with no SRSF1 detected in the input lane (Figure 5.7). This might suggest that more protein was loaded in the SAFB2 immunodepleted lane compared with the input lane.

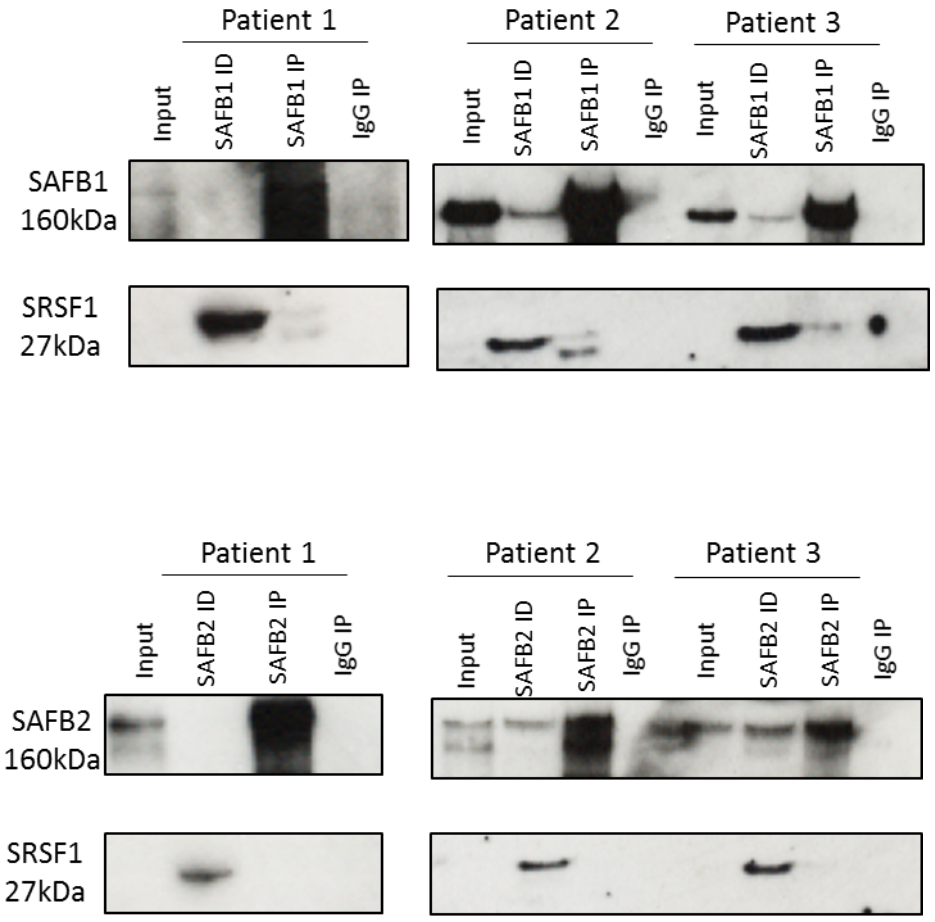

Figure 5.7 Investigating the interaction between SAFB1 or SAFB2 with SRSF1 in primary T-ALL cells. Co-IP was performed with 500µg of pre-cleared lysate incubated with SAFB1 (Invitrogen), SAFB2 (Bethyl) or IgG (Invitrogen) antibody crosslinked beads. The immunoprecipitate was run on Western blots and probed with SAFB1 (Bethyl), SAFB2 (Bethyl) and SRSF1 (Invitrogen) antibodies. Input and immunodepleted (ID) lysates were run as controls. Co-IP was performed on cell lysates from 3 patients.

5.2.6 Identification of novel SAFB1 and SAFB2 protein-protein interactions

Following the co-IPs performed in Figure 5.3 and Figure 5.4, co-IP samples were labelled by Tandem Mass Tag (TMT) and analysed by Nano-LC Mass Spectrometry. It is known that SAFB1 and SAFB2 are similar proteins, in which SAFB2 shares 74% similarity with SAFB1 (7). However, little is known about the specific protein interactions of SAFB1 and SAFB2. In order to investigate these interactions, the abundance of proteins in SAFB1 and SAFB2 immunoprecipitates was normalised to the corresponding IgG immunoprecipitate and the relative abundance was measured and analysed by student's t-test. SAFB1 and SAFB2 interacting proteins in HeLa and T-ALL cells, with a significant difference of ($P<0.05$) compared to the IgG control were selected for further analyses. Lists of SAFB1 and SAFB2 interacting proteins in HeLa and T-ALL cells were uploaded to VENNY 2.1 website (http://bioinfogp.cnb.csic.es/tools/venny/) and a Venn diagram was created (Figure 5.8). Results showed that a total of 1061 proteins were identified as interacting with SAFB1, while a total of 605 proteins interacted with SAFB2 in HeLa cells. Results also showed that in HeLa cells there were more unique partners of SAFB1 (476 proteins, 44%) than SAFB2 (20 proteins, 1.9%). Furthermore, a significant number of proteins interacted with both SAFB1 and SAFB2 (585 proteins, 54.1%). In contrast, in T-ALL cells a total of 146 proteins were found to interact with SAFB1, while a total of 348 proteins interacted with SAFB2. There were also more unique partners of SAFB2 (269 proteins, 64.8%) than SAFB1 (67 proteins, 16.1%) in T-ALL cells. Also, there was a large portion of proteins interacting with both SAFB1 and SAFB2 (79 proteins, 19%) (Figure 5.8).

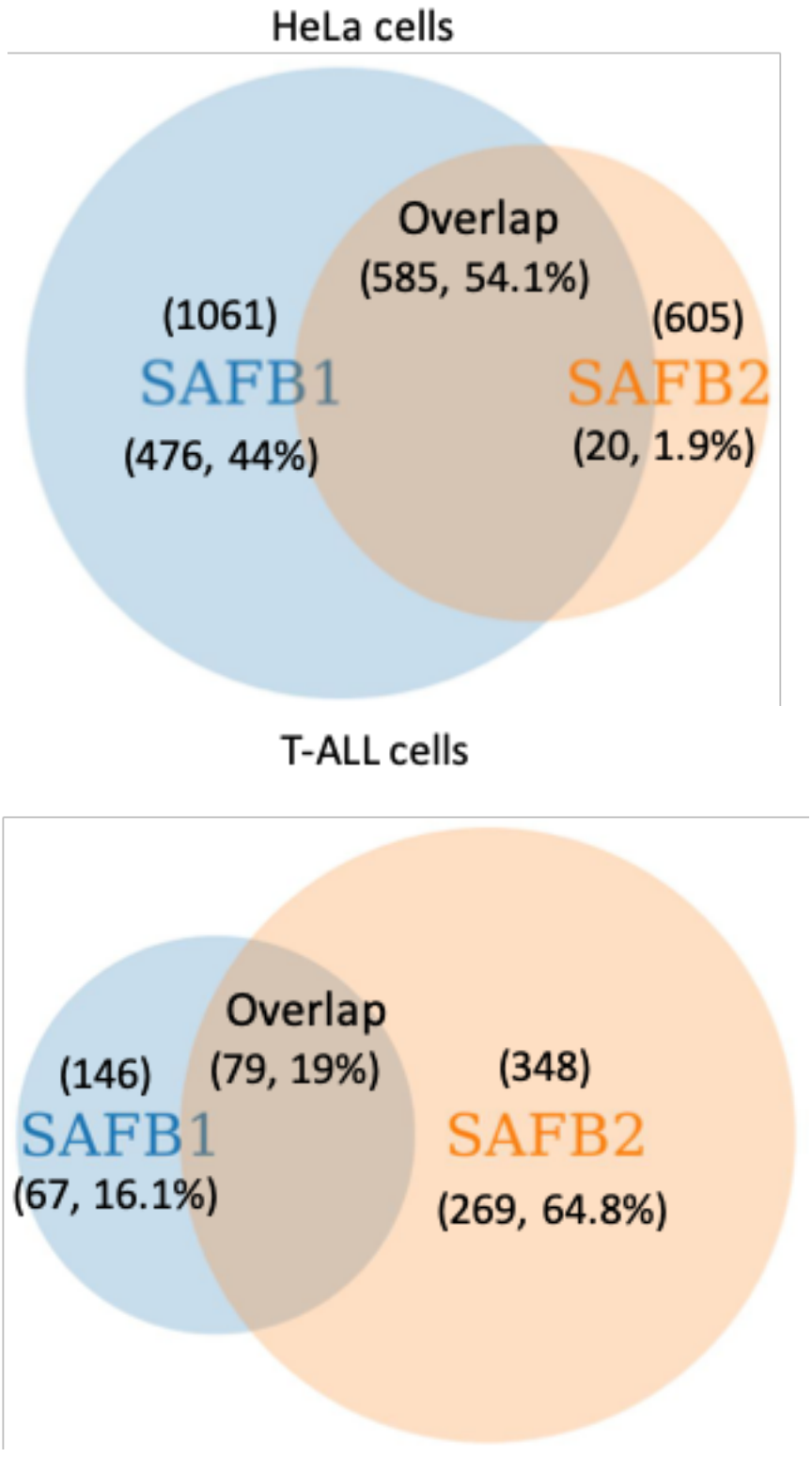

Figure 5.8 SAFB1 and SAFB2 protein interactions. A Venn diagram showing the total number of SAFB1 and SAFB2 interacting proteins in HeLa and T-ALL cells and highlighting SAFB1 unique partners (blue), SAFB2 unique partners (light brown) and the SAFB1/SAFB2 shared partners. Total number of proteins and corresponding percentage in each group are indicated.

The top interactions for SAFB1 in HeLa cells are shown (Table 5.1). Overall, SAFB1 binding proteins were associated with a higher statistical significance (lower p values) compared with SAFB2. SAFB1 interacted with several RNA binding proteins, including ELAVL1, LARP4, RBN27 with roles in regulating gene expression. In addition, SAFB1 was shown to interact with HNRNPR and HNRNPAB with roles in RNA processing. Furthermore, SAFB1 binding proteins were involved in regulating the chromosome and the cell cycle (CDC20, CCAR1, PRC1, CEP170).

Table 5.1 Top SAFB1 interactions in HeLa cells

Protein ID	Protein description	Gene ID	P value
Q15717	ELAV-like protein 1	ELAVL1	0.00E-06
Q71RC2	La-related protein 4	LARP4	0.00E-06
Q6IQ30	Polyadenylate-binding protein	PABPC1	2.58E-03
Q6NSW5	Putative protein	FAM45B	2.58E-03
Q12834	Cell division cycle protein 20 homolog	CDC20	2.58E-03
Q9P2N5	RNA-binding protein 27	RBN27	2.58E-03
Q8WXF1	Paraspeckle component 1	PSPC1	2.82E-03
A0A024R4E2	TAR DNA binding protein	TARDBP	2.82E-03
Q8N684	Cleavage and polyadenylation specificity factor subunit 7	CPSF7	2.82E-03
A0A0F7KYT8	Fragile X mental retardation autosomal homolog variant p2K	FXR1	2.82E-03
Q3MHD2	Protein LSM12 homolog	LSM12	3.10E-03
Q6FI03	G3BP protein	G3BP	3.10E-03
A8K6Q4	cDNA FLJ76888	N/A	3.10E-03
Q08211	ATP-dependent RNA helicase A	DHX9	3.10E-03
Q8IX12	Cell division cycle and apoptosis regulator protein 1	CCAR1	3.44E-03
P38919	Eukaryotic initiation factor 4A-III	EIF4A3	3.44E-03
Q9P0K7	Ankycorbin	RAI14	3.44E-03
Q5T1Z8	Pumilio homolog 1	PUM1	4.08E-03
Q13310	Polyadenylate-binding protein 4	PABPC4	4.17E-03
Q96N66	Lysophospholipid acyltransferase 7	MBOAT7	4.17E-03
A0A024RC67	Protein regulator of cytokinesis 1	PRC1	4.17E-03
A0A024QZ19	TNF receptor-associated factor 4	TRAF4	4.17E-03
Q9BY77	Polymerase delta-interacting protein 3	POLDIP3	4.17E-03
O43390	Heterogeneous nuclear ribonucleoprotein R	HNRNPR	4.17E-03
O60826	Coiled-coil domain-containing protein 22	CCDC22	4.17E-03
O43896	Kinesin-like protein	KIF1C	4.43E-03
O43143	Pre-mRNA-splicing factor ATP-dependent RNA helicase	DHX15	4.43E-03
Q5SW79	Centrosomal protein of 170	CEP170	4.50E-03
A0A024QZD5	Small nuclear ribonucleoprotein 70kDa polypeptide	SNRP70	4.50E-03
P51116	Fragile X mental retardation syndrome-related protein 2	FXR2	4.50E-03
F8W0Q9	Periphilin-1	PPHLN1	5.16E-03
Q53F64	Heterogeneous nuclear ribonucleoprotein AB	HNRNPAB	5.16E-03
A0A024R395	MRE11 meiotic recombination 11 homolog A	MRE11A	5.16E-03
O14965	Aurora kinase A	AURKA	5.16E-03
Q6P158	Putative ATP-dependent RNA helicase	DHX57	5.16E-03
A0A0S2Z4Z9	Non-POU domain containing octamer-binding isoform 1	NONO	5.16E-03
A8K9T5	E3 ubiquitin-protein ligase	UHRF1	5.29E-03
Q9HBB9	HC56	N/A	5.29E-03
P61964	WD repeat-containing protein 5	WDR5	6.12E-03
O75643	U5 small nuclear ribonucleoprotein 200 helicase	SNRNP200	6.12E-03
J3QR07	YTH domain-containing protein 1	YTHDC1	6.45E-03
Q14444	Caprin-1	CAPRIN1	6.45E-03
A0A024RAZ7	Heterogeneous nuclear ribonucleoprotein A1	HNRNPA1	6.45E-03
Q92878	DNA repair protein	RAD50	6.45E-03
Q9HCD5	Nuclear receptor coactivator 5	NCOA5	6.51E-03
Q8IYV2	DEAD (Asp-Glu-Ala-Asp) box polypeptide 20	ddx20	6.51E-03
Q9UK61	Protein TASOR	TASOR	6.60E-03
Q15182	Small nuclear ribonucleoprotein-associated protein	SNRPB	6.60E-03
Q9Y4W2	Ribosomal biogenesis protein LAS1L	LAS1L	6.60E-03
A0A087WVQ6	Clathrin heavy chain	CLTC	6.60E-03

The top interactions for SAFB2 in HeLa cells are shown (Table 5.2). Like SAFB1, SAFB2 binding proteins were associated with some RNA binding proteins, such as RBMXL1 and LARP4. Also, SAFB2 was associated with many HNRNPs, including HNRNPU, HNRNPH1, HNRNPR, HNRNPK and HNRNPM. Furthermore, SAFB2 was involved in regulating protein translation (EIF4A3, MRPL4, SRP68, RPS27). In addition, some proteins with roles in gene silencing were found to interact with SAFB2 (XPO1).

Table 5.2 Top SAFB2 interactions in HeLa cells

Protein ID	Protein description	Gene ID	P value
Q6IQ30	Polyadenylate-binding protein	PABPC1	1.10E-02
Q00839	Heterogeneous nuclear ribonucleoprotein U	HNRNPU	1.10E-02
Q96E39	RNA binding motif protein, X-linked-like-1	RBMXL1	1.10E-02
Q3MHD2	Protein LSM12 homolog	LSM12	1.10E-02
Q9NV31	U3 small nucleolar ribonucleoprotein protein	IMP3	1.10E-02
Q13601	KRR1 small subunit processome component homolog	KRR1	1.10E-02
Q12834	Cell division cycle protein 20 homolog	CDC20	1.10E-02
G8JLB6	Heterogeneous nuclear ribonucleoprotein H	HNRNPH1	1.10E-02
Q8TCJ2	Dolichyl-diphosphooligosaccharide--protein glycosyltransferase subunit	STT3B	1.10E-02
A0A024RDQ8	Replication factor C (Activator 1) 3	RFC3	1.10E-02
P11940	Polyadenylate-binding protein 1	PABPC1	1.10E-02
Q9HCD5	Nuclear receptor coactivator 5	NCOA5	1.10E-02
A0A1C7CYX1	ELM2 and SANT domain-containing protein 1	ELMSAN1	1.10E-02
Q12905	Interleukin enhancer-binding factor 2	ILF2	1.10E-02
A0A087WTW0	E3 ubiquitin-protein ligase	UHRF1	1.10E-02
Q6FI03	G3BP protein	G3BP	1.10E-02
P38919	Eukaryotic initiation factor 4A-III	EIF4A3	1.10E-02
O43390	Heterogeneous nuclear ribonucleoprotein R	HNRNPR	1.10E-02
Q5EC54	Heterogeneous nuclear ribonucleoprotein K	HNRNPK	1.10E-02
O00425	Insulin-like growth factor 2 mRNA-binding protein 3	IGF2BP3	1.10E-02
P52272	Heterogeneous nuclear ribonucleoprotein M	HNRNPM	1.10E-02
J3KTA4	Probable ATP-dependent RNA helicase	DDX5	1.10E-02
Q96F88	Processing of 1, ribonuclease P/MRP subunit	POP1	1.10E-02
Q9BZH6	WD repeat-containing protein 11	WDR11	1.10E-02
A8MXP9	Matrin-3	MATR3	1.10E-02
Q08211	ATP-dependent RNA helicase A	DHX9	1.10E-02
Q13310	Polyadenylate-binding protein 4	PABPC4	1.20E-02
P67809	Nuclease-sensitive element-binding protein 1	YBX1	1.20E-02
P38159	RNA-binding motif protein, X chromosome	RBMX	1.20E-02
Q9BYD3	39S ribosomal protein L4, mitochondrial	MRPL4	1.20E-02
A0A024QZ19	TNF receptor-associated factor 4	TRAF4	1.20E-02
C9JJ19	28S ribosomal protein S34, mitochondrial	MRPS34	1.20E-02
Q9BZI7	Regulator of nonsense transcripts 3B	UPF3B	1.20E-02
A0A024QZD5	Small nuclear ribonucleoprotein 70kDa polypeptide	SNRP70	1.20E-02
Q15398	Disks large-associated protein 5	DLGAP5	1.20E-02
Q9UHB9	Signal recognition particle subunit	SRP68	1.20E-02
O43896	Kinesin-like protein KIF1C	KIF1C	1.20E-02
Q9HBB9	HC56	N/A	1.20E-02
A0A024R1I7	Tuftelin-interacting protein 11	TFIP11	1.20E-02
Q71RC2	La-related protein 4	LARP4	1.20E-02
Q14966	Zinc finger protein 638	ZNF638	1.20E-02
Q15058	Kinesin-like protein KIF14	KIF14	1.20E-02
Q8IV48	3'-5' exoribonuclease 1	ERI1	1.30E-02
O14980	Exportin-1	XPO1	1.30E-02
H0YJZ4	Striatin-3	STRN3	1.30E-02
Q9UHK0	Nuclear fragile X mental retardation-interacting protein 1	NUFIP1	1.30E-02
P42677	40S ribosomal protein S27	RPS27	1.30E-02
Q08379	Golgin subfamily A member 2	GOLGA2	1.30E-02
D9HTE9	Plasma membrane citrate carrier	SLC25A1	1.30E-02
F8W0Q9	Periphilin-1	PPHLN1	1.30E-02

Also, the most significant interactions for SAFB1 in T-ALL are highlighted (Table 5.3). There were several proteins were bound SAFB1 that have roles in protein translation (RPL34, RPL37, RPL15, RPL18A, RPS10, RPL27, RPL6, RPL4, RPL8, RPL3, RPL13, RPL13A). SAFB1 was involved in regulating splicing (SRPK1, CWC25).

Table 5.3 Top SAFB1 interactions in T-ALL cells

Protein ID	Protein name	Gene ID	P value
A0A024RDH8	Ribosomal protein L34	RPL34	2.84E-04
A0A024R029	Activator of basal transcription 1	ABT1	5.41E-04
H3BLV9	SRSF protein kinase 1	SRPK1	8.75E-04
J3KNL6	Protein transport protein sec16	SEC16A	1.10E-03
Q13045	Protein flightless-1 homolog	FLII	1.17E-03
P61927	60S ribosomal protein L37	RPL37	1.25E-03
A0A024R2Q4	Ribosomal protein L15	RPL15	1.56E-03
Q96HS1	Serine/threonine-protein phosphatase	PGAM5	1.58E-03
B2R4C0	60S ribosomal protein L18a	RPL18A	2.23E-03
P46783	40S ribosomal protein S10	RPS10	2.24E-03
Q9H8M2	Bromodomain-containing protein 9	BRD9	2.91E-03
Q9H7Z3	Protein NRDE2 homolog	NRDE2	3.71E-03
Q02040	A-kinase anchor protein 17A	AKAP17A	3.75E-03
Q9NXE8	Pre-mRNA-splicing factor CWC25 homolog	CWC25	3.91E-03
L0R588	Alternative protein C11orf48	C11orf48	4.91E-03
E9PGC8	Microtubule-associated protein 1A	MAP1A	5.49E-03
P00387	NADH-cytochrome b5 reductase 3	CYB5R3	6.07E-03
J3KNR0	Non-specific serine/threonine protein kinase	MARK3	6.53E-03
A0A024QZW2	Nucleolar protein 7, 27kDa	NOL7	6.95E-03
B3KX14	cDNA FLJ44463 fis	MORF4L2	7.09E-03
Q15149	Plectin	PLEC	7.12E-03
O43684	Mitotic checkpoint protein	BUB3	7.49E-03
P07437	Tubulin beta chain	TUBB	7.56E-03
V9HW31	ATP synthase subunit beta	ATP5F1B	8.37E-03
Q9BU76	Multiple myeloma tumour-associated protein 2	MMTAG2	8.47E-03
J3KQN4	60S ribosomal protein L36a	RPL36A	8.50E-03
A0A090N7Y2	ATP-binding cassette, sub-family F (GCN20), member 2	GCN20	9.16E-03
P61353	60S ribosomal protein L27	RPL27	9.61E-03
Q16630	Cleavage and polyadenylation specificity factor subunit 6	CPSF6	9.68E-03
Q96GA3	Protein LTV1 homolog	LTV1	9.80E-03
Q9NP58	ATP-binding cassette sub-family B member 6, mitochondrial	ABCB6	9.87E-03
Q9HBB3	60S ribosomal protein L6	RPL6	1.01E-02
Q9BVP2	Guanine nucleotide-binding protein-like 3	GNL3	1.01E-02
A0A024R711	E3 ubiquitin-protein ligase	UHRF1	1.05E-02
Q96F86	Enhancer of mRNA-decapping protein 3	EDC3	1.06E-02
Q59GY2	Ribosomal protein L4	RPL4	1.07E-02
P62917	60S ribosomal protein L8	RPL8	1.08E-02
A0A024R704	SFRS protein kinase 2	SRPK2	1.09E-02
P39023	60S ribosomal protein L3	RPL3	1.10E-02
P26373	60S ribosomal protein L13	RPL13	1.10E-02
V9HW22	Epididymis luminal protein 33	HEL-S-72p	1.10E-02
Q13573	SNW domain-containing protein 1	SNW1	1.11E-02
Q12873	Chromodomain-helicase-DNA-binding protein 3	CHD3	1.13E-02
Q8N684	Cleavage and polyadenylation specificity factor 7	CPSF7	1.22E-02
B4DWA6	cDNA FLJ60094	N/A	1.22E-02
P0DPB5	Protein POLR1D, isoform 2	POLR1D	1.23E-02
A0A1U9X972	PRRC2A	PRRC2A	1.26E-02
Q9UGY1	Nucleolar protein 12	NOL12	1.26E-02
A0A024R6W2	Nudix (Nucleoside diphosphate linked moiety X)-type motif 21	NUDT21	1.28E-02
P40429	60S ribosomal protein L13a	RPL13A	1.30E-02

Also, the most significant interactions for SAFB2 in T-ALL are highlighted (Table 5.4). SAFB2 interacted with proteins with roles in gene silencing (SRRT). In addition, SAFB2 seemed to be important in regulating splicing (U2AF, SF3B1, DHX15, SF3B6, SRPK1, KHDRBS1). Furthermore, some serine proteases interacted with SAFB2 with implication in the immune system and NK and T cells (GZMH, CTSG).

Table 5.4 Top SAFB2 interactions in T-ALL cells

Protein ID	Protein name	Gene ID	P value
Q13045	Protein flightless-1 homolog	FLII	1.72E-04
Q658Y4	Protein FAM91A1	FAM91A1	1.88E-04
Q9NZB2	Constitutive coactivator of PPAR-gamma-like protein 1	FAM120A	4.88E-04
Q53HH4	Ras-GTPase-activating protein SH3-domain-binding protein variant	N/A	6.98E-04
Q9Y520	Protein PRRC2C	PRRC2C	7.32E-04
P26368	Splicing factor U2AF 65 kDa subunit	U2AF	7.46E-04
Q9BXP5	Serrate RNA effector molecule homolog	SRRT	7.61E-04
A8K588	cDNA FLJ76823	SFRS6	8.70E-04
Q8ND56	Protein LSM14 homolog A	LSM14	1.07E-03
B4DUQ1	cDNA FLJ54552	N/A	1.11E-03
P20718	Granzyme H	GZMH	1.17E-03
Q07666	KH domain-containing, RNA-binding, signal transduction-associated protein 1	KHDRBS1	1.53E-03
A3RJH1	ATP-dependent RNA helicase	DDX1	1.55E-03
P51116	Fragile X mental retardation syndrome-related protein 2	FXR2	1.59E-03
A0A2R8YEM9	TPR and ankyrin repeat-containing protein 1	TRANK1	1.65E-03
P08579	U2 small nuclear ribonucleoprotein B''	SNRPB2	1.81E-03
A0A0S2Z4Z0	RNA binding motif protein 14 isoform 1	RBM14	1.95E-03
Q15365	Poly(rC)-binding protein 1	PCBP1	2.35E-03
B4DI41	cDNA FLJ55972	N/A	2.37E-03
O75533	Splicing factor 3B subunit 1	SF3B1	2.40E-03
O15042	U2 snRNP-associated SURP motif-containing protein	U2SURP	2.46E-03
A0A024RAC5	Regulator of chromosome condensation 2	RCC2	2.85E-03
Q9NUD5	Zinc finger CCHC domain-containing protein 3	ZCCHC3	2.90E-03
Q59EC0	Adenosine deaminase, RNA-specific isoform ADAR-a	ADAR	3.06E-03
O43143	Pre-mRNA-splicing factor ATP-dependent RNA helicase	DHX15	3.09E-03
A0A024RDB4	Heterogeneous nuclear ribonucleoprotein D	HNRNPD	3.45E-03
A8K9U6	cDNA FLJ76121	N/A	3.67E-03
Q9GZR7	ATP-dependent RNA helicase	DDX24	3.74E-03
P62081	40S ribosomal protein S7	RPS7	3.76E-03
Q9BZH6	WD repeat-containing protein 11	WDR11	4.07E-03
A0A024R3R5	Lamin B receptor	LBR	4.08E-03
Q9P2N5	RNA-binding protein 27	RBM27	4.28E-03
Q9Y2X3	Nucleolar protein 58	NOP58	4.82E-03
A8K7N0	cDNA FLJ75556	N/A	5.04E-03
A8K9C4	Elongation factor 1-alpha	EEF1A1	5.09E-03
P09661	U2 small nuclear ribonucleoprotein A'	SNRPA1	5.10E-03
P41091	Eukaryotic translation initiation factor 2 subunit 3	EIF2S3	5.39E-03
Q9Y3B4	Splicing factor 3B subunit 6	SF3B6	5.42E-03
B2RE11	cDNA, FLJ96865	N/A	5.44E-03
Q13422	DNA-binding protein Ikaros	IKZF1	5.61E-03
Q8IY37	Probable ATP-dependent RNA helicase	DHX37	5.67E-03
Q9UKM9	RNA-binding protein Raly	RALY	5.69E-03
Q7L2E3	ATP-dependent RNA helicase	DHX30	5.72E-03
Q15366	Poly(rC)-binding protein 2	PCBP2	5.72E-03
P08311	Cathepsin G	CTSG	6.08E-03
Q27975	Synaptosomal-associated protein 47	SNAP47	6.09E-03
O60506	Heterogeneous nuclear ribonucleoprotein Q	SYNCRIP	6.39E-03
H3BLV9	SRSF protein kinase 1	SRPK1	6.64E-03
P38919	Eukaryotic initiation factor 4A-III	EIF4A3	6.72E-03
O43447	Peptidyl-prolyl cis-trans isomerase H	PPIH	6.90E-03

5.2.7 Protein-protein interactions and gene ontology (GO) analysis of SAFB1 and SAFB2 interacting proteins in HeLa cells

In order to gain more information on the functional relevance of SAFB1 and SAFB2 interactions, protein-protein interactions network (PPIs), GO analysis and pathway analysis were conducted. The Search Tool for the Retrieval of Interacting Genes (STRING 11.0 version) database was used to identify PPIs (https://string-db.org). An interaction score of not < 0.7 (medium confidence score) was considered to be significant and the PPI were visualised.

There are many web based enrichment tools (174),(175) of which some are commonly used; Enrichr (https://amp.pharm.mssm.edu/Enrichr/) (176) and the Database for Annotation, Visualization and Integrated Discovery (DAVID) version 6.8 (https://david.ncifcrf.gov/). DAVID was used as it is commonly used by proteomic and RNA-seq users (174),(177). Also, GO of the biological processes (BP) in DAVID can be shown at different levels of enrichment. Also, BP-FAT was used to provide specific BPs and to filter out very broad GO terms based on a measured specificity of each term with reduced GO term redundancies.

Using DAVID, the significant total SAFB1 and SAFB2 interacting protein lists were profiled for BP (177), pathway analysis; Kyoto Encyclopaedia of Genes and Genomes (KEGG, version 2019) (178) and tissue specific enrichment (179). P value scores were computed for all categories and false discovery rates (FDR) with the thresholds of P-value < 0.05 and enrichment gene count > 2.

5.2.7.1 Specific tissue enrichment by GNF database in HeLa cells

A specific tissue enrichment tool (GNF database), adopted from DAVID, was used to show enrichments for up-regulated proteins in human tissue for SAFB1 and SAFB2 interacting proteins in HeLa cells. GNF database is a gene online portal that provides information of gene expression in human tissues. Interestingly, results showed that the SAFB1 and SAFB2 interacting proteins were highly up-regulated in different blood-related tissues. For example, both SAFB1 and SAFB2 interacting proteins were most enriched in promyelocytic leukaemia (HL-60) cell line. In addition, SAFB1 and SAFB2 interacting proteins were also enriched in another leukaemia cell line, T lymphoblastic leukaemia (MOLT-4) (Figure 5.9). As SAFB1 and SAFB2 interacting proteins were enriched in HL-60 and MOLT-4 leukaemia cell lines, the interacting proteins were found to be enriched in specific lymphoid cells, such as $CD56^+$ NK cells and $CD4^+$ and $CD8^+$ T cells. Also, SAFB1 and SAFB2 interacting proteins were enriched in $CD14^+$ monocytes, $CD33^+$ myeloid cells and $CD71^+$ early erythroid cells (Figure 5.9).

SAFB1 and SAFB2 interacting proteins were enriched in lymph nodes and the Burkitts lymphoma (Raji) cell line with less significant enrichment compared with HL-60 and MOLT-4 leukaemia cell lines. Finally, SAFB1 and SAFB2 interacting proteins were found to be widely up-regulated in other tissues, including heart, adipocyte, placenta, uterus corpus and testis (Figure 5.9).

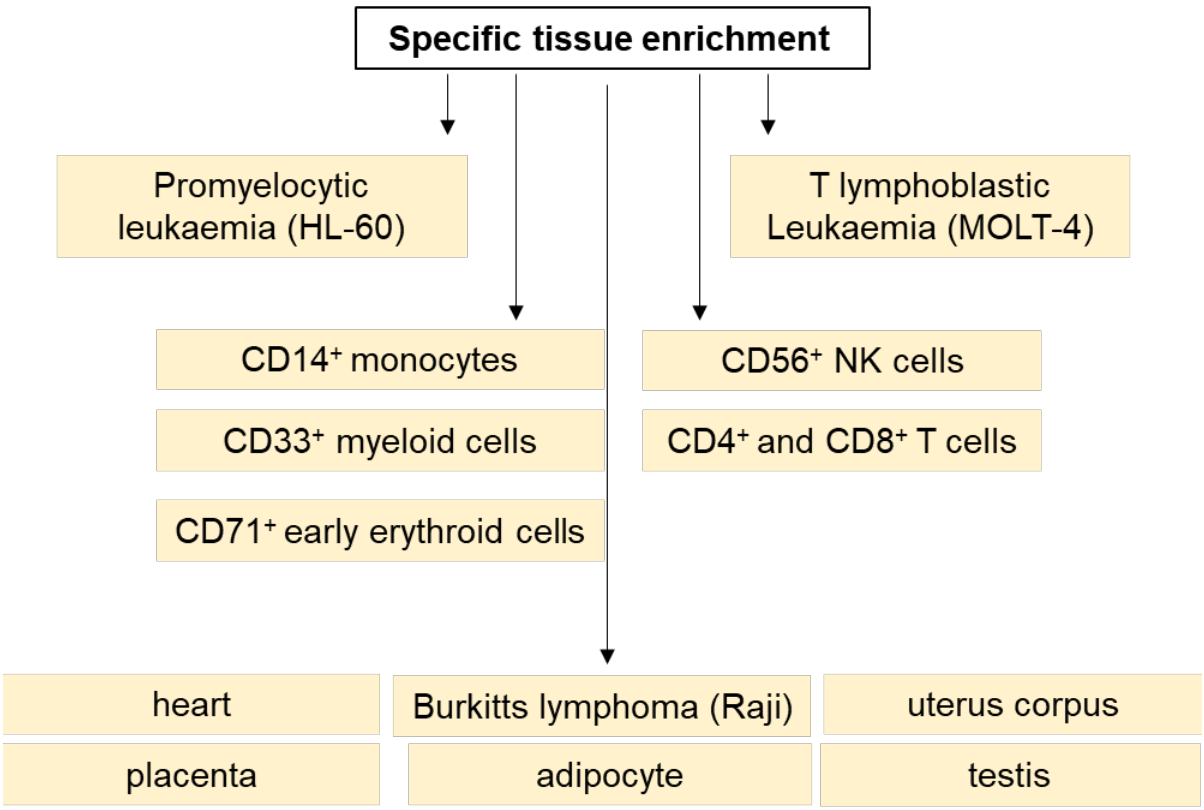

Figure 5.9 Specific tissue enrichment for SAFB1 and SAFB2 interacting proteins in HeLa cells. SAFB1 and SAFB2 lists were loaded into DAVID and the tissue specific enrichment tool was selected. The protein enrichments were based on thresholds of P-value < 0.05 and enrichment gene count > 2.

5.2.7.2 Protein-protein interactions for SAFB1 interacting proteins in HeLa cells

In order to show the SAFB1 protein interaction network and the processes associated with the distinct clusters (in HeLa cells), STRING analysis was used. STRING analysis was computed with a high degree of connectivity for the network edges and the highest confidence for the interaction score. Results showed that total SAFB1 interacting proteins (1061) could be grouped into 6 broad functional categories, highlighted in black rectangles (Figure 5.10). The STRING analysis showed a cluster of: (i) ribosomal proteins, important in protein translation; (ii) mitochondrial ribosomal proteins ; (iii) DEAD-box proteins and hnRNPs, which are known to essential in RNA processing; (iv), proteins involved in the transcription processes (initiation, elongation, termination); (v) histones enzymes and chromatin modifiers, suggesting a role in the nucleosome organisation; (vi) centromere regulators and microtubules, which are involved in the cytoskeleton organisation and cell cycle.

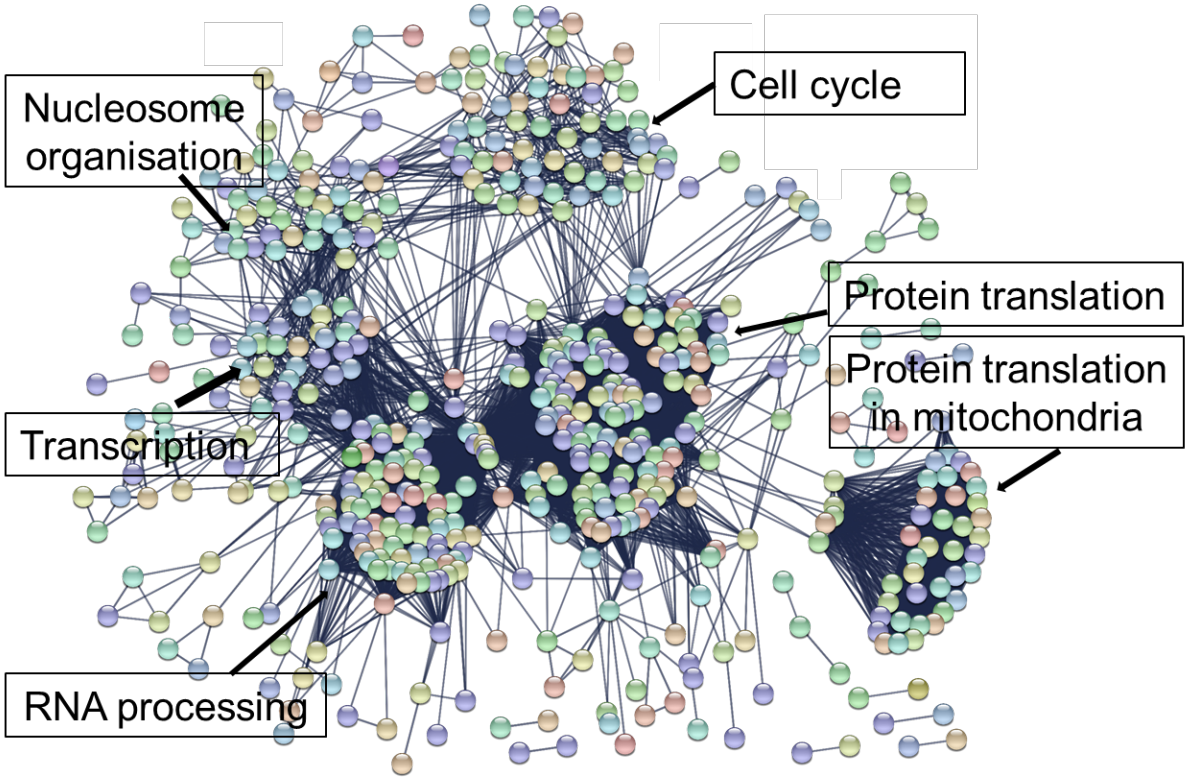

Figure 5.10 STRING analysis of SAFB1 interacting proteins in HeLa cells. SAFB1 interacting proteins were loaded into STRING and the network edges were based on confidence. The interaction score was set for the highest confidence (≥0.7). Circles represent SAFB1 interacting proteins.

5.2.7.3 Protein-protein interactions for SAFB2 interacting proteins in HeLa cells

The total SAFB2 binding proteins (605) were also loaded into STRING to give insight on the broad processes that SAFB2 interacting proteins regulate in HeLa cells. Similar to the SAFB1 data, results showed that the main processes regulated by SAFB2 interacting proteins were RNA processing, protein translation, protein translation in mitochondria, nucleosome organisation, transcription and the cell cycle (Figure 5.10). Regulating similar processes is not surprising, as SAFB2 interacting proteins were mostly overlapped with SAFB1 binding proteins and only 20 proteins were unique to SAFB2 (Figure 5.11).

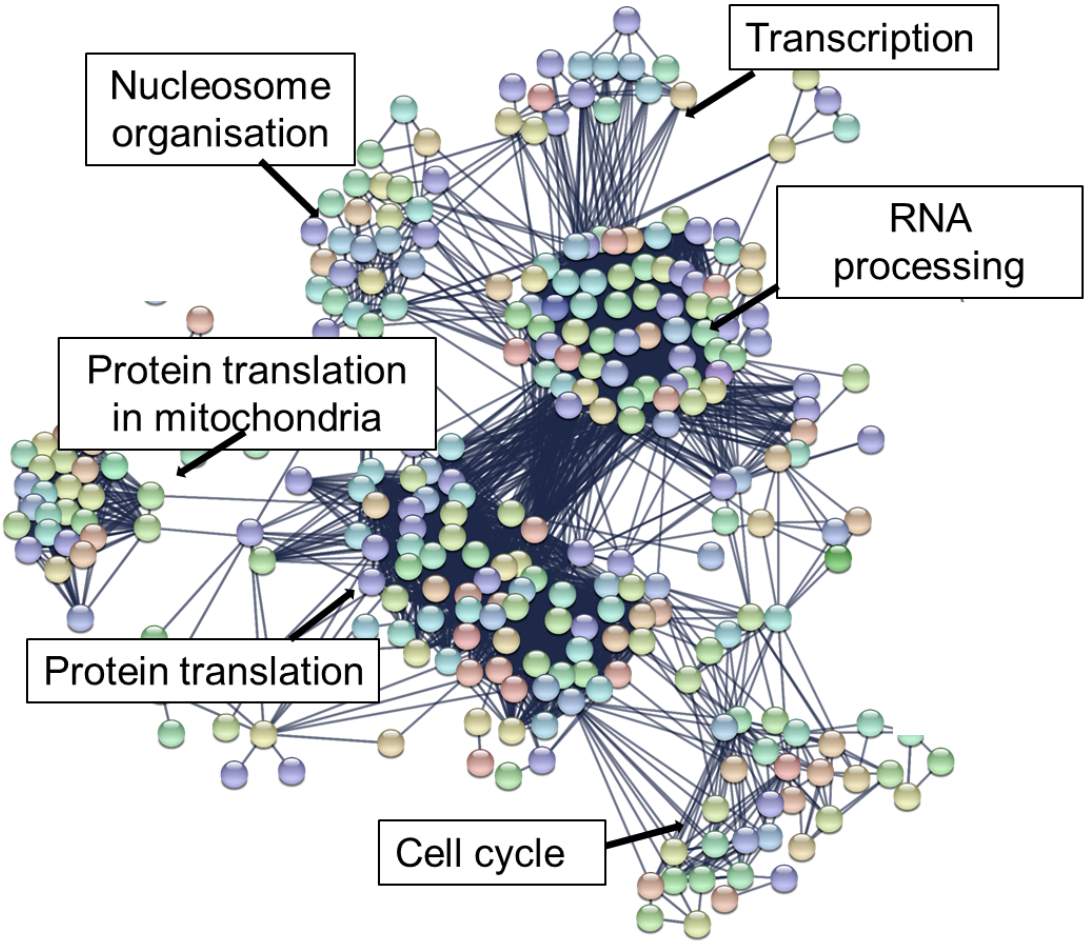

Figure 5.11 STRING analysis of SAFB2 interacting proteins in HeLa cells. SAFB2 interacting proteins were loaded into STRING and the network edges were based on confidence. The interaction score was set for the highest confidence (≥0.7). Circles represent SAFB2 interacting proteins.

5.2.7.4 Pathway analysis (KEGG) in HeLa cells

The next aim was to explore the main pathways that SAFB1 (1061) and SAFB2 (605) interacting proteins regulate in HeLa cells. The KEGG database was used as it is thought to be the gold standard for pathway analysis (Qi *et al.*, 2016). Results showed that SAFB1/2 regulated the same pathways with lower FDRs for SAFB1 binding proteins compared with SAFB2. Results also showed that the most enriched pathway for both SAFB1 and SAFB2 interacting proteins was the ribosome for SAFB1 (8.5%) and SAFB2 (7.7%) with FDR of 2.60E-59 and 2.60E-26, respectively (Table 5.5). These data reflect the observations on STRING where there was a cluster of proteins involved in protein translation and they were mainly ribosomal proteins. The second most enriched pathway was the spliceosome for SAFB1 (6.6%) and SAFB2 (7.6%) with FDR of 8.70E-37 and 1.50E-25, respectively. Another pathway that was found to be enriched by SAFB1 and SAFB2 interacting proteins was RNA transport for SAFB1 (5.2%) and SAFB2 (5.2%) with FDR of 3.50E-17 and 1.70E-10, respectively (Table 5.5). Lastly, SAFB1 interacting proteins (3.5%) were found to be more enriched than SAFB2 (3.9%) in regulating the RNA transport and mRNA surveillance pathways with FDR of 5.20E-14 and 8.00E-09, respectively (Table 5.5).

Table 5.5 Pathway analysis (KEGG) for SAFB1 and SAFB2 interacting proteins in HeLa cells.

	SAFB1		SAFB2	
Term	**%**	**FDR**	**%**	**FDR**
Ribosome	8.5	2.60E-59	7.7	2.60E-26
Spliceosome	6.6	8.70E-37	7.6	1.50E-25
RNA transport	5.2	3.50E-17	5.5	1.70E-10
mRNA surveillance pathway	3.5	5.20E-14	3.9	8.00E-09

FDR= false discovery rate, %= percentage of proteins involved from the whole list.

5.2.7.5 The top overlapping GO biological processes for SAFB1/2 in HeLa cells

The next aim was to identify specific SAFB1 and SAFB2 functions. Thus, SAFB1 (1061) and SAFB2 (605) lists were loaded into DAVID and searched against BP-FAT to provide specific functions. There were 535 and 402 biological processes (BP-FAT) that were significantly enriched for SAFB1 and SAFB2 interacting proteins in HeLa cells, respectively. The key most enriched categories for SAFB1 and SAFB2 interacting proteins were selected (Table 5.6). Overall, the top BP for SAFB1/2 is similar but is variable in SAFB1 compared with SAFB2. Also, the BP for SAFB1 was associated with lower FDRs compared with SAFB2. Specifically, SAFB1 (33.4%) and SAFB2 (37.8%) interacting proteins were highly enriched for RNA processing with FDR of 4.10E-180 and 4.70E-125, respectively. Also, there were several processes related to RNA, including mRNA, rRNA, ncRNA processing, RNA splicing, RNA localisation and RNA transport found to be enriched.

In addition, SAFB1 (22%) and SAFB2 (23.1%) interacting proteins were found to be associated with ribonucleoprotein complex biogenesis with FDR of 1.30E-135 and 6.00E-79, respectively (Table 5.6). Broadly, SAFB1 (62.8%) and SAFB2 (66.1%) interacting proteins were highly enriched for gene expression with FDR of 4.00E-106 and 1.10E-71, respectively. Furthermore, there are other processes found to be enriched, such as translation with FDR of 1.90E-85 and 1.20E-48 for SAFB1 (19.8%) and SAFB2 (20.3%) interacting proteins, respectively. Also, SAFB1 and SAFB2 interacting proteins were enriched for chromosome organisation, transcription and cell cycle processes.

Table 5.6 The top 10 GO biological processes for total SAFB1 and SAFB2 interacting proteins in HeLa cells

	SAFB1		SAFB2	
Term	**%**	**FDR**	**%**	**FDR**
RNA processing	33.4	4.10E-180	37.8	4.70E-125
ribonucleoprotein complex biogenesis	22	1.30E-135	23.1	6.00E-79
gene expression	62.8	4.00E-106	66.1	1.10E-71
ncRNA processing	16.7	1.40E-90	17.3	4.30E-52
translation	19.8	1.90E-85	20.3	1.20E-48
RNA splicing	15	4.60E-75	18.1	1.50E-57
RNA localisation	6.6	5.0E-26	6.8	3.4E-14
chromosome organisation	15.7	1.90E-20	14.6	7.20E-08
RNA transport	5.3	1.1E-19	5.7	2.0E-11
DNA-templated transcription	3.6	1.20E-14	4.6	6.80E-12

FDR= false discovery rate, %= percentage of proteins involved from the whole list.

5.2.7.6 The involvement of SAFB1/2 in regulating the cell cycle

SAFB1/2 interacting proteins were significantly involved in regulating the cell cycle. STRING was used to show the functional connections between the SAFB1/2 interactome (Figure 5 12). For instance, the BRCA1 protein is known to interact with regulators of the cell cycle (CDKN2A) and cell division (CDC20 and CDC27). Another interesting protein is BUB3 which is important in regulating the centromere.

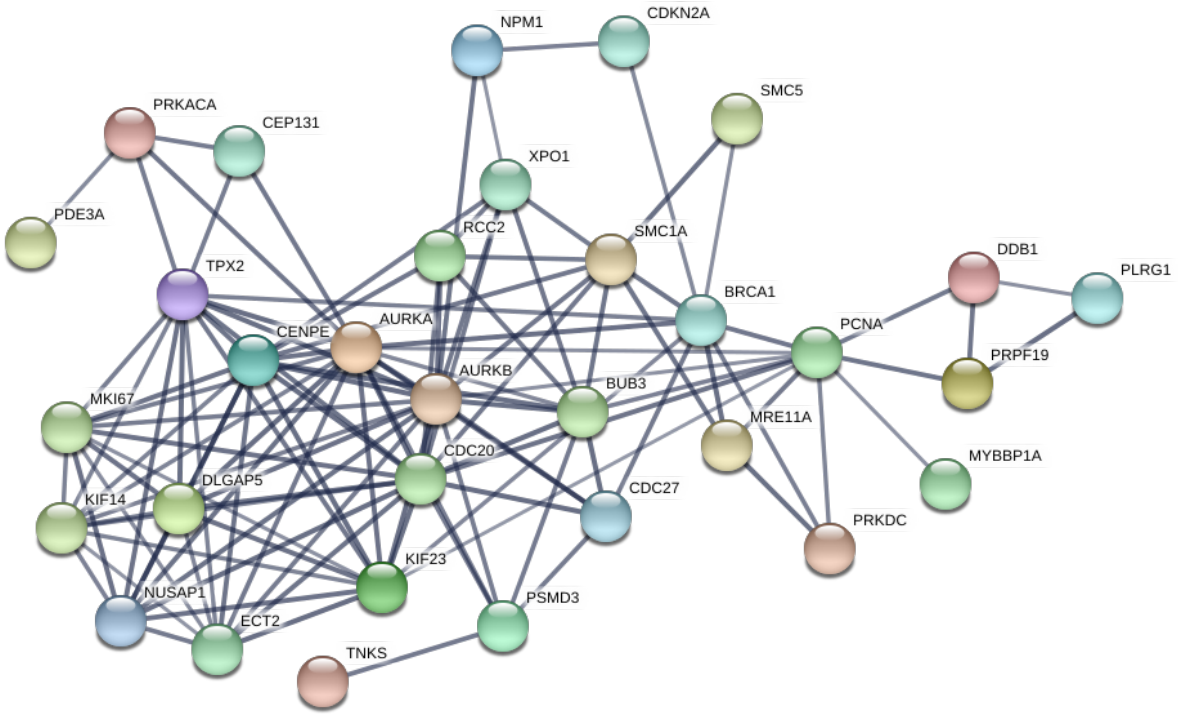

Figure 5.12 STRING analysis of SAFB1/2 interacting proteins implicated in regulating the cell cycle in HeLa cells. SAFB1/2 interacting proteins implicated in regulating the cell cycle were loaded into STRING and the network edges were based on confidence. The interaction score was set for the highest confidence (≥0.7). Circles represent SAFB1/2 interacting proteins.

5.2.7.7 The involvement of SAFB1/2 in regulating the gene silencing by miRNA

DAVID analyses showed that SAFB1/2 binding proteins were important regulators of gene silencing. The binding proteins were loaded into STRING to investigate how those proteins associated together (Figure 5.13). ELAVL1, which was shown to be the top interactor with SAFB1 (Table 1.1), found to interact with important regulators of miRNA processing, including DROSHA, SRRT, DGCR8 and AGO2.

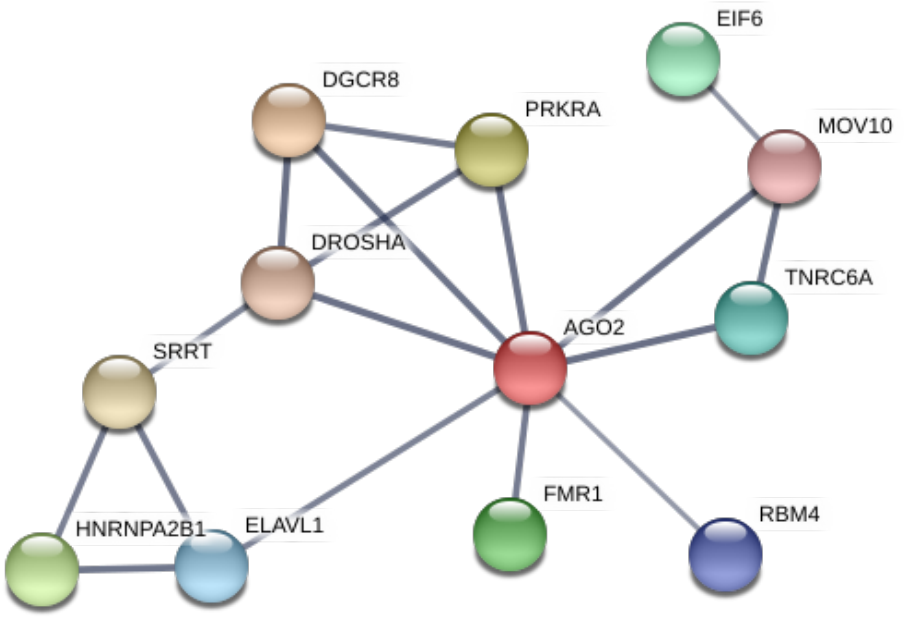

Figure 5.13 STRING analysis of SAFB1/2 interacting proteins implicated in regulating gene silencing in HeLa cells. SAFB1/2 interacting proteins implicated in regulating gene silencing were loaded into STRING and the network edges were based on confidence. The interaction score was set for the highest confidence (≥0.7). Circles represent SAFB1/2 interacting proteins.

5.2.7.8 The involvement of SAFB1/2 in regulating methylation

SAFB1/2 interacting proteins were shown to regulate protein methylation using DAVID. It was found that SAFB proteins are methylated differentially with RGG/RG motifs (Norman et al., 2016; Scott et al., 2017; Nozawa et al., 2017). STRING analysis showed that SAFB1/2 binding proteins interacted with histones (HIST1H1C, HIST1H1E, HIST1H1B) and DNA methyltransferases (DNMT1), thereby regulating methylation (Figure 5.14). Small nuclear ribonucleoprotein Sm D3 (SNRPD3) were shown as a cluster with CHTOP and SNW1 and the former proteins was shown to interact with PRMT5 (Hiroki et al., 2014).

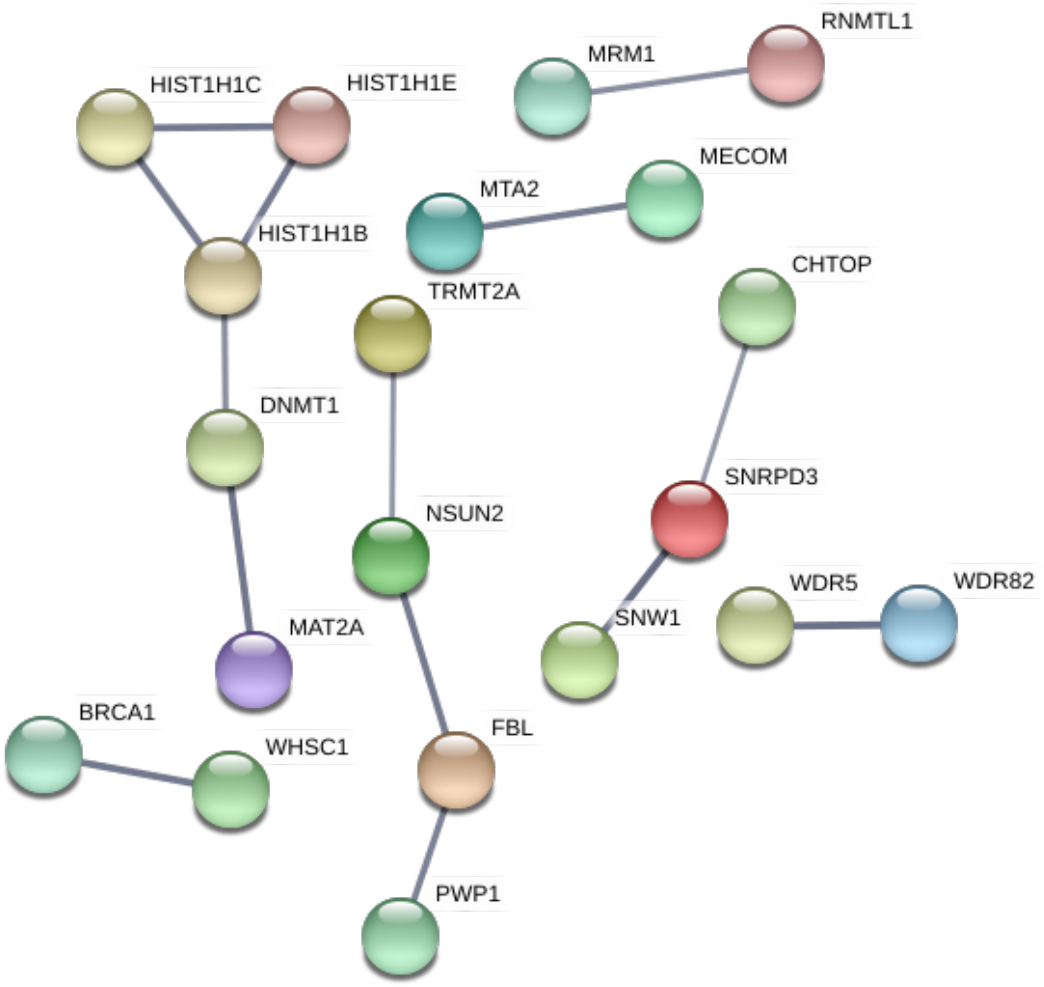

Figure 5.14 STRING analysis of SAFB2 interacting proteins implicated in regulating methylation in HeLa cells. SAFB2 interacting proteins implicated in regulating methylation were loaded into STRING and the network edges were based on confidence. The interaction score was set for the highest confidence (≥0.7). Circles represent SAFB2 interacting proteins.

5.2.7.9 Unique GO BP terms identified in HeLa cells following analysis of all proteins pulled down by SAFB1 (1061) and SAFB2 (605)

Data in Table 5.6 shows that SAFB1 and SAFB2 interacting proteins shared a lot of functions (BP) in HeLa cells. The aim here was to identify unique SAFB1 and SAFB2 biological processes. Thus, total SAFB1 (1061) and SAFB2 (605) interacting proteins were loaded into DAVID and unique biological processes for SAFB1/2 were identified. From a total of 535 and 402 biological processes that were significantly enriched for

SAFB1 and SAFB2, respectively, some BP terms were only unique to SAFB1 or SAFB2.

Results showed that SAFB1 has more unique BP processes than SAFB2. SAFB1 was enriched and involved in regulating protein localisation (19.1%) and transport (15%, Table 5.7). Data also showed that SAFB1 is important in the formation of the translation preinitiation complex (0.9%) and in regulating chromatin organisation (2.1%). Furthermore, SAFB1 regulates other processes, including small nuclear RNA (snoRNA) localisation (0.4%), anatomical structure homeostasis (3.5%) and cellular response to oxidative stress (2.5%, Table 5.7).

Table 5.7 Unique SAFB1 BP terms in HeLa cells following analysis of all proteins pulled down by SAFB1 (1061)

Term	%	FDR
protein localisation	19.1	3.10E-05
protein transport	15	8.48E-05
formation of translation preinitiation complex	0.9	4.27E-04
protein-DNA complex assembly	2.7	0.011
chromatin organisation	2.1	0.021
snoRNA localisation	0.4	0.023
anatomical structure homeostasis	3.5	0.024
cellular response to oxidative stress	2.5	0.029

FDR= false discovery rate, %= percentage of proteins involved from the whole list.

SAFB1 is expressed in the nucleus, while SAFB2 is found in the nucleus and cytoplasm, suggesting that SAFB2 function is likely to differ from SAFB1. Thus, it was interesting to identify unique functions for SAFB2 in HeLa cells. Results showed that SAFB2 is important in regulating the cytoskeleton (9.2%) and centrosome organisation (1.6%, Table 5.8). Furthermore, SAFB2 functions as an important regulator for mitotic spindle elongation (0.5%, Table 5.8). All GO terms were significantly enriched ($P<0.05$) but associated with higher FDR values.

Table 5.8 Unique SAFB2 BP terms in HeLa cells following analysis of all proteins pulled down by SAFB2 (605)

Term	%	FDR
cytoskeleton organisation	9.2	0.106
centrosome organisation	1.6	0.223
mitotic spindle elongation	0.5	0.289

FDR= false discovery rate, %= percentage of proteins involved from the whole list.

5.2.7.10 Biological process analyses of SAFB1/2 binding proteins in HeLa cells that only found in SAFB1 (476) or SAFB2 (20) pull downs

Data in Figures (5.10- 5.15) and Tables (5.5, 5.6, 5.7, 5.8) were all based on SAFB1 (1061) interacting proteins and most SAFB1 binding proteins were also bound to SAFB2 (54.1%). Thus, those (476) proteins bound by SAFB1 and not bound by SAFB2 were analysed using DAVID (Figure 5.9). Results showed that SAFB1 binding proteins were predominantly enriched in regulating ribonucleoprotein complex biogenesis (20.3%), RNA processing (26.3%), RNA splicing (20.3%) and translation (18.6%). Consistent with Table (5.7), protein localisation (15.7%), protein transport (18.8%), chromatin organisation (8.7%) and protein-DNA complex assembly (3.4%) were found enriched for the proteins that only bound by SAFB1 and associated with significant FDRs.

Table 5.9 BP terms in HeLa cells following analysis of proteins (476) only found in SAFB1 pull down

Term	%	FDR
ribonucleoprotein complex biogenesis	20.3	5.00E-46
RNA processing	26.3	6.60E-45
RNA splicing	20.3	1.70E-34
translation	18.6	5.50E-30
protein localisation	15.7	8.30E-13
protein transport	18.8	3.50E-04
chromatin organisation	8.7	8.80E-03
protein-DNA complex assembly	3.4	3.20E-03

FDR= false discovery rate, %= percentage of proteins involved from the whole list.

A total of 585 SAFB2 out of 605 interacting proteins were found to bind SAFB1. However, only 20 proteins were uniquely bound to SAFB2 in HeLa cells (Figure 5.9). Therefore, the BP for those proteins were investigated (Table 5.10). Consistent with Table 5.8, SAFB2 binding proteins were enriched and involved in the regulation of microtubule-based process (26.3%), mitotic cell cycle (15.8%) and cytoskeleton organisation (26.3%), suggesting a role in regulation cell division and associated with significant FDRs. Furthermore, the binding proteins were involved in regulating the natural killer cell mediated cytotoxicity (10.5%).

Table 5.10 BP terms in HeLa cells following analysis of proteins (20) only found in SAFB2 pull down

Term	%	FDR
microtubule-based process	26.3	3.00E-03
mitotic cell cycle	15.8	1.50E-02
cytoskeleton organisation	26.3	2.60E-02
natural killer cell mediated cytotoxicity	10.5	5.30E-02

FDR= false discovery rate, %= percentage of proteins involved from the whole list.

5.2.8 Protein-protein interactions and GO analysis of SAFB1 and SAFB2 interacting proteins in T-ALL cells

5.2.8.1 Specific tissue enrichment for SAFB1 and SAFB2 interacting proteins found in T-ALL cells

The SAFB1 and SAFB2 interacting proteins in T-ALL cells were highly up-regulated in different blood-related cell lines. Similar to HeLa cell data, results showed that both SAFB1 and SAFB2 interacting proteins were up-regulated in promyelocytic leukaemia (HL-60) cell line, which was found to be the most highest enriched. T lymphoblastic leukaemia (MOLT-4) cell line was also enriched for both SAFB1 and SAFB2 interacting proteins.

Although the interacting proteins were also up-regulated in specific lymphoid cells including, $CD4^+$ T cells and $CD8^+$ T cells, $CD33^+$ myeloid cells, $CD14^+$ monocytes and

CD56^{+} NK were also enriched. In addition, CD71^{+} early erythroid cells were also enriched (Figure 5.15).

SAFB1 and SAFB2 interacting proteins were enriched in a wide range of different tissues, including thyroid, heart, whole brain and uterus corpus. Trachea tissue was only found to be enriched for SAFB1 interacting proteins. In contrast, Burkitts lymphoma cells lines, Raji and Daudi, CD34^{+}, CD19^{+} cells and placenta were significantly enriched for only SAFB2 interacting proteins (Figure 5.15).

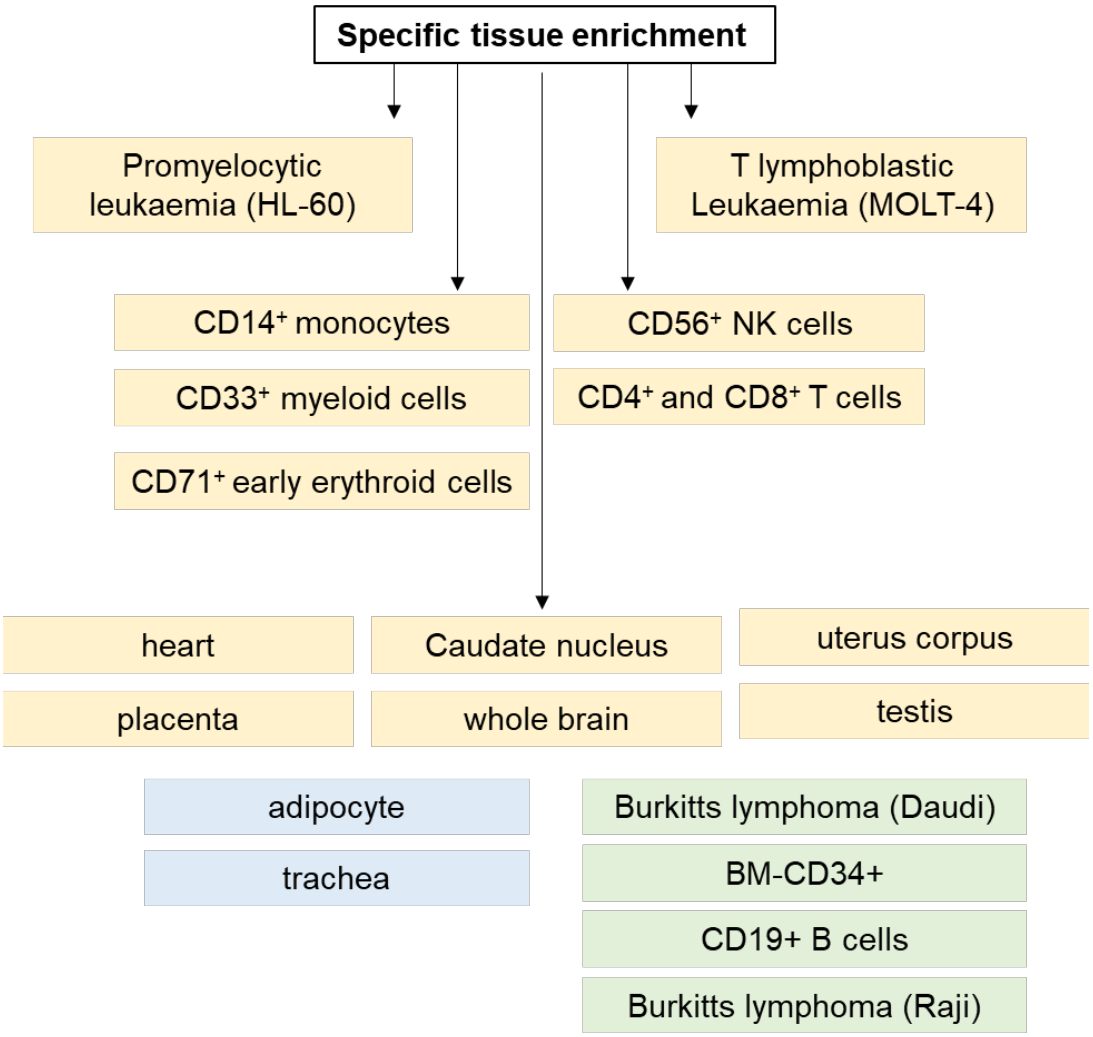

Figure 5.15 Specific tissue enrichment for SAFB1 and SAFB2 interacting proteins found in T-ALL cells. SAFB1 and SAFB2 lists were loaded into DAVID and the GO-BP was selected for BP-1 and BP-2. The protein enrichments were based on the thresholds of P-value < 0.05 and enrichment gene count > 2. Shared tissues for SAFB1 and SAFB2 are indicated in orange boxes. Unique SAFB1 tissues are indicated in blue, while unique SAFB2 tissues are indicated in green.

5.2.8.2 Protein-protein interactions for SAFB1 interacting proteins in T-ALL cells

Data in Figure 5.6 showed that SAFB1 interacting proteins in HeLa cells were mainly involved in regulating RNA processing, protein translation, protein translation in mitochondria, transcription, nucleosome organisation and the cell division. However, it is not known which processes are regulated in primary T-ALL cells. Thus, SAFB1 interacting proteins (146) for T-ALL were uploaded into STRING and the interaction networks are shown (Figure 5.16). Results show that there was a cluster of ribosomal proteins, which are known to be involved in protein translation (Figure 5.16). Also, another group of DEAD-box proteins and hnRNPs were strongly clustered and these are known to play a role in RNA processing (Figure 5.16). Furthermore, another cluster of histone enzymes was highlighted, suggesting they were involved in nucleosome organisation (Figure 5.16).

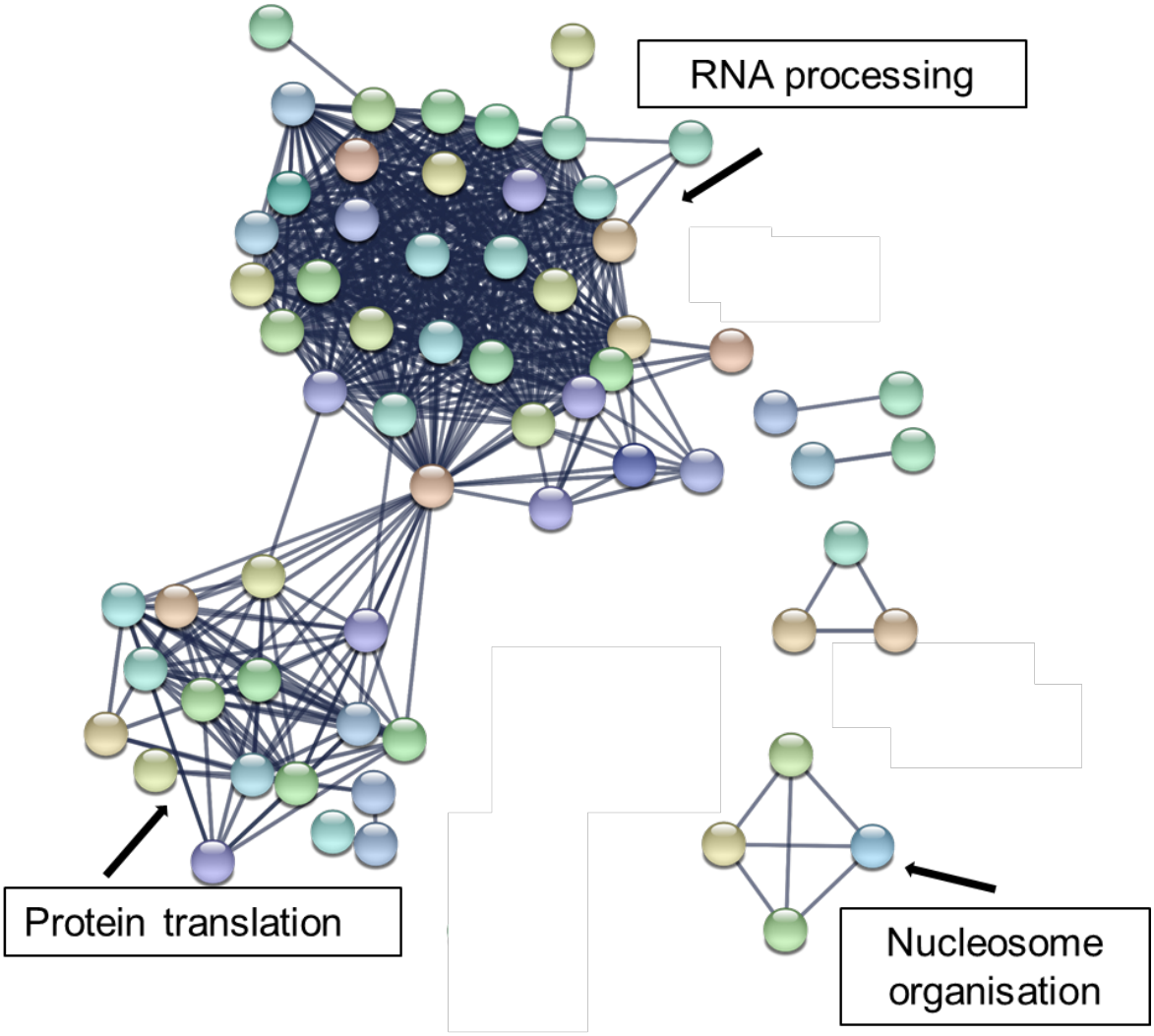

Figure 5.16 STRING analysis of SAFB1 interacting proteins in T-ALL cells. SAFB1 interacting proteins were loaded into STRING and the network edges were based on confidence. The interaction score was set for the highest confidence (≥0.7). Circles represent SAFB1 interacting proteins.

5.2.8.3 Protein-protein interactions for SAFB2 interacting proteins in T-ALL cells

Next, it was interesting to examine the interaction network for SAFB2 (348) interacting proteins using STRING in primary T-ALL cells. Overall, there were more SAFB2 interacting proteins than SAFB1. Similar to SAFB1 network in T-ALL cells, results showed 2 clusters of strongly connected proteins. The first cluster represents a group of DEAD-box proteins and hnRNPs, which are known to be involved in regulating RNA processing (Figure 5.17). The other cluster contains many ribosomal proteins, which are known to regulate protein translation (Figure 5.17). Furthermore, microtubules and cyclin kinases were clustered, indicating they were involved in regulating the cell division. Also, several histone enzymes and chromatin modifiers were found in a cluster, suggesting they were important in the chromatin organisation (Figure 5.17). Lastly, SAFB2 binding proteins were involved in regulation of transcription.

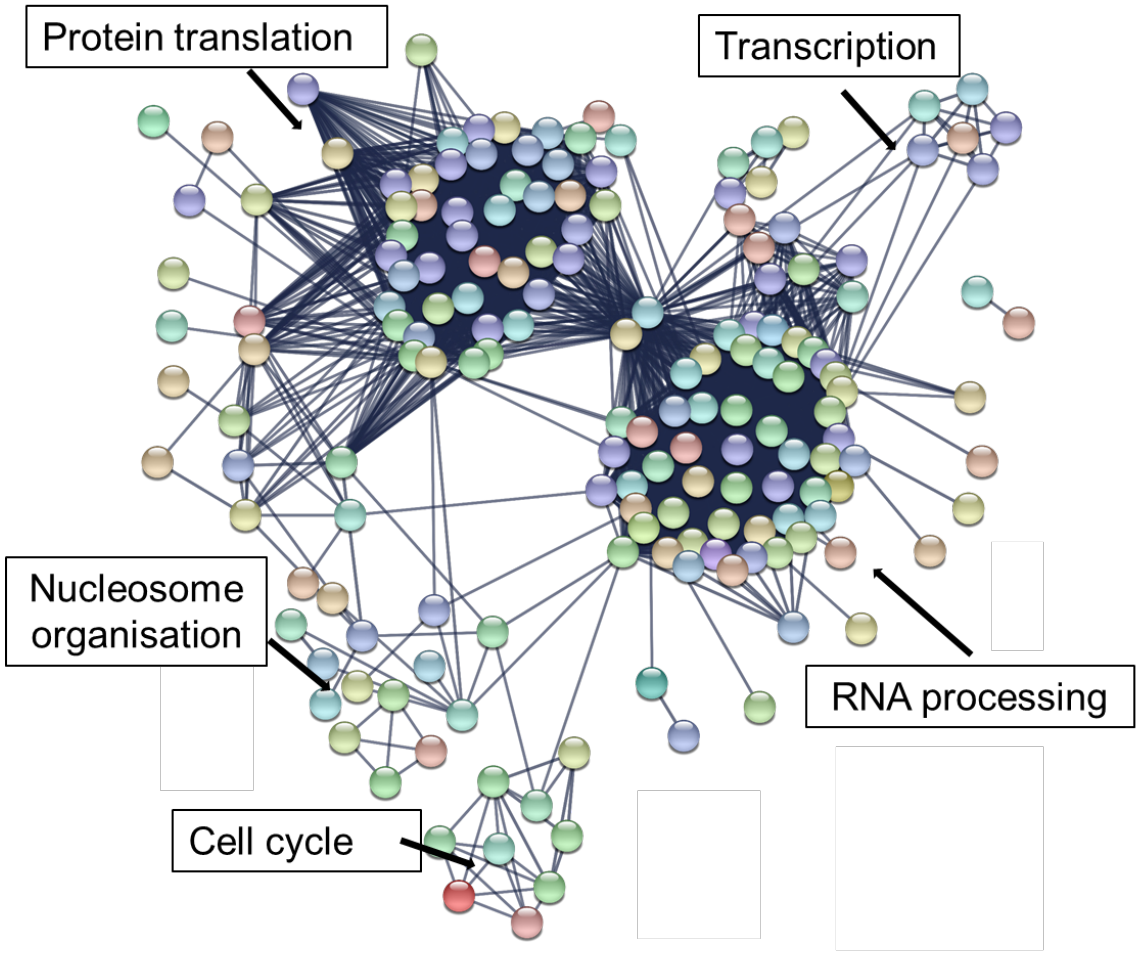

Figure 5.17 STRING analysis of SAFB2 interacting proteins in T-ALL cells. SAFB2 interacting proteins were loaded into STRING and the network edges were based on confidence. The interaction score was set for the highest confidence (≥0.7). Circles represent SAFB2 interacting proteins.

5.2.8.4 GO pathway analysis (KEGG) in T-ALL cells

The pathway analysis by KEGG was used to investigate the SAFB1 (146) and SAFB2 (348) interacting proteins in primary T-ALL cells. SAFB1 and SAFB2 interacting proteins were found to be important in regulating similar pathways. However, they were associated with distinct FDR values and lower FDRs for SAFB2 binding proteins. The spliceosome pathway was found to be the most significant enriched pathway for SAFB1 interacting proteins (16.9%, FDR= 3.80E-17), while the FDR rate was higher for SAFB2 (13.4%, 1.70E-30). In contrast, the ribosome pathway was the highest enriched pathway for SAFB2 (13.7%) interacting proteins and the least for SAFB1 (7.3%) with FDR of 1.80E-31 and 2.30E-02, respectively (Table 5.11). Furthermore, the mRNA surveillance pathway was enriched for SAFB1 (8.9%) and less so for SAFB2 (6.2%) interacting proteins with FDR of 5.10E-06 and 5.80E-09, respectively. Lastly, RNA transport was found to be enriched for both SAFB1 (8.1%) and SAFB2 (5.8%) interacting proteins with FDR of 1.70E-02 and 7.90E-04, respectively (Table 5.11).

Table 5.11 Pathway analysis for SAFB1 and SAFB2 interacting proteins in T-ALL cells

	SAFB1		SAFB2	
Term	**%**	**FDR**	**%**	**FDR**
Spliceosome	16.9	3.80E-17	13.4	1.70E-30
mRNA surveillance pathway	8.9	5.10E-06	6.2	5.80E-09
RNA transport	8.1	1.70E-02	5.8	7.90E-04
Ribosome	7.3	2.30E-02	13.7	1.80E-31

FDR= false discovery rate, %= percentage of proteins involved from the whole list.

5.2.8.5 Overlapping GO biological processes for SAFB1/2 in T-ALL cells

Next, the aim was to identify more specific biological process terms for SAFB1 and SAFB2 interacting proteins in T-ALL cells. Total SAFB1 (146) and SAFB2 (348) binding proteins were uploaded into DAVID and BP-FAT was selected to identify more specific biological terms. Results found a total of 245 and 315 biological processes (BP-FAT) were enriched for SAFB1 and SAFB2 interacting proteins, respectively. The

key most enriched categories for SAFB1 and SAFB2 interacting proteins were selected (Table 5.12). Overall, results showed that SAFB1/2 binding proteins had similar BP terms. Although most of BP terms are similar to data in HeLa cells (Table 5.6), BPs for SAFB2 binding proteins in T-ALL cells were associated with lower FDRs compared with SAFB1. Results also showed that both SAFB1 and SAFB2 interacting proteins were most highly enriched in the regulation of gene expression for SAFB1 (82.3%) and SAFB2 (74.9%) with FDR of 5.80E-32 and 2.30E-59, respectively. RNA processing was the second highest enriched process for SAFB1 (56.5%) and SAFB2 (54.6%) interacting proteins with FDR of 7.20E-54 and 1.20E-127, respectively (Table 5.11). There were other RNA-related processes enriched for SAFB1 and SAFB2 interacting proteins. For example, they were highly enriched for RNA splicing, RNA localisation ncRNA processing and RNA transport (Table 5.11). Furthermore, ribonucleoprotein complex biogenesis processes were enriched for SAFB1 (20.2%) and SAFB2 (25.4%) interacting proteins with FDR of 3.90E-11 and 1.50E-47, respectively. In addition, there were other processes found to be enriched for SAFB1 (20.2%) and SAFB2 (24.4%) interacting proteins, including translation with FDR of 2.00E-08 and 1.40E-35, respectively (Table 5.11).

Table 5.12 The 10 top GO biological process for total SAFB1 and SAFB2 interacting proteins in T-ALL cells

	SAFB1		SAFB2	
Term	**%**	**FDR**	**%**	**FDR**
RNA processing	56.5	7.20E-54	54.6	1.20E-127
RNA splicing	41.1	4.00E-47	33.3	5.80E-85
gene expression	82.3	5.80E-32	74.9	2.30E-59
ribonucleoprotein complex biogenesis	20.2	3.90E-11	25.4	2.70E-48
translation	20.2	2.00E-08	24.4	1.00E-36
ncRNA processing	14.5	2.40E-07	21.6	4.00E-32
RNA localisation	10.5	1.20E-06	11.7	1.80E-21
DNA-templated transcription, termination	6.5	1.50E-04	6.9	1.20E-13
chromosome organisation	18.5	3.50E-04	13.1	1.50E-03
RNA transport	4.7	7.5E-3	10.1	9.9E-20

FDR= false discovery rate, %= percentage of proteins involved from the whole list.

5.2.8.6 The involvement of SAFB1/2 in regulating the cell cycle

SAFB1/2 interacting proteins were shown to be important regulators of the cell cycle in T-ALL using DAVID. Thus, it was interesting to see how they are related to each other. STRING analysis showed that some cell cycle check-point regulators were involved (CDK7, CDK13, CDKN2A). Also, BUB3, the important regulator of the centromere was shown. Interestingly, the oncogene LEF1 was found to be a member in regulating the cell cycle (Figure 5.18).

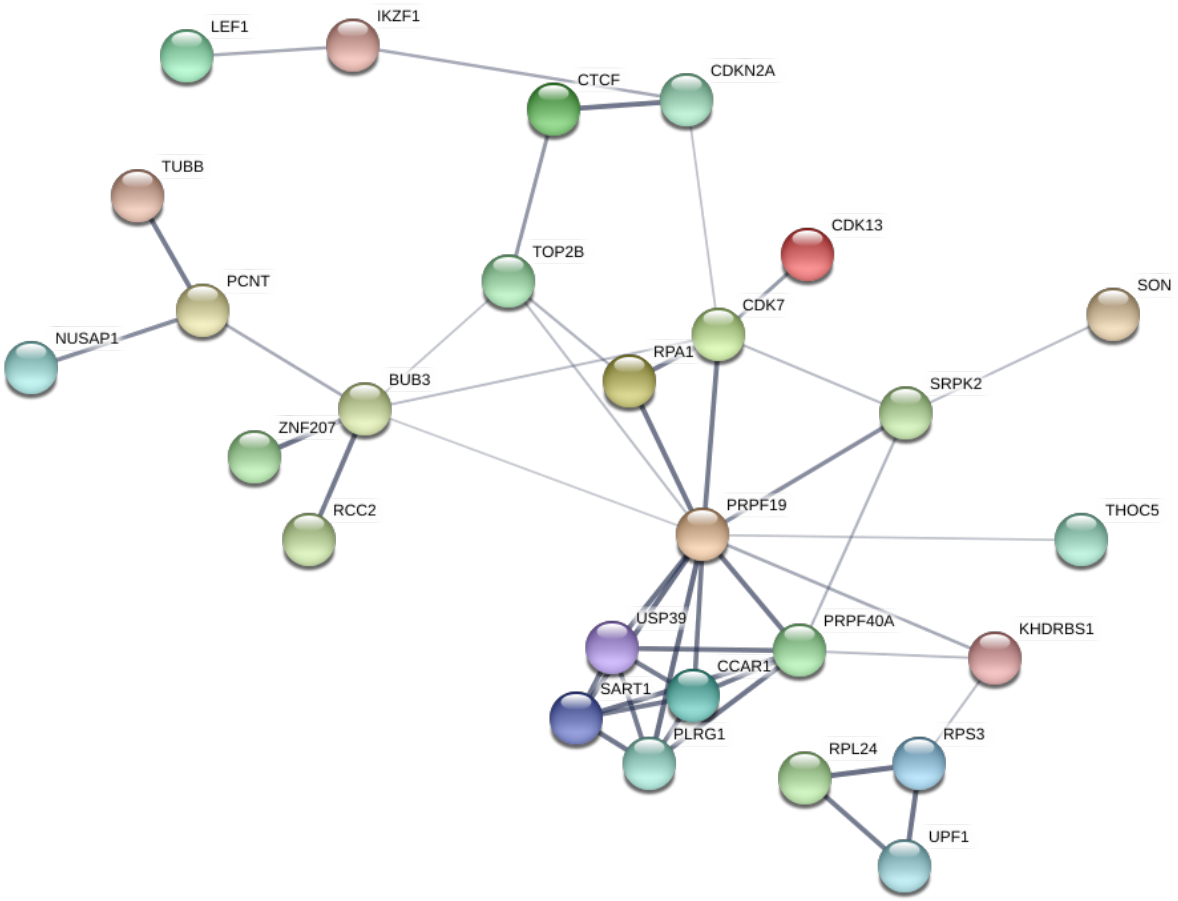

Figure 5.18 STRING analysis of SAFB1/2 interacting proteins implicated in regulating the cell cycle in T-ALL cells. SAFB1/2 interacting proteins implicated in regulating the cell cycle were loaded into STRING and the network edges were based on confidence. The interaction score was set for the highest confidence (≥0.7). Circles represent SAFB1/2 interacting proteins.

5.2.8.7 The involvement of SAFB2 only in regulating gene silencing by miRNA

SAFB1/2 were shown to regulate gene silencing in HeLa cells (Figure 5.14). However, DAVID analyses showed that SAFB2 interacting proteins only were involved in regulating gene silencing in T-ALL. Next, it was interesting to investigate the interaction network using STRING. The analyses showed that the proteins involved in regulating gene silencing were highly connected (Figure 5.19). ELAVL1, SRRT and HNRNPA2B1 proteins were found to be important in regulating gene silencing in HeLa cells.

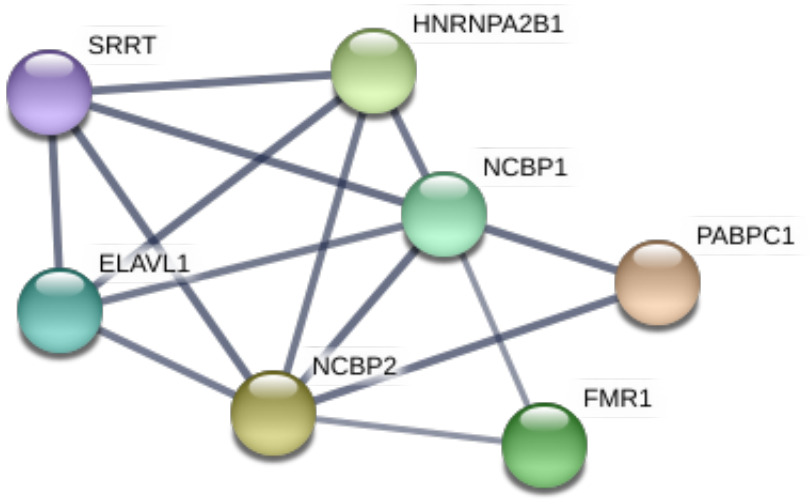

Figure 5.19 STRING analysis of SAFB2 interacting proteins implicated in regulating gene silencing in T-ALL cells. SAFB2 interacting proteins implicated in regulating the gene silencing were loaded into STRING and the network edges were based on confidence. The interaction score was set for the highest confidence (≥0.7). Circles represent SAFB2 interacting proteins.

5.2.8.8 The involvement of SAFB2 only in regulating methylation

SAFB2 interacting proteins but not SAFB1 appeared to be important in regulating protein methylation. STRING was used to identify those proteins and see how they interact with each other. Like the HeLa cell data, results showed that histones were involved (HIST1H1C, HIST1H1D), SNW1, SNRPD3 and CHTOP (Figure 5.20).

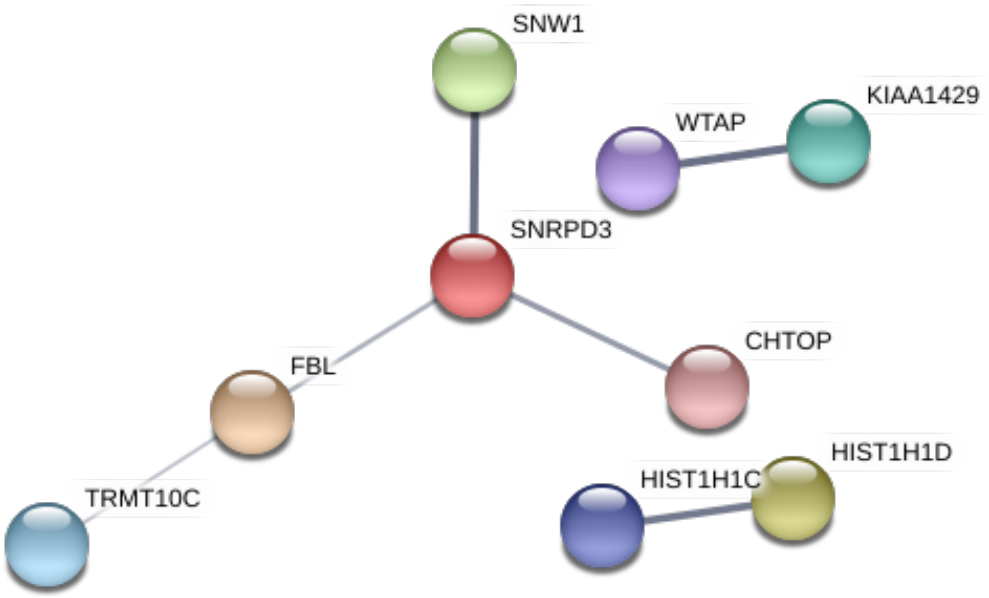

Figure 5.20 STRING analysis of SAFB2 interacting proteins implicated in regulating methylation in T-ALL cells. SAFB2 interacting proteins implicated in regulating the methylation were loaded into STRING and the network edges were based on confidence. The interaction score was set for the highest confidence (≥0.7). Circles represent SAFB2 interacting proteins.

5.2.8.9 Unique GO biological processes for total SAFB1/2 interacting proteins in T-ALL cells

It was interesting to identify novel functions of SAFB1 (146) in T-ALL cells and investigate whether they are similar to those identified in HeLa cells. Specific SAFB1 functions were investigated using BP-FAT using DAVID. Interestingly, results found that SAFB1 in T-ALL cells have some functions that were unique to SAFB2 in HeLa cells, such as the regulation of transcription from RNA polymerase II promoter (19.6%) and cytoskeleton organisation (3.1%, Table 5.12). However, SAFB1 also has specific functions in T-ALL cells, which were not found in HeLa cells, including positive

regulation of type I interferon production (4.7%) and intermediate filament-based process (3.1%, Table 5.12).

Table 5.13 Unique SAFB1 BP terms in T-ALL cells following analysis of all proteins pulled down by SAFB1 (146)

Term	%	FDR
positive regulation of type I interferon production	4.7	0.002
regulation of transcription from RNA polymerase II promoter	19.6	0.018
cytoskeleton organisation	3.1	0.033
intermediate filament-based process	3.1	0.035

FDR= false discovery rate, %= percentage of proteins involved from the whole list.

Also, unique functions for SAFB2 (348) interacting proteins were explored. Similarly, SAFB2 possesses some functions that were exclusive to SAFB1 in HeLa cells, such as protein localisation (23.0%), protein transport (18.9%), protein-DNA complex assembly (4.4%) and snoRNA localisation (1.0%, Table 5.13). In contrast, SAFB2 has distinct functions in T-ALL cells, including mRNA cleavage (2.0%), UTR-mediated mRNA stabilisation (1.7%), rRNA modification (2.0%), gene silencing by miRNA (2.0%) and regulation of DNA damage checkpoint (1.0%, Table 5.13).

Table 5.14 Unique SAFB2 BP terms in T-ALL cells following analysis of all proteins pulled down by SAFB2 (348)

Term	%	FDR
protein localisation	23.0	2.35E-04
protein transport	18.9	2.37E-04
mRNA cleavage	2.0	0.001
UTR-mediated mRNA stabilisation	1.7	0.002
rRNA modification	2.0	0.003
protein-DNA complex assembly	4.4	0.007
gene silencing by miRNA	2.0	0.033
regulation of DNA damage checkpoint	1.0	0.037
snoRNA localisation	1.0	0.037

FDR= false discovery rate, %= percentage of proteins involved from the whole list.

5.2.8.10 Biological process analyses of binding proteins in T-ALL cells that are only found in SAFB1 (67) or SAFB2 (269) pull downs

Sixty seven proteins were uniquely bound to SAFB1 in T-ALL cells (Figure 5.9). Thus, it was interesting to investigate if the BP for the SAFB1 binding proteins (67) were comparable to the BPs identified for the whole SAFB1 interactome (146). The unique SAFB1 interacting proteins (67) were loaded into DAVID and biological processes were identified (Table 5.14). Results showed that SAFB1 binding proteins were enriched and involved in regulating ribonucleoprotein complex biogenesis (43.9%), RNA processing (35.1%) and translation (31.6%). However, these BP terms were also associated with the total SAFB2 (348) interactome (Table 5.14). However, SAFB1 binding proteins were enriched in regulating the cytoskeleton organisation (8.8%).

Table 5.15 BP terms in T-ALL cells following analysis of proteins (67) only found in SAFB1 pull down

Term	%	FDR
ribonucleoprotein complex biogenesis	43.9	1.00E-20
RNA processing	35.1	5.50E-18
translation	31.6	4.90E-09
cytoskeleton organisation	8.8	4.20E-02

FDR= false discovery rate, %= percentage of proteins involved from the whole list.

Many proteins (269) were uniquely bound to SAFB2 (and not SAFB1) in T-ALL cell from the total SAFB2 (348) interacting proteins (Figure 5.9). Therefore, the BP for those proteins were investigated (Table 5.15). Similar to SAFB1 binding proteins, SAFB2 was involved in regulating RNA processing (55.5%), ribonucleoprotein complex biogenesis (24.2%), and translation (22%). In contrast, SAFB2 binding proteins were enriched in regulating protein localisation (20.3%), protein transport (15.7%), mRNA cleavage (1.7%) and rRNA modification (1.7%), gene silencing by miRNA (3.4%), and regulation of DNA damage checkpoint (1.3%).

Table 5.16 BP terms in T-ALL cells following analysis of proteins (269) only found in SAFB2 pull down

Term	%	FDR
RNA processing	55.5	1.80E-104
ribonucleoprotein complex biogenesis	24.2	4.10E-34
translation	22	1.10E-22
protein localisation	20.3	4.30E-03
mRNA cleavage	1.7	4.70E-03
gene silencing by miRNA	3.4	5.10E-03
rRNA modification	1.7	9.90E-03
protein transport	15.7	1.10E-02
regulation of DNA damage checkpoint	1.3	1.60E-02

FDR= false discovery rate, %= percentage of proteins involved from the whole list.

5.3 Discussion

SAFB1 was previously reported to interact with the splicing factor SRSF1 (2),(4),(40),(9) and both are co-localised in nSBs, suggesting that they might play important roles in splicing (2). However, whether stress related PTM, such as methylation and SUMOylation, can alter SAFB1/2 interactions is not known. The interaction between WT-SAFB1/WT-SAFB2 and SRSF1 was reduced significantly following heat shock and this may occur due to stress induced PTM of the proteins facilitating new interactions (e.g. with SATII transcripts in nSBs) and/or promoting a looser association between the proteins so as to allow a cessation of their non-stress related, constitutive actions. During stress, most constitutive transcription, splicing and translation is stopped to prevent damage to nascent RNA transcripts and proteins (4),(18). Hence, the decrease in SAFB1/2:SRSF1 interactions likely reflects a general stress induced mechanism whereby proteins responsible for coordinating RNA processing are 'inactivated'. Interestingly, the SAFB2:SRSF1 interactions had recovered to basal levels 1hr after HS while SAFB1:SRSF1 interaction remained significantly decreased. This may well reflect the need for SAFB2:SRSF1 mediated functions to be 'turned back on' following a stress sooner than those mediated by SAFB1:SRSF1. In addition, it suggests that the reversal of stress mediated PTMs occurs in an order that favours SAFB2 being reactivated prior to SAFB1.

Studies using SAFB1/2 constructs with mutated RGG/RG methylation and SUMOylation sites revealed that SAFB1 SUMOylation mutants had a significantly increased interaction with SRSF1 compared with WT-SAFB1 following heat shock and recovery. SUMOylation regulate many processes, including DNA damage repair, cell cycle, protein-protein interaction, stress response and apoptosis (182),(183). SAFB1 SUMOylation status was linked to the stress response, with SAFB1/2 becoming de-SUMOylated upon heat stress (27). Also, it was found that SUMOylation was required for transcriptional repression to be mediated by SAFB1 (29). Furthermore, it was found that transcription of ribosomal proteins was enhanced by SUMOylated SAFB1 (28). SRSF1 was reported to regulate the SUMOylation pathway and promotes SUMO conjugation to RNA processing factors (184),(185). It was also reported that the dysregulation of SUMOylation pathway is associated with development of cancer (183). Together these results strongly suggest that the de-SUMOylation of SAFB1 that

occurs following a stress has a marked effect on its functional interactions.

In addition, the results suggested that the SAFB1 Δ-methylation mutant had a reduced interaction with SRSF1 under basal levels (p=0.55). In contrast, the interaction between the SAFB2 RGG/RG methylation mutants and SRSF1 was significantly reduced when compared to WT-SAFB2 under basal and HS+R, conditions. Overall, the data suggest that SAFB1 SUMOylation status appears to be important for SRSF1 interactions following heat shock and recovery, while the methylation status of SAFB2 is important for regulating interactions with SRSF1 under basal conditions. It is however acknowledged that further experiments to increase the n number and analyse the importance of individual mutation sites are needed before we can be totally confident of these conclusions.

Interestingly, the interaction between SAFB1/2 and SRSF1 appeared to be reduced in T-ALL cells compared to HeLa cells. As repeated attempts to conduct IP experiments in NBM cells failed we do not have a bone marrow SAFB1/2: SRSF1 control, we can therefore only conclude that this result may reflect the diminished need for SAFB1/2: SRSF1 interactions in T-ALL cells or that this interaction is lost in primary T-ALL cells. The homology (65-100%) between SAFB1 and SAFB2 suggests that both proteins are likely to share many functions. However, the differences in SAFB1 and SAFB2 expression in human tissues suggest that both proteins will also have distinct functions. The observation that the interaction between two important proteins with roles in gene expression, splicing and the regulation of the cell cycle is altered by methylation and SUMOylation status has important implications. In many cancers, the methylation and SUMOylation status is altered (180),(181), our data suggests that the decreased expression of SAFB1 plus potential stress/cancer induced changes in PTM status would alter their function and interactions with SRSF1, a powerful oncogene (180). SRSF1 is overexpressed in many cancers and correlated with poor prognosis (180). SRSF1 overexpression is associated with oncogenic transformation of human mammary epithelial cells and immortalized rodent fibroblasts (180).

Arginine methylation has been implicated in regulating gene expression, RNA processing and protein translocation (30). The RGG/RG motif mediates nucleic acid and protein interactions and regulates many physiological processes, including

transcription, pre-mRNA splicing, DNA damage signalling, mRNA translation and the regulation of apoptosis. Several RGG/RG containing motif proteins, such as Bromodomain-containing protein 4 (BRD4), Bromodomain adjacent to zinc finger domain protein 1A (BAZ1A), DROSHA, Inhibitor of growth protein 5 (ING5) and hnRNPK are reported to be mis-regulated in cancer (186).

The RGG domain and SAF–box of SAF-A have been shown to play a role in anchoring Xist RNA to DNA (187) and suggests that both SAFB2 and SAFB1 may play similar roles in RNA recognition (188),(30). Scaffold attachment factor A (SAF-A), like SAFB proteins contains a SAF-box, RRM domain and C-terminal GAR motifs and has functions similar to SAFB-1 (11). The GAR motifs of SAF-A were reported to mediate the binding of the lnc-RNA Xist and transcriptional silencing (188). A subsequent study found that the SAF box of SAF-A also tethered Xist to DNA (189). In addition, SAF-A also interacts with the SWI/SNF complex and RNA Pol II to mediate transcription (190). Recently, hnRNPG, an interactor of SAFB1, was found to bind RNA and proteins using RGG motifs interacts directly with the CTD of RNA polymerase II via the RGG motifs (191).

PRMT5, an enzyme that catalyses RG/RGG arginine methylation, was reported to be important in haemopoiesis where PRMT5 knockout in mouse bone marrow haemopoietic stem and progenitor cells impaired T and B lymphocyte development (192). PRMT5 was overexpressed in a wide range of cancers, including leukaemia and inhibiting PRMT5 was associated with anti-cancer activity in lymphomas (193) and AML *in vitro* (194),(195). PRMT5 was expressed at high levels in primary BCP-ALL at diagnosis but decreased at complete remission, indicating that PRMT5 might have an oncogenic role in BCP-ALL progression (181). PRMT5 overexpression in BCP-ALL was partially by the dysregulation of B-cell lineage differentiation, suggesting that PRMT5 can be a potential biomarker in BCP-ALL (181). However, the role of PRMT5 has never been investigated in T-ALL. Profiling of the whole genome DNA methylation was performed in primary BCP-ALL and found SAFB proteins were hypermethylated (196). Together these data suggest that SAFB proteins, in common with several other proteins regulated by arginine methylation, may play important roles in regulating the cell cycle. PRMT5 was also shown to regulate DNA double-strand breaks (DSBs), p53 activation, cell-cycle arrest and cell death in AML cell lines

(197),(192). PRMT5 was reported to be essential for cell proliferation and correlated with G_1 phase regulators, including CDK4 and CDK6 (198). PRMT5 knockdown was reported to result in the cell cycle arrest and eventually apoptosis (198). Given that SAFB1 are arginine methylated by PRMT5 and interacted with many cell cycle regulators suggest that targeting PRMT5 might be an interesting strategy to disrupt the cell cycle. GSK3326595 (a PRMT5 inhibitor) has been shown to be a promising drug candidate in phase I (solid tumours and non- Hodgkin lymphoma) and phase I/II trials (myelodysplastic syndromes and acute myeloid leukaemia) and associated with lower IC_{50} *in vitro* (204). The cell cycle regulator, CDKN2A was found to interact with SAFB1/2 in T-ALL and reported to co-depleted with 5-methylthioadenosine phosphorylase (MTAP), leading to methylthioadenosine (MTA) accumulation and further sensitisation of cells to PRMT5 inhibition (192).

Advances in proteomic technologies and the availability of new antibodies, enabled analyses to identify novel SAFB1 and SAFB2 interactions in HeLa and primary T-ALL cells. The analyses also helped to identify potential SAFB1/2 functions. Interestingly, the number of SAFB1 and SAFB2 interactions were reversed in T-ALL cells compared with HeLa cells with more SAFB1 interactions identified in HeLa compared with T-ALL. Likewise, more SAFB2 interactions were found in T-ALL compared with HeLa cells, indicating that SAFB2 may substitute for the decreased expression of SAFB1 in T-ALL cells. SAFB1 and SAFB2 interacting proteins shared many functions, such as RNA processing, translation and transcription but they also have distinct functions, such as protein localisation and transport. Interestingly, some of the unique SAFB1 functions in HeLa cells were found to be unique for SAFB2 in T-ALL, such as protein localisation and transport. Similarly, some unique SAFB2 functions in HeLa cells were functions for SAFB1 in T-ALL, such as cytoskeleton organisation. These data suggest that although SAFB1 and 2 functions are largely overlapping, both proteins have distinct functions, some of which are reversed for SAFB1 in HeLa compared with T-ALL cells and vice versa.

It was interesting to investigate potential novel protein interactions for SAFB1 and SAFB2 in HeLa and T-ALL cells, so genome-wide proteomic analyses using TMT technology were performed. For the first time, proteomic analyses for SAFB1/2 were generated in HeLa and T-ALL which helped us to give insights and understand

SAFB1/2 functions. It was shown that the majority of proteins were interacting with SAFB1 in HeLa cells and with SAFB2 in T-ALL cells. This could be related to the data presented in chapter 3 when SAFB1/2 ratio was altered in T-ALL cells compared with NBM cells and SAFB2 protein expression was elevated in T-ALL, suggesting that SAFB2 is likely to play more fundamental roles in T-ALL. The abundance of SAFB2 interactions in T-ALL cells compared with SAFB1 might be supported by the tissue expression data where SAFB1 and SAFB2 interacting proteins were found to be highly up-regulated in various blood cells, such as lymphoid and myeloid cells in T-ALL cells and surprisingly in HeLa cells. The abundance of SAFB1/2 interacting proteins in lymphoid and myeloid cells suggest that SAFB1/2 play more significant roles in blood cell regulation and function than previously thought. Also, it was reported that SAFB1 and 2 are regulated by a bidirectional promotor and knockdown of SAFB1 results in the up-regulation of SAFB2 (39).

SAFB1 has been implicated in a variety of processes, including transcriptional regulation, chromatin organisation, cellular stress response, DNA damage response, apoptosis, RNA splicing and metabolism (11). However, whether SAFB2 has similar or distinct functions to SAFB1 is not known. Bioinformatics analyses found that both SAFB1 and SAFB2 were involved in regulating similar processes, such as RNA processing and splicing. Sharing similar functions could be due to the fact that both proteins have 65-100% similarity for their domains or SAFB1/2 antibodies used for the co-IP cross-react with each other. Furthermore, the bioinformatics analyses showed that SAFB1 and 2 interacted with many hnRNPs and DEAD-boxes, indicating they are important in regulating the RNA processing. Also, the involvement of SAFB1/2 in regulating RNA is not surprising as they interact with RNA via the RRM domain. SAFB1 was previously reported to interact with several hnRNP proteins, including hnRNPC (4), hnRNPD (40), hnRNPG (9) and hnRNPPI (4). SAFB1 was identified to be a component of the spliceosomes (42), macromolecular complexes of snRNA and small nuclear ribonucleoproteins assisting in removal of introns (43), thus suggesting that both proteins are involved in the regulation of RNA splicing. The role of SAFB1 in RNA processing was supported by transcriptomic analyses using iCLIP, which found that SAFB1 is involved in the regulation of RNA processing, such as RNA splicing (38), (39).

The bioinformatics analyses showed that both SAFB1 and SAFB2 are likely involved in the regulation of the cell cycle, chromosome and cytoskeleton organisation. This was consistent with previous data that found high levels of SAFB1 arrested human urinary bladder cancer (T24) cells in the G_2-M phase suggesting a role in the control of cell division (23). It was shown that binding proteins found in SAFB2 pull down (20 proteins) in HeLa cells were mainly microtubule proteins, suggesting that SAFB2 might have predominant roles in regulating the cytoskeleton and thereby cell division. However, SAFB1 binding proteins were found to be important in regulating the cytoskeleton in T-ALL cells. Further to the genetic alterations that are observed in T-ALL, which was discussed in chapter 1, the cell cycle is frequently altered in T-ALL (70),(69). CDKs are set of proteins with functions in regulating the cell cycle include cell renewal, differentiation, transcription and epigenetic regulation (199). CDKN2A deletions are one of the most frequent abnormalities and found in over 70% of T-ALL patients. The p16INK4A and p14ARF tumour suppressor genes are found in the short arm of chromosome 9 where CDKN2A is located. However, patients with CDKN2A deletions are associated with good prognosis (70),(69). CDK7 is a component of the transcription factor IIH complex (TFIIH) and regulates transcription elongation process. Inhibitions of CDK7 using THZ1 was shown to generally dampens mRNA transcription of key drivers of T-ALL, such as RUNX-1 (62).

In the present study, it was found that LEF1 was bound with SAFB1/2 and therefore might be involved in regulating the cell cycle in T-ALL. The Wnt signalling pathway regulates many processes, including differentiation and proliferation of progenitor cells. β-Catenin is the main mediator of this pathway and accumulates in the cytoplasm and moves to the nucleus where it interacts with the T-cell factor (Tcf)/lymphoid enhancer factor (LEF) family (200), leading to activation of target genes, including c-Myc and cyclin D1 (important regulators of G_1 to S cell cycle transition) (201). LEF1 is a member of the Tcf/LEF family of DNA-binding transcription factors (202). β-Catenin and LEF1 expression was up-regulated in T-ALL patients (200). LEF1 was found to be mutated in 15% of cases in T-ALL (70),(69). LEF1 inactivation was reported in T-ALL patients and associated with activating NOTCH1 mutations (202). LEF1 was shown to function as an oncogene or tumour suppressor gene. LEF1 is associated with T and B lymphocyte development. High levels of LEF1 is associated with good prognosis in T-ALL (202). These data suggest that SAFB1/2 might control Wnt

signalling by interacting with LEF1 transcription factor and thereby regulating cell differentiation and proliferation in T-ALL cells.

In the current study, it was found that SAFB1 and SAFB2 were might be involved in regulation of chromatin organisation and transcription. Evidence showed that SAFB1 has been found to interact with several important modifiers of chromatin structure e.g. CHD1 (46), NCOR (29), HDAC3 (29), BRG1 (15), Matrin 3 (47) and suggests that SAFB1 might be important for chromatin organisation. Another interesting finding was the potential involvement of SAFB1/2 proteins in the regulation of transcription. SAFB1 was identified as a protein that bound and repressed hsp27 promoter activity (3) and hence SAFB1 was believed to be a negative regulator of transcription. Another study demonstrated that knockdown of SAFB1 and SAFB2 resulted in the induction of 457 genes and repression of 259 genes (12). SAFB1 represses the androgen receptor and SAFB1 knockdown resulted in higher transcription of PSA in cultured prostate cells (16). It was evident that SAFB1 resulted in transcriptional repression of XOR (15) and SAFB1 knockdown inhibited the expression of skeletal muscle genes, indicating a positive regulatory role of SAFB1 (17). In addition, SAFB1 interacts with proteins involved in transcription, such as RNA polymerase III (2) and p53 (45). The involvement of SAFB1 in regulating such processes emphasises the previous findings and indicates that SAFB2 is playing similar roles.

The bioinformatics data suggested that SAFB1 and 2 were involved in regulating protein translation in T-ALL cells and HeLa cells. Also, it was found that SAFB1/2 interacted with many ribosomal proteins in HeLa and T-ALL cells. SAFB1 and SAFB2 were shown to interact with RNA polymerase II at the C-terminal (2),(9). The SUMOylated SAFB1 and SAFB2 were shown to be associated with recruiting RNA polymerase II to the promotor of ribosomal genes (15). Also, it was shown that knockdown of both proteins was associated with reduction in RNA expression of the ribosomal genes (15). These data suggest that SAFB1 and SAFB2 are important proteins involved in the regulation of protein translation and synthesis. Protein synthesis and ribosome biogenesis are essential processes for cancer cell growth and several defects in the translation machinery have been reported. Some ribosomal proteins include ribosomal protein L5 (RPL5), RPL10 and RBL22 have been reported to be mutated in 20% of T-ALL patients (203),(69). RPL5 and RPL22 are associated

with inactivating mutations and deletions, whereas RPL10 is associated with missense mutations (69). It was reported that many ribosomal proteins were arginine methylated by PRMT5 and involved in mRNA translation (204).

Although SAFB1 and SAFB2 share many potential functions, it was interesting to investigate whether both proteins have distinct functions in HeLa and T-ALL cells. It was found that protein localisation and transport processes were potentially exclusive functions for SAFB1 in HeLa cells, however, these functions were found to be specific for SAFB2 in T-ALL. These data suggest that some SAFB1/2 functions were reversed in HeLa cells compared T-ALL cells and vice versa. The previous observations that SAFB1/2 is reversed in T-ALL compared with NBM cells support these findings. However, it should be highlighted that the reverse SAFB1 or SAFB2 functions were generated when HeLa cells were compared with T-ALL cells, rather than comparing T-ALL with NBM cells. The involvement of SAFB1 or SAFB2 in regulating protein localisation and transport was not surprising as SAFB1/2 have a protein-protein interaction domain to mediate and regulate protein interactions (204).

In conclusion, SAFB1/2 RGG/RG methylation and SUMOylation are likely significant for its interaction with SRSF1. The proteomic analyses for SAFB1 and SAFB2 interactions were undertaken for the first time in HeLa and T-ALL cells. Also, SAFB1/2 interactions and functions seem to be altered in HeLa cells compared with T-ALL, indicating unique functions of both proteins in HeLa and T-ALL cells. SAFB1/2 were involved in regulating RNA processing, transcription, translation and the cell division in both cell types. These data form the foundation for SAFB1/2 interactions and functions and highlighted the importance of SAFB1/2 in potentially regulating critical processes. However, further experiments are needed to comprehensively elucidate the roles SAFB1/2 play in T-ALL cells and define the binding partners in NBM cells.

CHAPTER 6 : General discussion and future directions

The SAFB proteins help regulate a number of important cellular processes (e.g. gene expression (38), the cellular stress response (19), DNA repair (22), apoptosis (162), RNA processing and splicing (38) whose dysregulation is linked to cancer formation. The down-regulation of SAFB1 is linked to the aetiology of some cancers, however little was known about the biological relevance/significance of SAFB proteins in primary BCP-ALL and T-ALL cancers.

Experiments detailed in this thesis, attempt to explore the significance and/or functions of SAFB proteins in ALL using different strategies. Firstly, investigating the expression levels of SAFB proteins in ALL subtypes in comparison with NBM cells. Following that, examining whether modulating SAFB1/2 expression in ALL cells has a compensatory pro-apoptotic effect with minimal cytotoxicity on various normal cells was investigated (Chapter 3). Secondly, characterising the expression/localisation of SAFB1/2, HSF1 and HSP70 proteins following Hsp90 inhibitors and heat shock in ALL cells was conducted. HSP90 inhibitors (e.g. 17-DMAG and celastrol) were reported to induce the expression of heat shock proteins and hence it has been inferred they induce a stress response (128),(129),(131),(95). However, a heat shock/stress response is characterised by the expression of heat shock proteins and the formation of nuclear stress bodies. Thus, the aim was to characterise a heat induced stress response in primary ALL cells and HeLa cells and determine whether Hsp90 inhibitors (Chapter 4) instigated a similar response. The results of these experiments may also help identify additional mechanisms by which HSP90 inhibitors mediate selective cytotoxicity in cancer cells. Lastly, I hypothesised that by identifying the proteins that SAFB1/2 interacted with in T-ALL (and HeLa) cells a better understanding of the biological processes/functions and pathways regulated by SAFB1/2 in health and disease would be obtained (Chapter 5).

6.1 SAFB1/2 expression in ALL

In Chapter 3, SAFB levels were measured in BCP-ALL and T-ALL cells and compared with NBM cells and the results showed there was decreased SAFB1 mRNA and protein expression in T-ALL cells. These results are in broad agreement with previous findings where SAFB1 expression was lower in colorectal (35), prostate (16) and

breast cancers (33). The expression of SAFB2 has not been investigated in many human cancers. However, SAFB2 protein expression was found to be significantly elevated in both ALL subtypes. Also, the SAFB1/SAFB2 ratio was reduced significantly in both BCP- and T-ALL cells compared with NBM. SAFB proteins have been shown to play important roles in regulating gene expression and the cell cycle, suggesting that aberrant SAFB1/2 expression may be associated with the development of cancer. Going forward, as SAFB1 and SAFB2 expression is controlled by a bidirectional promoter (39), it was of interest to investigate the ratio of SAFB1/2 in ALL cells. Results showed that modulating the SAFB1/SAFB2 ratio was associated with pro-apoptotic effects. Data showed that SAFB1 overexpression was associated with apoptosis in both BCP-ALL and T-ALL cells, with no significant alterations in viability on different normal cells, including NBM, MEFs or primary neuronal cells. SAFB1 was reported to play a role in the apoptotic process (162) and SLTM overexpression (which shares 30% homology with SAFB1), has been shown to induce apoptosis in cancer lines (6), suggesting that cancer cells are uniquely sensitive to SAFB1 overexpression. The possible mechanisms for the potential pro-apoptotic of SAFB1 overexpression were detailed in chapter 3, including methylation and binding to chromatin modifiers. The effect of SAFB2 overexpression on ALL cells was also examined. It was shown that SAFB2 overexpression induced apoptosis in both primary T-ALL and BCP-ALL cells to less extent compared with SAFB1. However, SAFB2 overexpression did not induce apoptosis in NBM cells. The potential pro-apoptotic effect of SAFB2 is not well established compared with SAFB1 role and further experiments are warranted to define these observations. However, there are a number of possible reasons for the potential pro-apoptotic actions of SAFB2 overexpression: (i) SAFB2 could be competing with SAFB1, as SAFB2 was shown to co-localise with SAFB1 (9) (ii) SAFB1 and SAFB2 are under the control of a bidirectional promoter and it could be that a feedback mechanism for SAFB1/2 regulation can be involved. If more time was available, the effect of knocking down SAFB2 on tumour cell viability could also have been investigated. Data in Chapter 5 revealed that SAFB1/2 binding proteins were implicated in regulating methylation, chromatin organisation and the cell cycle and hence altered SAFB1/2 expression could be important in promoting cancer in T-ALL cells.

6.2 Effect of HSP90 inhibitors (17-DMAG and celastrol) on the stress response in ALL

The HSP90 inhibitors, celastrol and 17-DMAG, are considered to be inducers of a stress response (128),(129),(131) and they induce apoptosis in T-ALL and BCP-ALL cells (95). Whether primary ALL cells respond to Hsp90 inhibitors by inducing a stress response is not known. In addition, the contribution of stress response pathways (e.g. heat shock protein expression and nSB formation) to cancer cell survival has not been investigated in ALL. Evidence shows that SAFB1 localises to nSBs with HSF1. However, it is not known if its paralogue, SAFB2, also translocates to nSBs following a stress in HeLa cells (4),(142). In chapter 4, the expression/localisation of SAFB1/2, HSF1 and HSP70 proteins were evaluated following treatment with HSP90 inhibitors (17-DMAG and celastrol) and heat shock in HeLa and ALL cells. HeLa cells exposed to a HS showed SAFB2 and HSF1 were recruited into nSBs earlier than SAFB1, and that HSP70 was induced. This may indicate SAFB2 is possibly needed to stabilise Sat III lncRNAs and/or plays a role in recruiting further proteins to nSBs. SAFB1 may need to be inactivated during stress or that it is forming new processing centres (21). The stress response following HSP90 inhibitors was different in comparison to heat shock. For example, 17-DMAG but not celastrol increased HSP70 expression and induced HSF1 puncta but SAFB1 and SAFB2 were not recruited into HSF1 puncta, suggesting that 17-DMAG is an effective inducer of Hsp70 transcription but does not induce the formation of SAFB1/2 containing SBs at 48 hours. Whether NBM and ALL cells exposed to HSP90 inhibitors or heat shock can induce the formation of nSBs and the transcription of HSP70 has not been investigated. Data showed that SAFB1 and SAFB2 expression was not altered following heat shock compared with basal conditions, however HSF1 expression was significantly increased in BCP-ALL and T-ALL compared with NBM. In addition, HSF1 nuclear border expression was significantly increased in T-ALL and BCP-ALL cells compared with NBM following a heat shock and 17-DMAG treatment (but no discrete nuclear puncta are seen), suggesting that HSF1 does not mediate nSB formation in NBM and ALL cells. Under normal conditions, HSF1 is normally diffusely enters the nucleus upon stress. In this study, HSF1 was aggregating at the nuclear border upon stress in ALL cells, which is unusual staining pattern and has never shown in other cells (HeLa cells). It is not

known what does that mean but could be that HSF1 is not fully activated in these cells and further experiments are needed to define these observations.

6.3 SAFB1/2 interaction with SRSF1

SAFB1 was previously reported to interact with the splicing factor SRSF1 (2),(4),(40),(9) and both co-localised in nSBs, possibly suggesting that they need to be inactivated during stress or that they are forming new processing centres (21). However, whether stress related PTM, such as methylation, can alter SAFB1/2 interactions is not known. The interaction between WT-SAFB1 or WT-SAFB2 with SRSF1 was reduced significantly following heat shock and this may occur due to stress induced PTMs of the proteins facilitating new interactions (e.g. with SATII transcripts in nSBs) and/or promoting a looser association between the proteins to allow a cessation of their non-stress related, constitutive actions. During stress, most constitutive transcription, splicing and translation is stopped to prevent damage to nascent RNA transcripts and proteins. Hence, the decrease in SAFB1/2:SRSF1 interactions likely reflects a general stress induced mechanism whereby proteins responsible for coordinating RNA processing are ‘inactivated’. Interestingly, the SAFB2:SRSF1 interactions had recovered to basal levels 1hr after HS while SAFB1:SRSF1 interaction remained significantly decreased. This may well reflect the need for SAFB2:SRSF1 mediated functions to be ‘turned back on’ following a stress sooner than those mediated by SAFB1:SRSF1. In addition, it suggests that the reversal of stress mediated PTMs occurs in an order that favours SAFB2 being reactivated prior to SAFB1. Interestingly, the interaction between SAFB1/2 and SRSF1 appeared to be reduced in T-ALL cells compared to HeLa cells. As repeated attempts to conduct IP experiments in NBM cells failed we do not have a bone marrow SAFB1/2: SRSF1 control, we can therefore only conclude that this result may reflect the diminished need for SAFB1/2: SRSF1 interactions in T-ALL cells or that this interaction is lost in primary T-ALL cells.

6.4 Influence of RGG/RG methylation of SAFB1/2 proteins

SAFB proteins have been found to undergo several PTMs (methylation, SUMOylation), which are important in regulating protein-protein interactions (2),(25), (27),(28),(11). The RGG/RG motifs may be methylated differentially to mediate important cellular functions such as RNA binding and protein-protein interactions (30), (11),(172),(173). Little is known about the significance of the methylation of SAFB proteins in regulating the cellular response to stress. Studies in Chapter 5 using SAFB1/2 mutants with the RGG/RG methylation sites mutated found that the interaction between the SAFB2 RGG/RG methylation mutants and SRSF1 was significantly reduced when compared to WT-SAFB2 under basal and HS+R, conditions. However, SAFB1 Δ-methylation mutant had a reduced interaction with SRF1 under basal levels, this was not significant. These data suggest that the methylation status of SAFB2 is important for regulating interactions with SRSF1 under basal conditions. It is however acknowledged that further experiments to increase the n number and analyse the importance of individual mutation sites are needed before we can be totally confident of these conclusions. The demonstration that the interaction between two important proteins with roles in gene expression, splicing and the regulation of the cell cycle is altered by methylation status has important implications. In many cancers, the methylation status of gene and proteins is altered (181). These data suggest that the decreased expression of SAFB1/2 plus potential stress/cancer induced changes in PTM status would alter their function and interactions with SRSF1. PRMT5, an enzyme that catalyses RGG/RG arginine methylation, was overexpressed in a wide range of cancers, including leukaemia, and inhibiting PRMT5 was associated with anti-cancer activity in lymphomas (193) and AML *in vitro* (194),(195). PRMT5 was reported to be essential for cell proliferation and correlated with G_1 phase regulators (198). PRMT5 was proposed as an important regulator of the cell cycle and was reported to result in the cell cycle arrest (198). Evidence showed that SAFB proteins were methylated in primary BCP-ALL (196). Thus, it would be interesting to explore whether SAFB proteins are also methylated in T-ALL. If this is the case, a PRMT5 inhibitor, such as GSK3326595 inhibitor, could be used to treat T-ALL cells and viability assessed using annexin-PI assay. GSK3326595 has been shown to be a promising drug candidate in phase I (solid tumours and non-

Hodgkin lymphoma) and phase I/II trials (myelodysplastic syndromes and acute myeloid leukaemia) and associated with lower IC_{50} of GSK3326595 *in vitro* (204).

6.5 Influence of SUMOylation of SAFB1/2 proteins

SUMOylation regulates many processes, including DNA damage repair, cell cycle, protein-protein interactions, stress response and apoptosis (182),(183). SAFB1 SUMOylation status was linked to the stress response, with SAFB1/2 becoming de-SUMOylated upon heat stress (27). Also, it was found that SUMOylation was required for transcriptional repression to be mediated by SAFB1 (29). Furthermore, it was found that transcription of ribosomal proteins was enhanced by SUMOylated SAFB1 (28). SRSF1 was reported to regulate the SUMOylation pathway and promotes SUMO conjugation to RNA processing factors (184),(185). It was also reported that the dysregulation of SUMOylation pathway is associated with development of cancer (183). Studies using SAFB1/2 constructs with mutated SUMOylation sites revealed that SAFB1 SUMOylation mutants had a significantly increased interaction with SRSF1 compared with WT-SAFB1 following heat shock and recovery. Together these results strongly suggest that the de-SUMOylation of SAFB1 that occurs following a stress has a marked effect on its functional interactions and that SAFB1 SUMOylation status appears to be important for SRSF1 interactions following heat shock and recovery.

6.6 Characterising SAFB1 and SAFB2 protein: protein interaction

The main aim of chapter 5 was to identify potential protein-protein interactions in HeLa and T-ALL cells. Interestingly, more SAFB2 interactions were found in T-ALL compared with HeLa cells, indicating that SAFB2 may substitute for the decreased expression of SAFB1 in T-ALL cells that was observed in Chapter 3. The abundance of SAFB1/2 interacting proteins in lymphoid and myeloid cells plus the increase in SAFB2 expression in T-ALL (Chapter 3) might suggest that SAFB1/2 play more crucial roles in blood cell regulation and function than previously thought. Data in Chapter 5 suggested that SAFB1/2 binding proteins were implicated in regulating many known important processes, including RNA processing, splicing, transcription and translation,

all of which were reported to be regulated by arginine methylation (204). For example, it was reported that many ribosomal proteins were arginine methylated by PRMT5 and involved in mRNA translation (204). The proteomic data also found to be involved in potentially regulating unique SAFB1/2 processes, including gene silencing. However, SAFB1/2 binding proteins profile in T-ALL should be compared with normal cells.

6.7 Future directions

In Chapter 3, it was shown that the ratio of SAFB1/2 was altered in ALL cells. As SAFB1 and SAFB2 expression is controlled by a bidirectional promoter (39), it could be that genetic mutations might be identified in this region which would be responsible for the alter expression of SAFB1/2. To do this, the SAFB1/2 promotor can be sequenced in both ALL subtypes and compared with NBM. Also, a lentiviral vector made in the laboratory expressing the SAFB1/2 promotor could be used as a strategy to investigate the transcriptional regulation of the SAFB1/2 promotor in ALL in comparison to NBM. SAFB1 is tagged to EGFP and SAFB2 was tagged to mScarlet to allow for visualisation/quantification. Thus, ALL and NBM cells can be transduced with the lentiviral vector and EGFP and mScarlet levels would be measured by flow cytometer. Furthermore, as SAFB2 protein levels were shown to be elevated in ALL subtypes compared with NBM, it would be interesting to investigate if ALL cells are dependent on SAFB2 for their survival. One strategy would be to knockdown SAFB2 and evaluate viability to see if reducing SAFB2 expression would be associated with apoptosis using annexin-PI assay.

In Chapter 4, 17-DMAG but not celastrol increased HSP70 expression and induced HSF1 puncta but SAFB1 and SAFB2 were not recruited into HSF1 puncta. Why SAFB1/2 were nor recruited to HSF1 puncta is not known. Further experiments using different time-points should be performed to investigate if the co-localisation between SAFB1/2 and HSF1 following 17-DMAG would be attained as the optimal time-point would have been missed or this would be via a different mechanism. Under normal conditions, HSF1 is normally diffusely enters the nucleus upon stress. In this study, HSF1 was aggregating at the nuclear border (detected by measuring the average intensities of HSF1 in the nucleus and cytoplasm- explained in the Method section)

upon stress in ALL cells, which is unusual staining pattern and has never shown in other cells (HeLa cells). It is not known what does that mean but could be that HSF1 is not fully activated in these cells and further experiments are needed to define these observations. To differentiate localisation of cytoplasmic and nuclear proteins, cytoplasmic markers techniques (e.g. immunofluorescence staining) could be employed to assess whether HSF1 is also detected in the cytoplasm.

In Chapter 4, the assumption that nSBs were present or absent following stress was based on the recruitment of SAFB1/2 with HSF1 into nSBs. Upon stress, in addition to HSP production, HSF1 also transcribes G-rich lncSatIII RNAs (135) mediating nSB formation (136). To confirm whether SAFB1/2 were found in nSBs with HSF1, fluorescence in situ hybridization (FISH) can be used to investigate whether SAFB1/2 would be detected in SATIII in ALL compared with NBM cells. FISH probes targeting SATIII that were described (136) can be used and this should be followed by staining SAFB1/2 and HSF1 using immunofluorescence techniques. This would allow to see if SAFB1/2 and HSF1 are co-localised with SATIII loci following a stress, as SATIII transcription was shown to be associated with formation of nSBs (136). Furthermore, the transcription of SATIII can be measured using qPCR, which was shown to be highly induced following heat shock (136). The absence of nSBs following heat shock in NBM and ALL cells might be due to the fact that bone marrow cells did not induce normal stress response (nSBs formation and hsp70 transcription) or they can be more resistant to heat stress. NBM and ALL cells have been heat shocked at 42^0C; however, evidence suggests that different temperatures (42^0C, 43^0C, 45^0C) resulted in various levels of SATIII transcription (136).

In Chapter 5, the potential significance of the RGG/RG status of SAFB1/2 on the interaction with SRSF1 needs to be refined. The mutants used in this study contain 7 and 8 sites for SAFB1 and SAFB2, respectively. Future studies should focus to investigate the specific methylation sites that were responsible for the significant effect of SAFB1/2 interaction with SRSF1 using single mutations of RGG/RG sites. Data in Chapter 5 revealed that SAFB1/2 binding proteins were implicated in regulating the cell cycle and methylation. Future studies could establish the biological link between the cell cycle and the RGG/RG methylation of SAFB1/2 and investigate whether inhibiting methylation would trigger the cell cycle arrest and eventually apoptosis.

Therefore, T-ALL can be treated with GSK3326595 inhibitor and viability can be assessed using annexin-PI assay.

The proteomic data in Chapter 5 lacked normal control cells to compare the SAFB1/2 proteome with. A few attempts using SAFB1 and SAFB2 pulldowns were made in NBM cells but were unsuccessful. NBM cells are a heterogeneous population of cells so a purified subset bone marrow cells would be ideal to isolate using fluorescence-activated cell sorting (FACS) method. $CD7^+$, a marker that is expressed on normal lymphoid cells and highly expressed in many T-ALL patients, can be isolated using FACS in NBM cells and eventually yield pure population of cells. The $CD7^+$ NBM cells would be used as controls for SAFB1/2 pulldowns and thereby TMT-MS analysis. Therefore, SAFB1/2 interactions in T-ALL can be compared with $CD7^+$ NBM cells.

6.8 Conclusions

This thesis provided insights of SAFB1/2 expression in ALL compared with NBM cells and showed that modulating SAFB1 levels induce apoptosis selectively in ALL cells. The altered expression of SAFB1 and SAFB2 influenced the mechanisms regulating the stress response in malignant cells. In addition, HSF1 was found to be constitutively significantly increased in primary BCP-ALL and T-ALL cells compared with NBM following HS and HSP90i treatment, indicating that the stress response is altered. In addition, HSF1 was found enriched at the nuclear border in primary NBM, BCP-ALL and T-ALL cells. HSF1 nuclear border aggregation was more abundant in BCP-ALL and T-ALL cells compared to NBM. The altered stress response in ALL, as typified by the lack of SAFB2 containing nSBs, also suggest an altered stress response could be involved. SAFB1/2 RGG/RG methylation and SUMOylation are likely significant for its interaction with SRSF1. The proteomic analyses for SAFB1 and SAFB2 interactions were undertaken for the first time in HeLa and T-ALL cells and it highlighted the pivotal role SAFB1/2 might play in regulating critical cellular processes.

REFERENCES

1. Renz A, Fackelmayer FO. Purification and molecular cloning of the scaffold attachment factor B (SAF-B), a novel human nuclear protein that specifically binds to S/MAR-DNA. Nucleic Acids Research. 1996;24(5):843–9.

2. Nayler O, Strätling W, Bourquin JP, Stagljar I, Lindemann L, Jasper H, et al. SAF-B protein couples transcription and pre-mRNA splicing to SAR/MAR elements. Nucleic Acids Research. 1998;26(15):3542–9.

3. Oesterreich S, Lee A V., Sullivan TM, Samuel SK, Davie JR, Fuqua SAW. Novel nuclear matrix protein HET binds to and influences activity of the HSP27 promoter in human breast cancer cells. Journal of Cellular Biochemistry. 1997 Nov 1;67(2):275–86.

4. Weighardt F, Cobianchi F, Cartegni L, Chiodi I, Villa a, Riva S, et al. A novel hnRNP protein (HAP/SAF-B) enters a subset of hnRNP complexes and relocates in nuclear granules in response to heat shock. Journal of cell science. 1999;112 (Pt 1(April 2016):1465–76.

5. Townson SM, Dobrzycka KM, Lee A V., Air M, Deng W, Kang K, et al. SAFB2, a new scaffold attachment factor homolog and estrogen receptor corepressor. Journal of Biological Chemistry. 2003;278(22):20059–68.

6. Chan CW, Lee Y-B, Uney J, Flynn A, Tobias JH, Norman M. A novel member of the SAF (scaffold attachment factor)-box protein family inhibits gene expression and induces apoptosis. Biochemical Journal. 2007;407(3):355–62.

7. Garee JP, Oesterreich S. SAFB1's multiple functions in biological control - Lots still to be done! Journal of Cellular Biochemistry. 2010;109(2):312–9.

8. Hong EA, Gautrey HL, Elliott DJ, Tyson-Capper AJ. SAFB1- and SAFB2-mediated transcriptional repression: relevance to cancer. Biochemical Society Transactions [Internet]. 2012;40(4):826–30. Available from: http://biochemsoctrans.org/lookup/doi/10.1042/BST20120030

9. Sergeant KA, Bourgeois CF, Dalgliesh C, Venables JP, Stevenin J, Elliott DJ. Alternative RNA splicing complexes containing the scaffold attachment factor SAFB2. Journal of Cell Science. 2007;120(2):309–19.

10. Uhlén M, Fagerberg L, Hallström BM, Lindskog C, Oksvold P, Mardinoglu A, et al. Tissue-based map of the human proteome. Science. 2015;347(6220).

11. Norman M, Rivers C, Lee Y-B, Idris J, Uney J. The increasing diversity of functions attributed to the SAFB family of RNA-/DNA-binding proteins. Biochemical Journal. 2016;473(23):4271–88.

12. Hammerich-Hille S, Kaipparettu BA, Tsimelzon A, Creighton CJ, Jiang S, Polo JM, et al. SAFB1 mediates repression of immune regulators and apoptotic genes in breast cancer cells. Journal of Biological Chemistry. 2010;285(6):3608–16.

13. Ivanova M, Dobrzycka KM, Jiang S, Michaelis K, Meyer R, Kang K, et al. Scaffold Attachment Factor B1 Functions in Development , Growth , and Reproduction Scaffold Attachment Factor B1 Functions in Development , Growth , and Reproduction. Molecular and cellular biology. 2005;25(8):2995–3006.

14. Jiang S, Katz TA, Garee JP, DeMayo FJ, Lee A V, Oesterreich S. Scaffold attachment factor B2 (SAFB2)-null mice reveal non-redundant functions of SAFB2 compared with its paralog, SAFB1. Disease models & mechanisms [Internet]. 2015;8(9):1121–7. Available from: http://dmm.biologists.org/content/8/9/1121.abstract

15. Lin J, Xu P, LaVallee P, Hoidal JR. Identification of proteins binding to E-Box/Ku86 sites and function of the tumor suppressor SAFB1 in transcriptional regulation of the human xanthine oxidoreductase gene. Journal of Biological Chemistry. 2008;283(44):29681–9.

16. Mukhopadhyay NK, Kim J, You S, Morello M, Hager MH, Huang WC, et al. Scaffold attachment factor B1 regulates the androgen receptor in concert with the growth inhibitory kinase MST1 and the methyltransferase EZH2. British Dental Journal [Internet]. 2014;217(1):3235–42. Available from: http://dx.doi.org/10.1038/onc.2013.294

17. Hernández-Hernández JM, Mallappa C, Nasipak BT, Oesterreich S, Imbalzano AN. The Scaffold attachment factor b1 (Safb1) regulates myogenic differentiation by facilitating the transition of myogenic gene chromatin from a

repressed to an activated state. Nucleic Acids Research. 2013;41(11):5704–16.

18. Biamonti G, Caceres JF. Cellular stress and RNA splicing. Vol. 34, Trends in Biochemical Sciences. 2009. p. 146–53.

19. Chiodi I, Biggiogera M, Denegri M, Corioni M, Weighardt F, Cobianchi F, et al. Structure and dynamics of hnRNP-labelled nuclear bodies induced by stress treatments. Journal of cell science [Internet]. 2000;113 (Pt 2(May 2014):4043–53. Available from: http://www.ncbi.nlm.nih.gov/pubmed/11058091

20. Denegri M, Chiodi I, Corioni M, Cobianchi F, Riva S, Biamonti G. Stress-induced nuclear bodies are sites of accumulation of pre-mRNA processing factors. Molecular biology of the cell. 2001;12(11):3502–14.

21. Montecucco A, Biamonti G. Pre-mRNA processing factors meet the DNA damage response. Frontiers in Genetics. 2013;4(June):1–14.

22. Altmeyer M, Toledo L, Gudjonsson T, Grøfte M, Rask MB, Lukas C, et al. The chromatin scaffold protein SAFB1 renders chromatin permissive for DNA damage signaling. Molecular Cell [Internet]. 2013;52(2):206–20. Available from: http://dx.doi.org/10.1016/j.molcel.2013.08.025

23. Townson SM, Sullivan T, Zhang Q, Clark GM, Osborne CK, Lee A V. HET / SAF-B Overexpression Causes Growth Arrest and Multinuclearity and Is Associated with Aneuploidy in Human Breast Cancer 1. 2000;6(September):3788–96.

24. Lee YB, Colley S, Norman M, Biamonti G, Uney JB. SAFB re-distribution marks steps of the apoptotic process. Experimental Cell Research. 2007;313(18):3914–23.

25. Beli P, Lukashchuk N, Wagner SA, Weinert BT, Olsen J V., Baskcomb L, et al. Proteomic Investigations Reveal a Role for RNA Processing Factor THRAP3 in the DNA Damage Response. Molecular Cell [Internet]. 2012;46(2):212–25. Available from: http://dx.doi.org/10.1016/j.molcel.2012.01.026

26. Picard N, Caron V, Bilodeau S, Sanchez M, Mascle X, Aubry M, et al. Identification of Estrogen Receptor as a SUMO-1 Target Reveals a Novel

Phosphorylated Sumoylation Motif and Regulation by Glycogen Synthase Kinase 3 . Molecular and Cellular Biology. 2012;32(14):2709–21.

27. Golebiowski F, Matic I, Tatham MH, Cole C, Yin Y, Nakamura A, et al. System-wide changes to SUMO modifications in response to heat shock. Science signaling [Internet]. 2009;2(72):ra24. Available from: http://www.ncbi.nlm.nih.gov/pubmed/19471022

28. Liu HW, Banerjee T, Guan X, Freitas MA, Parvin JD. The chromatin scaffold protein SAFB1 localizes SUMO-1 to the promoters of ribosomal protein genes to facilitate transcription initiation and splicing. Nucleic Acids Research. 2015;43(7):3605–13.

29. Garee JP, Meyer R, Oesterreich S. Co-repressor activity of scaffold attachment factor B1 requires sumoylation. Biochemical and Biophysical Research Communications [Internet]. 2011;408(4):516–22. Available from: http://dx.doi.org/10.1016/j.bbrc.2011.04.040

30. Guo A, Gu H, Zhou J, Mulhern D, Wang Y, Lee KA, et al. Immunoaffinity enrichment and mass spectrometry analysis of protein methylation. Molecular & cellular proteomics : MCP [Internet]. 2014;13(1):372–87. Available from: http://www.ncbi.nlm.nih.gov/pubmed/24129315%0Ahttp://www.pubmedcentral.nih.gov/articlerender.fcgi?artid=PMC3879628

31. Boisvert F-M, Côté J, Boulanger M-C, Richard S. A proteomic analysis of arginine-methylated protein complexes. Molecular & cellular proteomics : MCP [Internet]. 2003;2(12):1319–30. Available from: http://www.ncbi.nlm.nih.gov/pubmed/14534352

32. Dobrzycka KM, Kang K, Jiang S, Meyer R, Rao PH, Lee A V., et al. Disruption of scaffold attachment factor B1 leads to TBX2 up-regulation, lack of p19ARF induction, lack of senescence, and cell immortalization. Cancer Research. 2006;66(16):7859–63.

33. Oesterreich S, Allredl DC, Mohsin SK, Zhang Q, Wong H, Lee a V, et al. High rates of loss of heterozygosity on chromosome 19p13 in human breast cancer. British journal of cancer [Internet]. 2001;84(4):493–8. Available from: papers3://publication/doi/10.1054/bjoc.2000.1606

34. Hammerich-Hille S, Bardout VJ, Hilsenbeck SG, Osborne CK, Oesterreich S. Low SAFB levels are associated with worse outcome in breast cancer patients. Breast Cancer Research and Treatment. 2010;121(2):503–9.

35. Jiao H-L. Down-regulation of SAFB sustains the NF-κB pathway by targeting TAK1 during the progression of colorectal cancer.pdf. Clinical Cancer Research. 2017;23(22):7108–18.

36. Baltz AG, Munschauer M, Schwanhäusser B, Vasile A, Murakawa Y, Schueler M, et al. The mRNA-Bound Proteome and Its Global Occupancy Profile on Protein-Coding Transcripts. Molecular Cell. 2012;46(5):674–90.

37. Castello A, Fischer B, Eichelbaum K, Horos R, Beckmann BM, Strein C, et al. Insights into RNA Biology from an Atlas of Mammalian mRNA-Binding Proteins. Cell [Internet]. 2012;149(6):1393–406. Available from: http://dx.doi.org/10.1016/j.cell.2012.04.031

38. Rivers C, Idris J, Scott H, Rogers M, Lee YB, Gaunt J, et al. iCLIP identifies novel roles for SAFB1 in regulating RNA processing and neuronal function. BMC Biology [Internet]. 2015;13(1):1–15. Available from: http://dx.doi.org/10.1186/s12915-015-0220-7

39. Hong E, Best A, Gautrey H, Chin J, Razdan A, Curk T, et al. Unravelling the RNA-binding properties of SAFB proteins in breast cancer cells. BioMed Research International. 2015;2015.

40. Arao Y, Kuriyama R, Kayama F, Kato S. A nuclear matrix-associated factor, SAFB-B, interacts with specific isoforms of AUF1/hnRNP D. Archives of Biochemistry and Biophysics. 2000;380(2):228–36.

41. Stoilov P, Dauod R, Nayler O, Stamm S. Human tra2-beta1 autoregulates its protein concentration by infuencing alternative splicing of its pre-mRNA. Human Molecular Genetics. 2004;13(5):509–24.

42. Rappsilber J, Ryder U, Lamond AI, Mann M. Large-scale proteomic analysis of the human spliceosome. Genome Research. 2002;13(1):1231–45.

43. Will CL, Lührmann R. Spliceosome structure and function. Cold Spring Harbor Perspectives in Biology. 2011;3(7):1–2.

44. Agafonov DE, Deckert J, Wolf E, Odenwalder P, Bessonov S, Will CL, et al. Semiquantitative Proteomic Analysis of the Human Spliceosome via a Novel Two-Dimensional Gel Electrophoresis Method. Molecular and Cellular Biology. 2011;31(13):2667–82.

45. Peidis P, Voukkalis N, Aggelidou E, Georgatsou E, Hadzopoulou-Cladaras M, Scott RE, et al. SAFB1 interacts with and suppresses the transcriptional activity of p53. FEBS Letters [Internet]. 2011;585(1):78–84. Available from: http://dx.doi.org/10.1016/j.febslet.2010.11.054

46. Tai HH, Geisterfer M, Bell JC, Moniwa M, Davie JR, Boucher L, et al. CHD1 associates with NCoR and histone deacetylase as well as with RNA splicing proteins. Biochemical and Biophysical Research Communications. 2003;308(1):170–6.

47. Zeitz MJ, Malyavantham KS, Seifert B, Berezney R. Matrin 3: Chromosomal distribution and protein interactions. Journal of Cellular Biochemistry. 2009;108(1):125–33.

48. Bryder D, Rossi DJ, Weissman IL, Al E. Hematopoietic stem cells: The paradigmatic tissue-specific stem cell. American Journal of Pathology. 2006;169(2):338–46.

49. Doulatov S, Notta F, Laurenti E, Dick JE. Hematopoiesis: A human perspective. Cell Stem Cell [Internet]. 2012;10(2):120–36. Available from: http://dx.doi.org/10.1016/j.stem.2012.01.006

50. Orkin SH, Zon LI. Hematopoiesis: An Evolving Paradigm for Stem Cell Biology. Cell. 2008;132(4):631–44.

51. Mikkola HKA. The journey of developing hematopoietic stem cells. Development [Internet]. 2006;133(19):3733–44. Available from: http://www.ncbi.nlm.nih.gov/pubmed/16968814

52. Teitell MA, Mikkola HKA. Transcriptional activators, repressors, and epigenetic modifiers controlling hematopoietic stem cell development. Pediatric Research. 2006;59(4 PART. 2):33–9.

53. Aggarwal R, Lu J, J. Pompili V, Das H. Hematopoietic Stem Cells:

Transcriptional Regulation, Ex Vivo Expansion and Clinical Application. Current Molecular Medicine. 2011;12(1):34–49.

54. Carotta S, Nutt SL, Wu L, Al E. Surprising new roles for PU.1 in the adaptive immune response. 2010;238:63–75.

55. Huang X, Cho S, Spangrude GJ, Marrow B. Hematopoietic stem cells : generation and self-renewal Circulation. 2007;1851–9.

56. Hunger SP, Mullighan CG. Acute Lymphoblastic Leukemia in Children. New England Journal of Medicine [Internet]. 2015;373(16):1541–52. Available from: http://www.nejm.org/doi/10.1056/NEJMra1400972

57. Terwilliger T, Abdul-Hay M. Acute lymphoblastic leukemia: a comprehensive review and 2017 update. Blood cancer journal [Internet]. 2017 Jun;7(6):e577. Available from: http://www.ncbi.nlm.nih.gov/pubmed/28665419

58. Hunger SP, Lu X, Devidas M, Camitta BM, Gaynon PS, Winick NJ, et al. Improved survival for children and adolescents with acute lymphoblastic leukemia between 1990 and 2005: A report from the children's oncology group. Journal of Clinical Oncology. 2012;30(14):1663–9.

59. Schwab C, Harrison CJ. Advances in B-cell Precursor Acute Lymphoblastic Leukemia Genomics. HemaSphere. 2018;1.

60. Hiroto Inaba, MD, Prof.Mel Greaves, PhD, and Charles G.Mullighan M. Acute Lymphoblastic Leukemia. Lancet. 2013;381(9881):1–27.

61. Ghazavi F, Lammens T, Van Roy N, Poppe B, Speleman F, Benoit Y, et al. Molecular basis and clinical significance of genetic aberrations in B-cell precursor acute lymphoblastic leukemia. Experimental Hematology [Internet]. 2015;43(8):640–53. Available from: http://dx.doi.org/10.1016/j.exphem.2015.05.015

62. Durinck K, Goossens S, Peirs S, Wallaert A, Van Loocke W, Matthijssens F, et al. Novel biological insights in T-cell acute lymphoblastic leukemia. Experimental Hematology [Internet]. 2015;43(8):625–39. Available from: http://dx.doi.org/10.1016/j.exphem.2015.05.017

63. Moorman A V. The clinical relevance of chromosomal and genomic

abnormalities in B-cell precursor acute lymphoblastic leukaemia. Blood Reviews. 2012;26(3):123–35.

64. Mullighan CG. The molecular genetic makeup of acute lymphoblastic leukemia. Hematology Am Soc Hematol Educ Program. 2012;2012:389–96.

65. Harrison CJ. Cytogenetics of paediatric and adolescent acute lymphoblastic leukaemia. British Journal of Haematology. 2009;144(2):147–56.

66. Pui C-H, Mullighan CG, Evans WE, Relling M V. Pediatric acute lymphoblastic leukemia: Where are we going and how do we get there? [Internet]. Vol. 120, Blood. 2012. p. 1165–74. Available from: http://www.embase.com/search/results?subaction=viewrecord&from=export&id=L365469319%0Ahttp://bloodjournal.hematologylibrary.org/content/120/6/1165.full.pdf+html%0Ahttp://dx.doi.org/10.1182/blood-2012-05-378943

67. Aifantis I, Raetz E, Buonamici S, Al E. Molecular pathogenesis of T-cell leukaemia and lymphoma. Nature Reviews Immunology. 2008;8(5):380–90.

68. Vlierberghe P Van, Ferrando A, Vlierberghe P Van, Ferrando A. The molecular basis of T cell acute lymphoblastic leukemia Find the latest version : Review series The molecular basis of T cell acute lymphoblastic leukemia. 2012;122(10):3398–406.

69. Girardi T, Vicente C, Cools J, De Keersmaecker K. The genetics and molecular biology of T-ALL. Blood. 2017;129(9):1113–23.

70. Vlierberghe P Van, Ferrando A, Vlierberghe P Van, Ferrando A. The molecular basis of T cell acute lymphoblastic leukemia Find the latest version : Review series The molecular basis of T cell acute lymphoblastic leukemia. The Journal of Clinical Investigation. 2012;122(10):3398–406.

71. Iacobucci I, Mullighan CG. Genetic basis of acute lymphoblastic leukemia. Journal of Clinical Oncology. 2017;35(9):975–83.

72. Burke MJ, Salzer WL, Devidas M, Dai Y, Gore L, Hilden JM, et al. Replacing cyclophosphamide/cytarabine/mercaptopurine with cyclophosphamide/etoposide during consolidation/delayed intensification does not improve outcome for pediatric B-cell acute lymphoblastic leukemia: a

report from the COG. Haematologica. 2019;104(5):986–92.

73. Lee-Sherick AB, Linger RMA, Gore L, Keating AK, Graham DK. Targeting paediatric acute lymphoblastic leukaemia: Novel therapies currently in development. British Journal of Haematology. 2010;151(4):295–311.

74. Sutton R, Venn NC, Law T, Boer JM, Trahair TN, Ng A, et al. A risk score including microdeletions improves relapse prediction for standard and medium risk precursor B-cell acute lymphoblastic leukaemia in children. British Journal of Haematology. 2018;180(4):550–62.

75. Cooper SL, Brown PA. Treatment of Pediatric Acute Lymphoblastic Leukemia. 2016;118(24):6072–8.

76. Medical Research Council. United K ingdom National Randomised Trial For Children and Young Adults with A cute L ymphoblastic L eukaemia and. 2011;27.

77. Tucci F, Maurizio Aricò. Treatment of pediatric acute lymphoblastic leukemia. Clinical and Transfusion Haematology. 2009;45(1–2):23–7.

78. Wook Jae L, Bin C. Prognostic factors and treatment of pediatric acute lymphoblastic leukemia. Korean Journal of Pediatrics [Internet]. 2017;60(5):129–37. Available from: http://dx.doi.org/10.3345/kjp.2017.60.5.129%25Q???

79. Chatterjee T, Mallhi RS, Venkatesan S. Minimal residual disease detection using flow cytometry: Applications in acute Leukemia. Medical Journal Armed Forces India [Internet]. 2016;72(2):152–6. Available from: http://dx.doi.org/10.1016/j.mjafi.2016.02.002

80. Dongen JJM Van, Velden VHJ Van Der, Brüggemann M, Orfao A. Minimal residual disease (MRD) diagnostics in acute lymphoblastic leukemia (ALL): need for sensitive , fast and standardized technologies. Blood. 2015;125(26):3996–4010.

81. Kotrova M, Van Der Velden VHJ, Van Dongen JJM, Formankova R, Sedlacek P, Brüggemann M, et al. Next-generation sequencing indicates false-positive MRD results and better predicts prognosis after SCT in patients with childhood

ALL. Bone Marrow Transplantation. 2017;52(7):962–8.

82. Sekiya Y, Xu Y, Muramatsu H, Okuno Y, Narita A, Suzuki K, et al. Clinical utility of next-generation sequencing-based minimal residual disease in paediatric B-cell acute lymphoblastic leukaemia. British Journal of Haematology. 2016;176(2):248–57.

83. Tan SH, Bertulfo FC, Sanda T, AL E. Leukemia-Initiating Cells in T-Cell Acute Lymphoblastic Leukemia. Frontiers in Oncology. 2017;7(September).

84. Cox C V., Martin HM, Kearns PR, Virgo P, Evely RS, Blair A. Characterization of a progenitor cell population in childhood T-cell acute lymphoblastic leukemia. Blood. 2007;109(2):674–82.

85. Gerby B, Clappier E, Armstrong F, Deswarte C, Calvo J, Poglio S, et al. Expression of CD34 and CD7 on human T-cell acute lymphoblastic leukemia discriminates functionally heterogeneous cell populations. Leukemia. 2011;25(8):1249–58.

86. Diamanti P, Cox C V., Blair A. Comparison of childhood leukemia initiating cell populations in NOD/SCID and NSG mice. Leukemia. 2012;26(2):376–80.

87. Shultz LD, Lyons BL, Burzenski LM, Gott B, Chen X, Chaleff S, et al. Human lymphoid and myeloid cell development in NOD/LtSz-scid IL2R gamma null mice engrafted with mobilized human hemopoietic stem cells. Journal of immunology (Baltimore, Md : 1950) [Internet]. 2005;174(10):6477–89. Available from: http://www.ncbi.nlm.nih.gov/pubmed/15879151

88. Dworzak MN, Fröschl G, Printz D, De Zen L, Gaipa G, Ratei R, et al. CD99 expression in T-lineage ALL: Implications for flow cytometric detection of minimal residual disease. Leukemia. 2004;18(4):703–8.

89. Cox C V., Diamanti P, Moppett JP, Blair A. Investigating CD99 expression in leukemia propagating cells in childhood t cell acute lymphoblastic leukemia. PLoS ONE. 2016;11(10):1–13.

90. Cobaleda C, Gutie´rrez-Cianca N, Rez-Losada JP, Al E. A primitive hematopoietic cell is the target for the leukemic transformation in human Philadelphia-positive acute lymphoblastic leukemia A primitive hematopoietic

cell is the target for the leukemic transformation in human Philadelphia-positive acute lymp. Hematology. 2000;95(3):1007–13.

91. Cox C V, Evely RS, Oakhill A, Pamphilon DH, Goulden NJ, Blair A. Characterization of acute lymphoblastic leukemia progenitor cells. Hematology. 2004;104(9):2919–25.

92. Kong Y, Yoshida S, Saito Y, Al E. CD34 þ CD38 þ CD19 þ as well as CD34 þ CD38?CD19 þ cells are leukemia- initiating cells with self-renewal capacity in human B-precursor ALL.pdf. 2008.

93. Cox C V., Diamanti P, Evely RS, Kearns PR, Blair A. Expression of CD133 on leukemia-initiating cells in childhood ALL. Blood. 2009;113(14):3287–96.

94. Diamanti P, Cox C V., Moppett JP, Blair A. Parthenolide eliminates leukemia-initiating cell populations and improves survival in xenografts of childhood acute lymphoblastic leukemia. Blood. 2013;121(8):1384–93.

95. Diamanti P, Cox C V., Moppett JP, Blair A. Dual targeting of Hsp90 in childhood acute lymphoblastic leukaemia. British Journal of Haematology. 2018 Jan;180(1):147–9.

96. Starý J, Hrušák O. Recent advances in the management of pediatric acute lymphoblastic leukemia. F1000Research. 2016;5(May):2635.

97. Goetz MP, Toft DO, Ames MM, Erlichman C. The Hsp90 chaperone complex as a novel target for cancer therapy. Annals of oncology : official journal of the European Society for Medical Oncology / ESMO. 2003;14(8):1169–76.

98. Thyagu S, Minden MD, Gupta V, Yee KWL, Schimmer AD, Schuh AC, et al. Treatment of Philadelphia chromosome-positive acute lymphoblastic leukaemia with imatinib combined with a paediatric-based protocol. British Journal of Haematology. 2012;158(4):506–14.

99. Du Z, Lovly CM. Mechanisms of receptor tyrosine kinase activation in cancer. Molecular Cancer. 2018;17(1):1–13.

100. Schultz KR, Bowman WP, Aledo A, Slayton WB, Sather H, Devidas M, et al. Improved early event-free survival with imatinib in Philadelphia chromosome - Positive acute lymphoblastic leukemia: A Children's Oncology Group Study.

Journal of Clinical Oncology. 2009;27(31):5175–81.

101. Aoe M, Shimada A, Muraoka M, Washio K, Nakamura Y, Takahashi T, et al. ABL kinase mutation and relapse in 4 pediatric Philadelphia chromosome-positive acute lymphoblastic leukemia cases. International Journal of Hematology. 2014;99(5):609–15.

102. Fei F, Stoddart S, Müschen M, Kim YM, Groffen J, Heisterkamp N. Development of resistance to dasatinib in Bcr/Abl-positive acute lymphoblastic leukemia. Leukemia. 2010;24(4):813–20.

103. Cortes JE, Kim DW, Pinilla-Ibarz J, le Coutre PD, Paquette R, Chuah C, et al. Ponatinib efficacy and safety in Philadelphia chromosome–positive leukemia: final 5-year results of the phase 2 PACE trial. Blood. 2018;132(4):393–404.

104. Miller GD, Bruno BJ, Lim CS. Resistant mutations in CML and Ph+ALL – role of ponatinib. Biologics: Targets and Therapy. 2014;8:243–54.

105. Farhadfar N, Litzow MR. New monoclonal antibodies for the treatment of acute lymphoblastic leukemia. Leukemia Research [Internet]. 2016;49:13–21. Available from: http://dx.doi.org/10.1016/j.leukres.2016.07.009

106. Schlegel P, Lang P, Zugmaier G, Ebinger M, Kreyenberg H, Witte KE, et al. Pediatric posttransplant relapsed/refractory B-precursor acute lymphoblastic leukemia shows durable remission by therapy with the T-cell engaging bispecific antibody blinatumomab. Haematologica. 2014;99(7):1212–9.

107. Raetz EA, Teachey DT. T-cell acute lymphoblastic leukemia. American Society of Hematology. 2016;580–8.

108. van de Donk NWCJ, Janmaat ML, Mutis T, Lammerts van Bueren JJ, Ahmadi T, Sasser AK, et al. Monoclonal antibodies targeting CD38 in hematological malignancies and beyond. Immunological Reviews. 2016;270(1):95–112.

109. Bride KL, Vincent TL, Im SY, Aplenc R, Barrett DM, Carroll WL, et al. Preclinical efficacy of daratumumab in T-cell acute lymphoblastic leukemia. Blood. 2018;131(9):995–9.

110. Lee DW, Kochenderfer JN, Stetler-Stevenson M, Cui YK, Delbrook C, Feldman SA, et al. T cells expressing CD19 chimeric antigen receptors for

acute lymphoblastic leukaemia in children and young adults: A phase 1 dose-escalation trial. The Lancet [Internet]. 2015;385(9967):517–28. Available from: http://dx.doi.org/10.1016/S0140-6736(14)61403-3

111. Turtle CJ, Hanafi L-A, Berger C, Hudecek M, Al E. Immunotherapy of non-Hodgkin's lymphoma with a defined ratio of CD8 + and CD4 + CD19-specific chimeric antigen receptor–modified T cells. Science Translational Medicine. 2016;8(355):355ra116-355ra116.

112. Gomes-Silva D, Srinivasan M, Sharma S, Lee CM, Wagner DL, Davis TH, et al. CD7-edited T cells expressing a CD7-specific CAR for the therapy of T-cell malignancies. Blood [Internet]. 2017;130(3):285–96. Available from: http://www.bloodjournal.org/content/early/2017/05/24/blood-2017-01-761320%5Cnhttp://www.ncbi.nlm.nih.gov/pubmed/28539325

113. Sanchez-Martınez D, Baroni ML, Gutierrez-Aguera F, Al E. Fratricide-resistant CD1a-speci fi c CAR T cells for the treatment of cortical T-cell acute lymphoblastic leukemia. Blood. 2019;133(21).

114. Richardson PG, Mitsiades CS, Laubach JP, Lonial S, Chanan-Khan AA, Anderson KC. Inhibition of heat shock protein 90 (HSP90) as a therapeutic strategy for the treatment of myeloma and other cancers. British Journal of Haematology. 2011;152(4):367–79.

115. M. T, F. K, S. Y, K. K. Heat shock protein 90 targeting therapy: State of the art and future perspective. EXCLI Journal [Internet]. 2015;14:48–58. Available from: http://www.embase.com/search/results?subaction=viewrecord&from=export&id=L601876365%0Ahttp://dx.doi.org/10.17179/excli2014-586

116. Yamaki H, Nakajima M, Shimotohno KW, Tanaka N. Molecular basis for the actions of Hsp90 inhibitors and cancer therapy. Vol. 64, Journal of Antibiotics. 2011. p. 635–44.

117. Lazenby M, Hills R, Burnett AK, Zabkiewicz J. The HSP90 inhibitor ganetespib: A potential effective agent for Acute Myeloid Leukemia in combination with cytarabine. Leukemia Research. 2015;39(6):617–24.

118. Solárová Z, Mojžiš J, Solár P. Hsp90 inhibitor as a sensitizer of cancer cells to different therapies (review). International Journal of Oncology. 2015;46(3):907–26.

119. Den RB, Lu B. Heat shock protein 90 inhibition: Rationale and clinical potential. Vol. 4, Therapeutic Advances in Medical Oncology. 2012. p. 211–8.

120. Butler LM, Ferraldeschi R, Armstrong HK, Centenera MM, Workman P. Maximizing the Therapeutic Potential of HSP90 Inhibitors. Molecular Cancer Research. 2015;13(11):1445–51.

121. Peron M, Bonvini P, Rosolen A, Al E. Effect of inhibition of the Ubiquitin-Proteasome System and Hsp90 on growth and survival of Rhabdomyosarcoma cells *in vitro*. BMC Cancer. 2012;12.

122. Qu Z, Dong H, Xu X, Feng W, Yi X. Combined effects of 17-DMAG and TNF on cells through a mechanism related to the NF-kappaB pathway. Diagnostic pathology [Internet]. 2013;8(1):70. Available from: http://www.pubmedcentral.nih.gov/articlerender.fcgi?artid=3716826&tool=pmcentrez&rendertype=abstract

123. Hertlein E, Wagner AJ, Jones J, Lin TS, Maddocks KJ, Towns WH, et al. 17-DMAG targets the nuclear factor-κB family of proteins to induce apoptosis in chronic lymphocytic leukemia: Clinical implications of HSP90 inhibition. Blood. 2010;116(1):45–53.

124. Zhang T, Li Y, Yu Y, Zou P, Jiang Y, Sun D. Characterization of celastrol to inhibit Hsp90 and Cdc37 interaction. Journal of Biological Chemistry. 2009;284(51):35381–9.

125. Calderwood SK. Molecular Cochaperones: Tumor Growth and Cancer Treatment. Scientifica. 2013;2013:1–13.

126. Hieronymus H, Lamb J, Ross KN, Peng XP, Clement C, Rodina A, et al. Gene expression signature-based chemical genomic prediction identifies a novel class of HSP90 pathway modulators. Cancer Cell. 2006;10(4):321–30.

127. Peng B, Xu L, Cao F, Wei T, Yang C, Uzan G, et al. HSP90 inhibitor, celastrol, arrests human monocytic leukemia cell U937 at G0/G1 in thiol-containing

agents reversible way. Molecular Cancer. 2010;9:1–13.

128. Westerheide SD, Bosman JD, Mbadugha BNA, Kawahara TLA, Matsumoto G, Kim S, et al. Celastrols as inducers of the heat shock response and cytoprotection. Journal of Biological Chemistry. 2004;279(53):56053–60.

129. Trott A, West JD, Klaic L, Westerheide SD, Silverman RB, Morimoto RI, et al. Activation of Heat Shock and Antioxidant Responses by the Natural Product Celastrol: Transcriptional Signatures of a Thiol-targeted Molecule. Molecular biology of the cell. 2008;19(September):308–17.

130. Matokanovic M, Barisic K, Filipovic-Grcic J, Maysinger D. Hsp70 silencing with siRNA in nanocarriers enhances cancer cell death induced by the inhibitor of Hsp90. European Journal of Pharmaceutical Sciences. 2013;50(1):149–58.

131. Ambade A, Catalano D, Lim A, Mandrekar P. Inhibition of heat shock protein (molecular weight 90 kDa) attenuates proinflammatory cytokines and prevents lipopolysaccharide-induced liver injury in mice. Hepatology. 2012;55(5):1585–95.

132. Åkerfelt M, Morimoto RI, Sistonen L, Al E. Heat shock factors: Integrators of cell stress, development and lifespan. Vol. 11, Nature Reviews Molecular Cell Biology. 2010. p. 545–55.

133. Calderwood SK, Wang Y, Xie X, Khaleque MA, Chou SD, Murshid A, et al. Signal Transduction Pathways Leading to Heat Shock Transcription. Signal Transduction Insights. 2010 Jan;2:STI.S3994.

134. de Billy E, Travers J, Workman P. Shock about heat shock in cancer. Oncotarget. 2012 Aug 11;3(8).

135. Denegri M, Chiodi I, Corioni M, Cobianchi F, Riva S, Biamonti G. Stress-induced Nuclear Bodies Are Sites of Accumulation of Pre-mRNA Processing Factors. Molecular Biology of the Cell. 2001;12(11):3502–14.

136. Valgardsdottir R, Chiodi I, Giordano M, Rossi A, Bazzini S, Ghigna C, et al. Transcription of Satellite III non-coding RNAs is a general stress response in human cells. Nucleic Acids Research. 2008;36(2):423–34.

137. Mahl P, Lutz Y, Puvion E, Fuchs JP. Rapid effect of heat shock on two

heterogeneous nuclear ribonucleoprotein-associated antigens in HeLa cells. Journal of Cell Biology. 1989;109(5):1921–35.

138. Sarge KD, Murphy SP, Morimoto RI. Activation of heat shock gene transcription by heat shock factor 1 involves oligomerization, acquisition of DNA-binding activity, and nuclear localization and can occur in the absence of stress. Molecular and cellular biology [Internet]. 1993;13(3):1392–407. Available from: http://www.ncbi.nlm.nih.gov/pubmed/8441385%0Ahttp://www.pubmedcentral.nih.gov/articlerender.fcgi?artid=PMC359449

139. Chiodi I, Corioni M, Giordano M, Valgardsdottir R, Ghigna C, Cobianchi F, et al. RNA recognition motif 2 directs the recruitment of SF2/ASF to nuclear stress bodies. Nucleic Acids Research. 2004;32(14):4127–36.

140. Musch, Anne, Cohen David, Yeaman Charles, Nelson James, Rodriguez-Boulan Enrique and BP. Human Chromosomes 9, 12, and 15 Contain the Nucleation Sites of Stress-Induced Nuclear Bodies. Molecular biology of the cell. 2002;13(6):158–68.

141. Jolly C, Metz A, Govin J, Vigneron M, Turner BM, Khochbin S, et al. Stress-induced transcription of satellite III repeats. Journal of Cell Biology. 2004;164(1):25–33.

142. Biamonti G, Vourc'h C. Nuclear stress bodies. Vol. 2, Cold Spring Harbor perspectives in biology. 2010.

143. Jolly C, Lakhotia SC. Human sat III and Drosophila hsrω transcripts: A common paradigm for regulation of nuclear RNA processing in stressed cells. Nucleic Acids Research. 2006;34(19):5508–14.

144. Vihervaara A, Sistonen L. HSF1 at a glance. Journal of Cell Science [Internet]. 2014;127(2):261–6. Available from: http://jcs.biologists.org/cgi/doi/10.1242/jcs.132605

145. Mendillo ML, Santagata S, Koeva M, Bell GW, Hu R, Tamimi RM, et al. HSF1 drives a transcriptional program distinct from heat shock to support highly malignant human cancers. Cell. 2012 Aug 3;150(3):549–62.

146. Calderwood SK. HSF1, A Versatile Factor in Tumorogenesis. Current Molecular Medicine. 2012;12(9):1102–7.

147. Dai C, Sampson SB. HSF1: Guardian of Proteostasis in Cancer. Vol. 26, Trends in Cell Biology. 2016. p. 17–28.

148. Santagata S, Mendillo ML, Tang YC, Subramanian A, Perley CC, Roche SP, et al. Tight coordination of protein translation and HSF1 activation supports the anabolic malignant state. Science. 2013;341(6143).

149. Fok JHL, Hedayat S, Zhang L, Aronson LI, Mirabella F, Pawlyn C, et al. HSF1 Is essential for myeloma cell survival and a promising therapeutic target. Clinical Cancer Research. 2018;24(10):2395–407.

150. Tang D, Khaleque MA, Jones EL, Theriault JR, Li C, Wong WH, et al. Expression of heat shock proteins and heat shock protein messenger ribonucleic acid in human prostate carcinoma *in vitro* and in tumors *in vivo*. Cell Stress and Chaperones. 2005;10(1):46–58.

151. Ganguly S, Home T, Yacoub A, Kambhampati S, Shi H, Dandawate P, et al. Targeting HSF1 disrupts HSP90 chaperone function in chronic lymphocytic leukemia. Oncotarget. 2015;6(31).

152. Frezzato F, Raggi F, Martini V, Severin F, Trimarco V, Visentin A, et al. HSP70/HSF1 axis, regulated via a PI3K/AKT pathway, is a druggable target in chronic lymphocytic leukemia . International Journal of Cancer. 2019;1–13.

153. Dai C, Whitesell L, Rogers AB, Lindquist S. Heat Shock Factor 1 Is a Powerful Multifaceted Modifier of Carcinogenesis. Cell. 2007;130(6):1005–18.

154. Fang F, Chang R, Yang L, Al E. Heat shock factor 1 promotes invasion and metastasis of hepatocellular carcinoma *in vitro* and *in vivo*. Cancer. 2012;118(7):1782–94.

155. Nakamura Y, Fujimoto M, Fukushima S, Nakamura A, Hayashida N, Takii R, et al. Heat shock factor 1 is required for migration and invasion of human melanoma *in vitro* and *in vivo*. Cancer Letters [Internet]. 2014;354(2):329–35. Available from: http://dx.doi.org/10.1016/j.canlet.2014.08.029

156. Dai C. The heat-shock, or HSF1-mediated proteotoxic stress, response in

cancer: From proteomic stability to oncogenesis. Philosophical Transactions of the Royal Society B: Biological Sciences. 2018;373(1738).

157. Murphy ME. The HSP70 family and cancer. Carcinogenesis. 2013;34(6):1181–8.

158. Kudryavtsev VA, Khokhlova A V., Mosina VA, Selivanova EI, Kabakov AE. Induction of Hsp70 in tumor cells treated with inhibitors of the Hsp90 activity: A predictive marker and promising target for radiosensitization. PLoS ONE. 2017 Mar 1;12(3).

159. Nikolakaki E, Kohen R, Hartmann AM, Stamm S, Georgatsou E, Giannakouros T. Cloning and Characterization of an Alternatively Spliced Form of SR Protein Kinase 1 that Interacts Specifically with Scaffold Attachment Factor-B. Journal of Biological Chemistry. 2001;276(43):40175–82.

160. Hartmann AM, Nayler O, Schwaiger FW, Obermeier A, Stamm S, Et al. The interaction and colocalization of Sam68 with the splicing-associated factor YT521-B in nuclear dots is regulated by the Src family kinase p59(fyn). Molecular Biology of the Cell. 1999;10(11):3909–26.

161. Stoss O, Schwaiger FW, Cooper TA, Stamm S, Al E. Alternative splicing determines the intracellular localization of the novel nuclear protein Nop30 and its interaction with the splicing factor SRp30c. Journal of Biological Chemistry. 1999;274(16):10951–62.

162. Lee YB, Colley S, Norman M, Biamonti G, Uney JB. SAFB re-distribution marks steps of the apoptotic process. Experimental Cell Research. 2007;313(18):3914–23.

163. Den RB, Lu B. Heat shock protein 90 inhibition: rationale and clinical potential. Therapeutic advances in medical oncology [Internet]. 2012;4(4):211–8. Available from: http://www.pubmedcentral.nih.gov/articlerender.fcgi?artid=3384095&tool=pmcentrez&rendertype=abstract

164. Ciocca DR, Arrigo AP, Calderwood SK. Heat shock proteins and heat shock factor 1 in carcinogenesis and tumor development: An update. Vol. 87,

Archives of Toxicology. 2013. p. 19–48.

165. de Nadal E, Ammerer G, Posas F. Controlling gene expression in response to stress. Nature Reviews Genetics [Internet]. 2011; Available from: http://www.nature.com/doifinder/10.1038/nrg3055

166. Jurivich DA, Choo M, Welk J, Qiu L, Han K, Zhou X. Human aging alters the first phase of the molecular response to stress in T-cells. Experimental Gerontology. 2005 Dec;40(12):948–58.

167. Hardy L, Goodman M, Vasquez A, Chauhan D, Anderson KC, Voellmy R, et al. Activation signals regulate heat shock transcription factor 1 in human B lymphocytes. Journal of Cellular Physiology. 1997;170(3):235–40.

168. Gandhapudi SK, Murapa P, Threlkeld ZD, Ward M, Sarge KD, Snow C, et al. Heat Shock Transcription Factor 1 Is Activated as a Consequence of Lymphocyte Activation and Regulates a Major Proteostasis Network in T Cells Critical for Cell Division During Stress. The Journal of Immunology. 2013 Oct 15;191(8):4068–79.

169. Boudesco C, Rattier T, Garrido C, Jego G. Do not stress, just differentiate: Role of stress proteins in hematopoiesis. Vol. 6, Cell Death and Disease. Nature Publishing Group; 2015.

170. Creagh EM, Sheehan D, Cotter TG. Heat shock proteins--modulators of apoptosis in tumour cells. Leukemia : official journal of the Leukemia Society of America, Leukemia Research Fund, UK. 2000;14(January):1161–73.

171. Kudryavtsev VA, Khokhlova A V., Mosina VA, Selivanova EI, Kabakov AE. Induction of Hsp70 in tumor cells treated with inhibitors of the Hsp90 activity: A predictive marker and promising target for radiosensitization. PLoS ONE. 2017;12(3).

172. Scott H, Smith AE, Barker GR, Uney JB, Warburton EC. Contrasting roles for DNA methyltransferases and histone deacetylases in single-item and associative recognition memory. Neuroepigenetics [Internet]. 2017;9:1–9. Available from: http://dx.doi.org/10.1016/j.nepig.2017.02.001

173. Nozawa RS, Boteva L, Soares DC, Naughton C, Dun AR, Buckle A, et al.

SAF-A Regulates Interphase Chromosome Structure through Oligomerization with Chromatin-Associated RNAs. Cell [Internet]. 2017;169(7):1214-1227.e18. Available from: http://dx.doi.org/10.1016/j.cell.2017.05.029

174. Huang DW, Sherman BT, Lempicki RA. Bioinformatics enrichment tools: Paths toward the comprehensive functional analysis of large gene lists. Nucleic Acids Research. 2009;37(1):1–13.

175. Ashburner M, Ball CA, Blake JA, Botstein D, Butler H, Cherry JM, et al. Gene Ontology : tool for the unification of biology. Nature genetics [Internet]. 2011;25(1):25–9. Available from: http://www.nature.com/ng/journal/v25/n1/abs/ng0500_25.html

176. Kuleshov M V, Jones MR, Rouillard AD, Fernandez NF, Duan Q, Wang Z, et al. Enrichr: a comprehensive gene set enrichment analysis web server 2016 update. Nucleic acids research [Internet]. 2016;44(W1):W90-7. Available from: http://www.ncbi.nlm.nih.gov/pubmed/27141961%0Ahttp://www.pubmedcentral.nih.gov/articlerender.fcgi?artid=PMC4987924

177. Huang DW, Sherman BT, Lempicki RA. Systematic and integrative analysis of large gene lists using DAVID bioinformatics resources. Nature protocols [Internet]. 2009;4(1):44–57. Available from: http://www.ncbi.nlm.nih.gov/pubmed/19131956

178. Qi M, Wang R, Jing B, Jian F, Ning C, Zhang L. KEGG: Kyoto Encyclopedia Genes and Genomes. Infection, Genetics and Evolution. 2016;44(1):313–7.

179. Su AI, Wiltshire T, Batalov S, Lapp H, Ching KA, Block D, et al. A gene atlas of the mouse and human.pdf. Proceedings of the National Academy of Sciences. 2004;101(16):6062–7.

180. Das S, Krainer AR. Emerging functions of SRSF1, splicing factor and oncoprotein, in RNA metabolism and cancer. Molecular Cancer Research. 2014;12(9):1195–204.

181. Mei M, Zhang R, Zhou ZW, Ying Z, Wang J, Zhang H, et al. PRMT5-mediated H4R3sme2 confers cell differentiation in pediatric B-cell precursor acute lymphoblastic leukemia. Clinical Cancer Research. 2019;25(8):2633–43.

182. Enserink JM. Sumo and the cellular stress response. Cell Division [Internet]. 2015;10(1):1–13. Available from: http://dx.doi.org/10.1186/s13008-015-0010-1

183. Han ZJ, Feng YH, Gu BH, Li YM, Chen H. The post-Translational modification, SUMOylation, and cancer (Review). International Journal of Oncology. 2018;52(4):1081–94.

184. Pelisch F, Gerez J, Druker J, Schor IE, Muñoz MJ, Risso G, et al. The serine/arginine-rich protein SF2/ASF regulates protein sumoylation. Proceedings of the National Academy of Sciences of the United States of America. 2010;107(37):16119–24.

185. Pozzi B, Bragado L, Will CL, Mammi P, Risso G, Urlaub H, et al. SUMO conjugation to spliceosomal proteins is required for efficient pre-mRNA splicing. Nucleic Acids Research. 2017;45(11):6729–45.

186. Thandapani P, O'Connor TR, Bailey TL, Richard S. Defining the RGG/RG Motif. Molecular Cell. 2013;50(5):613–23.

187. Helbig R, Fackelmayer FO. Scaffold attachment factor A (SAF-A) is concentrated in inactive X chromosoe territories through its RGG domain. Chromosoma. 2003;112(4):173–82.

188. McHugh CA, Chen CK, Chow A, Surka CF, Tran C, McDonel P, et al. The Xist lncRNA interacts directly with SHARP to silence transcription through HDAC3. Nature. 2015;521(7551):232–6.

189. Kolpa HJ, Fackelmayer FO, Lawrence JB. SAF-A Requirement in Anchoring XIST RNA to Chromatin Varies in Transformed and Primary Cells. Developmental Cell [Internet]. 2016;39(1):9–10. Available from: http://dx.doi.org/10.1016/j.devcel.2016.09.021

190. Vizlin-Hodzic D, Runnberg R, Ryme J, Simonsson S, Simonsson T. SAF-A forms a complex with BRG1 and both components are required for RNA polymerase II mediated transcription. PLoS ONE. 2011;6(12).

191. Zhou KI, Shi H, Lyu R, Wylder AC, Matuszek Ż, Pan JN, et al. Regulation of Co-transcriptional Pre-mRNA Splicing by m6A through the Low-Complexity Protein hnRNPG. Molecular Cell. 2019;70–81.

192. Zhu F, Rui L. PRMT5 in gene regulation and hematologic malignancies. Genes and Diseases [Internet]. 2019;6(3):247–57. Available from: https://doi.org/10.1016/j.gendis.2019.06.002

193. Chan-Penebre E, Kuplast KG, Majer CR, Boriack-Sjodin PA, Wigle TJ, Johnston LD, et al. A selective inhibitor of PRMT5 with *in vivo* and *in vitro* potency in MCL models. Nature Chemical Biology [Internet]. 2015;11(6):432–7. Available from: http://dx.doi.org/10.1038/nchembio.1810

194. Kaushik S, Liu F, Veazey KJ, Gao G, Das P, Neves LF, et al. Genetic deletion or small-molecule inhibition of the arginine methyltransferase PRMT5 exhibit anti-tumoral activity in mouse models of MLL-rearranged AML. Leukemia. 2018;32(2):499–509.

195. Tarighat SS, Santhanam R, Frankhouser D, Radomska HS, Lai H, Anghelina M, et al. The dual epigenetic role of PRMT5 in acute myeloid leukemia: Gene activation and repression via histone arginine methylation. Leukemia. 2016;30(4):789–99.

196. Chaber R, Gurgul A, Wróbel G, Haus O, Tomoń A, Kowalczyk J, et al. Whole-genome DNA methylation characteristics in pediatric precursor B cell acute lymphoblastic leukemia (BCP ALL). PLoS ONE. 2017;12(11).

197. Hamard PJ, Santiago GE, Liu F, Karl DL, Martinez C, Man N, et al. PRMT5 Regulates DNA Repair by Controlling the Alternative Splicing of Histone-Modifying Enzymes. Cell Reports [Internet]. 2018;24(10):2643–57. Available from: https://doi.org/10.1016/j.celrep.2018.08.002

198. Raposo AE, Piller SC. Protein arginine methylation: An emerging regulator of the cell cycle. Cell Division [Internet]. 2018;13(1):1–16. Available from: https://doi.org/10.1186/s13008-018-0036-2

199. Aleem E, Arceci RJ. Targeting cell cycle regulators in hematologic malignancies. Frontiers in Cell and Developmental Biology. 2015;3(APR):1–22.

200. Ng OH, Erbilgin Y, Firtina S, Celkan T, Karakas Z, Aydogan G, et al. Deregulated WNT signaling in childhood T-cell acute lymphoblastic leukemia.

Blood Cancer Journal. 2014;4(3).

201. Hadjihannas M V., Bernkopf DB, Brückner M, Behrens J. Cell cycle control of Wnt/β-catenin signalling by conductin/axin2 through CDC20. EMBO Reports. 2012;13(4):347–54.

202. Jia M, Zhao HZ, Shen HP, Cheng YP, Luo ZB, Li SS, et al. Overexpression of lymphoid enhancer-binding factor-1 (LEF1) is a novel favorable prognostic factor in childhood acute lymphoblastic leukemia. International Journal of Laboratory Hematology. 2015;37(5):631–40.

203. Goudarzi KM, Lindström MS. Role of ribosomal protein mutations in tumor development (Review). International Journal of Oncology. 2016;48(4):1313–24.

204. Guccione E, Richard S. The regulation, functions and clinical relevance of arginine methylation Nature reviews | Molecular cell Biology. Nature Reviews Molecular Cell Biology [Internet]. 2019;20(Box 1). Available from: www.nature.com/nrm.

APPENDIX

Publications

Mamdouh Allahyani, Youn-Bok Lee, Renata Raele, Paraskevi Diamanti, Helen Scott, Allison Blair, James B. Uney. (In preparation). Expression of SAFB1 is decreased in ALL and its overexpression induces translational arrest and apoptosis selectively in cancer cells.

Mamdouh Allahyani, Paraskevi Diamanti, Allison Blair, James B. Uney. Characterising the Expression of the Stress Responsive Genes SAFB1 and SAFB2 in Childhood ALL. (2019). **Abstract**. British Journal of Haematology, 185, (Suppl. 1), 3–20

Presentations

27/07/2016 Investigating the roles SAFB proteins play in controlling Haemopoiesis and in acute lymphoblastic leukaemia. (Oral presentation, SCRM Seminar, Bristol University).

28/03/2017 Investigating the roles SAFB proteins play in controlling Haemopoiesis and in acute lymphoblastic leukaemia. (Oral presentation, SCRM Seminar, Bristol University).

27/02/2018 Investigating the roles SAFB proteins play in controlling Haemopoiesis and in acute lymphoblastic leukaemia. (Oral presentation, SCRM Seminar, Bristol University).

10/01/2019 SAFB1 and SAFB2 expression is altered in ALL and its overexpression induces apoptosis selectively in primary cancer cells. (Poster presentation, Cellular and Molecular Medicine away day, Wills Hall, Bristol).

26/03/2019 Characterising the Expression of the Stress Responsive Genes SAFB1 and SAFB2 in Childhood ALL. (Oral presentation, SCRM Seminar, Bristol University).

1-3/04/2019 Characterising the Expression of the Stress Responsive Genes SAFB1 and SAFB2 in Childhood ALL. (Poster presentation, British Society for Haematology Annual Scientific meeting, SEC, Glasgow).